

UNCLASSIFIED

AD NUMBER: AD0481856

LIMITATION CHANGES

TO:

Approved for public release; distribution is unlimited.

FROM:

Distribution authorized to Us Government Agencies only; Export Control; 1 Sep 1965. Other requests shall be referred to US Army Corps of Engineers, Washington, DC 20314

AUTHORITY

OCE D/A ltr dtd 30 Oct 1969

THIS PAGE IS UNCLASSIFIED



481856

**Translation 74**  
**RHEOLOGICAL PROPERTIES**  
**AND**  
**BEARING CAPACITY**  
**OF**  
**FROZEN SOILS**

by

**S. S. Vialov**

**SEPTEMBER, 1965**

**CONDUCTED FOR**  
**CORPS OF ENGINEERS, U.S. ARMY**  
**BY**

**U.S. ARMY MATERIEL COMMAND**  
**COLD REGIONS RESEARCH & ENGINEERING LABORATORY**  
**HANOVER, NEW HAMPSHIRE**



**DDC**  
**RECEIVED**  
**MAY 17 1966**  
**REGULATED**  
**B**

Translation 74

RHEOLOGICAL PROPERTIES AND BEARING CAPACITY  
OF FROZEN SOILS

(Reologicheskie Svoistva i Nesushchaia Sposobnost'  
Merzlykh Gruntov)

by  
S. S. Vialov

Izdatel'stvo Akademii Nauk SSSR Moscow (1959)

Translated from the Russian by Aztec School of Languages

CONDUCTED FOR  
CORPS OF ENGINEERS, U. S. ARMY

by

U. S. ARMY MATERIEL COMMAND  
COLD REGIONS RESEARCH AND ENGINEERING LABORATORY  
HANOVER, NEW HAMPSHIRE

This document is subject to special export controls and each  
transmittal to foreign governments or foreign nationals may be  
made only with prior approval of the Office, Chief of Engineers

## FOREWORD

This translation was prepared for the Office, Chief of Engineers, Directorate of Military Construction, Civil Engineering Branch, Mr. T. B. Pringle, Chief, in connection with Military Construction Investigations, Investigation of Arctic Construction, Sub-Project 21; Creep of Frozen Soils. Sub-Project authority, contained in FY 1961 through FY 1965 Instructions and Outline, Military Construction Investigations, Engineering Criteria and Investigations and Studies, provided for the translation of pertinent foreign language publications.

Translation from the Russian was performed for the U. S. Army Cold Regions Research and Engineering Laboratory (USA CRREL) under supervision of the Liaison and Technical Publications Branch, Mr. W. R. Floyd, Chief, by Aztec School of Languages, Inc., West Acton, Massachusetts with technical editing and copy preparation by Professional Writers, Inc., Beverly, Massachusetts. Mr. F. J. Sanger, USA CRREL, served as technical reviewer.

Sub-Project 21 is a project of the Applied Research Branch, Mr. A. F. Wuori, Chief, of the Experimental Engineering Division, Mr. K. A. Linell, Chief, USA CRREL. Mr. F. H. Sayles of the Applied Research Branch is the project leader.

Colonel Philip G. Krueger was Commanding Officer of USA CRREL during the preparation of this publication, and Mr. W. K. Boyd was Technical Director.

USA CRREL is an Army Materiel Command Laboratory.



## CONTENTS

	Page
Foreword -----	ii
List of illustrations -----	vi
List of tables -----	ix
Notes by technical reviewer-----	xi
Preface-----	1
Introduction -----	3
Part I. Strength and creep of frozen soils -----	6
Chapter I. Basic principles -----	6
1. Survey of previous study on strength of frozen soils -----	6
2. Basic principles for the theory of rheology (Survey) -----	10
3. Purpose of the experiments and conditions under which they were conducted -----	23
Chapter II. Investigation of the cohesion of frozen soils -----	39
1. Purpose of the investigation ----	39
2. Experimental method -----	40
3. Evaluation of the plastic characteristics of frozen soil -----	49
4. Relaxation of cohesion and limiting long-term strength -----	49
5. Dependence of the cohesion of frozen soils upon the gradation, moisture content, and temperature -----	54
6. Cohesion of ice -----	58
Chapter III. Investigation of the adfreeze strength of soils and ice with wooden rods ---	65
1. Concept of adfreeze strength ----	65
2. Experimental methods -----	66
3. Deformation process for constant loads and reduction of the adfreeze strength -----	67
4. Deformation process for an increasing load -----	74
5. Visco-plastic flow -----	78
6. Conditions for similarity of piles of various dimensions -----	82
7. Limiting long-term adfreeze strength of soil with wooden rods -----	86
8. The adfreeze strength of ice with wooden rods -----	89
Chapter IV. Tensile strength and compressibility of frozen soils -----	91
1. Long-term tensile strength of frozen soils -----	91
2. Compressibility of frozen soils -	93

	<u>Page</u>
Chapter V. Limiting stress-condition of frozen soils -----	96
1. General principles -----	96
2. Method of testing frozen soils in shear -----	97
3. Limiting stress condition of frozen soils taking into account the time factor -----	97
Chapter VI. The laws of deformation and resistance of frozen soils under load ----	103
1. The nature of frozen soil deformation -----	103
2. Distinguishing the rheological process of frozen soils from the deformation processes of an idealized solid -----	109
3. The relationship among load, deformation, and the rate of flow -----	113
4. The laws of the process of deformation in frozen soils -----	117
5. The laws of the reduction in strength of frozen soils -----	123
6. Methods of determining the limits of long-term strength -----	127
Part II. The resistance of frozen soils in structural foundations -----	130
Chapter VII. Experimental investigations on the resistance of frozen soil to indentation by a punch -----	130
1. Experimental methods -----	130
2. The character of the failure of frozen soil under penetration by a punch -----	134
3. The development of the penetration of frozen soil with time ---	138
4. The relationship between the penetration and the load -----	141
Chapter VIII. Determination of the bearing capacity of frozen soils taking their rheological properties into account -----	148
1. Theoretical value of the limiting stress -----	148
2. Determination of the limiting stress from the results of penetration by spherical indenters --	150
3. Comparison of the experimental and theoretical values of the limiting stress -----	151
4. Influence of ice inclusions on the bearing capacity of frozen soils -----	152
5. Computed strength of frozen soils in structural foundations -----	157

# CONTENTS (cont'd)

v

	<u>Page</u>
Chapter IX. Pressure distribution in frozen soils under a footing -----	163
1. Survey -----	163
2. Experimental determination of the frozen soil reaction at the base of the rigid footing -----	163
Part III. Resistance of pile foundations in frozen soil -----	169
Chapter X. Behavior of piles in frozen soils ---	169
1. General principles -----	169
2. Conditions for conducting field tests -----	170
3. On the nature of the resistance of frozen soil to displacement along the lateral surface of the pile -----	175
4. The relationship between the resistance of piles to loads and the method of placement -----	180
Chapter XI. Limiting load capacity of piles -----	185
1. Pull-out tests on piles -----	185
2. Pile testing for resistance to penetration [down loads] -----	188
3. Point-bearing resistance of frozen soil -----	194
4. Bearing capacity of piles and design values of the adfreeze strength -----	196
5. Heave forces -----	201
Conclusion -----	205
Literature -----	207

## ILLUSTRATIONS

	<u>Figure</u>		<u>Page</u>
Chapter I:	1.	Time variations of stress and strain --	12
	2.	Variation of the deformation of ideal bodies -----	14
	3.	Mechanical model of an elasto-plasto- viscous body -----	17
	4.	Rheological curves for liquid-form bodies and solid-form bodies -----	20
Chapter II:	5.	Results of experiment 53 for evaluation of the limit of long-term cohesion of permafrost soils -----	42
	6.	Results of repeated determinations of the cohesion - heavy loam -----	45
	7.	Results of repeated determinations of the cohesion - varved clay -----	45
	8.	Results of tests with spherical indenters of various dimensions -----	46
	9.	Relationship between the cohesion $c_{lt}$ and load $p$ for ball indenters -----	47
	10.	Test of pressing a ball with loading --	48
	11.	Curves of plastic deformations and reduction of cohesion for various soils	55
	12.	Diagrams of the plastic strains, and the lowering of cohesion for different temperatures of heavy, sandy loam -----	59
	13.	Dependence of the cohesion of frozen soils upon temperature -----	60
	14.	Dependence of the 'instantaneous' com- pressive strength of frozen loam upon temperature -----	60
	15.	Relaxation curves for the cohesion of ice at various temperatures -----	63
Chapter III:	16.	Combined curves of the growth of the displacement for various stresses -----	68
	17.	Growth of the displacement for a constant stress -----	69
	18.	Punching of model piles -----	70
	19.	Curves of the long-term adfreeze strength -----	73
	20.	Growth of the displacement for pull-out model piles under a gradually applied load -----	77
	21.	Relationship between the rate of dis- placement of model piles and the applied stress -----	80
	22.	Region of visco-plastic deformation of the soil -----	81
	23.	Pull-out tests of model piles of var- ious diameters -----	83
	24.	Influence of the dimensions of the pile on the adfreezing strength -----	84
	25.	Curves of the long-term adfreeze strength at various soil temperatures -	88

## ILLUSTRATIONS (cont'd)

	<u>Figure</u>		<u>Page</u>
	26.	Variation of the adfreeze strength with temperature -----	88
	27.	Adfreeze of ice with piles -----	90
Chapter IV:	28.	Curve of the long-term tensile strength -----	91
	29.	Curves of the compressibility of frozen soils -----	94
Chapter V:	30.	Envelopes and curves of the long-term shearing strength of frozen soils -----	99
	31.	Test of frozen loam for shear -----	100
Chapter VI:	32.	The melting of ice and the displacement of water in frozen soil -----	105
	33.	The melting of ice and the displacement of water under pressure -----	106
	34.	Scheme for probing for the moisture content -----	107
	35.	Kinetics of the deformations of frozen soils -----	108
	36.	Experimental and calculated according to the Maxwell-Shwedoff formula; curves of relaxation of the cohesion in normal and semilogarithmic coordinates -----	110
	37.	The change of the relaxation time $n$ and its dependence on time $t$ and stress $\sigma$ -	111
	38.	Curve of the long-term adfreeze strength on semilogarithmic and logarithmic coordinates -----	112
	39.	Relationship between the deformation and stress taking into account the time factor -----	114
	40.	Change of the deformation rate with time -----	117
	41.	Rectification of the curves of the long-term adfreeze strength -----	124
Chapter VII.	42.	Diagram of the setup for tests of frozen soils under load tests -----	133
	43.	Section of a block of soil after the penetration of a punch -----	134
	44.	The character of the deformation of soil when a punch penetrates it -----	136
	45.	A sectioned block of frozen soil (varved clay) after the penetration of a punch -----	137
	46.	The settlement of frozen soil (varved clay) upon the penetration of a punch -	138
	47.	The settlement in frozen soil of a punch under a constant load -----	139
	48.	Tests of the penetration of a punch into plastic frozen soil under field conditions -----	140
	49.	The recoverable deformation with long-term penetration of a punch into clay -	142

## ILLUSTRATIONS (cont'd)

	<u>Figure</u>		<u>Page</u>
	50.	The deformation of frozen soil upon the penetration of a punch -----	142
	51.	The relationship between the settlement and the load in the penetration of a punch into frozen soil -----	144
Chapter VIII:	52.	Investigation of frozen soils by punching -----	153
	53.	Cross-section of blocks of frozen soil with ice inclusions after punching ----	154
	54.	Influence of the structure of frozen soil on the strength under punching ---	155
Chapter IX:	55.	Diagram of the reaction pressure of unfrozen soils on a rigid footing at the soil surface -----	163
	56.	Profiles of the reaction pressures of frozen soil under rigid punches for various loads: varved clay -----	165
	57.	Diagrams of the reaction pressures of frozen soils under various loads on the punch -----	166
	58.	Variation of the reaction pressures with time -----	168
Chapter X:	59.	Cross-sections of soil along piles placed in frozen soil by different methods -----	176
	60.	The redistribution of moisture during the freezing of argillaceous soil around the model piles -----	177
Chapter XI:	61.	Tests for pulling-out piles driven by hand with steaming -----	186
	62.	Pull-out test for piles driven by hand with steaming -----	187
	63.	Test for pulling-out piles driven by hand with steaming -----	189
	64.	Curves of the development of deformation in pressing-down piles under constant stresses -----	191
	65.	The growth of settlement in pressing-down a pile under load increasing by steps -----	192
	66.	Relation between the deformation and the stress in ordinary and logarithmic coordinates -----	193
	67.	Relation between the stress and the speed of the relative displacement of the piles -----	194
	68.	Test for pressing-down piles driven by hand with steaming -----	195



## TABLES

	<u>Table</u>		<u>Page</u>
Chapter I:	1.	Physico-mechanical characteristics of frozen soils -----	28
	2.	Phase composition of water in frozen soils -----	38
Chapter II:	3.	Value of the coefficient M as a function of the angle of internal friction $\phi$ ----	40
	a.	Data of long-term experiments -----	43
	b.	Data of five short-duration experiments -----	43
	c.	Physico-mechanical characteristics of the soil -----	44
	d.	Gradation and plasticity -----	44
	4.	Statistical processing of the experimental data -----	46
	5.	Combined data of tests concerning the determination of the cohesion of undisturbed frozen soils at various temperatures -----	50
	6.	Reduction of cohesion with time -----	52
	7.	Data on the relaxation properties of undisturbed frozen soil -----	53
	8.	Relationships between the equivalent cohesion, mechanical composition, and plasticity of undisturbed frozen soils -	56
	9.	Reduction of the long-term cohesion of undisturbed frozen loams with increase in moisture content -----	57
	10.	Value of the relaxation time $n$ frozen soils at various temperatures $\theta$ -----	59
	11.	Compiled data of the value of the limiting long-term equivalent cohesion of undisturbed frozen soil -----	61
	12.	Compiled data of the determination of the cohesion of ice -----	62
	13.	Values of $c_{inst}$ ( $\text{kg/cm}^2$ ) for ice and frozen soils -----	64
Chapter III:	14.	Growth of strain for the pull-out of model piles -----	70
	15.	Results of pull-out tests of model piles under constant stresses -----	71
	16.	Results of pull-out tests on model piles with loads rising in steps -----	75
	17.	Experimental and theoretical values of the displacement -----	79
	18.	Values of $r_{lt}$ and $n_{pv}$ -----	80
	19.	Resistance of frozen soils to movement along the surface of wooden rods (adfreeze strength) according to laboratory experiments -----	87
Chapter IV:	20.	Instantaneous and limiting long-term tensile strength of undisturbed frozen soils -----	92
	21.	Relative compression $e$ of frozen soils -	94

## TABLES (cont'd)

	<u>Table</u>		<u>Page</u>
	22.	Values of the reduced coefficient of compressibility $a_0$ for silty, sandy loam	95
Chapter V:	23.	Instantaneous shearing strength of frozen soils -----	98
	24.	Instantaneous and limiting long-term shearing strength of frozen soils -----	99
Chapter VI:	25.	The cohesion of frozen clayey soil, undisturbed and remolded -----	104
	26.	Redistribution of the moisture in frozen soil after penetration by a punch -----	107
	27.	Rate of deformation $v$ , mm/hr -----	121
	28.	Results from experiment 24 -----	125
	29.	Experimental and theoretical values $\tau$ ( $\text{kg}/\text{cm}^2$ ), calculated according to (55) and (57) -----	126
Chapter VII:	30.	The physico-mechanical characteristics of the soils -----	131
	31.	The values of the parameters $A$ and $\alpha$ for plastic frozen soil -----	145
	32.	Experimental and analytical values of the settlement in the penetration of a punch -----	146
Chapter VIII:	33.	Values of $c$ ( $\text{kg}/\text{cm}^2$ ) for various values of $\phi$ and $c_e$ -----	149
	34.	Values of $p_{lim}$ ( $\text{kg}/\text{cm}^2$ ) for various $c_e$ , $q$ , and $\phi$ -----	149
	35.	Values of the limiting pressure of frozen soils -----	151
	36.	Experimental and analytical values of the limiting stress $p_{lim}$ -----	154
	37.	Computed strength (permissible pressures) of frozen soils under footings -----	158
	38.	Comparison of the values of $R$ , $\text{kg}/\text{cm}^2$ --	160
Chapter IX:	39.	Value of the reaction pressures $\sigma_z = 0$ -	167
Chapter X:	40.	Mechanical gradation of the soils in locations of driven piles -----	173
	41.	The effect on the adfreeze strength of grooves in the pile -----	179
	42.	Adfreeze strength of soil with piles driven by different methods -----	181
	43.	Adfreeze strength of the soil with temperature $0^\circ\text{C}$ to $-0.2^\circ\text{C}$ with piles driven by different methods -----	183
Chapter XI:	44.	Results of pull-out tests on piles under constant stresses driven by hand steaming into sandy loam and argillaceous, silty loam -----	186
	45.	Values of long-term adfreeze strength of soil with piles driven by hand with steaming -----	190

## TABLES (cont'd)

<u>Table</u>	<u>Page</u>
46. Comparison of the results of tests for pressing-down and pulling-out piles under constant stresses -----	194
47. Design values of long-term adfreeze strength of sandy loam and argillaceous silty loam with wooden piles driven with steaming -----	198
48. Limiting long-term adhesion of undisturbed frozen soil and soil disturbed by steaming -----	200
49. Observed data on heave of the soil in Igarka in 1952 -----	203

Notes by Technical Reviewer

Some Russian terms have no word-for-word equivalent in English and occasional clumsiness is unavoidable.

A brief explanation of some terms and an outline of Russian ideas on soils classification are presented to help in the reading of the translation.

Terms

Base. The word for "base", "origin", etc. in Russian is also used to mean the mass of soil that supports a structure. This is usually translated as "base" whereas "subgrade", or a phrase, applying to the ground not the structure, would be better.

Foundation. The Russian word for "foundation" means the part of the structure supported by the "base". Quite commonly the best translation is "footing".

Ground. "Ground" in Russian has caused trouble in other translations. It strictly means "subsoil" or "ground", never "topsoil". It is commonly used in the plural which makes a literal translation difficult. The best translation is usually "soil" or "soils" used in the engineering sense.

Loam. The word "loam" is used here to save writing "mixed fine-grained soil". In the USSR these soils are classified very usefully and because they give the most trouble with frost action they are discussed in more detail below.

Permafrost Institute. The word "Permafrost" in "Permafrost Institute" is more strictly "the study of the frozen condition", but the phrase "Institute for the study of the frozen condition", while correct, is unusable. "Geocryology" might be acceptable but a good Russian word exists for this and is not used in this context.

Instantaneous. This is a direct translation, (sometimes other translations use "temporal" or "momentary"). It means "in a very short interval of time", usually dictated by the testing machine, and is often from 5 to 10 seconds.

Long-term. This is a direct translation meaning many hours up to years (usual).

Punch. The Russian word is literally "stamp". Sometimes the best translation is "rigid footing" but this is not very good for an object a few inches in diameter. Where the "stamp" is a ball we have used the word "indenter" after hardness-testing terminology.

Kernel. Near failure in shear a rigid footing on soil usually develops a hard, so-called "elastic" wedge or cone of highly compressed soil beneath it, here described by "kernel", which means, literally, nucleus, core, kernel, center, etc.

Silty. In Russian usage, a soil is silty if the proportion of silt-sized particles exceeds that of the sand-sized ones.

Muddy. The word describes a soft highly sensitive (or perhaps thixotropic) soil that has low stability when undisturbed but has negligible strength when remolded.

#### Soil sizes

<u>Name</u>	<u>Diam in mm</u>
Sand	>0.05
Silt	0.05 to 0.005
Clay	<0.005

The word for "silt" can also be "dust" and some translations use "dusty" for "silty" -- even "loessial" has been used.

Soil types (Refer to figure for soils used for this book.)

<u>Name</u>	<u>Clay content % by wt.</u>	<u>Minimum diam of roll in plastic limit procedure</u>	<u>Liquid limit (in soils described in book)</u>	<u>Plasticity index</u>
Glina (clay)	>30	<1	53-68	23-24 and up
Suglinok	30 to 10	1 to 3	32-38	12-16
Supes	10 to 3	>3	22-38	1-14
Pesok (sand)	<3	N. P.	-----	-----

It will be remembered that 3 mm is the size for the Plastic Limit test. Suglinok is variously translated. Here the translation is "clayey silty loam". Another good translation would be "clayey silt with some sand". Supes is translated by: "sandy silty loam". Another good translation is "silty sand with some clay".

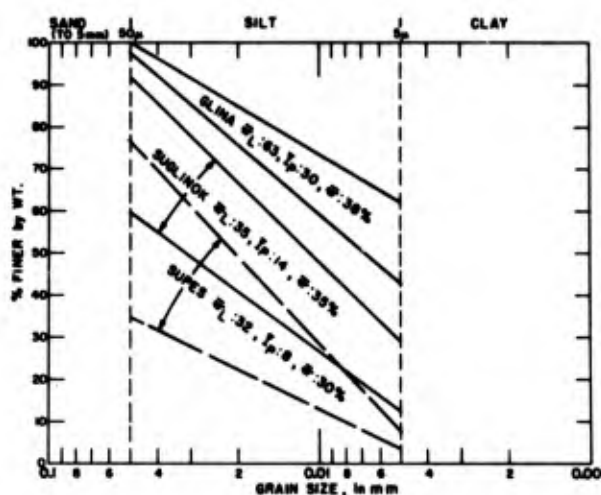
The best descriptions are given by examples (see figure).

The void ratio of these two soils is usually between 1 and 1-1/2.

Another index property is the Liquidity Index ( $I_L = w - w_p / I_p$ ) well-known in Soil Mechanics.

$I_L = 0$  - "stiff" or "firm"  
 0.25 - semi-stiff  
 0.25-0.50 - stiff-plastic  
 0.50-0.75 - soft-plastic  
 0.75-1.0 - flow-plastic  
 >1.0 - flowing.

Granular soils are described by gradation, relative density and void ratio.



Approximate gradations water content, liquid limit and plasticity index.

#### List of Symbols

A, A'	Deformation modulus
	Tyabin number
	Parameter
$A_w$	Coefficient of pressure distribution
B	Parameter in the basic creep equation for strength
	at a given time
	Liquidity index
C	A function
E	Young's modulus of elasticity
$E_u$	Euler number
F	Force
	Surface area of adfreezing
G	Shear modulus of elasticity
H	Abscissa for cycloid equations
$H_M$	Depth of embedment in permafrost

xiv

I	Hydraulic gradient	
$I_p$	Plasticity index	
K	A function in creep theory	--
$K_1, K_2$	Coefficients	
M	Coefficient in cohesion equation	--
N	Design stress for a pile	
P	Force	
	Load	
Q	A function	
	Self-weight	
R	Permissible pressure	
	Radius of influence	
	Point resistance of a pile	
$R_e$	Reynolds number	--
S	Heave force	
$S_M$	Long-term adfreeze strength	--
T	Absolute temperature	
	Adfreeze force	
	Axial load on pile	
a	Soil parameter	
	Coefficient of compressibility	
b	Soil parameter	
	Width of footing	
c	Cohesion	
	Adhesion	
d	Diameter of rod, pile, ball indenter	--
	Distance from center	
e	Relative compression (conventional strain)	.



f	A function
	Cross-sectional area of a pile
	Area of base of footing
	Coefficient of friction
h	Thickness
	Depth
	Sample height
k	Constant
	Factor of safety
	Load factor
	Uniformity coefficient
l	Length of rod or of pile
	Embedded length
m	Reaction time
n	A parameter
	Number of observations
	Relaxation time
p	Pressure on a footing
	Compressive load
q	Soil pressure at footing depth
r	Radius of a rod or a pile
s	Computed settlement
	Penetration of ball indenter
	Displacement
t	Time
u	Linear displacement
	Perimeter of pile
v	Rate of linear displacement
	Rate of shear displacement
w	Water content

xvi

y	Intercept on vertical axis	
z	Depth	
	A variable in gamma function	--
$\Gamma$	Gamma function	
	Ratio of length/diameter of a pile	--
$\alpha$	Soil parameters	
	Ratio of viscosity coefficients	
	Scale ratios	
	Coefficient of consolidation	0
$\beta$	Soil parameters	
	Parameter in the basic creep equation for strength	
	at a given time	
$\gamma$	Unit weight	
	Vertical displacement	--
	Shear displacement	
	Soil parameter	~
$\delta$	Soil parameter	
	Deviation from a mean	
e	Void ratio	
n	Coefficient of viscosity	
$\theta$	Temperature	
	Tensor of yield stresses	
$\lambda$	Ratio of displacement to diameter	
	Displacement along a normal	
$\mu$	Poisson's ratio	
v	Time in creep theory	-
$\xi$	Rate of flow	
$\rho$	A radius	.
	Density	

## Coefficient of variation

$\sigma$	Normal stress
$\tau$	Tangential stress
	Shear stress
$\phi$	A function
$\phi$	Angle of internal friction
	Round bar diameter
$x$	Angle parameter in cycloid equations
$w$	Acceleration

Suffixes

av	Average
c	Cohesion
cr	Critical
dc	Damped creep
e	Linear dimensions
el	Elastic
es	Delayed elastic
ex	Experimental
f	Final
	Footing
fl	Flow
fr	Frictional
i	Initial
	General value
incl	Inclusions
inst	Instantaneous; i.e., very short time
lim	Limiting
lt	Long-term, i.e., very long time

xviii

M	Model	
m	Mean	
mn	Mineral layers	--
N	Nature (full scale or prototype)	
n	Normal	--
o	Initial or average	
p	Plastic	
per	Permissible	
pr	Press-down	
pul	Pull-up	
q	Body forces	
res	Residual	
s	Equivalent layer	
t	Time	--
	Tensile	
T	Time	--
$\tau$	Shear stress	

## RHEOLOGICAL PROPERTIES AND BEARING CAPACITY OF FROZEN SOILS

### PREFACE

This investigation is for the purpose of studying the strength and stability of frozen soil under building foundations. These questions are examined as they concern the rheological processes which occur in frozen soil, i.e., the processes of changes of load-deformation conditions with time.

The necessity of such investigations arose as a result of practical requirements, and the investigations were intended to solve several engineering problems. Experimental investigations were carried out from 1950 to 1953 at the Igarskii Permafrost Scientific Research Station (INIMS) of the V. A. Obruchev Permafrost Institute of the Academy of Sciences of the U.S.S.R., together with the Northern Project - Exploration Expedition (SPIE) of the Arctic Project (GUSMP). The experiments were carried out both under laboratory conditions (in the vault of the INIMS, dug in a stratum of permafrost), and under field conditions in two experimental areas\*. Since the investigations were related to studying the influence of the time factor, part of the investigations were conducted over a period of several months, and, in some instances, several years.

Such complicated investigations were made possible by close contact with the Arctic Project, and by the interest shown by the management of SPIE and the Arctic Project.

The Author wishes to extend his deep thanks to all the collaborators from INIMS and SPIE who participated in the experimental investigations; he expresses his sincere gratitude to N. A. Tsyтовich, Corresponding Member of the Academy of Sciences of the U.S.S.R., for invaluable advice, and to Dr. N. I. Saltykov for the interest shown in the investigations.

---

\* Approximately 1300 individual experiments were conducted under laboratory conditions, and approximately 100 under field conditions.

## INTRODUCTION

The strength of frozen soil and its resistance to stress cannot be considered as fixed properties which are determined once and for all. These characteristic properties undergo continuous changes in accordance with thermodynamic, physico-mechanical, mechanical, and other processes which occur in the ground. One of the most important factors other than temperature which causes change in the stress-deformation condition of the frozen soil is the time of action of the load. In such soils, because of the presence of water both in solid and liquid phases, deformations increasing with time arise (phenomenon of creep), the stress weakens (relaxation), and a reduction in strength occurs with a protracted application of the load. The specific rheological processes are quite general in natural conditions, both for frozen and for unfrozen strata. Flow of glaciers, solifluction, creep of ground masses, flow of mud streams, etc., are simply rheological processes occurring during time intervals ranging from comparatively short periods to centuries. The various tectonic dislocations, i.e. fold formation, bending of strata, and other similar phenomena, are explained in many instances precisely as a consequence of the flow of a deep stratum of rock under the influence of the weight of overlying layers. For large values of the average pressure in the rock stratum, and for high temperatures, there is an insignificant difference between vertical and horizontal pressures. However, this is sufficient to cause a flow of the hard rock layers which lasts for centuries (Gogoladze, 1939; Nadai, 1954, and others). According to geophysicists, these situations are realized particularly where rock masses of extremely old formation overlie a layer of younger geological age (Jeffreys and Gutenberg, 1939).

Just as often, we encounter rheological processes in the ground, perceptible during comparatively short periods, which are commensurate with the time for engineering construction; these rheological processes lead to the effects of the loading of these buildings. It is well known that the long-term settlement of structures is the result of flow in the clay soils under the foundations; flow in soils is also responsible for the displacements of retaining walls, shore protective structures, etc.

As has been shown in the investigations by N. A. Tsytovich, V. G. Berezantsev, M. N. Goldshtein, and others, as well as by this work, rheological phenomena occur with particular intensity in frozen soil.

The calculation of rheological effects becomes particularly significant in the study of the behavior of frozen soils having a temperature close to 0C (descriptively called "plastic frozen soil"). Such soils are highly plasto-viscous because of the large amount of unfrozen water which they contain; under the influence of a load, significant deformations develop and the soils quickly lose their strength. This condition is very important because "plastic frozen" soils are prevalent in many areas important for industry, and on



which intensive construction is being undertaken. But even in the calculations for construction in areas with severe permafrost conditions, we must take into account the periodic plastic condition of the frozen soils, since foundations are usually laid at a small depth below the permafrost table; in the summer, the temperature at this depth rises sharply.

The present investigation plans to explain, on the basis of experimental and theoretical investigations, the mechanism of rheological processes occurring in frozen soils. Several instances of the theory (even if only phenomenological) for the strength of these soils, originating from physical representation of the mechanism of deformation, will also be examined. The practical purpose of the investigation is to determine the strength properties of frozen soils and to evaluate the bearing capacity of footings and piled foundations in frozen soils. This analysis is divided into three parts according to the problem under investigation.

In the first part, the general problems of strength and rheology of frozen soils are examined on the basis of analysis of the results of laboratory experiments which have been conducted. On the basis of the above experiments, a hypothesis is introduced concerning the physical nature of rheological processes occurring in frozen soils; rules characterizing the relation of load, deformation, and time (rate of deformation) are determined. The condition of a limiting stress state of frozen soils is also examined. In this part, the data for the values of the long-term strength, cohesion, adfreezing, tension shear, etc. are introduced.

The second part of the investigation is devoted to the problem of bearing capacity of frozen soils when they are used as natural construction foundation soils. Results of laboratory and field experiments concerning the long-term resistance of frozen soils to indentation (foundation models) by a punch are also given in this part. Values of the calculated, permissible pressures on these soils, originating from the basic principles shown in Part I, are also estimated.

In the third part, the problems of the bearing capacity of pile foundations in frozen soils are examined. Such foundations are increasingly used in construction on frozen soils; yet the use of piles in frozen soil is almost completely uninvestigated. Limited information, mainly on the method of use and rate of adfreeze, is available in the literature. In the present investigation, the data of the field experiments for determining the long term resistance to load and extraction, using piles driven by various means, are shown. The value of the limiting load, obtained by the simplest method, is determined as the sum of the resistance of the soil along the lateral surface of the pile and the resistance under its tip. Formulae for calculating the bearing capacity of the pile in frozen soil are introduced, and the calculated parameters for the strength of adfreezing, which have been obtained experimentally, are given.

The investigations were carried out with undisturbed frozen soil. Hence, a considerable part was assigned to the field experiments. In all the investigations, considerable attention was devoted to frozen

soils having a temperature close to 0C. In these soils, which are of great significance in engineering, rheological processes occur with maximum intensity.

## PART I. STRENGTH AND CREEP OF FROZEN SOILS

## CHAPTER I. BASIC PRINCIPLES

## 1. Survey of previous study on strength of frozen soils

The necessity of studying the strength properties of frozen soil was a direct consequence of industrial utilization of permafrost areas. The first large-scale engineering enterprises in these areas, such as the construction of the Transbaikal and Amur Railroads (in the 1900's), directed the attention of engineers toward the importance of studying the relation of frozen soils to construction, as well as the physico-mechanical properties of these soils. The problems mentioned above were first examined in the investigation of N. S. Bogdanov, and were reflected in the general construction procedure of V. Statsenko. Since that time, isolated investigators and builders have made scattered calculations on the strength of frozen soil. But systematic investigations, with broad theoretical generalizations, were initiated in the Soviet Era, when industrial utilization of the North began. In 1927, the famous monograph of M. I. Sumgin (1927) was published; in 1928, the first investigations concerned with the problems of calculating foundations in frozen soils appeared (Tsytoich, 1928). It is interesting to note that because of the complete lack of experimental data, the bearing capacity of frozen soils was estimated in the early investigations to approximate the 'instantaneous' compressive strength of ice.

For the first time, in 1930, investigations of "Technical Conditions for Designing Structural Foundations in Areas of Permafrost" were conducted at the Leningrad Structural Institute; this project generalized the experience which had already been acquired for structures in these areas. From 1930-1936, systematic experimental investigations in the field of frozen soil mechanics were developed. These investigations, carried out by N. A. Tsytoich and his collaborators, I. S. Vologdina, M. L. Sheikov and O. M. Gumenskaia, were of the utmost significance. Simultaneously, the investigations of 'instantaneous' compressive strength for frozen soils were conducted by M. I. Evdokimov-Rokotovskiy, N. M. Belyev, V. N. Skhepochkin, and others.

Experiments for determining the adfreeze strength of soil were carried out for the first time in 1928, by M. Ya. Chernyshev, and after him by M. I. Evdokimov-Rokotovskiy. The concept of adfreezing forces in engineering practice was introduced. The above problem was examined in greater detail in 1930-1936 by N. A. Tsytoich and I. S. Vologdina.

During this initial phase of the development of Permafrostology, frozen soil was considered as a brittle solid body, similar to rock layers. Thus, the instantaneous strength, i.e. the rupture stress for a rapid increase of load, was taken as the characteristic strength of frozen soil. These views, which persisted for an extremely long time

and continue to persist among many builders even today, are reflected in the "Standards for Planning and Construction on Frozen Soil" (OST 4555). Issued in 1935, the values of the computed characteristics were taken from the instantaneous strength. For this reason, the permissible pressure on frozen soils was determined according to the specimen strength, disregarding the special behavior of the soil as a mass.

The monograph by N. A. Tsytoich and M. I. Sumgin (1937) was an important contribution; the basic principles of frozen soil mechanics were formulated, thus creating a new scientific field. In this investigation, considerable attention was devoted to the problem of stability of frozen soils, hence obtaining a more adequate concept of the actual properties of frozen soil. The soil began to be considered as an elasto-plastic body capable of developing plastic deformation, even under small loads, rather than as an absolutely rigid body. It was shown that the compressive yield stresses at which plastic deformation arises are 6-10 times smaller than the instantaneous strength for the frozen soil. For determination of the bearing capacity of frozen soils under structural foundations, i.e. to determine the strength of a plastic medium under a rigid punch, it was suggested that Prandtl's formula be used. The fact that this formula has preserved its importance to the present despite new refinements proves the validity of such an approach.

In the experiments conducted from 1933-1936 by N. A. Tsytoich, N. S. Vologdina and M. S. Sheikov (Tsytoich and Sumgin, 1937), it was noted for the first time that a change in the rate of loading would affect the ultimate resistance of frozen soils. At that time, however, an explanation of this phenomenon had not been discovered, and investigators restricted themselves to its observation only. The stability of frozen soils continued to be determined by using the instantaneous resistance. This approach was kept in use, even in the standards of OST 90032-39, up to 1955. In these standards, the value of the adfreeze strength and the resistance to shear were computed on the basis of "instantaneous" tests (under laboratory conditions), and were of course excessively large. To determine the permissible stresses on frozen soil, an attempt was made to calculate the influence of plastic deformation and also the influence of restrained lateral expansion of the soil under the action of a local load. This was done by introducing correction factors in the data of the tests for three-dimensional instantaneous compressive strength. Such an approach was an improvement on the standards of 1935. However, because of limitations in the given method and insufficient understanding of the problem, the permissible pressures recommended by OST 90032-39 were too small.

Further industrial utilization of the North caused increased attention to the investigations of the mechanical properties of frozen soils. These investigations were conducted by the USSR Academy of Sciences (Committee of Permafrost, then the Permafrost Institute), by departmental scientific-investigating organizations and frost stations, as well as by large-scale construction enterprises (Dalstroï, Norilstroï, Vorkutugol, Glavsevmorput, and others).

Mention should also be made of the experimental investigations by N. I. Bykov and P. N. Kapterev (1940), the monograph by A. V. Liverovskiy and K. D. Morozov (1941), which generalized experiments of

building on frozen soil, and the books by V. A. Elenevskiy and G. A. Nizovkin, K. D. Morozov, and others. Field experiments concerning determination of the adfreezing strength and resistance to shearing of frozen soil were conducted in Igarka by L. A. Meister and P. I. Melnikov (1940). The compressive strength of undisturbed frozen soils was determined by the Norilsk Group of KOVM, Yakutsk Permafrost Station, and others. Laboratory investigations on stability were carried out at the Leningrad Institute of Construction Engineers (LISI), and then at the Central Laboratory of the Institute of Geocryology. In all these investigations, the influence of time on the stability of frozen soils and soil's ability to develop plastic deformations were increasingly observed. Thus, in 1937-1940, in the laboratory of LISI, special experiments were conducted for determining the yield stress of frozen soil for compression, shear and adfreeze. The work by N. A. Tsytoich (1940) was devoted to the investigation of elastic and plastic deformations of frozen soils.

Simultaneously, experiments in the field were carried out by several investigators. Many interesting experiments were made in 1936-1940 by N. I. Bykov (Bykov and Kapterev, 1940) for determining the ultimate resistance of frozen soils; the experiments showed that the actual values are significantly smaller than those obtained in the laboratory for "rapid-tests" (included in the 1939 standards). However, N. I. Bykov did not give a correct explanation for the causes of these discrepancies. He assumed that they were due to inadequate calculation procedures, whereas, in fact, they appeared as a result of the influence of the time factor (instantaneous loading in the laboratory experiments vs. long-term action of the load in the field experiments). The excess of the standard values of the adfreeze strength and shear resistance was noted also in other investigations (Liverovskiy and Morozov, 1941; Saltykov, 1944; and others). The data from the experiments by N. I. Bykov were used in 1941 in "Technical Specifications Concerning the Investigations, Planning and Construction of Railroads in Permafrost Areas." However, because of the limitations of the experiments, the values of the adfreeze strength were not differentiated according to temperature and were assumed to be identical for all temperatures; this is, of course, incorrect.

The theory formulated by N. A. Tsytoich (1945-1952) for the equilibrium composition of water in both solid and liquid phases is important for explaining the nature of the cohesion of frozen soils. Numerous investigations of this problem were carried out by Jung, A. E. Fedosov, M. N. Goldshtein, Z. A. Nersesova, and others.

In developing the theory of stability of frozen soils, an important role was played by the investigations which considered these soils as visco-elastic bodies. For the first time, M. N. Goldshtein (1941-1948) applied the theory of relaxation to frozen soils. He investigated long-term adfreeze strength as it concerned the problem of heaving. On the basis of the data from experiments concerning the punching through of piles frozen in the soil, M. N. Goldshtein showed that the punching resistance diminished with an increase in the time of action of the load. Following Yu. M. Ivanov (1948), M. N. Goldshtein used, for describing the process of lowering stability, the relaxation equation from Maxwell-Shwedoff, and he introduced the concept of the limit of long-term adfreeze strength for frozen soils. N. I. Saltykov (1944) devoted his work to investigating the force of heaving with regard to relaxation, also using the

Maxwell-Shwedoff equation.

Under field conditions, the long-term adfreeze strength of the soil with piles was determined in 1941-43 by I. D. Dergunov (1945) and I. D. Belokrylov (1944), who conducted extremely interesting investigations and showed that, in nature, the time of action of the load strongly affects the adfreeze strength.

In extensive experimental and theoretical investigations, V. G. Berezantsev (1947-1949, 1953) studied the long-term resistance of frozen soils under a local load. To determine the critical load on frozen foundations, he proceeded from the Saint-Venant principle for plasticity, but he took the relaxation phenomena into account. This introduced into the computational formula a limit for the long-term value of the cohesion, wherein it was assumed that the weakening of cohesion obeys the Maxwell-Shwedoff relaxation law. V. G. Berezantsev conducted interesting investigations on the long-term resistance of frozen soil to punching shear.

The monograph by N. A. Tsyтовich (1952) was a broad study of the mechanics of frozen soil, summing up the latest results obtained by the author, as well as by other investigators. In this last investigation, considerable attention was devoted to the strength of frozen soil and to the phenomena of yield and relaxation. As in the previously mentioned studies, lowering of the strength of the soil, for various forms of resistance, was assumed to obey the Maxwell-Shwedoff law. Determination of the limiting load for foundations on frozen soils by Prandtl's formula for a plastic medium was suggested, introducing, in addition, the long-term limiting cohesion as a characteristic property.

As far as foreign research on the mechanics of frozen soil and engineering investigations of permafrost is concerned, it was practically non-existent up to the Second World War, if we disregard isolated articles on the physico-mechanical properties of seasonally frozen soils. This situation changed (in the U. S. A., and partially in Canada) during the Second World War, and even more in the post-war period. The American scientist R. Black (Black, 1954) wrote: "... it is only in the last few years that the properties of permafrost soils have captured the attention of North American scientists. If it had not been for the difficulties encountered by our armed forces in the Subarctic during the Second World War, the study of permafrost would not have progressed with such speed, as it has during the past ten years." Muller's abstract (Muller, 1945) can be considered the first large-scale investigation published concerning the engineering problems; published in three parts, it was largely based, as the author himself wrote, upon the studies of Soviet scientists. Later, several articles devoted to construction on frozen soils and, in particular, to the problems of building foundations on these soils were published (Hardy and D'Appolonia, 1946; Barnes, 1946; Carlson, 1948; Hemstock, 1949; Roberts and Cooke 1950; Nees, 1951; Rathjens, 1951; Legget, 1951; McKinley, 1952; Waterhouse and Nelson, 1952; Sturgis, 1953; and others). The problems of road construction on frozen soil and the physico-mechanical properties of the soil are considered in a special collection translated into Russian\*. In 1951 and 1954, Black

\* Frost Phenomena in Soil. Collected articles. M. Izd. in foreign literatures 1955.



(1954) published a new survey; a review article by Terzaghi (1952) appeared, whose aim, as the author indicated, was "to give basic engineering information which is necessary to predict results for permafrost soil work and to adapt a construction project to the anticipated changes in the subsoil." A description of the interesting engineering problems encountered in constructing Thule Air Base is given by S. Sturgis (1953). Some of the foundations of this project were of the pile type, and preservation of the frozen condition of the soil was assured through natural and artificial cooling. In general, wide use of piled foundations is noteworthy in American construction practice on frozen soil.

It must be noted that the investigations of foreign scientists on the stability of frozen soils disregarded rheological processes; there is, however, an indication in Terzaghi's article (Terzaghi, 1952) of the fact that frozen soils possess yield characteristics. However, this question has not been investigated in detail.

The investigations conducted in recent years have increased our knowledge of the mechanics of frozen soil; they have shown the necessity of reconsidering a variety of existing situations which require a new approach to the problem of strength in these soils. These problems are investigated in the present analysis.

## 2. Basic principles for the theory of rheology (survey)

Before proceeding to an investigation of the special behavior of frozen soils, it is advisable to review the basic principles of the theory of rheology, since our analysis is based on such principles. Such a review will also be useful, since the application of this theory to frozen soils is recent.

The classical theories of elasticity and plasticity consider the stress-condition of a body as stationary, and assume that strains arise immediately after the application of a stress, hence excluding the time factor. Rheology\*, in the widest sense of the term, includes the theories of elasticity and plasticity, introducing time as an independent variable in the stress-strain relationships. In other words, rheology, by studying the stress-strain history of a body, must answer the question: what are the stresses and strains at a given point of the body at a given time? The creep, i.e., the growth of a deformation in time, even for a constant load, is one of the manifestations of the rheological properties of a body. For this reason, the process of development of deformations can have multiple characteristics (Rebinder 1947; 1950).

For sufficiently small stresses, smaller than some value  $\tau_0$ , which is called the limiting stress (or the yield stress), the strain approaches a limit as the time increases (Figure 1a). This process is called "elastic after-effect, and sometimes "damped creep." For a stress exceeding the limiting value mentioned above, a continuous growth of a residual strain takes place, with a transition to a

\* Rheology is (from the Greek  $\rho\epsilon\omega$ -flow, and  $\lambda\acute{o}\gamma\omicron\varsigma$ -science) the science dealing with the flow of matter; it is a division of physical mechanics.

steady flow once the elastic reaction is completed (Figure 1b). This process is called "creep", or "visco-plastic flow."\*

The dynamics of damped creep (Figure 1a) are characterized by the following stages. Immediately after application of a load, an initial, conditionally instantaneous (with respect to the speed of sound) elastic strain,  $\gamma_i$ , arises. Then, as time goes on, the elastic strain (so-called by P. A. Rebinder)  $\gamma_{es}$  develops; its rate of growth gradually decreases, approaching zero, and the strain approaches a certain maximum final value,  $\gamma_f$ , for a given stress. Thus, the strain of a damped creep after-effect is equal to:

$$\gamma_{dc} = \gamma_i + \gamma_{es} \quad (1)$$

for any time,  $t$ .†

The ideal visco-elastic body exhibits deformations which completely disappear when the stress is removed; the initial elastic strain would vanish instantaneously, while the delayed elastic strain vanishes after a period of time.

The process of creep includes several stages:

(1) the initial, characteristic formation of instantaneous purely elastic strain.

(2) the stage of non-uniform creep (delayed elastic strain,  $\gamma_{es}$ ), characterized by a decrease in the rate of strain, approaching a certain minimum value (part of curve A-B, Figure 1b).

(3) The stage of steady creep  $\gamma_{f1}$ , where the growth of the rate of strain, having reached a minimum value, becomes constant:  $\epsilon_{f1} = \frac{d\gamma_{f1}}{dt} = \text{const}$ ; this is reflected by the straight-line section of the curve B-C (Figure 1b). This stage is called visco-plastic (or simply plastic) flow, because of its superficial similarity to the flow of liquids.

\* The first of these terms, creep, is generally applied to solid crystalline bodies, whereas the second, flow, is applied to viscous liquids, dispersed (colloidal) and high molecular weight systems, and others. But the above concepts often become confused. Several authors (P. A. Rebinder and others) imply by "creep" only the process of slow strain growth, where no breaking of the structural bonds occurs.

† All the discussions and notations for stress and strains refer to shear, since it is precisely the shear resistance that determines the stability and strength of soils. However, the cited formulae will also be accurate for other types of simple stress situations, provided that the appropriate substitutions of parameters are made. As far as rheological mechanisms for complex stress situations are concerned, we refer those interested to the specialized literature (Kachanov, 1948; Ishlinskiy, 1945; Nadai, 1954; Reiner, 1947; Goldenblat, 1952; and others).

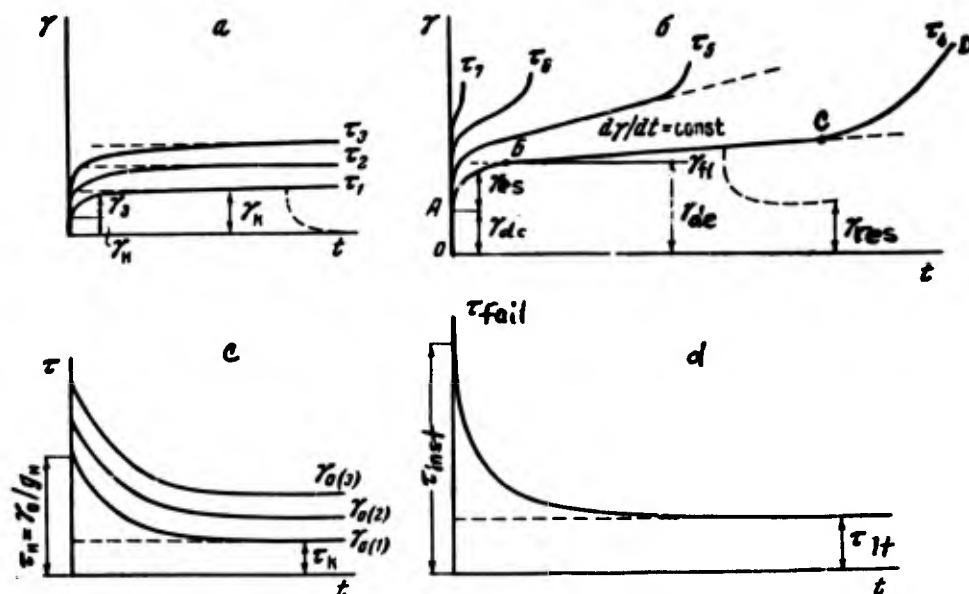


Figure 1. Time variations of stress and strain.

a. Damped creep  $\tau_1 < \tau_2 < \tau_3 < \tau_{lt}$ . b. Un-damped creep  $\tau_{lt} < \tau_4 < \tau_5$ . c. Relaxation stress. d. Reduction of ultimate strength.  $\tau$  is shearing stress;  $t$  is time;  $\gamma$  is strain.

(4) The stage of progressive flow, characterized by an increasing rate of strain (part CD of the curve, Figure 1b), leading to collapse. For several colloidal media this stage is absent, since a continuous restoration of the broken bonds takes place in the flow.

Thus, up to the transition in the fourth stage, the strain during "undamped creep" is equal to :

$$\gamma_{cr} = \gamma_i + \gamma_{es} + \gamma_{fl}. \quad (2)$$

Here, only the components  $\gamma_i$  and  $\gamma_{es}$  of the strain are reversible, while  $\gamma_{fl}$  is irrecoverable.

The nature of the curves for creep and rate of the visco-plastic flow depends upon the load, i.e. the larger the load, the greater the speed, and the faster the transition to the stage of progressive flow.

Another manifestation of the rheological properties of a body is relaxation, i.e. the lowering of resistance of the body for a constant strain. With the appearance of relaxation, a lowering of the strength of the material occurs, i.e. its resistance to failure for the long-term action of a load. If the load is applied for a short time, the creep-strain cannot develop and a brittle break occurs, during which resistance to failure, the so-called instantaneous strength  $\tau_{inst}$  (theoretically corresponding to loading with the speed of sound), is a maximum. For practical purposes, we are concerned either with the instantaneous resistance, or, for a standard rate of growth of the load, with a temporary resistance. However, the failure of the body

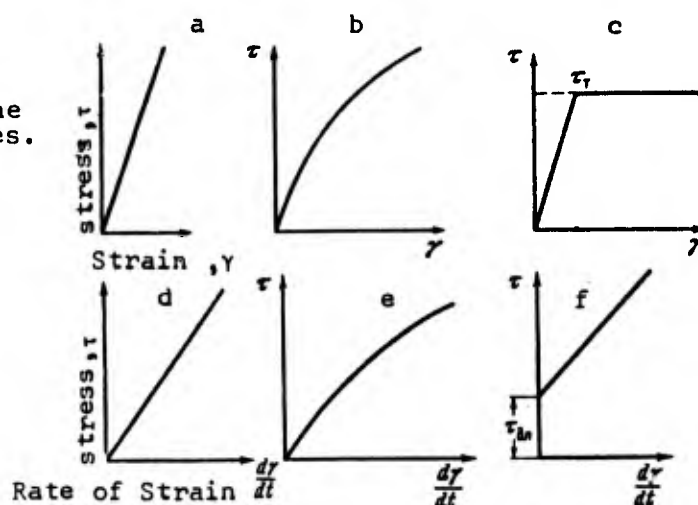
can also occur for a load smaller than  $\tau_{inst}$  if this load acts, not instantaneously, but during a certain time which allows for the development of the creep strain; the smaller the load, the longer the time necessary for failure to occur (the bearing capacity condition). The resistance to such a failure is called the long-term strength. It is assumed that for some materials (metals at high temperatures for instance), the lowering of resistance occurs infinitely. Calculations for stability of such materials are carried out at a given moment in the construction operation. Nevertheless, for certain of these materials, we assume existence of the so-called limit of long-term strength,  $\tau_{lt}$ . Until this limit is exceeded, failure will not occur during the practically realizable period of application of the load. On the basis of the experiments conducted, it will later be shown that the limiting value  $\tau_{lt}$  is the limit of the cohesive  $\tau_{fl}$  for an infinitely slow failure. Thus, the limit of the long-term strength can be considered as the stress up to which the strain becomes constant after a period of time. Above this stress, increasing strain arises, yielding to failure after a certain period. Lowering the resistance, as a function of the long-term action of the load is represented by the curve of the long-term strength, plotted as failure stress vs. time coordinates. The initial ordinate of the curve corresponds to  $\tau_{inst}$ , while the ordinate of the asymptote is  $\tau_{lt}$  (Figure 1d). The curve of the long-term strength can be deduced from the curves for undamped creep if they are plotted with  $\tau - t$  coordinates.

The above processes are non-uniform (Frenkel 1951) and their peculiarity lies in the fact that the same force induces both reversible elastic strains, by which the shape of the body is permanently changed. All real bodies possess elastic and plastic properties, but the evidence of these properties depends upon several conditions: pressure, temperature, and interval of time during which the process is observed, compared to the so-called "relaxation." If a force is applied on water during a time interval shorter than 10-11 sec, which is its relaxation time, the water will display elastic properties. On the contrary, forces acting on soil layers (the relaxation time of which is estimated in milleniums) cause flows of these layers lasting for centuries, within the course of geological periods. Since the classification of bodies as "elastic," "plastic," and "viscous" is a conventional one, we usually resort to a specified scheme; we examine certain idealized flows whose deformations characterize the conditions investigated for the real flow. The six deformation patterns of the simplest flows are shown in Figure 2. The diagrams a, b, and c (Figure 2) characterize flows for which no influence of time on the deformation process is taken into account. These diagrams show the stress-strain relation: linear,  $\tau = G\gamma$ , for an elastic Hooke body (Figure 2a), and non-linear for a non-linear elastic body (Figure 2b). For the elasto-plastic body (Figure 2c), the strain obeys Hooke's law until the stress is equal to the yield stress  $\tau_{fl}$ ; thereafter, when  $\tau = \tau_{fl} = c = \text{const}$  (Saint-Venant's condition of plasticity), the strain grows irreversibly for a constant stress. Furthermore, the change of the shape of the flow is not accompanied by volumetric changes. The graphs 2e and 2f characterize idealized viscous flows. The diagrams show the dependence of stress upon rate of strain. The ideal Newtonian viscous body (Figure 2d) flows for any non-zero stress with a velocity proportional to the shearing stress,

$$\tau = \eta \frac{dv}{dr} = \eta \frac{d\gamma}{dt}, \quad (3)$$

Figure 2. Variation of the deformation of ideal bodies.

- a. Ideal Elastic.
- b. Non-linear elastic.
- c. Ideal elasto-plastic.
- d. Ideal viscous.
- e. Non-linear viscous.
- f. Ideal visco-plastic.



where  $\frac{dv}{dr}$  is the gradient of the velocity,  $v = \frac{d\lambda}{dt}$ ;  $\lambda$  is the displacement along the normal  $r$  to its direction: this is equivalent to the concept for rate of shear strain  $\frac{dy}{dt} = \xi_{fl}$ . The quantity  $\eta$  is the coefficient of viscosity\*, determined as the slope of the straight line  $\frac{dy}{dt} = f(\tau)$ .

For several bodies (Figure 2e), the dependence between stress and the rate of strain is non-linear: the slope of the curve  $\frac{dy}{dt} = f(\tau)$  is often interpreted as the variable coefficient of viscosity. Many bodies (Figure 2f) begin to develop a noticeable flow when the shearing stress exceeds a certain limiting value (which we have agreed to designate by  $\tau_{lt}$ ). The process of deformation of such visco-plastic bodies, according to Shwedoff-Bingham, is characterized by a linear dependence between rate of strain and excess of stress,

$$\tau - \tau_{lt} = \eta_{pv} \frac{dy}{dt}, \quad (4)$$

where  $\eta_{pv}$  is the plastic viscosity.

The law for visco-plastic flow has had extremely wide coverage in practice.†

\* Measured in poise:  $1 \text{ poise} = 1 \frac{\text{g(mass)}}{\text{cm/sec.}} = 1 \frac{\text{dyn/sec.}}{\text{cm}^2} = 0.00102 \frac{\text{g(force)/sec.}}{\text{cm}^2}$ .

† The works of many investigators are devoted to the problem of the visco-plastic flow: Shwedoff (1889), Bingham (1922), Reiner (1947, 1949), Rebinder, et al (1947, 1950), Volarovich (1949), Tyabin (1952), and others. A survey of these investigations is given in the article by Volarovich (1954).

For a more general point of view and for more complicated stress conditions, reference is made to G. Genka (1948), A. A. Ilyushin (1940), M. P. Volarovich and A. M. Gutkin (1946). Although the schemes of viscous deformation (Figure 2d, e, f) are for liquid bodies, they also describe the behavior of idealized solid bodies, whose time deformation reflects the dependence between stress and steady rate of creep.

The superficial analogy between the graphs of  $\gamma = f(\tau)$  (Figure 2a, b, c) and  $\frac{d\gamma}{dt} = f(\tau)$  (Figure 2d, e, f) makes it possible to formally

take over the equations of linear and non-linear elasticity and the equations of plasticity for solving the problem of steady creep (flow). It is necessary only to replace a strain in the corresponding formulas by its first derivative (rate of strain) and to substitute the modulus of elasticity in shear by the coefficient of viscosity.\*

The rheological behavior of a body is determined by an equation which relates stresses, strains, and their rate of change:

$$R(\tau, \gamma, \frac{d\tau}{dt}, \frac{d\gamma}{dt}) = 0. \quad (5)$$

The form of the relationship is obtained from the properties and the condition of the body. The diagrams in Figure 2 represent the simplest cases, but the majority of actual bodies deform in a more complex manner: they have elastic and plastic deformations as well as viscous deformations which occur simultaneously. For the idealized description of the behavior of these bodies, schemes are adapted which combine the schemes of Figure 2. In particular, the widely used method of mechanical models, where the visco-elastic body is considered as composed of separate elastic and viscous elements, is very graphic (Reiner, 1947; Rebinder, 1947; Ishlinskiy, 1945; Rzhantsyn, 1949; Mewes, 1953; and others).

The elastic elements are modelled by springs which obey Hooke's law and the viscous elements are modelled by perforated pistons moving in a cylinder filled with a viscous liquid, for which the speed of immersion of the piston obeys Newton's Law (3). Depending upon the combination of the elements, it is possible to obtain a model for any idealized body. The most general is the model of the linearly deformed, elasto-visco-plastic body presented in Figure 3. Combinations of the upper cylinder (3) and the pistons (1) and (2) model the idealized visco-elastic body capable of both elastic reaction and relaxation. The lower cylinder (4) corresponds to the visco-plastic flow (Bingham), arising for a load exceeding the limiting stress  $\tau_{lt}$ .

Let us first examine the visco-elastic deformation. The "elasticity" of the piston (1) is the analogy of the initial modulus of elasticity  $G_0$ ; the elasticity of piston (2) is the analogy of the modulus of elasticity (developing in time)  $G_{es}$ . The viscous properties of elements (3) model the viscosity  $\eta_{es}$  (elastic after-effect). The

\* The coefficient of viscosity for tension or compression for an ideal elasto-plastic body is related to the coefficient of viscosity for shear by a relation which is analogous to the relation between the modulus of elasticity in tension and the shear modulus;  $E = 3 G$ .

general modulus of the deformation of all the systems will be variable in time, changing from the initial value  $G_i$  to the final limiting long-term value  $G_f$ ,

$$G_f = \frac{G_i G_{es}}{G_i + G_{es}} \quad (6)$$

By examining the operation of a model, the equation for the linear deformation of an ideal visco-elastic body can be obtained; this was carried out by Hohenemser and Prager (Hohenemser and Prager, 1932) and examined in detail by A. I. Ishlinskiy (1945), A. R. Rzhanitsyn (1949), and others,

$$nG_i \frac{dy}{dt} + G_f y = \tau + n \frac{d\tau}{dt} \quad (7)$$

where  $n = \frac{\eta_{es}}{G_i + G_f}$  is the relaxation time.

Integrating equation (7) for  $y = \text{const}$ , we obtain Maxwell-Shwedoff's relaxation law, according to which the stress decreases from the maximum initial stress  $\tau_i$  to some final value  $\tau_f$  (Figure 1c).

$$\tau = \tau_f + (\tau_i - \tau_f) e^{-\frac{t}{n}} \quad (8)$$

where  $\tau$  is the stress at any given time.

Integrating equation (7) for  $\tau = \text{const}$ , we obtain the law of elastic after-effect (Figure 1a),

$$y_{dc} = y_f - (y_f - y_i) e^{-\frac{t}{m}} \quad (9)$$

where  $y_{dc}$  is the strain of the after-effect at any given time;  $y_i$  and  $y_f$  are the initial and final strains, and  $m = n \frac{G_i}{G_f}$  is the time (period) of reaction ( $m > n$ ).

From the solution of equation (8) for  $t=n$ , it is apparent that the relaxation time  $n$  corresponds to the time for which the difference between initial and final stresses decreases by a factor  $e$  ( $=2.72$ ), i.e. when  $\tau - \tau_f = 0.368 (\tau_i - \tau_f)$ . This parameter characterizes the rate of relaxation: the larger  $n$ , the faster the stress decreases.

There are simpler laws for particular cases of equation (7). For  $G_i = \infty$  and  $n=0$  (but  $nG_i = \eta$ ), we obtain the equation for a visco-elastic, non-relaxing body,  $\tau = G_f y + \eta \frac{dy}{dt}$ , described by Kelvin's model (the elastic element (2), in parallel with the viscous element (3) of Figure 3). Let us note that the detailed model was used at the same time by K. Terzaghi and N. A. Gersevanov to describe the consolidation of soils. For  $G_f = 0$ , we obtain Maxwell's equation of relaxation

$$\tau + \frac{\eta}{G} \frac{d\tau}{dt} = \eta \frac{dy}{dt} \quad (10)$$

By solving this equation, it follows that, for  $y = \text{const}$ , lowering of the stress occurs not down to the final limit  $\tau_f$  (this correction was introduced by Shwedoff) but down to 0; the model of

\* Non-relaxing, since for  $y = \text{const}$ , we obtain  $\tau = \text{const}$ .



such a body is obtained by the elastic element (1) in series with the viscous element (3).

A. P. Bronskiy (1941), proceeding from the Boltzman-Volterra integral equation, obtained an expression for relaxation which differs from equation (7) by the more complicated aspect of the exponent,

$$\tau = \tau_f + (\tau_i - \tau_f) e^{-\left(\frac{t}{\tau}\right)^n}; \quad (10)$$

an analogous equation for the after-effect was also obtained. The formulas are developed for rubber (Bronskiy, 1941) and wood pulp (Ivanov, 1948), and independently derived by another method for metals.

Let us now examine the process of permanent deformation (creep) which arises when the stress exceeds the limiting value  $\tau_{lt}$ . The above process can be modelled by the supplementary addition of the viscous element (4) with a coefficient of visco-plasticity  $\eta_{pv}$ , as is shown in Figure 3.

This element is included in the operation only in the event that the load exceeds  $\tau_{lt}$ , which is modelled by the retarding device (5) (dry friction).\*

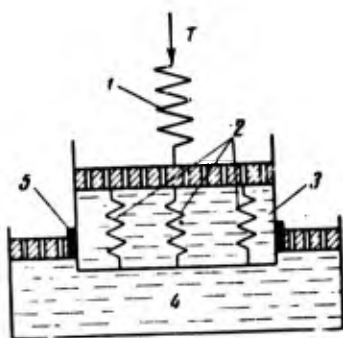


Figure 3. Mechanical model of an elasto-plasto-viscous body.

- (1) Elastic element with a modulus of elasticity  $J_i$
- (2) Elastic element with a modulus of elasticity  $J_{es}$
- (3) Viscous element with a coefficient of viscosity  $\eta_{es}$
- (4) Viscous element with a coefficient of viscosity  $\eta_{pv}$
- (5) Blocking device modeling  $\tau_{lt}$ .

After  $\tau_{lt}$  is exceeded, the upper system begins to sink continuously into the cylinder (4), with a constant rate

$$\frac{dy}{dt} = \frac{\tau - \tau_{lt}}{\eta_{pv}},$$

corresponding to Bingham's model of visco-plastic flow. In addition, the strain of the whole system is composed of the sum of elastic deformation and the flow,  $\gamma_{cr} = \gamma_{dc} + \gamma_{fl}$ .

The value of  $\gamma_{dc}$  is determined from equation (9). The value of  $\gamma_{fl}$  is obtained from the integration of equation (4). Hence,

$$\gamma_{cr} = \gamma_f - (\gamma_f - \gamma_i) e^{-\frac{t}{\tau}} + \frac{\tau - \tau_{lt}}{\eta_{pv}} t. \quad (11)$$

\* Modelled rigorously for a constant of infinitesimally slow loading; for a varying load, the retarding device must model, depending upon the rate of loading, the yield limit or the constant value of the limiting deformation.



An analogous equation was derived by P. A. Rebinder and others (Sapalova, Rebinder, Senteryukhina, 1951); it was derived in another form by V. I. Likhtman (1950).

The mechanism of lowering stability of an ideal elasto-viscoplastic body can be obtained by examining the processes of permanent deformation. Assuming that the rate of strain is the sum of the elastic rate of strain  $\frac{dy_{ers}}{dt} = \frac{1}{G_f} \cdot \frac{d\tau}{dt}$  and the visco-plastic rate of strain  $\frac{dy_{fl}}{dt}$  determined by formula (4), we have

$$\frac{d\tau}{dt} = \frac{1}{G_f} \cdot \frac{d\tau}{dt} + \frac{1}{\eta_{pv}} (\tau - \tau_{lt}).$$

Integrating this expression for  $\tau = \text{const}$ , we obtain the relationship between failure stress  $\tau$  and time  $t$  (where failure occurs),

$$\tau = \tau_{lt} + (\tau_{inst} - \tau_{lt}) e^{-\frac{t}{n}}, \quad (12)$$

where  $\tau_{inst}$  and  $\tau_{lt}$  are, respectively, the instantaneous and limiting long-term strength, and  $n = \frac{\eta_{pv}}{G_f}$  is the time (period) of reduction of strength, or actual relaxation time.

Equation (12) was obtained in 1938-1942 by Yu. M. Ivanov (1948), who proceeded from the assumption that the curve of the long-term strength can be considered as the limiting relaxation curve for rupture stresses. This equation was also used by M. N. Goldshtein (1948) to describe dependence of the adfreeze strength of soils upon time, up to failure; it was generalized by N. A. Tsytoich (1952) for other aspects of the strength of frozen soils under long-term loading.

Substituting  $e^{-\frac{t}{n}} = z$  and writing formula (12) in the form (Berezantsev, 1953),

$$\tau_{lt} = \frac{\tau - z \tau_{inst}}{1 - z}, \quad (13)$$

we can compute the quantity of greatest interest to us, i.e. the limit of long-term strength. Since direct determination of  $z$  is complicated, V. G. Berezantsev proposed determining  $z$  by the value of  $\tau_{inst}$ , known experimentally, and by two values  $\tau_1$  and  $\tau_2$  for given times  $t_1$  and  $t_2$ , which are related to one another by the condition  $2t_1 = t_2$ . For such a relationship of the quantities, the value obtained for  $z$  by S. S. Vialov and V. M. Faintsimmer is equal to  $z = \frac{\tau_1 - \tau_2}{\tau_{inst} - \tau_1}$ .

The equation for the reduction of strength assumes a more complicated form if we proceed from A. P. Bronskiy's equation (10): then,

$$\tau = \tau_{lt} + (\tau_{inst} - \tau_{lt}) e^{-\left(\frac{t}{n}\right)^a}. \quad (14)$$

An equation which is somewhat different from (12) was suggested by V. N. Bykovsky (1951, 1954), who assumed that the stability of a body is determined by the elastic framework. Consequently failure will occur when the stress in element (2) of Figure 3 reaches the limiting value  $\tau_{lt} = \gamma_{dc} \cdot G_f$ . Substituting this value in formula (9), we obtain

$$\tau = \frac{\tau_{lt}}{1 - (1 - \frac{\tau_{lt}}{\tau_{inst.}}) e^{-\frac{t}{m}}}, \quad (15)$$

or

$$\tau = \frac{\tau_{lt}}{1 - (1 - \frac{\tau_{lt}}{\tau_{inst.}}) e^{-(\frac{t}{m})^\beta}}, \quad (16)$$

if we use equation (9) with the more complex exponent (according to Bronskiy). The nature of formula (15) differs from formula (12) in that the latter considers the time of failure to be determined by growth of a permanent plastic deformation, whereas the former considers the beginning of this deformation. In the limit for  $t \rightarrow 0$  and  $t \rightarrow \infty$ , both formulas coincide; it follows from both of them that

$$\frac{\tau_{inst.}}{\tau_{lt}} = \frac{G_i}{G_f}.$$

Using this relation, V. N. Bykovskiy (1954) proposed determining  $\tau_{lt}$  by using the data from experiments of a relatively short duration for behavior with continuous loading up to failure.

The mechanical models examined and the equations related to them (7-16) are only conventional descriptions of the real system and characterize only the qualitative aspect. They give only a poor quantitative agreement with the experimental investigations for the majority of real bodies. Primarily, this is because parameters  $n$  and  $m$  are actually variable (Rebinder, 1950; Dogadkin and Reznikovskiy, 1951; Likhtman, 1950; Tozovskiy, 1951).

As recent investigations have shown (Mikhailov and Rebinder, 1955), all systems based on the type of relationship that exists between the so-called effective (structural) viscosity and the shear stress can be divided into liquid-form and solid-form (Figure 4). For liquid-form bodies, the effective viscosity  $\eta(\tau)$  varies for an increase of the stress, and takes at the limits constant values  $\eta_0$  and  $\eta_m$ . In addition,  $\eta_0$  corresponds in practice to a non-collapsible structure and  $\eta_m$  corresponds to a collapsible structure\*. The relationship between shearing stress and rate of steady flow for such bodies is

\* The coefficient of viscosity remains constant, except for dependence upon  $\tau$ , only for Newtonian liquids.

## 20 RHEOLOGICAL PROPERTIES AND BEARING CAPACITY OF FROZEN SOILS

characterized by an equation derived from the so-called theory for rate of chemical reactions, based on statistical mechanics.\*

$$\frac{dy}{dt} = A \text{Sh} \frac{\tau}{\tau^*}, \quad (17)$$

where  $A = \frac{1}{t_0} e^{-\frac{u}{kT}}$  and  $\tau^* = \frac{kT}{\omega}$  are the constants of the medium, depending upon its absolute temperature  $T$ . The parameters entering into this expression are:

$u$ , the activation energy necessary for formation of "holes" (according to Frenkel) between the particles;

$k$ , a constant;

$t_0$ , the minimum rest time of the particle, and

$\omega$ , the molecular volume.

For  $\tau \ll \tau^*$ , we obtain  $\text{Sh} \frac{\tau}{\tau^*} \approx \frac{\tau}{\tau^*}$ , and formula (17) becomes a formal analogy of Newton's law.

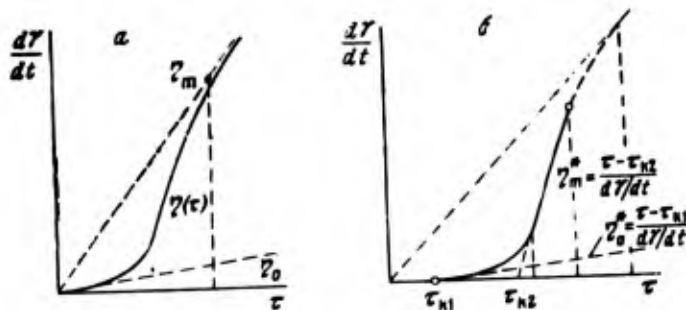


Figure 4. Rheological curves for liquid-form bodies (a) and solid-form bodies (b), according to N. V. Mikhailov and P. A. Rebinder (1955).

Formula (17) shows the dependence of viscosity upon  $\tau$ ; this is explicit in the following equation by N. V. Mikhailov, which can be considered as the equation of the complete rheological curve,

$$\eta = \eta_m + (\eta_0 - \eta_m) \frac{\frac{\tau}{\tau^*}}{\text{Sh} \left( \frac{\tau}{\tau^*} \right)},$$

for  $\tau \rightarrow 0$ ,  $\eta \rightarrow \eta_0 = \frac{\tau^*}{A} = \frac{kT_0}{\omega} \text{Te}^{\frac{u}{kT}} = \text{const}$ , and for  $\tau \rightarrow \infty$ ,  $\eta \rightarrow \eta_m = \text{const}$ .

In practice, the limit of the yield is the stress for which an abrupt change of viscosity, i.e. rate of deformation, occurs; this is determined by the point of inflection in the curve  $1 - \alpha = \gamma(\tau)$ , where

$$\alpha = \frac{\eta - \eta_m}{\eta_0 - \eta_m}$$

\* See Eyring, 1936; Frenkel, 1951; Mikhailov and Rebinder, 1955.

Rigid-form bodies are characterized by an intermittent change in the rate of flow and by a correspondingly abrupt fall in the effective viscosity for a certain value of the stress. This makes it possible to use the (practical) concept of a limit or yield stress for these bodies. For bodies which P. A. Rebinder and N. V. Mikhailov called truly elasto-plastic, the above-mentioned value coincides with the limit of elasticity. Until it is exceeded, the deformations have only a resilient or elastic character (damped creep), and no flow is detected in practice (by using existing methods of measurement). The question of existence, in principle, of such a flow (for time intervals measured in centuries) has not been answered as yet. For certain bodies, which are said to be almost plastic, a flow is observed even for very small stresses, and although it is extremely slow, it can still be measured upon failure of the structure.\* When the stress exceeds the yield limit ( $\tau_f$ ), a sharp intermittent increase in the rate of flow and a large drop in the viscosity occur. For a rigid-form system (either actually or almost plastic), N. V. Mikhailov and P. A. Rebinder recommended using the concept of maximum plastic vis-

cosity  $\eta_{pv} = \eta_0^* \frac{\tau - \tau_{f1}}{\frac{d\gamma}{dt}}$ ; this corresponds to a creep-type flow in a

system which is generally non-collapsible for stresses larger than  $\tau_{f1}$ . They also recommended using the concept of minimum plastic viscosity

$\eta_m^* = \frac{\tau - \tau_{f1}}{\frac{d\gamma}{dt}}$ , which corresponds to the flow for a generally collapsible

structure in the presence of large velocity gradients that occur when the stress exceeds a second dynamic limit  $\tau$  (Figure 4).

Besides the mechanism examined, various technical theories for creep adapted from descriptions of the deformation process with time for metal are widespread.† Almost all these theories are based on the assumption that a non-linear dependence exists between stress and steady rate of creep. The curve which characterizes this dependence proceeds from the origin of the coordinates; this corresponds to the computed scheme (Figure 2). Because of this fact, only the process of permanent deformation is considered. The most widely used empirical relations between stress  $\sigma^{**}$  and steady rate of creep  $\frac{d\epsilon}{dt}$  are either the "common relation"  $\frac{d\epsilon}{dt} = A\sigma^a$ , or the "hyperbolic relation"

$\frac{d\epsilon}{dt} = A \sinh \frac{\sigma}{B}$ , which corresponds to Eyring's equation (17).

The equation of deformation, which describes the entire growth process of the deformation according to one of the existing theories of creep (the so-called theory of yield), can be obtained by summing the elastic and plastic rates of strain (Kachanov, 1949),

\* This deformation is called "creep" by the author.

† A vast literature is devoted to these theories: Oding, 1949; Rabotnov, 1948; Madlinin, 1949; Kachanov, 1949; Goldenblat, 1952; Arutyunyan, 1952; Nadai, 1954, and others.

\*\* We are usually concerned with normal stresses for the theory of creep.

$$\frac{d\epsilon}{dt} = \frac{1}{E_i} \frac{d\sigma}{dt} + A(t)\sigma^\alpha,$$

where  $A(t)$  is a function which corresponds to the rate of creep for a stress equal to unity.

The function decreases with time and approaches an asymptotic limiting value  $A \rightarrow A_\infty = \text{const}$  (for  $t \rightarrow \infty$ ), which corresponds to the minimum constant rate of strain for steady creep. The properties of the medium under study can be represented by Maxwell's model (the series connection of the elastic element (1) and the viscous element (3) of Figure 3), but with a variable value for the coefficient of viscosity  $\eta$ , i.e. the liquid in cylinder (3) is assumed to thicken.

According to another theory (theory of "age-hardening"), the relationship exists between strain, stress and time (this relation being clearly time dependent),\*

$$\epsilon = \epsilon_{\text{lim}} + \epsilon_{\text{cr}} = \frac{\sigma}{E_i} + \int_0^t A(t)\sigma^\alpha dt,$$

rather than between rates of strain and stress.

Several authors (Yoh-Han Pao and Marin, 1953) divide the strain into three parts instead of two: resilient, elastic (unsteady creep), and flow,

$$\epsilon = \epsilon_{\text{lim}} + \epsilon_{\text{el}} + \epsilon_t = \frac{\sigma}{E_i} + \int_0^t A(B\sigma^\alpha - \epsilon_{\text{el}}) dt + \int_0^t D \sigma^\alpha dt.$$

For simplicity, many authors replace the curve which characterizes creep by a broken straight line that consists of a vertical section coinciding with the vertical axis and an inclined section. In some cases (Odquist and Folke, 1953, and others), the first section replaces the instantaneous and (delayed) elastic deformation; in others (Mahinin, 1948; Yoh-Han Pao and Marin, 1953), it replaces only the instantaneous deformation and disregards the elastic part. Finally, many authors consider only the stage of steady creep, i.e. they examine the linear part of the deformation curve and disregard both the instantaneous and the "elastic" deformations.

At present, the so-called theory of "hereditary creep," based on the integral equations by Volterra-Boltzman (Volterra, 1932), is gaining increasing importance. For our purposes, the theory of non-linear hereditary creep suggested by Yu. N. Rabotnov (Rabotnov, 1948; Zhukov, Rabotnov, Churikov, 1953) is of great interest; we shall discuss it more extensively later.

Equation (7) for the linear deformation of idealized bodies, derived from an examination of the simplest models, can give only a general, qualitative representation of the character of rheological processes in frozen soils. The peculiar behavior of bodies with as complex a natural history as frozen unconsolidated deposits does not permit using elementary mechanical schemes with the laws corresponding

\* For a constant stress, the formulas for flow theory and "age-hardening" theory give identical results.

to these schemes. Therefore, the most important tasks in the present investigations consist of studying the rheological processes which occur in frozen soil, of determining the possibilities and limits of validity in the classical equations of rheology, and developing the characteristic mechanisms which describe the actual processes that occur in frozen soils. These investigations are necessary since the equations for deformation of idealized bodies yield no solutions which agree qualitatively with the experimental data, and since they also do not reflect the actual processes. The problems mentioned above will be examined later in this investigation.

3. Purpose of the experiments and conditions under which they were conducted

The experiments were intended to

(1) study the physical phenomena which occur in frozen soils under the action of an external load;

(2) formulate the laws of rheological processes which occur in frozen soils;

(3) determine the stability characteristics for frozen soils and explain the dependence of these characteristics upon the properties and conditions of the soils, and

(4) evaluate the bearing capacity of frozen soils under footings and piled foundations.

To attain these objectives, the investigations included:

(1) laboratory tests on samples of undisturbed frozen soils for basic, simple forms of stress conditions (resistance to shear, tension compression, determination of cohesion, adfreeze strength, etc.);

(2) experiments on frozen soils to determine the strength under punching by stamps in field and laboratory conditions, and

(3) field and laboratory tests of piles driven into frozen soils for load capacity.

From the experimental data, a relationship among stress, strain, and rate of visco-plastic flow was obtained, as well as the mechanism for reduction of strength and values of the limiting long-term resistance of frozen soils under stresses. Each experiment consisted of several tests, both of short-term duration (up to 2 hr) and long-term duration (up to several months, or even years).

A description of the purpose and methods used for the experiments on the punching by stamps and the testing of piles are given, together with the results obtained, in the second and third parts of the present study. In the present section, the conditions of the laboratory experiments related to the problems examined in the first part will be described. These experiments consisted of:

(1) investigation of the cohesive forces by penetration by spherical indenters. The experiments were both short-term (from



## 24 RHEOLOGICAL PROPERTIES AND BEARING CAPACITY OF FROZEN SOILS

30 min to 8 hr) and long-term, i.e. until complete cessation of the strain occurred (half a month to 1-3 months, or more);

(2) investigation of the adfreeze strength of the soil, using the lateral surface of wooden rods (similar to piles). The experiments consisted of the punching through and retraction of the rods;

(3) investigation of the resistance of frozen soils to tension;

(4) investigation of the resistance of frozen soils to shear. These experiments were conducted on the shearing apparatus of the Hidroenergoprojekt (Hydraulic Energy Project), and

(5) investigation of the compressibility of frozen soils under loads where no lateral expansion was possible. The experiments were conducted by using standard "compression" apparatus, but with strengthening of the machine, since the loads reach 20 kg/cm<sup>2</sup>.

The investigations were conducted\* at the Igarskiy Permafrost Station underground laboratory, which was built in a stratum of frozen soil at depths that ranged from 6-14 m. The great advantage of conducting the experiments under such conditions was the capability for maintaining a constant negative temperature (different for each room) in the laboratory rooms. This made it possible to conduct long-term experiments. In one of the rooms, a temperature of -4°C, with an annual fluctuation of  $\pm 0.4^\circ\text{C}$ , was maintained. In the second room, the temperature was -1.2°C, with a fluctuation of  $\pm 0.2^\circ\text{C}$ . In the third (at a depth of 14 m), the natural temperature of the permafrost stratum, i.e. -0.4°C with a fluctuation of  $\pm 0.1^\circ\text{C}$ , was preserved. In addition, supplementary measures were taken to insulate the samples.

The investigations with apparatus of small size and using small samples were conducted in special glass-covered niches built in the walls of the underground rooms. Several of these experiments (penetration and extraction of model piles, and also punching by stamps) were conducted with large blocks of frozen soil (30 cm x 30 cm x 30 cm, and 30 cm x 30 cm x 15 cm) that were embedded in the floor of the vault. This was achieved by making small holes, placing the blocks in them and filling up the gaps with semi-liquid soil to assure subsequent freezing of the blocks. The free surface of the soil was covered with sawdust to protect it from the air. The procedure mentioned above, which does not affect the properties of the tested soil, had several essential advantages:

(1) the testing conditions of the soil approximated actual conditions (the possibility of limited lateral expansion);

(2) the possible short term fluctuations of the air temperature in the chamber, due to the presence of people, were not reflected on the temperature of the embedded soil, i.e. maintenance of a completely constant temperature was assured;

\* S. I. Pimenova, Technical Associate at INIMS, M. V. Krasnianskaya, Sh. Z. Fatkulín, N. E. Fedotov, Research Assistants of SPIE and INIMS, and others, took part in these experiments.

(3) protection of the soil from the air was assured, and

(4) it was possible to use a simple lever apparatus instead of factory punching machines, which we possessed in a very limited quantity; this made it possible to run a large number (up to 30) of long-term experiments simultaneously.

Several of these devices aided the investigations and were standard; some were designed by the author and built in local workshops. The method of investigation will be described in more detail in the proper paragraph of this work. Let us introduce here only the main basic features.

The investigations on the long-term strength of frozen soils for those types of stress-condition where failure can be recorded, i.e. pulling out of bars, tension, etc., was accomplished by testing several samples (not less than 7-8 stamps) under constant loads. These loads differed for each sample, starting from loads which caused instantaneous rupture and ending with long-term loads which did not cause rupture. The first sample was loaded with a rapidly increasing stress, as a result of which instantaneous resistance was determined. A smaller load, whose value was 25-50% of the instantaneous ultimate load, was applied to the next sample. This load also caused rupture, not instantaneously however, but after some time. For each subsequent sample, increasingly smaller, constant loads were applied, and consequently the time to rupture increased. Finally, for a certain load, failure did not occur, no matter how long the load acted.

As testing of these samples under constant loads was being conducted, experiments on one of the samples were also performed for a gradually increasing load. This method was vital to the experiments when the time of collapse was difficult to record, or when a sufficiently large number of uniform samples was difficult to obtain. For these experiments, the load was applied in equal stages. Between two consecutive stages, the strain was allowed to become constant; this process was repeated until yield occurred. Even after a permanent strain appeared, thus indicating that the limiting long-term load had been exceeded, the load was increased further until it caused complete failure of the sample. Each step was maintained until a constant rate of strain had been established. In view of the long duration of such tests, some experiments of a cumulative nature were conducted for reduced intervals of time, equal for all the steps of loading.

The strain was recorded in all experiments. These measurements were taken with a dial type strain gauge with divisions spaced at 0.01 mm, (and for the "verification" experiments at 0.002 mm). In addition, servo-mechanisms were used in several tests (particularly for those tests where the time of failure had to be recorded). The strain was considered to have reached a stable value when, within the limits of possible reading precision, i.e. 0.002-0.005 mm, no variation occurred during the course of 10-15 days. To verify the constant strain and the absence of failure, certain samples were loaded with no change in the indicator reading for several months, and even for more than a year (in one case for more than 6 years).



Since the investigations were relatively new, considerable attention was devoted to developing operational methods.

The investigations were conducted with undisturbed soils extracted from holes in 30 cm x 30 cm x 30 cm blocks. To include the largest possible number of different types of soil, the blocks were taken from various excavations at different depths and stratigraphic levels. Altogether, 37 different types of soil were tested; they can be grouped into 6 categories: heavy clay (varved); heavy silty loam; light silty loam; heavy sandy loam; light sandy loam (60 - 80% sand); and sand. Separate investigations were conducted with ice taken from ice lenses in a natural stratum of frozen soil. The physico-mechanical characteristics of the soils are given in Table 1; data concerning phase composition of the water in several of these soils are given in Table 2. To avoid repetition, the data on these soils, as well as the results of laboratory experiments examined in the second part of the present investigation (resistance to punching by stamps), are also given in Table 1.\*

For convenient use of the tables, the number of experiments carried out with a given type of soil is shown in the last column. A different numbering system was used for each set of experiments (cohesion, shear, etc.).

Gradation of the soils was determined by the Sabanin-Robinson method. To avoid overcrowding the tables, the data on mechanical composition are given in abridged form (according to a trinomial classification) with the numbers rounded off. The phase composition of the water in the soils was determined by the calorimetric method used at the Permafrost Institute.

The characteristic property of the soils tested was their large silt content (this applies to most permafrozen unconsolidated deposits). As a rule the content of particles of 0.05 to 0.005 mm consists of approximately 40% clay, and 50 to 65% sandy loam and loam. Some exceptions are obvious from Table 1. Increase in the plasticity index for these soils, particularly for sandy loams, is obviously explained by the influence of the silt content. For clayey soils, this silt percentage varies from 12 to 16; for sandy loam, from 8 to 13. Thus, soils should be classified according to the plasticity index as recommended in the "Standards and Technical Conditions" (N and TU 127-55), rather than to the clay content (according to Okholi, as was done at the SPIE Laboratory). If this were done, then almost all the soils presently referred to as loam should actually be referred to as clayey soils, since their plasticity index is greater than 7. In only 3 out of a total of 15 blocks of heavy sandy loam was this index less than 7.

Experiments for developing initial basic principles were conducted on frozen soils that had no significant ice segregation to eliminate the complicating effect of heterogeneous soils, whose properties depend on their type of structure. The natural moisture content of these blocks, given in Table 1, usually equalled 25 to 35%, but was occasionally 35

---

\* Data concerning the soils in the experiments conducted under field conditions are given in the appropriate chapters.

to 45%.\* The liquidity index,  $I_L = \frac{w - w_p}{I_p}$ , is less than unity in most cases (17 out of 26). In this equation,  $w$  is the natural moisture content;  $w_p$  is the plastic limit, and  $I_p$  is the plasticity index.

The influence of ice inclusions was investigated with special attention. These investigations were carried out both in the laboratory using blocks of soil with various ice lenses and under field conditions. The results are examined in the second and third parts of this work. Among the soils examined, the Igarskiy varved clay played a special role. This clay consisted of alternating layers of different grain sizes, from heavy clay to silt. In the upper levels, the clay varves had a large content of ice inclusions. The number of these inclusions decreased with increasing depth while the width of the lens grew and reached 10 cm or more. The data on the physico-mechanical properties of clay varves, with respect to the mineral layers, are given in Table 1, i.e. the ice inclusions are disregarded. These layers differ only by their large density. Thus, their liquidity index varies between 0.4 and 0.1; this characterizes the condition of the soil after thawing from firm plasticity to almost rigidity.

Another characteristic, which indicates the high degree of consolidation and hardening of the mineral layers of varved clay, is that these soils neither swell nor crumble, either on thawing or on soaking. Therefore, as will be shown later, varved clay soils of glacier-lake origin (the Igarskiy type) possess very high stability, despite their large content of unfrozen water. This is an exception as compared to the usual fine grained frozen soils, whose stability is generally smaller than that of coarse-grained frozen soils.

---

\*From this point, the moisture content will be given as a percentage of the dry soil weight.

Table 1. Physico-Mechanical

Type and origin of soils	Depth at which sample was taken  m	Mechanical composition, %			Atterberg Limits			Natural moisture content %	Liquidity index	Maximum molecular water capacity, %
		Size, mm								
		Sand 0.05	Silt 0.05 -0.005	Clay 0.005	Liq-uid limit	Plas-tic limit	Plas-ticity index			
Silty varved clay (glacial lake sediment)	8.0	0.3	56.7	43	53	30	23	38	0.38	27
The same	14.0	1	37	62	65	31	34	35	0.11	27
The same, remolded.	14.0	1	37	62	65	31	34	42	0.3	27
Varved clay (glacial lake sediment)	3.25-3.55	2	47	51	61	29	32.5	37	0.26	--
The same	6.45-6.75	0.1	39	61	68.5	29.5	29	40	0.35	--
Heavy silty loam (alluvial sediment)	1.8-2.0	8	63	29	38	22	16	36	0.83	20

## Characteristics of frozen soils

Grain density g/cm <sup>3</sup>	Unit Wt. g/cm <sup>3</sup>	Dry unit Wt. g/cm <sup>3</sup>	Porosity %	Void ratio	Loss on ignition	Number of experiments carried out with a given soil while testing for:					
						Cohesion	Adfreezing	Tension	Shear	Compression	Penetration by a punch
2.79	1.80	1.30	53	1.14	5.0	---	--	--	--	---	12
2.8	1.77	1.28	54	1.15	6.0	11,14 17,18 19,20 21,22 23,24 26,27 28,33 52,59 72,96 116,118 139,148	2,3, 4,5, 6,7, 9,10, 14,16, 18,19 20,32 35,38 39,41	--	--	---	4,5,8,10, 11,13,15, 19
2.8	1.72	1.25	56	1.27	--	108,110	--	--	--	---	---
2.8	1.80	1.31	53	1.14	--	---	--	--	--	---	9,20,20a
2.80	1.80	1.29	54	1.17	--	---	--	--	--	---	22
2.81	1.91	1.47	47	0.89	4.0	43,44 45,46 47,50 54,57 88,141 142,143 144,145	8,12 17	212	--	---	---

Table 1. Physico-Mechanical

Type and Origin of soils	Depth at which sample was taken  m	Mechanical Composition, %			Atterberg Limits			Natural moisture content %	Liquidity index	Maximum molecular water capacity, %
		Size, mm								
		Sand ≥0.05	Silt 0.05 -0.005	Clay ≤0.005	Liq- uid limit	Plas- tic limit	Plas- ticity index			
Medium silty loam (alluvial sediment)	2.3-2.6	25	59	16	36	21	15	44	1.5	--
Light silty loam (alluvial)	4.2-4.5	26.5	61	12.5	37	23.5	13.5	38	1.3	--
The same	6.4-6.7	34.5	54.5	11	33.5	21.5	12	30	0.7	17
The same.	7.9-8.2	41	47	12	32	20	12	28	0.7	--
Heavy silty sandy loam (recent surface deposit)	1.05-1.40	25.5	65.5	9	58.5	45	13.5	47	0.15	--
Heavy silty sandy loam (recent surface deposit)	3.0	33	61	6	36	25	11	30	0.42	13
Heavy sandy loam (recent surface deposit)	1.2-1.5	55	39	6	22	18	4	20	0.5	--

## Characteristics of frozen soils (Cont'd)

Grain density g/cm <sup>3</sup>	Unit Wt. g/cm <sup>3</sup>	Dry unit Wt. g/cm <sup>3</sup>	Porosity %	Void ratio	Loss on ignition	Number of experiments carried out with a given soil while testing for:					
						Cohesion	Adfreezing	Tension	Shear	Compression	Penetration by a punch
2.68	1.73	1.20	55	1.23	5.8	---	45	--	--	---	---
2.77	1.85	1.34	52	1.08	4.8	---	26,27	--	--	---	---
2.78	1.7	1.2	55.5	1.26	4.9	146,189	--	215	--	---	---
2.78	1.90	1.42	49	0.96	3.1	258,259 260,261	28,29	--	--	---	---
2.49	1.64	1.12	55	1.22	15.6	---	13,21	--	--	---	---
2.69	1.77	1.30	53	1.15	3.6	137	--	211	--	---	---
2.76	2.03	1.69	39	0.63	4.4	---	15	--	--	---	---

Table 1. Physico-Mechanical

Type and origin of soils	Depth at which sample was taken  m	Mechanical Composition, %			Atterberg Limits			Natural moisture content %	Liquidity index	Maximum molecular water capacity, %
		Size, mm								
		Sand 0.05	Silt 0.05 -0.005	Clay 0.005	Liq- uid limit	Plas- tic limit	Plas- ticity index			
Heavy silty sandy loam (surface deposit)	2.0-2.3	26	65	9	38.5	24	14.5	43	1.35	18
The same	3.0-3.3	30	60.5	9.5	31.5	20.5	11	33	1.2	--
Heavy silty loam (alluvial sediment)	4.9-5.2	30	59	11	32.5	20.5	12	28	0.6	--
The same	7.6-7.9	42	50	8	27	17.5	9.5	28	1.1	16
The same	4.5	30.5 plus gravel 1.0	61	7.5	33	21	12	34	1.05	16
The same	4.25-4.55	26	64	10	31	22.5	8.5	29	0.8	--
Heavy sandy loam (alluvial sediment)	4.85-5.15	48	46	6	22.5	21	1.5	--	1.25	--
The same, silty	5.45-5.75	23	69	8	33	25.5	7.5	28	0.4	--
Light sandy loam (alluvial sediment)	3.05-3.55	65	29.5	5.5	27	26	1	25	0	--

## Characteristics of frozen soils (Cont'd)

Grain density g/cm <sup>3</sup>	Unit Wt. g/cm <sup>3</sup>	Dry unit Wt. g/cm <sup>3</sup>	Porosity %	Void ratio	Loss on ignition	Number of experiments carried out with a given soil while testing for:					
						Cohesion	Adfreezing	Tension	Shear	Compression	Penetration by a punch
2.74	1.76	1.33	50.5	1.02	5.0	55, 86, 140, 229, 247	--	213, 214	--	--	7
2.76	1.91	1.43	48	0.92	3.5	---	33, 34	--	--	--	--
2.77	1.97	1.54	44	0.80	3.6	---	---	---	--	6, 8, 10	--
2.76	1.82	1.37	48	0.93	7.7	147	--	217	--	--	--
2.76	1.94	1.5	46	0.83	2.8	31, 32, 36, 37, 40, 49, 51, 58, 117, 120, 134, 136	--	---	--	--	--
2.76	1.94	1.5	46	0.84	5.3	---	36	--	--	--	--
2.71	1.91	1.47	46	0.84	5.5	---	24, 25	--	--	--	--
2.76	2.03	1.58	43	0.75	--	238	--	--	--	--	--
2.69	1.88	1.5	44	0.79	4.5	---	40	--	--	--	--



Table 1. Physico-Mechanical

Type and origin of soils	Depth at which sample was taken  m	Mechanical Composition, %			Atterberg Limits			Natural moisture content %	Liquidity index	Maximum molecular water capacity, %
		Size, mm								
		Sand 0.05	Silt 0.05 -0.005	Clay 0.005	Liq- uid limit	Plas- tic limit	Plas- ticity index			
The same	3.35- 3.65	64	32	4	31	26	5	26	0	--
Light sandy loam (alluvial sediment)	3.65- 3.95	61	35	4	30	28	2	26	0	--
The same	3.95- 4.25	49	47	4	26	23	3	25	0.5	--
Silty sand (alluvial sediment)	4.0- 4.3	42 plus gravel 12	43.5	2.5	--	--	--	30	--	16
Silty sand (alluvial sediment)	3.0	51	46	2.6	--	--	--	26	--	21
Very fine sand	1.6- 1.9	55	42	2.8	--	--	--	37	--	--
The same	2.35- 2.65	59	39	2	--	--	--	33	--	--
Fine sand (marine sediment Kazantsevskii horizon).	12.8	98	2	--	--	--	--	23	--	--

## Characteristics of frozen soils (Cont'd)

Grain density g/cm <sup>3</sup>	Unit Wt. g/cm <sup>3</sup>	Dry unit Wt. g/cm <sup>3</sup>	Porosity %	Void ratio	Loss on ignition	Number of experiments carried out with a given soil while testing for:					
						Cohesion	Adfreezing	Tension	Shear	Compression	Penetration by a punch
2.76	1.99	1.58	43	0.75	--	--	--	--	--	--	17,21c,21d
2.76	1.96	1.55	44	0.78	4.3	--	--	--	--	--	14,21a,21b
2.77	2.02	1.62	42	0.71	--	--	--	--	--	--	16
2.65	1.86	1.50	55	0.81	--	131	--	210	--	--	--
2.63	1.85	1.47	44	0.79	10	--	--	--	--	--	1,2,3,6
2.66	1.73	1.26	53	1.11	7.1	233,234,235	--	--	--	--	--
2.71	1.83	1.37	50	0.98	4.9	--	22,23	--	--	--	--
2.73	--	1.28	--	--	--	60,61,62 63,64,65 66,67,84 90,149, 150,151, 152,153	--	--	--	--	--

### Table 1. Physico-Mechanical

[illegible]

## Characteristics of frozen soils (Cont'd)

Grain density g/cm <sup>3</sup>	Unit Wt. g/cm <sup>3</sup>	Dry unit Wt. g/cm <sup>3</sup>	Porosity %	Void ratio	Loss on ignition	Number of experiments carried out with a given soil while testing for:					
						Cohesion	Adfreezing	Tension	Shear	Compression	Penetration by a punch
2.78	--	--	--	--	--	91, 92, 93, 94, 95, 164, 165, 166, 167, 221, 222, 223, 225, 226	--	--	--	--	--
--	--	--	--	--	--	29, 30, 34, 58, 68, 69, 70, 73, 75, 76, 77, 78, 79, 80, 83, 154, 155, 156, 157, 158, 159, 160, 161, 162, 163, 168, 227, 231	--	--	--	--	--

Table 2. Phase composition of water in frozen soils  
(Calculations by S. I. Pimenova)

Type of soil	Depth at which the sample was taken m	Temperature °C	Natural moisture content, % of		Amount of unfrozen water %		Relative ice content
			Dry unit weight	Total unit weight	In relation to the damp soil	In relation to all moisture	
Varved clay	14.0	-4.0	36	27	16	45	0.55
		-1.4	35	26	21	59	0.41
		-0.3	37	27	30	83	0.18
Heavy silty loam	2.0	-1.5	33	25	12	37	0.63
		-0.4	31	25	15	47	0.53
Light silty loam	6.4	-4.3	30	23	10	33	0.67
Heavy silty sandy loam	2.0	-4.2	43	30	12	27	0.73
		-0.4	45	31	18	40	0.61
The same	4.5	-4.3	33	25	11	34	0.66
		-1.4	35	26	14	38	0.62
		-0.5	29	23	--	46	0.54
Light sandy loam	4.0	-4.2	30	23	12	39	0.60
Fine sand	12.8	-3.4	24	--	2	8	0.92
		-0.4	22	--	3	16	0.85

## CHAPTER II. INVESTIGATION OF THE COHESION OF FROZEN SOILS

## 1. Purpose of the investigation

The stability of frozen soils under load is determined by the strength of the inner bonds between the separate particles which compose an aggregate of frozen soil, and between the aggregates themselves. The sum of the above-mentioned bonds in the system, e.g. mineral particles, ice, unfrozen water, air,....., is usually called "cohesion (c)" in soil mechanics. Cohesion is the basis of the characteristic stability of frozen soils in correlation with the bonds from which all characteristic properties of strength under loads can be found. Cohesion in frozen soils is not constant, but varies with the moisture phase and time, weakening for the protracted action of a load (relaxation). This weakening, which is a consequence of the growth of plastic strains, depends upon ice melting in liquid interlayers in contact with the mineral particles, and dislocations in the mineral aggregates, as well as upon yield and change of ice structure contained in the soil. Weakening of the cohesion is restricted (in practice) by its reaching a certain limiting value  $c_{lt}$ . The present chapter is devoted to a study of cohesion, taking the relaxation phenomena into account.

Determination of cohesion was obtained by indentation with rigid spheres, as suggested by N. A. Tsytoovich (1954, 1956).\*

The principle of this method, analogous to the Brinell hardness test, is that cohesion is determined by the size of the imprint obtained as a result of a rigid ball penetrating under a constant load  $P$ . From the solution in the mathematical theory of plasticity (Ishlinskiy, 1944), it follows that a relationship exists between cohesion of an ideally plastic body (obeying the condition of Saint-

Venant  $\tau = \frac{\sigma}{2} = c = \text{const}$ ), and the hardness number  $H = \frac{P}{F}$  (where  $F$  is the area of imprint) determined by  $c = 0.18H$ . Hence, cohesion can be computed regardless of the depth of imprint of the sphere, i.e. by using the value of the plastic deformation  $s$ ,

$$c_t = 0.18 \frac{P}{\pi d s_t}, \quad (18)$$

where  $d$  is the diameter of the sphere, and  $\pi d s = F$ .

Since the penetration  $s$  of the sphere and the area of imprint increase with time,  $s = s(t)$ ; and the stress under the sphere will be correspondingly decreased. As a consequence, the value of  $c_t$ , determined from formula (18), also decreases. The initial penetration  $s_i$  determines the instantaneous cohesion  $c_{inst}$ ; the final stable penetration  $s_f$  determines the limiting long term cohesion  $c_{lt}$ .

\* See also S. S. Vialov and N. A. Tsytoovich (1955); S. S. Vialov (1954).

#### 40 RHEOLOGICAL PROPERTIES AND BEARING CAPACITY OF FROZEN SOILS

Formula (18) determines, in simple form, the cohesion of soils with a so-called internal friction close to zero. For soils which possess both cohesion and friction, we must introduce, as V. G. Berezantsev (1955) has shown, the correction  $N$  for the computed influence of the friction,

$$c_t = \frac{P}{N(ds_t - s_t^2)} \approx M \cdot 0.18 \frac{P}{ds_t} = Mc_e, \quad (19)$$

where  $M$  is a coefficient, whose value is given in Table 3.

Table 3. Value of the coefficient  $M$  as a function of the angle of internal friction  $\phi$

$\phi^\circ$	0	10	20	30
$M$	1.0	0.615	0.285	0.122

Hence, as suggested by S. S. Vialov and N. A. Tsytovich (1956), the strength determined by formula (18) can be considered as a complex characteristic-equivalent cohesion  $c_e$ . Later (Chapter VIII), it will be shown that through use of  $c_e$ , the limiting load for structural foundations on frozen soils can be determined directly.

#### 2. Experimental method

The ball instrument for determining cohesion of frozen soils and the method of operation are described in the handbook published by the laboratory of the Permafrost Institute (Tsytovich, 1954); these same questions, appropriate to our present investigation, are examined in S. S. Vialov's article (1954) and I will therefore not stop to discuss them. I will only point out that, in the experiments described below, a ball of 16 to 18 mm diam was used; the load, depending on the type of soil and on its temperature, was in the range from 1.2 to 5.5 kg, and in isolated cases up to 8 kg.\* Measurements on penetration of the ball, by using a dial type indicator graduated to 0.01 mm mounted on the device, were made after 5 sec, 15 sec, and 30 sec; 1 min, 2 min, 5 min, 10 min, 15 min, 30 min, and 60 min from the beginning of the experiment; afterwards, every hr (for a period of 8 hr); after 16 hr (the following days), and finally once a day until the end of the experiment. The time of initial reading was investigated (Vialov, 1954) with special interest. Consequently, the strain which was measured 5 sec after application of the stress was chosen as the initial value. For this time interval, which is practical for such measurements, no noticeable creep is able to grow, although the emerging strain includes a residual part as well as an elastic part. Further action of the stress leads to a noticeable growth in the strain,

\* The penetration of the ball had to be not more than 0.1 diam.

e.g. for silty, sandy loam at  $-0.3^{\circ}\text{C}$  to  $-4.2^{\circ}\text{C}$ , the penetration of the ball after 15 sec and 30 sec equals, respectively, 120 to 130% and 135 to 150% of the penetration observed after 5 sec.

Each experiment included short-duration tests lasting from 2 to 24 hr (conducted with 3, 4 and up to 10 repetitions), and long-term tests lasting until complete stabilization of the strain (without repetition). The processed results of experiment no. 53\* are given in Figure 5 and Tables a, b, c, and d.

The question of whether the curve representing the time variations of  $c_t$ , computed by means of formula (18), reflects the actual relaxation phenomena of the cohesion requires special examination, since this curve is obtained, not from direct experiments on relaxation, but by indirect means, i.e. through the data of the change of the area of imprint; this might include distortions of the ball. However, it is certain that the slow penetration of the ball in the soil (as distinguished from the rapid intrusion in plastic bodies, as for instance, steel) is caused by the growth of a visco-plastic deformation. Furthermore, since it is well known that the growth of such deformations depends upon the relaxation of the stresses, then the change of the reactive pressure under the ball, and consequently the values of  $c_t$ , are connected with the relaxation phenomena. For instance, if at any given time, we wish to discontinue further penetration of the ball, it will be necessary to gradually decrease the load on it, i.e. to decrease the specific stress (which also precisely characterizes the relaxation phenomena). The long-term strength (cohesion), which is determined through the value of the stabilized penetration (for more details see section 2, Chapter VIII), will be responsible for this steady condition.

This property will be fundamental in our investigations. To evaluate the degree of reproducibility of the repeated calculations, examine Figures 6 and 7, on which data for tests on samples of sandy loam and varved clay are given. Loam, sandy loam and sand of a homogeneous massive structure are in close agreement. Heterogeneous soils having ice inclusions give a large scatter of experimental points. The scatter increases with the growth of the ice-content and the lowering of the soil temperature. This can be explained by the difference in stability of ice and mineral aggregates (soil). The largest scatter of points is recorded for the 'instantaneous' strain, when, for a small area of contact of the ball, the influence of the dimensions of the soil particles is relevant. With the passage of time, the matrix of ice relaxes, and the pressure around the ball is distributed more evenly. As a result, the readings made some time after the beginning of the test, e.g. after 2 hr, are in completely satisfactory agreement.

The results of the statistical processing of the experimental data, presented in Table 4, are given in Figures 6 and 7 where the following nomenclature is used:

\* The data for all experiments constituting the body of the investigation are kept in the archives of the Permafrost Institute of AS, USSR (S. S. Vialov: "Bearing Capacity of Permafrost Soils" 1951, 1952-53 and appendices).



$$\sigma_i = \pm \sqrt{\frac{\sum_{i=1}^n \delta_i^2}{n-1}}$$

is the standard deviation of  $n$  individual experiments,

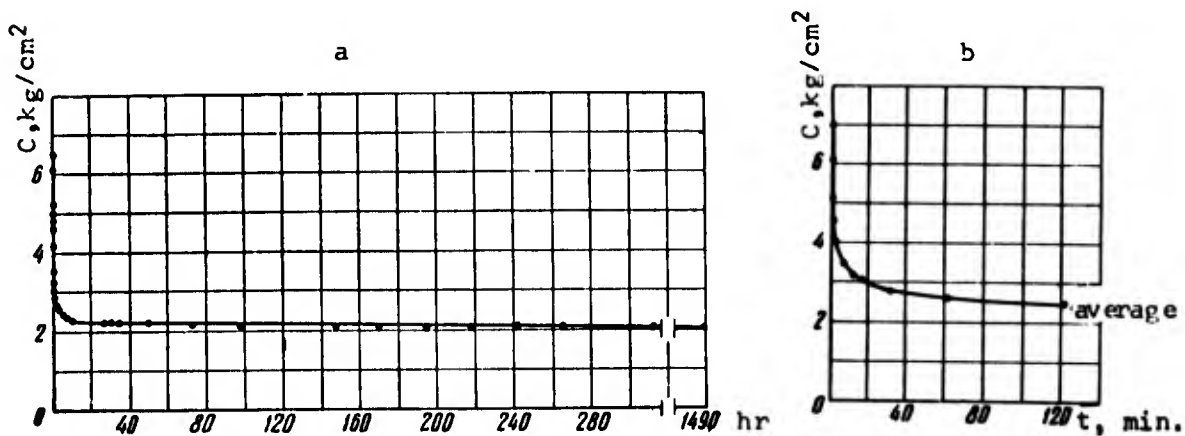
$$\sigma = \pm \frac{\sigma_i}{\sqrt{n}}$$

is the standard error of the mean, and

$$\rho = \frac{\sigma}{c_{av}} \cdot 100\% \quad \text{is the index of accuracy.}$$

The number of repeated tests on one sample is denoted by  $n$ ;  $c_{av}$  is the value of the arithmetic mean, and  $\delta_i = c_i - c_{av}$  is the departure from the value of the arithmetic mean.

Figure 5. Results of experiment 53 for the evaluation of the limit of long-term cohesion of permafrost soils. Heavy silty loam at a temperature of  $-1.2^\circ\text{C}$ .



- Variation of the cohesion with time of action of the load.
- Variation of the cohesion with time during early stages.

Table a. Data of the long-term experiments

t	s	c	t	s	c	t	s	c	t	s	c
5 sec	0.264	7.46	32hr	0.888	2.22	528hr	0.980	2.01	1056hr	1.011	1.95
15 "	0.323	6.11	48 "	0.889	2.22	552 "	0.980	2.01	1080 "	1.014	1.94
30 "	0.377	5.23	56 "	0.900	2.19	576 "	0.980	2.01	1105 "	1.014	1.94
1 min	0.428	4.61	72 "	0.924	2.13	600 "	0.991	1.99	1128 "	1.014	1.94
2 "	0.482	4.09	96 "	0.953	2.07	648 "	0.992	1.99	1152 "	1.014	1.94
5 "	0.557	3.54	144 "	0.955	2.07	672 "	0.992	1.99	1176 "	1.014	1.94
10 "	0.603	3.27	168 "	0.958	2.06	696 "	0.995	1.98	1200 "	1.016	1.94
15 "	0.648	3.04	192 "	0.960	2.05	720 "	0.998	1.97	1224 "	1.016	1.94
30 "	0.699	2.83	216 "	0.960	2.05	744 "	1.000	1.97	1248 "	1.019	1.93
60 "	0.740	2.67	240 "	0.962	2.05	768 "	1.001	1.97	1272 "	1.019	1.93
120 "	0.794	2.49	264 "	0.968	2.04	816 "	1.001	1.97	1296 "	1.023	1.92
3 hr	0.808	2.44	312 "	0.968	2.04	840 "	1.001	1.97	1320 "	1.023	1.92
4 "	0.820	2.40	336 "	0.969	2.04	864 "	1.001	1.97	1344 "	1.023	1.92
5 "	0.839	2.35	360 "	0.970	2.03	888 "	1.001	1.97	1368 "	1.024	1.92
6 "	0.845	2.34	384 "	0.972	2.03	912 "	1.001	1.97	1392 "	1.024	1.92
7 "	0.853	2.31	408 "	0.972	2.03	936 "	1.006	1.96	1416 "	1.024	1.92
8 "	0.860	2.29	432 "	0.972	2.03	984 "	1.009	1.95	1440 "	1.024	1.92
24 "	0.883	2.23	480 "	0.977	2.02	1008 "	1.010	1.95	1464 "	1.024	1.92
28 "	0.885	2.23	504 "	0.979	2.01	1032 "	1.011	1.95			

Nomenclature: s--penetration (mm)      c--cohesion (kg/cm<sup>2</sup>)  
t--time (hr)

Table b. Data of five short-duration experiments

	Max.		Min.		Average from five experiments	
t	s	c	s	c	s	c
5 sec	0.264	7.46	0.298	6.62	0.276	7.14
15 "	0.320	6.16	0.359	5.48	0.319	6.18
30 "	0.371	5.32	0.402	4.91	0.382	5.16
1 min	0.420	4.69	0.445	4.43	0.428	4.60
2 "	0.460	4.29	0.488	4.03	0.476	4.14
5 "	0.532	3.71	0.557	3.54	0.544	3.62
10 "	0.572	3.45	0.603	3.27	0.590	3.35
15 "	0.618	3.19	0.648	3.04	0.631	3.12
30 "	0.669	2.95	0.709	2.78	0.687	2.87
60 "	0.727	2.71	0.752	2.62	0.740	2.66
120 "	0.790	2.50	0.812	2.43	0.798	2.47

#### 44 RHEOLOGICAL PROPERTIES AND BEARING CAPACITY OF FROZEN SOILS

Table c. Physico-mechanical characteristics of the soil  
(soil from hole 31 K with a depth of 4.5 m)

Nomenclature	Units of measurement	Values
Grain density	g/cm <sup>3</sup>	2.76
Unit weight of the soil in natural condition	g/cm <sup>3</sup>	1.77
Natural moisture content	%	35.0
Dry unit weight	g/cm <sup>3</sup>	1.30
Porosity	%	52.9
Void ratio		1.15
Maximum molecular moisture capacity	%	16.2
Content of unfrozen water with respect to the dry weight for $\theta = -1.4^{\circ}\text{C}$	%	13.5
Content of unfrozen water with respect to all the moisture for $\theta = -1.4^{\circ}\text{C}$	%	38.2
Actual ice saturation for $\theta = -1.4^{\circ}\text{C}$		0.62
Temperature of the soil under natural conditions	$^{\circ}\text{C}$	-0.3 <sup>o</sup>
Loss on ignition	%	3.64

Table d. Gradation and plasticity

Gradation								Atterberg Limits			
Gravel				Sand		Silt		Clay	Liquid limit	Plastic limit in hole	Plasticity index
>10mm	10-5 mm	5-2 mm	2-1 mm	1.0-0.25 mm	0.25-0.05 mm	0.05-0.01 mm	0.01-0.005 mm	<0.05 mm			
0.5	0.2	0.1	0.1	3.0	27.4	30.7	30.6	7.4	33.5	21.3	12.2

Conditions and results of the experiments. The tests were carried out by pressing a ball of 15.8 mm diam; load on the ball:  $P=5.4$  kg; average temperature of the sample being tested:  $-1.2^{\circ}\text{C}$ ; limiting penetration  $s_f=1.02$  mm; limit of the long-term cohesion  $c_{lt}=1.9$  kg/cm<sup>2</sup>.

As is evident, the error decreases significantly for long-term values of  $c_i$ . If the error for  $c_{inst}$  in experiment no. 59 was 5.2%, then for  $c_{120}$  this error decreases to 1.9%. According to the data of other experiments, the value of  $\sigma$  for  $c_{inst}$  fluctuated between 2% and 12%, but was generally in the range from 2-3%. The data refer to the repeated tests on one sample; also, taking into account the inter-phase heterogeneity of the soil, the scatter of the points naturally increases.

The invariance of the value of the long-term cohesion is verified by "comparison tests" carried out with balls of different diameters (14 mm and 60.5 mm) for a proportional increase of the load. As is shown in Figure 8, discrepancies in the values of  $c$  are observed only for the initial points.

Figure 6. Results of repeated determinations of the cohesion. Heavy loam;  $\theta=-0.4^{\circ}\text{C}$  (experiment 37). Note: the experimental points corresponding to each repeated experiment are denoted by their conventional symbols on the diagram.

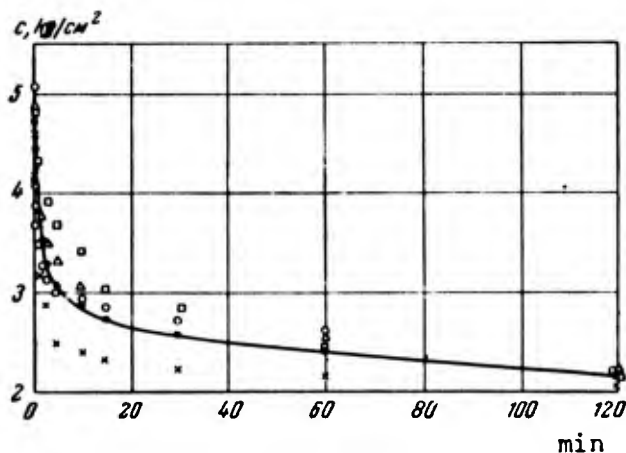
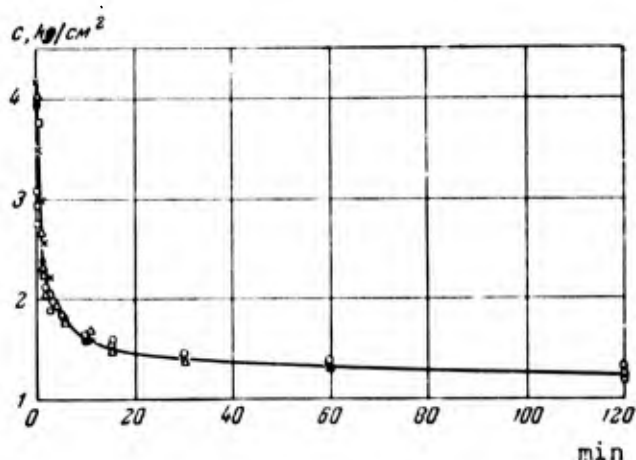


Figure 7. Results of repeated determinations of the cohesion. Varved clay;  $\theta=-0.4^{\circ}\text{C}$

(experiment 59). See note on Figure 6.

Table 4. Statistical processing of the experimental data

No. of the test	Soil	Time of reading	$c_t$ kg/cm <sup>2</sup>			$\sigma_i$ kg/cm <sup>2</sup>	$\sigma$ kg/cm <sup>2</sup>	$\rho$ %
			Mean	Minimum	Maximum			
59	Varved clay $\theta = -0.4^\circ\text{C}$	5 sec	4.79	4.06	5.14	0.50	0.25	5.2
		15 min	2.74	2.30	3.02	0.31	0.155	5.6
		60 min	2.44	2.15	2.60	0.20	0.100	4.1
		120 min	2.17	2.07	2.24	0.08	0.04	1.9
37	Heavy silty sandy loam $\theta = -0.4^\circ\text{C}$	5 sec	3.98	3.77	4.16	0.16	0.081	2.0
		15 min	1.51	1.48	1.54	0.032	0.016	1.1
		60 min	1.32	1.27	1.34	0.032	0.016	1.2
		120 min	1.23	1.20	1.26	0.024	0.012	1.0

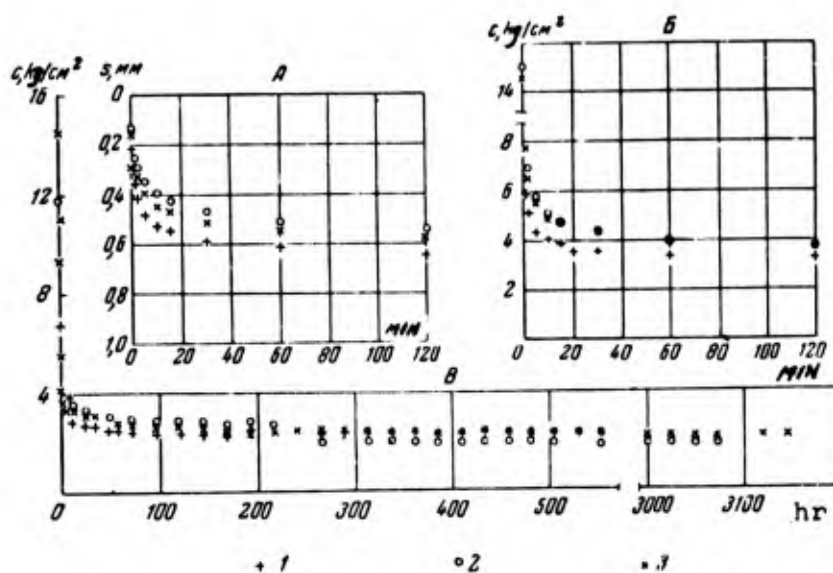


Figure 8. Results of the tests with spherical indenters of various dimensions. Sandy loam;  $\theta = -1.4^\circ\text{C}$ . a. Growth of penetration. b. Reduction of the cohesion. (1), (2), and (3) respectively for the apparatus:  
 INIMS  $D_{si} = 15$  mm,  $P = 5.5$  kg (1)  
 INMERO  $D_{si} = 14.3$  mm,  $P = 5.0$  kg (2)  
 INMERO  $D_{si} = 60.5$  mm,  $P = 20.5$  kg. (3)

As time elapses, the scatter of the points decreases and the values of the long-term cohesion turn out to be almost identical. Thus, the cohesion evaluated by the method of a loaded spherical indenter can be considered to be an actual characteristic of the frozen soil, reflecting its mechanical properties. This statement is applicable only to homogeneous frozen soil of massive structure containing ice only in the form of cement.

To evaluate the stability of frozen soils containing ice inclusions, we must use indenters of a sufficiently large size in order to carry out a test on the solid body. It is understood that for a massive structure as well a greater degree of simulation of natural conditions is achieved in the experiments by means of spherical indenters of large diameter.

Formulas (198) and (13) are deduced from the linear dependence of the load  $P$  on the punched ball and its penetration  $s$ , i.e. from the assumption that the cohesion  $c$  does not depend on the value of the load. However, experiments with ball indenters (Vialov, 1954) under different loads (both constant and increasing in steps) have shown that the relationship between  $P$  and  $s$  is in fact non-linear. Consequently, the value of  $c$  determined by formula (18) also increases with the increase of load (Figure 9), which indicates the strengthening of frozen soils.\*

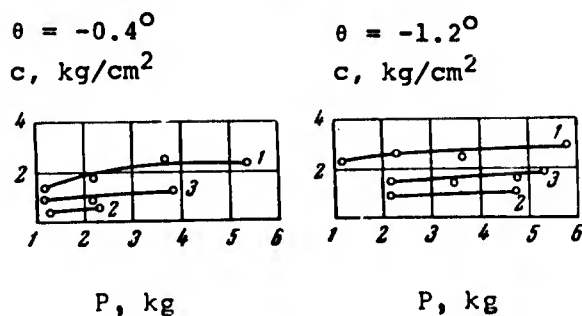


Figure 9. Relationship between the cohesion  $c_{lt}$  and load  $P$  for ball indenters:

(1) varved clay, (2) heavy silty loam, (3) heavy silty sandy loam.

The above phenomenon is explained by the irreversible bonding of the particles as a result of the flow of the ice, as well as of its melting at the contact of more densely packed particles, and consequently by the increase of the molecular forces of interaction. Let us note that the strengthening occurs for an increased load only up to a certain limit, beyond which the inner bonds break and yielding develops; the ball will continuously sink into the frozen soil as in a viscous medium. In a series of tests, it was interesting to note the existence of a minimum  $c$  for some value  $P$ . This obviously indicates a critical condition for which strengthening has not yet started to prevail over the weakening caused by breaking the structural bonds.

Owing to the large natural compactness of frozen soils (at a low temperature), their compression is insignificant (small inclination of the curves; see Figure 9) and therefore the effect of the strengthening is relatively small, especially for a small range of application of the

\* Let us note that strengthening during the penetration of a ball occurs even for materials such as steel.

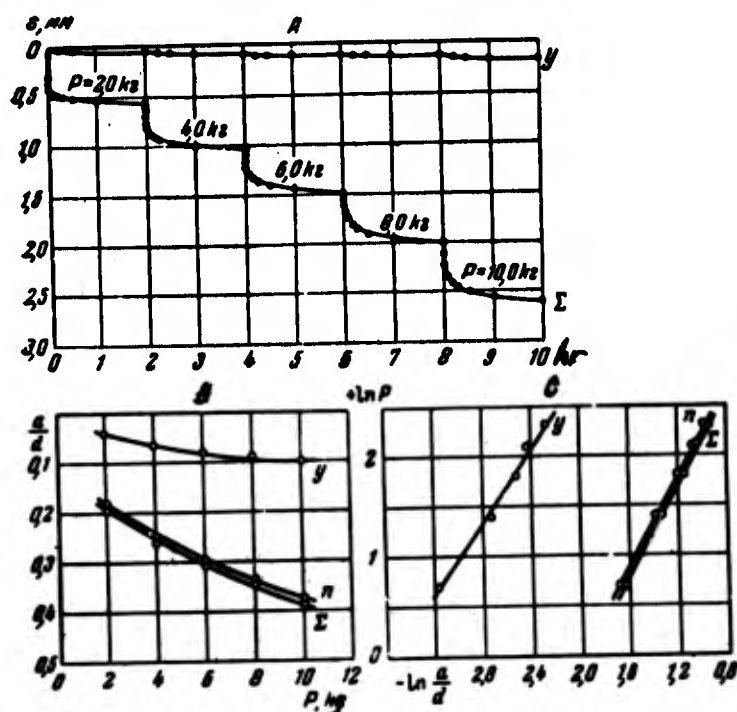


Figure 10. Test of pressing a ball with loading. Light silty loam,  $\theta = -0.30^\circ\text{C}$  (experiment 268). A. Growth of the strain with time. B. Relationship between the load and the radius of the imprint  $a$ . C. The same as B in logarithmic coordinates. Elastic strain  $y$ ; plastic strain  $n$ ; total strain  $\Sigma$ ; diam of the ball  $d$ .

stress. Hence, with sufficient accuracy for all practical purposes, the cohesion of frozen soils can be considered as a constant value independent of the pressure.

In the first section of the present chapter, we concluded that the cohesion should be determined by the value of the plastic strain. For the pressing of a ball into frozen soil, both a residual and a time-recoverable penetration were observed. To study the role of the recoverable penetration, several experiments were conducted for a gradual penetration with unloading after each step. Aiming at the influence of the time factor, the steps of the loading were maintained during the course of various time intervals (constant for each given experiment) ranging from 1 min - 24 hr. The analysis of the results of the tests (Figure 10) shows that the recoverable part of the penetration consists altogether of 2-10% of the value of the total; therefore, the more plastic the frozen soil, the greater is the duration of the tests, and the smaller is the relative importance of the elastic strain. Hence, the value of the long-term cohesion  $c$  can be determined with sufficient accuracy for all practical purposes by substituting in formulas (18) and (19) not the residual but the total value of the penetration; all the more since such an assumption gives a safety factor.



## 3. Evaluation of the plastic characteristics of frozen soil

To estimate the plastic properties of frozen soils, the nature of the relationship between the load on the ball and the dimensions of the imprint has an essential significance. From dimensional analysis, it follows (Zaitsev, 1950; Cherkasov, 1952) that for plastic bodies this relationship must be expressed by the formula:

$$P = Ar^2 \left( \frac{a}{r} \right)^n, \quad (20)$$

where  $r$  is the radius of the ball,  $a$  is the radius of the imprint, and  $A$  (kg/cm<sup>2</sup>) and  $n$  (dimensionless number) are plasticity parameters depending upon the type of soil, its temperature, and its moisture content.

The experiments indicated that this equation is completely applicable to frozen soils. This is confirmed by the good rectification of the experimental curves  $a/2r = f(P)$  when they are plotted with logarithmic coordinates (Figure 10b). From this graph, it also follows that the curves of the residual and total strains, as well as their absolute values, are very close and that formula (20) is correct both for plastic and total imprint. We must also note that the parameter  $A$  for frozen soils, unlike that for solid bodies, is time-dependent, changing correspondingly with the growth of the delayed elastic deformation.

Using formula (20) and following I. I. Cherkasov's method (1952), we can determine Poisson's ratio and evaluate the plastic properties of the soil. In order to do this, the parameter  $n$ , characterizing the above-mentioned properties, must be put in the form of  $n = m + k$ , where  $k$  is a constant depending upon the shape of the indenter (for a ball  $k = 2$ , for a circular cylinder  $k = 0$ ). Having experimentally obtained  $m = n - 2$ , we can compute Poisson's ratio from the following formula:

$$\mu = 0.25 \left( 1 + m^{\frac{3}{2}} \right). \quad (21)$$

For an ideally elastic material,  $\mu = 0.25$  since  $m = 0$  and  $n = 2$ ; for an ideally plastic body  $\mu = 0.5$ ,  $m = 1$ , and  $n = 3$ .

The degree of plasticity of the soil can be characterized by the coefficient  $k$ :

$$k = \frac{\mu - \mu_{el}}{\mu_p - \mu_{el}} = 4\mu - 1 = m^{\frac{3}{2}},$$

for which  $0 \leq k \leq 1$ .

For the experiments on sandy loam and loam for  $\theta = -0.3^\circ\text{C}$  and  $-1.4^\circ\text{C}$ , the parameter  $m$  ranged from 0.1 to 0.6, and Poisson's ratio  $\mu$  from 0.275 to 0.36; hence,  $k = 0.1$  to 0.45. These values of  $\mu$  are in good agreement with the data of N. A. Tsytovich (1940, 1952), who has determined  $\mu$  directly.

## 4. Relaxation of cohesion and limiting long-term strength

The averaged results of the experiments are condensed in Table 5. The values of the cohesion of frozen soil are given at the initial

Table 5. Combined data of tests concerning the determination of

SOIL	Depth at which the sample was taken, m	Moisture content, %	Temperature: -0.3C to -0.4C				
			$c_{inst}$	$c_{0.5}$	$c_2$	$c_8$	$c_{1t}$
Varved clay (mineral layers)	14.0	35	5.65	2.7	2.45	2.2	1.8
The same; artificial-ly prepared samples	14.0	43	--	--	--	--	--
Heavy silty loam	1.8	36	4.3	1.25	1.0	0.75	0.55
Light silty loam	6.4	30	--	--	--	--	--
The same	6.7	32	4.1	1.35	1.15	1.1	--
The same	7.9	28	4.0	1.45	1.2	1.0	--
Heavy silty sandy loam	2.0	43	5.95- 4.55	1.35- 1.5	1.05- 1.4	0.95- 1.3	0.75- 0.9
The same	2.35	35	4.7	1.8	1.6	1.55	--
"	4.5	34	4.5	1.4	1.25	1.1	0.95
"	3.0	30	--	--	--	--	--
"	7.6	28	--	--	--	--	--
"	5.45	28	3.9	1.45	1.3	--	1.0
"	4.5	28	4.3	1.4	1.25	1.15	--
Heavy sandy loam	2.6	24	5.8	1.9	1.6	--	1.3
The same	2.9	29	5.9	2.2	2.0	--	1.5
Light silty sandy loam	4.0	--	--	--	--	--	--
Silty sand	1.6	37	--	--	--	--	--
Fine sand	12.8	23	11.4	4.8	3.9	2.8	2.3
Medium sand	6.0	25	17.1	5.0	3.0	--	1.85

the cohesion of undisturbed frozen soils at various temperatures

Temperature: -1.1C to -1.2C

Temperature: -4.0C to -4.2C

c <sub>inst</sub>	c <sub>0.5</sub>	c <sub>2</sub>	c <sub>8</sub>	c <sub>1t</sub>	c <sub>inst</sub>	c <sub>0.5</sub>	c <sub>2</sub>	c <sub>8</sub>	c <sub>1t</sub>
8.0	4.5	4.05	3.4	2.6	14.4	9.1	7.5	6.5	4.2
--	--	--	--	--	8.8	--	3.8	2.9	1.4
8.55	2.5	2.2	1.85	1.0	11.7	5.0	4.15	--	--
--	--	--	--	--	12.8	5.9	4.8	4.7	2.6
5.4	4.0	3.9	3.75	--	8.4	6.3	6.15	5.9	--
--	--	--	--	--	--	--	--	--	--
--	3.8	3.2	--	--	11.0	4.5	4.0	3.4	1.95
5.35	3.25	3.65	3.05	--	--	--	--	--	--
7.35	2.7	2.35	2.15	1.6	7.7	4.2	3.8	3.3	2.8
--	--	--	--	--	8.2	4.1	3.9	3.35	3.0
--	--	--	--	--	15.1	--	5.0	4.55	3.2
--	--	--	--	--	--	--	--	--	--
--	--	--	--	--	--	--	--	--	--
--	--	--	--	--	--	--	--	--	--
--	--	--	--	--	--	--	--	--	--
--	--	--	--	--	9.0	4.1	3.8	3.4	2.0
13.1	4.1	3.6	3.4	2.0	--	--	--	--	--
13.8	5.7	4.85	--	2.7	18.7	--	6.55	6.1	4.5
19.0	5.1	4.2	--	2.2	20.2	7.5	6.2	5.6	3.7

## 52 RHEOLOGICAL PROPERTIES AND BEARING CAPACITY OF FROZEN SOILS

time ( $c_{inst}$ ), after 0.5 hr ( $c_{0.5}$ ), after 2 hr ( $c_2$ ), and after 8 hr ( $c_8$ ); after maximum penetration, the limiting long-term value ( $c_{lt}$ ) is also given.

Analysis of this data shows the character of the rheological processes occurring in frozen soils under the action of a load. The case in which the penetration of the indenter damps in time (if the load on the ball is not excessively large) has been verified. For instance, in experiment 238 (sandy loam,  $\theta = -0.3^\circ\text{C}$ ) for a total duration of the test of 2554 hr, an increment of the deformation, measured with a precision of 0.002 mm, was not recorded for the last 504 hr; in experiment 233 (sand,  $\theta = -1.2^\circ\text{C}$ ), during its 3352 hr, an increment of deformation was not recorded during the last 614 hr, etc. Although the period during which  $c$  varies is fairly large (from 100 to 3000 hr), the most intensive lowering of this quantity, nevertheless, occurs in the initial, extremely short time interval, which is a particular characteristic of frozen soils. From Table 6, in which the values of the cohesion forces at various times are given as percentages of  $c_{inst}$ , it can be seen that the cohesion decreases to 40 to 60% in the first 5 min, and after 1 hr is reduced to 25 to 50%, approaching a lower limit of 20 to 40%.

The relaxation time  $n$  introduced in formula (8) constitutes the characteristic time for the weakening. Even though it will later be shown that this parameter is in fact variable, it has a definite significance in the qualitative evaluation of the relaxation phenomena. In Table 7, the conditional\* values of this parameter are given, computed as the time after which the difference  $c_{inst} - c_t$  decreases by a factor of  $e$  in comparison with the difference  $c_{inst} - c_{lt}$ . In Table 7 are also inserted the data on the other properties characterizing the intensity of the reduction of the strength of frozen soils, namely, the relation between the cohesion at a given time and the limiting long-term cohesion  $\frac{c_t}{c_{lt}}$ .

Table 6. Reduction of cohesion with time (heavy, silty, sandy loam)

Temperature $^\circ\text{C}$	Value of the cohesion at various times							
	Instantaneous	1 min	5 min	30 min	1 hr	2 hr	8 hr	Limiting long-term
-4.2	100	72	63	56	52	47	45	37
-1.2	100	62	43	38	36	31	30	25
-0.4	100	52	37	26	24	20	19	18

As is evident, the limiting long-term cohesion turns out to be significantly less than instantaneous cohesion (3-9 times). This indicates the high relaxation properties of frozen soils. The data show conclusively the necessity of including the time factor in the

\* "Conditional" because they are obtained through indirect data, namely, the change of the area of imprint.

Table 7. Data on the relaxation properties of undisturbed frozen soil

Soil	Moisture content %	Temperature: -0.3C to -0.4C				Temperature: -1.0C to -1.2C				Temperature: -4.0C to -4.2C			
		$\frac{C_{lt}}{C_{inst}}$	$\frac{C_{lt}}{C_{lt}}$	$\frac{C_{lt}}{C_{lt}}$	n, min	$\frac{C_{lt}}{C_{inst}}$	$\frac{C_{lt}}{C_{lt}}$	$\frac{C_{lt}}{C_{lt}}$	n, min	$\frac{C_{lt}}{C_{inst}}$	$\frac{C_{lt}}{C_{lt}}$	$\frac{C_{lt}}{C_{lt}}$	n, min
Varved clay	35	3.2	1.35	1.2	10	3.1	1.5	1.3	2.2	3.4	1.7	1.5	40
Pulverized loam	36	7.8	1.8	1.35	2	5.2	1.8	--	3	5.1	1.9	--	--
Heavy pulverized sandy loam	34	4.75	1.4	1.15	1.7	4.6	1.45	1.35	3	2.75	1.35	1.2	10
The same, very damp	43	7.9	1.4	1.25	--	--	--	--	--	5.6	2.05	1.75	10
Sand	23-25	5.0-9.2	1.6-1.7	1.2	--	5.0-8.6	1.8	1.15	--	4.35-5.5	1.55-1.65	1.2-1.4	--

evaluation of the stability of frozen soils. The greatest lowering of the cohesion occurs for frozen soils with a high temperature (close to 0C) and a high ice content.

Determination of the limit of the long-term cohesion, which is a fundamental characteristic of the strength of frozen soils used in structural foundations, requires the undertaking of experiments of long duration. However, taking into account the fact that the most intensive weakening occurs in the initial period, it becomes possible to significantly shorten the duration of the experiments.

From Table 7, it is apparent that if the ratio  $c_{inst}/c_{lt}$  is between 3 and 8, then the cohesion determined 8 hr after the application of the load exceeds the limiting long-term value only by a factor of 1.1 to 1.35 (for  $\theta = -0.3C$  and  $-1.2C$ ). In addition, the ratio  $c_8/c_{lt}$  is approximately stable, unlike  $c_{inst}/c_{lt}$  which has very large fluctuations. Consequently, for practical purposes, the value of the limit of the long-term cohesion can be approximated by the data of a short-duration test (for instance, lasting 8 hr) with the introduction of a correction factor,  $k=0.75$ :

$$c_{lt} = 0.75c_8 \quad (22)$$

This relation is accurate for soils with a temperature from  $-0.2C$  to between  $-2C$  and  $-4C$ . For soils with a lower temperature and high ice content, the value of  $k$  is obviously somewhat smaller.

The value of  $c_{lt}$  can be determined also through the results of short-duration experiments (lasting for instance from 30 min to 2 hr); but in this case the value of  $k$  is less stable and the possibilities of error are greater: approximately,  $c_{lt} = 0.5 c_{0.5} = 0.6 c_8$ .

##### 5. Dependence of the cohesion of frozen soils upon the gradation, moisture content, and temperature

The influence of the gradation of frozen soils on the value of the equivalent cohesion is graphically illustrated by the diagrams in Figure 11, in which the curves of the penetration of indenters into various soils are presented. The curves for sandy loam and loam are very similar since the large silt content of these soils even up their mechanical properties. However, a difference in the value of  $c_{lt}$  is also observed for these soils; this is explained by their different sand and clay fractions. The dependence of the equivalent cohesion upon the ratio of these fractions is illustrated in Table 8, although the comparison is not carried out for the same conditions (in particular, different moisture content), since these data refer to undisturbed soils.

As is obvious from Table 8, with the increase of the sand fraction, as well as with the decrease of the plasticity index, the value of  $c_{lt}$  increases slightly. A sharp growth of  $c_{lt}$  is observed in sands; this is explained by their greater "frame" rigidity, by their smaller content of unfrozen water, etc. In addition, one must again emphasize that we are concerned (strictly speaking) not with the cohesion, but with the overall stability characterized by the equivalent cohesion. It is interesting to note that the relaxation curves for sand are different in character from those for silty loam and sandy loam soils; specifically,

they are smoother and do not have such a sharp curvature. This indicates the smaller intensity of the rheological processes in sandy soils in comparison to argillaceous soils. An exception must be made for the varved clay soils of Igarska. The mineral layers of this soil possess a greater stability (the value of  $c_{lt}$ , for instance, is the same as for sand) and a less marked relaxation, their relaxation time being 1.5 to 2 times larger than that for sandy loam soils (Table 5). As already mentioned, the above peculiarities depend upon the great compactness and small moisture content of the mineral layers of the varved clay (moisture content of 35% for a plastic limit in the hole of 32%, and a liquid limit of 65%), which is a consequence of the formation conditions of these lake sediments. The stability of an artificially prepared sample of the same clay was shown (Table 5) to be significantly smaller (up to 4 times). Such a large drop cannot be explained only by the slightly larger moisture content of the artificial sample; it must be a consequence of the removal of the so-called structural cohesion. This shows the necessity of taking into account the origin of the frozen soils when evaluating their mechanical properties, and the inadequacy of data obtained from tests on remolded samples.

Figure 11. Curves of plastic deformations (A) and reduction of the cohesion (B) for various soils.  $\theta = -0.3C$

- (1) Varved clay (experiment 59);
- (2) heavy silty loam (experiment 54);
- (3) heavy silty sandy loam (experiment 37)
- (4) Sand (experiment 62).

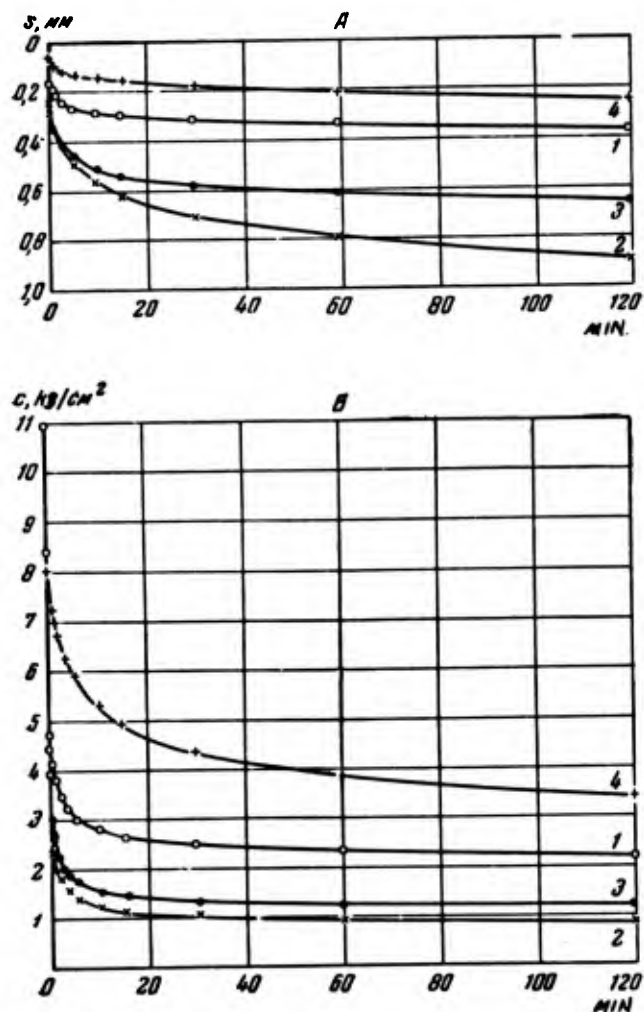




Table 8. Relationships between the equivalent cohesion, the mechanical composition, and plasticity of undisturbed frozen soils  
( $\theta = -3.8^\circ\text{C}$  to  $-4.2^\circ\text{C}$ )

Soil	Mois- ture content %	Plasticity index	Mechanical composition %			$c_{lt}$ , kg/cm <sup>2</sup>
			Sand	Silt	Clay	
Loam	30	12	35	54	11	2.5
Sandy loam	34	12	31	61.5	7.5	2.8
The same	30	11	33	61	6	3.0
The same	28	9.5	42	50	8	3.2
Sand	23	----	98	2	----	4.5

Investigating the 'instantaneous' resistance of frozen soils to compression, N. A. Tsytovich (1937) showed that for an incomplete filling of the pores of these soils with ice their stability grows with an increase of the ice content up to a certain fixed limit, corresponding, for a given porosity, to the complete filling of the pores with ice. For a further increase of the ice content, the strength decreases. From our data we can deduce that the long-term cohesion of frozen soils has an analogous behavior. This behavior can be explained as follows: in the process of freezing of the soil, additional new bonds arise, namely, the cementing caused by the ice; this cohesion increases the stability of the frozen soil, as compared to unfrozen soil. The higher the moisture content of the unfrozen soil, the greater the degree of ice saturation in the frozen soil (for a given temperature). Consequently, when the contact surface with the moisture film increases (Savelyev, 1953), the thickness of water films decreases, and as a result the interparticle bond increases. However, this is correct only under certain conditions, specifically when the amount of ice crystals is small and when, being separate, they react under the action of an external load as under a uniform pressure; the load itself is taken by the framework of the mineral particles. If the amount of ice is somewhat larger, then individual crystals of ice units form a semblance of an ice framework (the limiting case being ice impregnated with mineral particles). As a result, a large drop in the stability will occur (Table 9), since the long-term cohesion of ice is quite small (if not equal to zero). More details about the cohesion of ice are given later.

The influence of the ice content on the value of cohesion decreases somewhat as the temperature increases, since it is not only the absolute content of ice which is important, but also the ratio of ice to unfrozen water. For example, with an increase of moisture content from 34% to 43%,  $c_{lt}$  decreases, for  $\theta = -4.2^\circ\text{C}$ , by a factor of 1.5, whereas for  $\theta = -1.2^\circ\text{C}$ , it decreases by a factor of 1.25.

Table 9. Reduction of the long-term cohesion of undisturbed frozen loams ( $\theta = -4.2^\circ\text{C}$ ) with increase in moisture content

Mechanical composition, %			Liquid limit	Moisture content %	$c_{lt}, \text{kg/cm}^2$
Sand	Silt	Clay			
33	61	6	36	30	3.0
31	62	7	34	34	2.8
27	65	8	38	43	1.95

Influence of the temperature. The temperature of frozen soils is one of the main factors influencing their stability. This influence has been studied by several investigators in connection with the instantaneous strength. Let us consider the manner in which the temperature influences the long-term cohesion and the relaxation properties of frozen soils. From Figure 12 it follows that, with a lowering of the temperature, the relaxation curves become less steep, i.e. the intensity of the relaxation process decreases. This is also indicated by the increase of the relaxation time as  $\theta$  increases (Table 10).

The value of both the limiting long-term cohesion and the instantaneous cohesion significantly increase for sandy loam: at  $\theta = -0.3^\circ\text{C}$ ,  $c_{lt} = 0.95 \text{ kg/cm}^2$ ; at  $\theta = -1.2^\circ\text{C}$ ,  $c_{lt} = 1.6 \text{ kg/cm}^2$ ; and at  $\theta = 4.2^\circ\text{C}$ ,  $c_{lt} = 2.8 \text{ kg/cm}^2$ .

The dependence of the cohesion upon the temperature of the soil is illustrated in Figure 13. Analysis of the test data has shown that this dependence can be expressed by the following empirical formula,

$$c = c_0 + b\sqrt{|\theta|}, \quad (23)$$

where  $\theta$  is the absolute value of the negative temperature;  $c$  is the cohesion for any negative temperature;  $c_0$  is the cohesion for some temperature, for instance  $-0^\circ\text{C}$ , i.e. for a negative temperature approaching  $0^\circ\text{C}$ , and  $b$  is a parameter depending on the properties of the soil and its moisture-ice content.

In particular for varved clay  $c_{lt} = 1.0 + 1.5\sqrt{|\theta|}$ , and for heavy silty sandy loam  $c_{lt} = 0.3 + 1.2\sqrt{|\theta|}$ . Formula (23) shows (in a definite interval) the damping influence of temperature on the stability; the accuracy of the formula is verified by the rectification of the experimental curves, as shown in Figure 13b. The sands tested constitute an exception; they do not precisely follow the given formula. Formula (23) is also valid for instantaneous stability, and in particular, for the temporary strength of frozen soils under compression. This is verified by the graph in Figure 14, deduced from the test data of F. M. Faintsimmer.

The greatest changes in the stability of frozen soils occur in the range of significant phase transformations of water, i.e. from  $0^\circ\text{C}$  to  $-1.5^\circ\text{C}$ ,  $-2^\circ\text{C}$ . In addition, the influence of the mechanical composition,

the moisture content, and other factors becomes small for a temperature close to 0°C, because it is masked by the change in the phase composition of the water. Let us note that the parameters  $c_0$  and  $b$  depend upon the time of action of the load; in particular, they increase when  $t$  approaches zero. This means that the instantaneous strength depends upon the temperature to a greater extent than the long-term strength, since in the latter the influence of the temperature is somewhat covered by the time factor. The influence of the temperature on the stability of frozen soil is usually explained by the change in the content of unfrozen water. However, several other factors are important; otherwise, it would be difficult to explain why the strength of frozen sand, in which practically all the water is in solid form for a low  $\theta$ , changes with a temperature variation.

Frozen soils can be represented as a system of solid particles (mineral granules and crystals of ice-cement) connected by water films. The amount of unfrozen water decreases with the lowering of the temperature. Therefore, the content of ice-cement correspondingly increases. With the increase of the ice content, the surface of contact with the water film increases (Savelyev, 1953, 1955), and the film becomes thinner. A film no matter how thin, exists at the ice-mineral particles interface, even for low temperatures. A change in the amount of ice crystals, small enough not to affect the phase composition of the water in the soil, yields a noticeable increase in the cohesion of this film, i.e. an increase of the action of the molecular forces of attraction. As a result of the lowering of the temperature, the viscosity of the water film, as well as the stability of the ice, will increase. Finally, the lower the temperature, the greater is the load necessary to cause melting of the ice at the interface, and the intermixing of the particles upon which the growth of the creep deformation depends.

The compiled data of the values of the limit of long-term cohesion, determined by using a spherical indenter for various soils and at various temperatures, are given in Table 11. These data can also be used for the evaluation of the long-term strength of permafrozen soils.

#### 6. Cohesion of ice

The study of the plastic and rheological properties of ice is of great interest, since ice is one of the most important components of frozen soil; its properties determine to a large extent the behavior of such soil under stress. The data of this section were obtained by ball-indentation tests in ice, both in natural samples cut out of ice inclusions in a stratum of frozen varved clay at a depth of 14 m, and in artificially prepared samples. The initial tests were conducted for the ball loaded perpendicular to the plane of stratification of the ice lenses, i.e. parallel to the direction of the main optical axis of the crystals; parts of these tests were also conducted for loading parallel to this plane of stratification. As an illustration, the results of a 2r test on natural ice at various temperatures are shown in Figure 15. One can see that the relaxation curves for ice are less steep than the corresponding curves for frozen soils (Figure 12b), which indicates the slower rate of the relaxation process in ice as compared to frozen soils. This is explained by the smaller viscosity of frozen soils, due to their content of unfrozen water (Tsytovich, 1937).

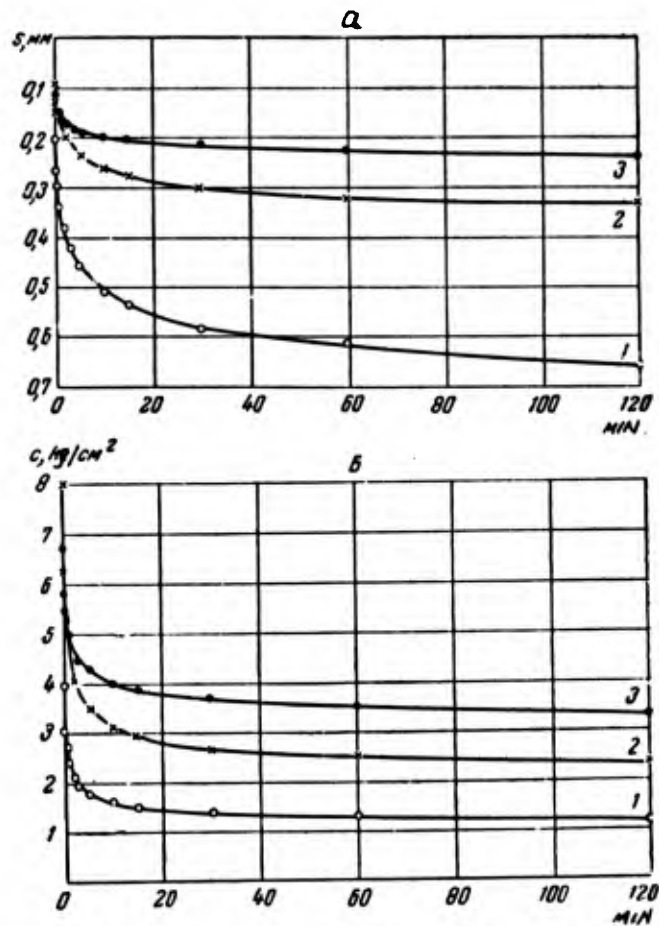


Figure 12. Diagrams of the plastic strains (a), and the lowering of the cohesion (b) for different temperatures of heavy, sandy loam.

(1), (2), and (3), represent respectively temperatures of -0.4C, -1.2C, and -4.2C.

Table 10. Value of the relaxation time  $\underline{n}$  of frozen soils at various temperatures  $\theta$ .

Soil	Value of $\underline{n}$ (in min) for a temperature of, °C		
	-0.3C	-1.2C	-4.0C
Varved clay	10	20	40
Heavy silty loam	2	3	--
Heavy silty sandy loam	1.7	3	10

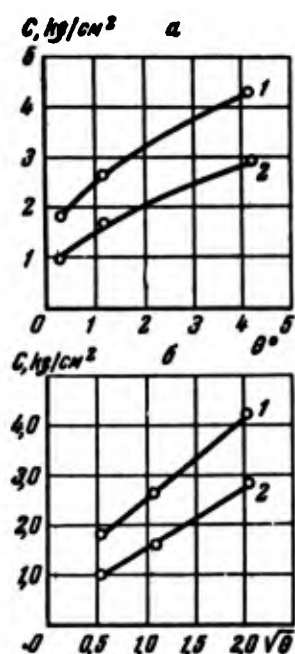


Figure 13. Dependence of the cohesion of frozen soils upon temperature.

- a. In the standard coordinates.  
 b. Rectified graph.  
 (1) Varved clay; (2) heavy sandy loam

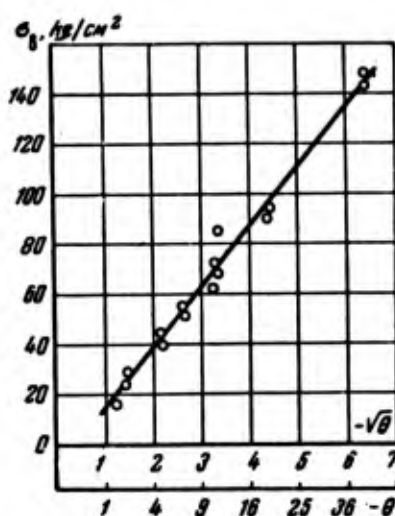


Figure 14. Dependence of the 'instantaneous' compressive strength of frozen loam upon the temperature.

It is significant that these relaxation curves of the cohesion of ice are analogous to the corresponding curves for sand at a low  $\theta$ . We should note the intermittent growth of deformation when testing ice; this has been pointed out also by other authors for short-duration, flexure, and other, tests of ice (Ivanov and Lavrov, 1950).

The processed data of the experiments on various ice samples under various stresses are given in Table 12. Instantaneous, 30 min and 2 hr values of the cohesion, as well as properties characterizing the scatter of the experimental data obtained after statistical processing, are also given in Table 12. The average value  $c_{av}$  was determined as the mean of  $n$  tests, each of which had  $m$  repeated evaluations,

$$c_{av} = \frac{\sum_{i=1}^n m_i c_{n(i)}}{\sum_{i=1}^n m_i},$$

where  $c_{n(i)} = \frac{1}{m_i} \sum_1^{m_i} c_i$  is the average value for each  $n^{\text{th}}$  test.

The index of accuracy (coefficient of variation) was determined as  $\rho = \frac{\sigma}{c_{av}} = \frac{\sigma_i}{c_{av} \sqrt{n}}$  %, where

$$\sigma_i = \sqrt{\frac{\sum_1^n m_i \delta_i^2}{(n-1) \frac{1}{n} \sum_1^n m_i}}$$

is the standard deviation of an individual experiment;  $\sigma$  is the weighted mean error, and  $\delta_i = c_{av} - c_{n(i)}$ .

Table 11. Compiled data of the value of the limiting long-term equivalent cohesion of undisturbed frozen soil

Soil	Value of $c_{lt}$ (kg/cm <sup>2</sup> ) for a temperature of, °C		
	-0.3C to -0.4C	-1.0C to -1.2C	-3.8C to -4.2C
Silty loams	0.6-0.9	1.0-1.5	2.0-2.5
Silty sandy loams	0.9-1.3	1.6-2.0	2.8-3.2
The same, very damp (W > 40%)	0.75	---	2.0
Sand	2.1-2.3	2.7	3.7-4.5
Dense varved clay	1.8	2.6	4.2

From Table 12, it is noted that the experimental data have a large departure from the mean values, and that  $\rho$  varies from 7 to 25%. This is explained by the marked anisotropy of ice and the heterogeneous orientation of its crystals. Examining the absolute values of  $c$ , we should note that they depend to a large extent upon the temperature, increasing as the latter decreases. The values of  $c$  for ice taken from ice-inclusions in a stratum of permafrozen soil and for artificially prepared ice turned out to be the same for all practical purposes. In each case, the instantaneous and even the 2 hr values of the cohesion of ice were significantly higher than those of frozen soils (Table 13).

Table 12. Compiled data of the determination of the cohesion of ice

Temperature °C	No. of exp.	No. of repeated determinations	c <sub>inst.</sub> kg/cm <sup>2</sup>				c <sub>0.5</sub> kg/cm <sup>2</sup>				c <sub>2</sub> kg/cm <sup>2</sup>			
			Average	Min.	Max.	ρ	Average	Min.	Max.	ρ	Average	Min.	Max.	ρ

Natural ice, stress parallel to the main optical axis of the crystals.

-3.8	6	23	108	48	210	19.2	17.8	44.8	22	85	8.5	19.0	32.3	16	67	5.6	17.3
-1.2	12	45	42.8	10	105	4.83	11.3	16.2	5	35	2.17	13.4	11.9	4	30	1.6	13.7
-0.4	7	7	19.5	10	34	4.17	21.3	4.9	3.7	7.6	0.41	8.5	3.9	2.8	5.0	0.27	7

Temperature °C	No. of exp.	No. of repeated determinations	c <sub>inst.</sub> kg/cm <sup>2</sup>				c <sub>0.5</sub> kg/cm <sup>2</sup>				c <sub>2</sub> kg/cm <sup>2</sup>			
			Average	Min.	Max.	ρ	Average	Min.	Max.	ρ	Average	Min.	Max.	ρ

Natural ice, stress perpendicular to the main optical axis of the crystals

-3.8	5	26	118	59	242	20.5	17.5	35.8	13.0	104	91	25.2	26.1	8.8	83	6.4	24.4
-1.2	5	32	89	31	288	13.9	15.8	29.6	12.7	52	58	19.5	21.2	8.5	38	5.1	19.4
Artificial ice, stress perpendicular to the plane of the freezing surface																	
-1.2	5	24	47.3	15	103	10.2	21.5	18.2	8.9	39	2.16	11.9	12.9	6.9	28	1.47	11.4



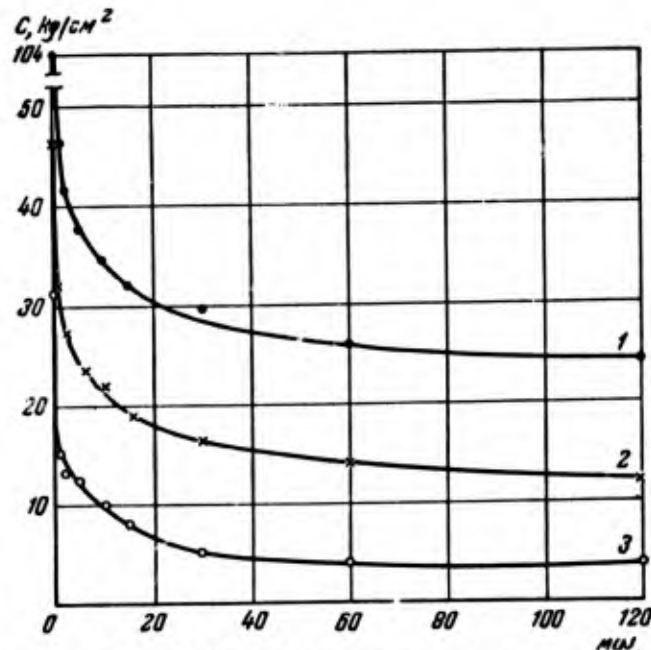


Figure 15. Relaxation curves for the cohesion of ice at various temperatures.

(1), (2), and (3) represent, respectively, temperatures of  $-3.6^{\circ}\text{C}$ ,  $-1.2^{\circ}\text{C}$ , and  $-0.4^{\circ}\text{C}$ .

It is interesting to note that according to the data of N. K. Pekarskaya (1957) the instantaneous shearing resistance of pure ice also turned out to be greater than that of frozen soil. At the same time, the instantaneous shearing resistance of ice is significantly smaller than the instantaneous cohesion. As a consequence, there is some doubt as to the possibility of using, as in formula (18), the plasticity condition of Saint-Venant  $\tau = c$ , for ice; nevertheless, this condition is used by several authors.

Hence, there is a doubt as to the possible interpretation of  $c$  determined through the indentation test as a plastic constant of ice. The data of these experiments must be considered as the characteristic hardness of ice ( $H$  kg/cm<sup>2</sup>), determined by the well-known metallurgical formula  $H_t = \frac{P}{\omega_t}$ , where  $\omega_t = \pi d_s^2$  is the area of imprint

of the ball, varying with time. The parameter  $H$  is connected to the parameter  $c$  by the relation  $H = 5.55 c$ .

Let us consider the question of the long-term cohesion of ice. It is well-known (Weinberg, 1940) that a body with a density greater than the density of ice will continuously sink in the ice at a constant rate. From these assumptions, one must expect that the ball will first sink with a decreasing speed (as the area of imprint increases), then with a constant speed when the diameter of the imprint is 0.5 larger than that of the ball. We have conducted 5 long-term experiments (from

Table 13. Values of  $c_{inst}$ . (kg/cm<sup>2</sup>) for ice and frozen soils.

Soil	Temperature °C		
	-3.8C	-1.2C	-0.4C
Ice	110	40	20
Sand	20	17	14
Sandy loam	8-15	5-8	4-6

3 to 5 years). However, the inadequacy of the instruments for such long-term tests under conditions of negative temperatures prevented our obtaining full-value results. In two of the experiments, the sinking of the ball stopped; this was obviously explained by the formation of hoarfrost on the rod. In the remaining three tests, the deformation continued uninterrupted, but it was discovered that the ice around the point of contact of the ball disintegrated, evidently affecting the value of the penetration.

Nevertheless, on the basis of the available data, it can be verified that the long-term cohesion of ice is either equal to zero, or is so small that it can hardly be determined in practice; at any rate, the long-term cohesion is significantly smaller than the limiting long-term cohesion of frozen soils.

The above discussion agrees with the newest data (Perutz, 1950; Glen, 1952; Nye, 1953; Voitkovskiy, 1957) according to which ice does not have a clearly defined elastic limit; at any rate, this limit does not exceed 0.1 kg/cm<sup>2</sup> (for shear).

The increased value of the instantaneous cohesion of ice and the sharp lowering of the stability for the protracted action of loads explain the diverse character of the influence of ice inclusions on the stability of frozen ground for short-term and long-duration application of the loads. The presence of ice inclusions can increase the instantaneous strength of frozen soil, and on the contrary decrease the long-term strength. In addition, it must be taken into consideration that the rate of weakening of ice is significantly lower than that of frozen soil.

### CHAPTER III. INVESTIGATION OF THE ADFREEZE STRENGTH OF SOILS AND ICE WITH WOODEN RODS

#### 1. Concept of adfreeze strength

In engineering calculations, the shearing strength of frozen soils along the lateral surface of a foundation is of great importance (Chernyshov, 1928; Tsytovich, 1937, 1952; Goldshtein, 1941, 1948). This type of strength is usually called adfreeze strength, because it is caused by adfreezing, i.e. the adhesion of the frozen moist soil to the foundation material. When the damp soil freezes, adhesion forces arise between it and the surface of the inserted body. These forces are distinct from the adhesion of pure ice. The bond between the frozen soil and the surface of the body occurs not only through the ice crystals, but also by means of direct contact (through a water film) of the mineral particles. In addition, both the border layer and a certain volume of the surrounding soil will be under stress. This is well corroborated by experiments on the pull-out of rods frozen in the soil, in which both the displacement of the pulled-out rod and deformation of the surface of the soil adjacent to the rod are observed. Let us consider a rod driven into a hole drilled in frozen soil. If the diameter of the rod is larger than the diameter of the hole, the shearing resistance along the lateral surface will be related to the frictional resistance\*. This frictional resistance depends upon the coefficient of friction of the frozen soil on the material of the rod, and upon the value of the normal stresses (squeezing force) developing in the soil. These forces arise not only from driving, but also as a result of the pressure caused by the volume expansion of the moisture freezing in the soil, as a consequence of the lateral pressure of the soil. Thus, the shearing strength of frozen soil along the lateral surface of foundations, piles, and other construction depends upon the adhesion  $c$  (adfreeze force) and upon the friction  $\sigma f$ .

$$\tau = c + \sigma f,$$

where  $f$  is the friction coefficient, and  $\sigma$  is the normal stress, i.e. normal to the lateral surface of the foundation.

The relationship between  $c$  and  $\sigma f$  will depend upon the emplacement method of the pile, upon its material, upon the moisture content of the soil, etc. From now on, we shall refer to the above-mentioned total shearing strength as the adfreeze strength (stability). This implies the stress which one must apply to the frozen soil surrounding the rod in order to break, in shear, its bond with the frozen soil, regardless of the method of emplacement†.

---

\* See Chapter V.

† A term, sometimes used is "Forces (Tangential) of Adfreezing", which must be considered as reactive forces arising from the punching through of a rod frozen in the soil.

## 2. Experimental methods

The experiments were conducted in the underground chambers of the laboratory and consisted of pulling out cylindrical wood rods (model piles) embedded in one way or another in the blocks of frozen soil under constant, and gradually increasing, stresses\*. The rods were turned on a lathe and, for the series of experiments, had the following dimensions: diam 35 mm; length of working piece 100 mm; length of point 20 mm. The load on the rod ( $\tau$  kg/cm<sup>2</sup>) was computed relative to a unit area of lateral surface.

Emplacement in the soil was accomplished by two methods. The first was the hammering of a pile into holes previously drilled in the blocks of undisturbed frozen soil embedded in the ground of the vault. The diameter of the holes was 0.9 times the diameter of the rods; these model piles were driven with a hammer. The depth of the drilled holes was greater than the length of the rods. The piles emplaced by this method will be referred to from now on as "driven" piles. The second method of emplacement was the driving-in of piles in frozen soils with the aid of steaming†. To accomplish this, 50 mm diam holes were drilled in the embedded frozen soil blocks and were filled up with soil of the chosen type, warmed to +50C or +60C; the model pile was embedded in this block. Under the influence of a cold current of air on the surface and the surrounding frozen strata, the soil block froze with time, forming the adfreeze of steamed soil. The models driven in by this method will be called "frozen-in" piles.

The initial moisture content of the inserted soil block corresponded to the moisture content of steamed soil in nature and consisted, for instance, of 50% for sand, 60 to 80% for sandy loams and loams, and up to 100% for clays. The final moisture content of the block sharply decreased after freezing as a result of the migration of the moisture during freezing (Tsvetova, 1954). This will be described in greater detail in Chapter XI.

The pull-out experiments of model piles were carried out by means of a special lever apparatus. Each test (having an ordinal number) was made with one block of soil and consisted of a set of 8 piles. Seven of them were tested under various stresses, constant for each pile, starting with a stress causing "instantaneous" pull-out and ending with "long-term" stresses which did not lead to pull-out. One of the piles was tested under a gradually increasing stress. In this case, the first stages of the loading were maintained unchanged until the deformation stopped; the subsequent ones were maintained until the establishment of steady flow. During the testing process, the vertical displacement  $\lambda$  (mm) of the rod was measured; in the appropriate cases this displacement was related to the diameter of the rod ( $d$ ), and was expressed by the dimensionless quantity  $\gamma = \frac{\lambda}{d}$ .

\* For the properties of the soils, see Table 1.

† Concerning this method of emplacing piles by steaming, see Chapter XI.

### 3. Deformation process for constant loads and reduction of the adfreeze strength

The combined curves of the deformation, i.e. the curves for the displacement of the rod with time, are represented in Figure 16. Each curve on the graphs corresponds to the given value of the pull-out stress  $\tau = \text{const.}$  It is evident that the curves are analogous to the classical curves for creep. The aspect of these curves changes with the value of the stress. For large values of  $\tau$ , the deformation process develops quickly; the plastic properties of the soil cannot develop and the collapse has a brittle character, i.e. the pull-out is accompanied by the characteristic snap and the displacement is small. For stresses equal to 50 to 70% of the instantaneous strength, the breaking occurs, although not immediately, in a very short time interval of the order of 100 to 300 sec; hence, the curves have an S-shape. For smaller values of the stress, e.g. equal to 25 to 40% of  $\tau_{\text{inst}}$ , the visco-plastic properties of the soil become clearly evident. The displacement curves for such stresses are typical creep curves reflecting all the stages of deformation: instantaneous (initial) displacement, the stage of steady creep, during which the sliding of the rod through the soil proceeds at a constant rate, and the stage of progressive flow in which the sliding occurs with an increasing speed; this stage is ended by the pull-out of the rod. With the scale used in Figure 16, this behavior is well represented only in the curves corresponding to small stresses, e.g. equal to 25 to 30% of  $\tau_{\text{inst}}$ . Even for stresses equal to 30 to 40%, the curves would have an analogous character if drawn on a larger scale (Figure 17), differing only by the greater intensity of the process.

It is significant that even a small change in the value of the stress leads to a sharp increase in the duration of the deformation process. For instance, when  $\tau = (0.3 - 0.4) \tau_{\text{inst}}$ , the pull-out occurs in 100 - 300 min, whereas for  $\tau = (0.25 - 0.3) \tau_{\text{inst}}$ , it occurs after 200 - 800 hr, and for  $\tau = 0.2 \tau_{\text{inst}}$ , after 2000 to 4000 hr. In addition, the stage of flow occupies 70 to 90% of the duration of the whole process. However, this stage does not set in immediately, but after a relatively long period, from 50 to 750 hr after the loading (for small values of  $\tau$ ). The duration of the steady stage is a feature of the creep process of frozen soil. Such a duration is also characteristic of the reaction process of frozen soil, i.e. the stabilization of the deformation occurs after 250 to 1000 hr and more.

Another distinguishing and extremely important property of frozen soils is that the deformation of creep inevitably develops into the progressive flow stage ending with collapse. For solid bodies, the transition into the final stage is usually due to a decrease in the cross-section of the sample, e.g. by the formation of a neck under tension. In several colloidal systems tested for shear by the torsion method, the working area does not change, and an uninterrupted growth of the flow is observed without transition into the collapse stage; this is explained by the continuous restoration (in the slow flow) of the broken structural bonds (Rebinder, 1950). However, in frozen soils, the transition into the stage of progressive flow and subsequent collapse occur also where the stressed area of the sample remains constant. This is graphically verified by the punching of rods through the soil (Figure 18).

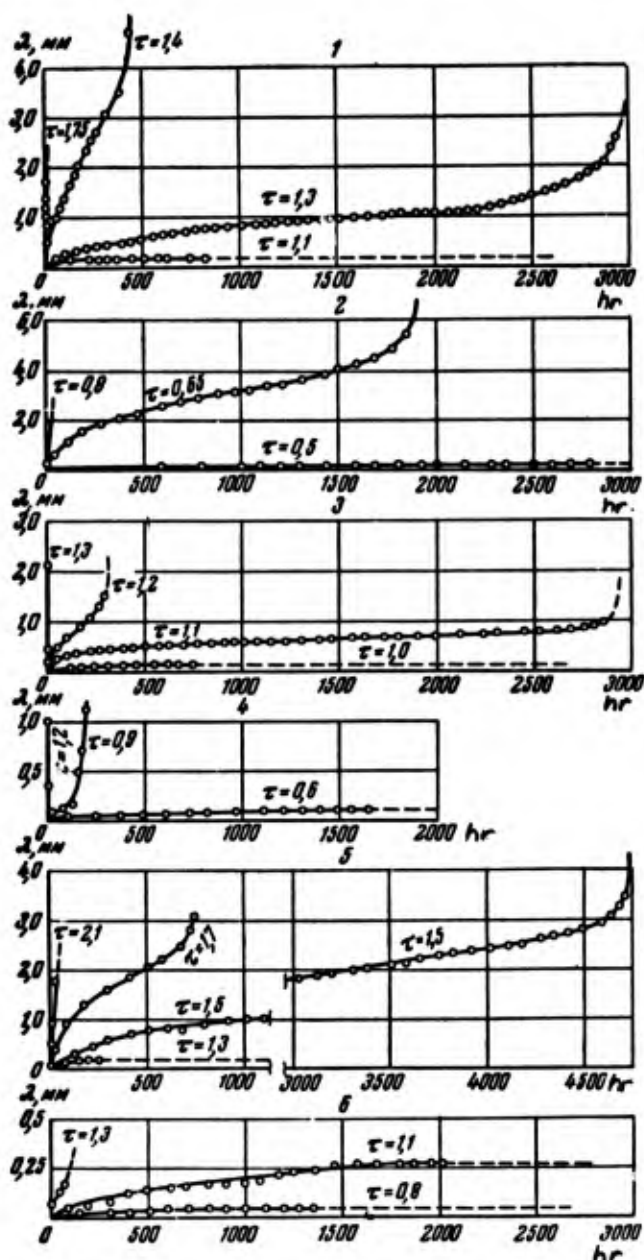


Figure 16. Combined curves of the growth of the displacement ( $\lambda$ ) for various stresses; ( $\tau$  kg/cm<sup>2</sup>) pull-out of model piles,  $\theta = -0.4^\circ$ .  
 (1) Varved clay, driven pile (experiment 16);  
 (2) Varved clay, frozen-in pile (experiment 14); (3) Light, silty loam, driven pile (experiment 26); (4) Light, silty loam, frozen-in pile (experiment 27); (5) Heavy, silty, sandy loam, driven pile (experiment 24); (6) Heavy, silty, sandy loam, frozen-in pile (experiment 25).



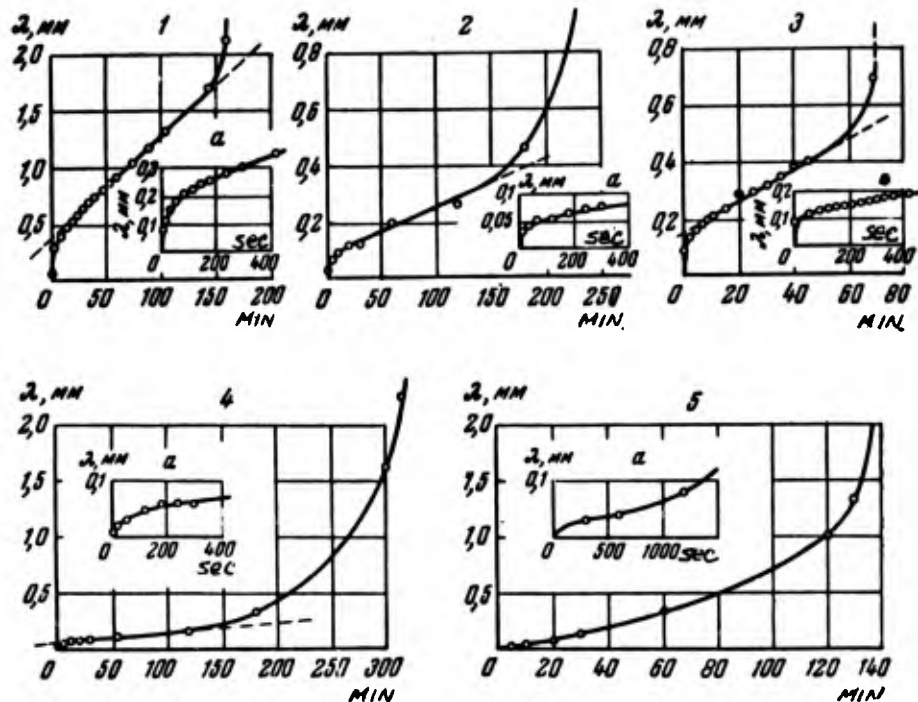


Figure 17. Growth of the displacement for a constant stress; pull-out of piles,  $\theta = -0.4^\circ\text{C}$ ; initial portion of the curve (a).

(1) Driven pile,  $\tau = 1.85 \text{ kg/cm}^2$ , heavy, silty, sandy loam (experiment 25); (2) Driven pile,  $\tau = 1.3 \text{ kg/cm}^2$ , light, silty loam (experiment 15); (3) Driven pile,  $\tau = 2.0 \text{ kg/cm}^2$ , varved clay (experiment 18); (4) Frozen-in pile,  $\tau = 1.5 \text{ kg/cm}^2$ , light, silty loam (experiment 28); (5) Frozen-in pile,  $\tau = 1.2 \text{ kg/cm}^2$ , light, silty loam (experiment 27).

It is obvious that the curves for pressing-in are analogous to those for pull-out and have a well marked bend, although the area of contact with the soil does not decrease in this case. In addition, analysis of the pull-out curves shows that progressive flow can begin for displacements of 1 to 2 mm, which corresponds to a total decrease of the working area of adfreezing of 1 to 2%; such a decrease is obviously not the cause of the transition in the progressive stage.

Thus, it might be assumed that the cause of the transition into this stage is the permanent destruction of the bonds, occurring as a result of the growth of creep strains and of their reaching a certain limiting value. It is interesting that the smallest increase of the stress can cause a sharp transition from a damped deformation to an undamped deformation and can lead to rupture. Thus in experiment 26, for  $\tau = 1 \text{ kg/cm}^2$ , the displacement of the pile stopped after 260 hr, whereas for  $\tau = 1.1 \text{ kg/cm}^2$ , an undamped deformation arose and the pile was pulled out in 2900 hr.



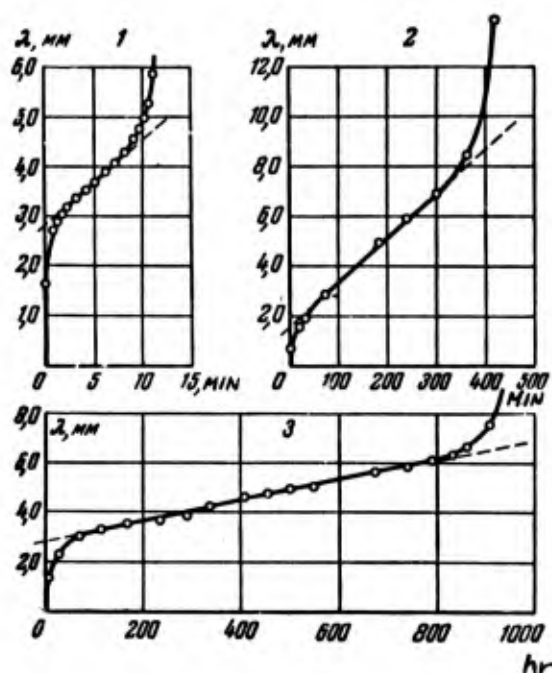


Figure 18.

Punching of model piles (disregarding the effect of the point). The piles are frozen-in; the soil is heavy silty loam;  $\theta = -0.4C$ ; (1), (2), and (3) represent respectively  $\tau = 1.7 \text{ kg/cm}^2$ ,  $0.9 \text{ kg/cm}^2$  and  $0.7 \text{ kg/cm}^2$ .

The third peculiarity of the creep process in frozen soils is the very small initial instantaneous displacements (Table 14); the main displacements develop with time.

Table 14. Growth of strain for the pull-out of model piles ( $\tau = 1.2 \text{ kg/cm}^2$ ,  $\theta = -0.4C$ ).

Soil	Deformation in mm vs time						
	10 sec	30 sec	1 min	5 min	10 min	30 min	1 hr
Sand, driven pile	0.02	0.07	0.07	0.09	0.09	0.12	0.16
Loam, driven pile	0.03	0.4	0.05	0.07	0.09	0.12	0.20
Loam, frozen-in pile	0	0	0.02	0.03	0.04	0.14	0.34

The character of the deformation curves depends somewhat on the mode of emplacement of the rods. Where they are driven into drilled holes, i.e. shearing occurs in the soil, the curves are in good agreement with the creep curves for visco-plastic bodies (Figure 1). When the rods are frozen in, the ice film, formed around the rod when the soil freezes back, has an essential influence on the shearing strength. The presence of such a film was also noted by M. N. Goldshtein (1940), and S. G. Tsvetkova (1954). The creep deformations for pull-out of

these rods (for large  $\tau$ ) have a tendency to increase indefinitely (Figure 17); this is a characteristic property of the displacement of rods frozen into pure ice; this will be further discussed later.

The compiled results of the experiments are given in Table 15 and in Figure 19, where the values of the pull-out stresses  $\tau$ , and the time  $t$ , after which the pull-out of the rod occurred (calculated from the beginning of loading), are also given. For each test, hypothetical values of the limit of the long-term strength of ad-freezing are also shown. It can be seen that the reduction process of the adfreeze strength can proceed for a very long time, up to 5000 to 6000 hr and more.

Table 15. Results of pull-out tests of model piles under constant stresses: relation between the load  $\tau$  (kg/cm<sup>2</sup>) and the time  $t$  until pull-out

Note: All experiments except 33 and 34 were conducted at a temperature of -0.4C while experiments 33 and 34 were conducted at a temperature of -3.6C.

Silty, muddy soil				Heavy, silty, sandy loam			
Experiment 22 Driven piles		Experiment 23 Frozen-in piles		Experiment 24 Driven piles		Experiment 25 Frozen-in piles	
$\tau$	t	$\tau$	t	$\tau$	t	$\tau$	t
4.5	7 sec	5.2	5 sec	4.8	14 sec	4.1	30 sec
2.3	45 "	2.4	65 "	2.3	5.3 hr	2.0	225 "
1.7	2.5 hr	2.4	205 "	2.1	33 "	1.5	0.25 hr
1.5	42 "	1.3	49 hr	1.9	429 "	1.3	95 "
1.3	77 "	1.2	465 "	1.7	788 "	1.1	no pull-out
1.2	>7300 "	1.0	3457 "	1.5	4735 "	1.0	same
1.1	4247 "	0.8	no pull-out	1.3	no pull-out	0.8	same
$\tau_{lt}=0.9-1.0$		$\tau_{lt}=0.8$		$\tau_{lt}=1.35$		$\tau_{lt}=1.0-1.1$	

Heavy, damp, sandy loam				Heavy, sandy loam			
Experiment 21 Driven piles		Experiment 13 Frozen-in piles		Experiment 15 Driven piles			
$\tau$	t	$\tau$	t	$\tau$	t		
3.8	10 sec	6.4	6 sec	4.0	10 sec		
2.3	42 "	4.2	30 "	2.7	113 "		
1.8	228 "	3.15	338 "	1.85	2.7 hr		
1.35	1.0 hr	2.1	1.25 hr	1.7	0.7 "		
1.1	1230 "	1.05	6 "	1.65	306 "		
1.0	2349 "	0.9	> 690 "	1.5	356 "		
0.9	2420 "	0.85	>4514 "	1.35	no pull-out		
0.8	3350 "	0.75	>1753 "				
$\tau_{lt}=0.75$		$\tau_{lt}=0.6-0.7$		$\tau_{lt}=1.3-1.4$			

Table 15 (continued)

Light, sandy, clayey soil				Heavy, sandy, clayey soil					
Experiment 28 Frozen-in piles		Experiment 26 Driven piles		Experiment 27 Frozen-in piles		Experiment 8 Driven piles		Experiment 12 Frozen-in piles	
$\tau$	t	$\tau$	t	$\tau$	t	$\tau$	t	$\tau$	t
4.2	13 sec	4.6	3 sec	3.5	7 sec	2.3	4 sec	4.2	7 sec
2	0.33 hr	1.7	215 "	2.0	0.3 hr	1.95	36 "	3.75	10 "
1.5	5.25 "	1.5	0.4 hr	1.5	0.5 "	1.5	156 "	2.85	32 "
1.2	8 "	1.3	4.1 "	1.2	2.2 "	1.0	0.6 hr	1.7	0.2 hr
1.0	130 "	1.2	310 "	1.0	13.1 "	1.0	6 "	1.15	1.5 "
0.8	97 "	1.1	2896 "	0.9	212 "	0.8	23 "	1.15	2.25 "
0.7	>2470 "	1.0	no pull-out	0.6	245 "	0.7	383 "	0.9	7 "
$\tau_{lt}=0.5$		$\tau_{lt}=1.0-1.05$		$\tau_{lt}=0.6-0.7$		$\tau_{lt}=0.6$		$\tau_{lt}=0.5-0.6$	
Varved clay									
Experiment 18 Driven piles with finished point in ground		Experiment 16 Driven piles		Experiment 14 Frozen-in piles		Experiment 33 Driven piles		Experiment 34 Frozen-in piles	
$\tau$	t	$\tau$	t	$\tau$	t	$\tau$	t	$\tau$	t
5.9	90 sec	3.25	7 sec	2.8	2 sec	10.3	10 sec	11.5	32 sec
4.0	25 "	2.9	9 "	2.1	4 "	6.0	0.6 hr	6.0	470 "
2.5	83 "	2.0	0.7 hr	1.8	17 "	5.15	9.5 "	4.0	55 hr
2.15	1.8 hr	1.75	6 "	1.2	115 "	4.75	6 "	3.25	745 "
2.0	1.2 "	1.6	289 "	0.8	16 hr	4.5	61 "	3.0	221 "
1.9	106 "	1.4	438 "	0.65	1866 "	4.25	50 "	2.75	no pull-out
1.8	145 "	1.3	240 "	0.5	no pull-out	4.0	no pull-out	2.5	no pull-out
1.7	no pull-out								
1.6	no pull-out								
$\tau_{lt}=1.6-1.7$		$\tau_{lt}=1.2$		$\tau_{lt}=0.6$		$\tau_{lt}=4.0$		$\tau_{lt}=2.75$	

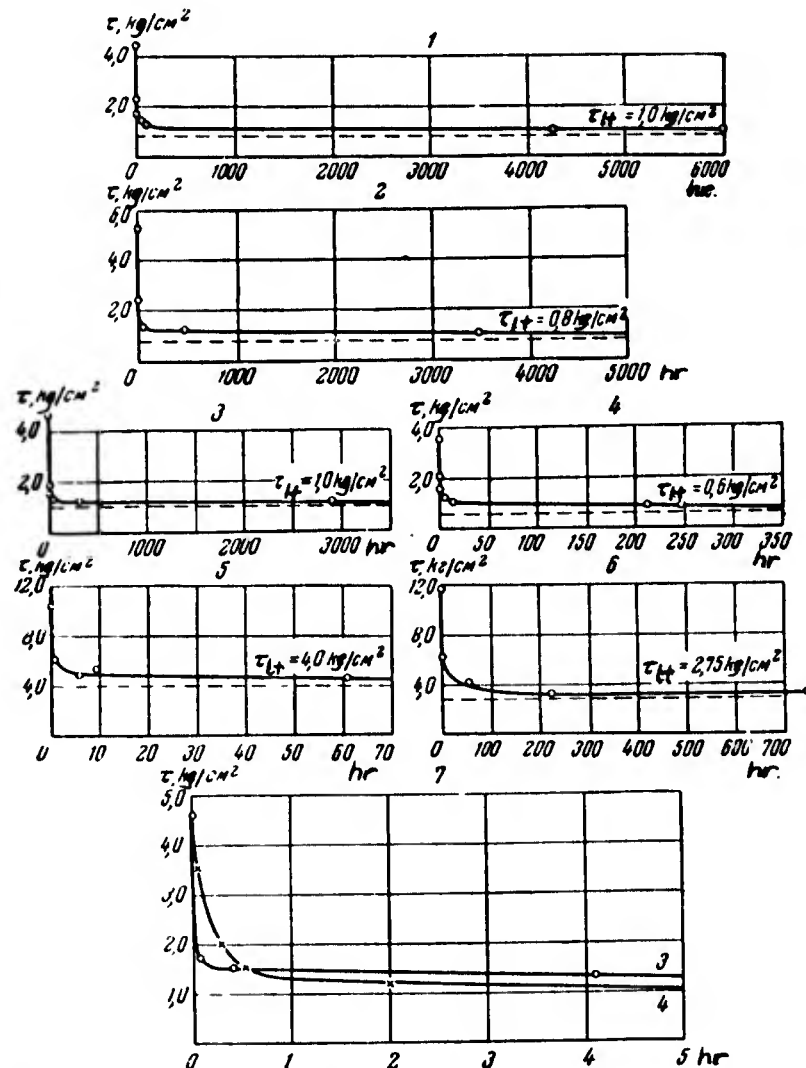


Figure 19. Curves of the long-term adfreeze strength.

(1) Silty, muddy soil,  $\theta = -0.4C$ , driven pile (experiment 22); (2) Silty, muddy soil,  $\theta = -0.4C$ , frozen-in pile (experiment 26); (3) Light, silty loam,  $\theta = -0.4C$ , driven pile (experiment 26); (4) Light, silty loam,  $\theta = -0.4C$ , frozen-in pile (experiment 27); (5) Heavy, silty loam,  $\theta = -3.6C$ , driven pile (experiment 33); (6) Heavy, silty loam,  $\theta = -3.6C$ , frozen-in pile (experiment 34); (7) Initial parts of curves (3) and (4).

The most intensive reduction of the adfreeze strength occurs, as in the case of cohesion, in the initial period; this is reflected by the sharp inflection of the curves shown. Thus, for  $\theta = -0.4C$ , during

the first 100 to 400 sec, the value of  $\tau$  decreases by a factor of 1.5 to 3 with respect to  $\tau_{\text{inst}}$ ; after 50 hr, the value of  $\tau$  decreases by a factor of 3 to 4 times. Further reduction becomes insignificant, and the curves of the long-term strength approach straight horizontal asymptotes.

In general, the adfreeze strength decreases for driven piles by 4.2 to 5.4 times for  $\theta = -0.4^\circ\text{C}$ , and by 2.6 times for  $\theta = -3.6^\circ\text{C}$ ; whereas for frozen-in piles, it decreases by 5.8 to 9.8 times for  $\theta = -0.4^\circ\text{C}$ , and by 4.2 times for  $\theta = -3.6^\circ\text{C}$ . Hence it follows, that first, the reduction of the strength occurs more intensively for plastic frozen soils with higher temperatures; secondly, this lowering occurs to a greater extent for frozen-in piles, where the relaxation properties of ice are the primary influences.

#### 4. Deformation process for an increasing load

The results of the pull-out tests of rods with a gradual load increase are shown in Table 16; the values of the load  $\tau$  for each stage, and the time interval  $\Delta t$  of their action, as well as the constant rate\* of the visco-plastic flow  $v = \frac{d\lambda}{dt} f_1$ , are given. Zero on this graph denotes the stabilization of the deformation. The appearance of a permanent deformation indicates that the stress has exceeded the limit of long-term strength, which determined  $\tau_{lt}$ .

Let us consider the curves of the displacement of the rod for gradual loading (Figure 20). The character of these curves is such that when loading with constant stresses: for small loads, the deformation (displacement) is damped with time; for loads exceeding  $\tau_{lt}$ , a permanent deformation develops with an increasing rate for larger  $\tau$ .

From the principle of superposition, the deformation caused by the action of some changing load is equal to the sum of the creep deformation due to the action of the increasing load. Assuming that the creep curves are similar, i.e. for various  $\tau = \text{const}$ , their ordinates are proportional to some function of the stress  $\phi(\tau)$ , we get an expression connecting the creep deformation to stress. For loading in steps at constant temperature,

$$\gamma(t_n) = \frac{\tau_n}{G_1} + \phi(\tau_0)F(t_0) + \sum_{i=1}^n [\phi(\tau_i) - \phi(\tau_i - 1)] F(\Delta t_i),$$

where  $\frac{\tau_n}{G_1} = \gamma_1$  is the initial displacement caused by the action of the total load  $\tau_n$ , assumed, in accordance with the test data, to be proportional to this load.  $\tau_0$  is the initial load (first stage);  $t_0$  is the time of action of this load;  $\Delta t_i$  is the interval of the time of action of each  $i$ -th stage of the loading;  $t_n$  is the time at which the displacement is determined, and  $F(t)$  is the analytical expression of the creep curve for a unit load  $\tau = 1$ .

Proceeding from the previous expression and taking into consideration that the failure is determined when the displacements reach a

\* Determined as the average of the last three days.

Table 16. Results of pull-out tests on model piles with loads rising in steps

Silty, muddy soil										Heavy, silty, sandy loam									
Experiment 22 Driven piles					Experiment 23 Frozen-in piles					Experiment 24 Driven piles					Experiment 25 Frozen-in piles				
$\tau$	$\Delta t$	$V$			$\tau$	$\Delta t$	$V$			$\tau$	$\Delta t$	$V$			$\tau$	$\Delta t$	$V$		
0.2	240	0			0.8	2178	0.2			1.3	240	0.6			0.8	1342	0		
0.4	240	0			0.9	262	0.4			1.4	240	1.8			0.9	240	0		
0.6	240	0			1.0	242	0.8			1.5	240	3.6			1.0	240	0.2		
0.8	240	0.33			1.1	89	pull-out			1.6	240	6.4			1.1	240	0.4		
1.0	240	1.67								1.7	50	pull-out			1.2	240	0.6		
1.2	240	3.33													1.3	240	0.6		
1.4	102	pull-out													1.4	166	pull-out		
$\tau_{lt} = 0.75 - 0.8$					$\tau_{lt} = 0.7 - 0.75$					$\tau_{lt} = 1.25$					$\tau_{lt} = 0.9$				
Heavy, sandy loam										Light, silty, sandy loam									
Experiment 15 Driven piles					Experiment 36 Frozen-in piles					Experiment 28 Frozen-in piles									
$\tau$	$\Delta t$	$V$			$\tau$	$\Delta t$	$V$			$\tau$	$\Delta t$	$V$			$\tau$	$\Delta t$	$V$		
1.35	1078	0			0.7	240	0			0.2	240	0			0.2	240	0		
1.45	288	0			0.8	240	0			0.3	240	0			0.3	240	0		
1.55	336	1.7			0.9	240	0.67			0.4	240	0.33			0.4	240	0.33		
2.2	0.15	pull-out			1.0	240	pull-out			0.5	240	1.33			0.5	240	1.33		
						49				0.6	240	4.0			0.6	240	4.0		
										0.7	240				0.7	240			
										0.8	240				0.8	240			
										0.9	pull-out				0.9	pull-out			
$\tau_{lt} = 1.4 - 1.5$					$\tau_{lt} = 0.75$					$\tau_{lt} = 0.45$									

Note: (1)  $\tau$  is in kg/cm<sup>2</sup>,  $\Delta t$  is in hr,  $v$  is in 0.01 mm/day; (2) all the experiments except 34 were carried out at -0.4C; experiment 34 was conducted at -3.6C.

Table 16 (continued)

Light, sandy, clayey soil						Heavy, silty, sandy loam (very damp)					
Experiment 26 Driven piles			Experiment 27 Frozen-in piles			Experiment 21 Driven piles					
$\tau$	$\Delta t$	$v$	$\tau$	$\Delta t$	$v$	$\tau$	$\Delta t$	$v$	$\tau$	$\Delta t$	$v$
1.0	742	0	0.6	1634	0	0.9	2420	3.0			
1.1	240	0	0.7	288	0.33	1.0	120	7.0			
1.2	240	0.33	0.8	240	1.0	1.2	90	pull-out			
1.3	240	4.0	0.9	240	4.5						
1.4	85	pull-out	1.0	3	pull-out						
$\tau_{lt} = 1.1$			$\tau_{lt} = 0.6 - 0.65$			$\tau_{lt} = 0.8$					
Varved clay											
Experiment 18 Driven piles			Experiment 16 Driven piles			Experiment 35 Frozen-in piles			Experiment 34 Frozen-in piles		
$\tau$	$\Delta t$	$v$	$\tau$	$\Delta t$	$v$	$\tau$	$\Delta t$	$v$	$\tau$	$\Delta t$	$v$
0.25	401	0	1.1	814	0	0.4	240	0	2.75	774	0
0.5	192	0	1.2	240	0	0.6	240	0	3.0	786	0.16
0.75	144	0	1.3	240	0	0.8	240	0.33	3.25	457	pull-out
1.0	240	0	1.4	240	0.2	1.0	240	2.56			
1.25	268	0	1.5	240	1.0	1.2	48	pull-out			
1.5	1274	pull-out	1.6	240	3.0						
			1.7	39	pull-out						
$\tau_{lt} = 1.4$			$\tau_{lt} = 1.3$			$\tau_{lt} = 0.7 - 0.75$			$\tau_{lt} = 2.5$		

Note: (1)  $\tau$  is in kg/cm<sup>2</sup>,  $\Delta t$  is in hr,  $v$  is in 0.01 mm/day. (2) All the experiments except 34 were carried out at -0.4°C; experiment 34 was conducted at -3.6°C.



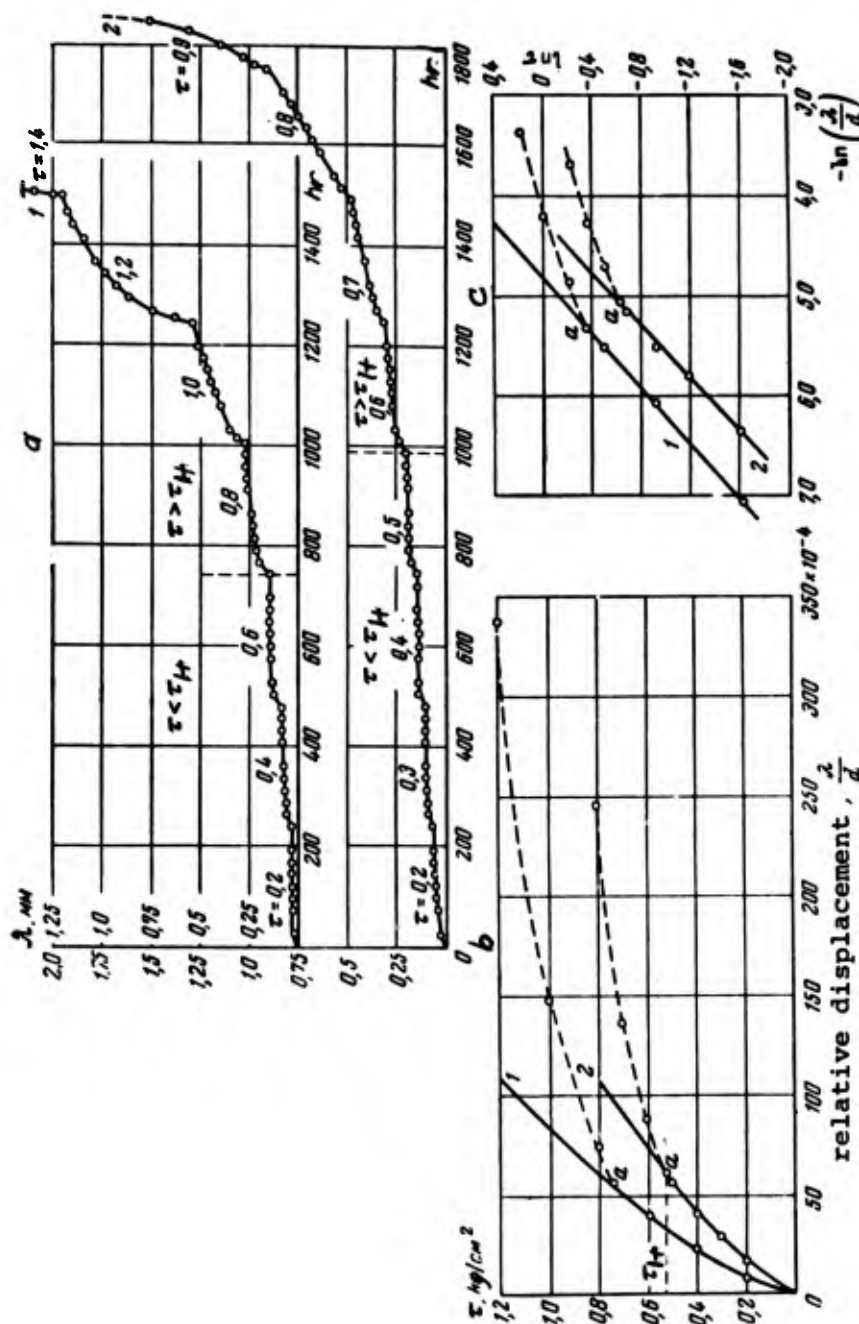


Figure 20. Growth of the displacement for pull-out model piles under a gradually applied load;  $\theta = -0.4C$

- Growth of the displacement with time.
- Dependence of the displacement upon the load.
- Same as diagram b but in logarithmic coordinates.
  - Silty, muddy sand, driven pile (experiment 22);
  - Light loam, frozen-in pile (experiment 28).

certain constant value, regardless of the type of loading, we must obtain matching values of  $\tau_{1t}$ , determined experimentally, both for gradually-increasing, and for constant, loads. Comparison of the data in Tables 15 and 16 corroborates the validity of such a matching.

Let us now proceed to the development of the relationship between tangential stress and strain. The appropriate curves are shown in Figure 20. The relative displacement of the pulled-out piles  $\gamma = \frac{\lambda}{d}$  is plotted as the abscissa, at the end of each stage. An analysis of the data has shown that the curves fit the exponential relation:

$$\tau = A\gamma^\alpha, \quad (24)$$

where  $A$  is the deformation modulus ( $\text{kg/cm}^2$ ), equal to the load for which the rod moves a distance equal to its diameter;  $\alpha$  is the strengthening coefficient. These parameters depend upon the type of soil, temperature, and moisture content, as well as upon the method of emplacing the rods.

The accuracy of equation (24) is verified by the rectilinearity of the curve when the experimental points are plotted logarithmically. From this graph, the parameter  $\alpha$  is determined as the slope of the straight line, as well as the value of  $\ln A$ , which corresponds to the intersection of the straight line with the ordinate axis. For example, in experiment 22 (silty, muddy soil;  $\theta = -0.4^\circ\text{C}$ , driven pile), we obtained  $A = 30.5 \text{ kg/cm}^2$ , and  $\alpha = 0.715$ ; for experiment 28 (sandy loam,  $\theta = -0.4^\circ\text{C}$ , frozen-in pile), we obtained  $A = 23.8 \text{ kg/cm}^2$ , and  $\alpha = 0.75$ . However, equation (24) is accurate only for stabilizing displacements, i.e. until the load reaches the limit of long-term strength. After this limit, a sharp departure of the experimental points from the curve occurs. This departure is explained by the appearance of permanent deformations, the values of which are determined not only by the load, but also by the time of action. Thus, the point of inflection "a" of the curve  $\gamma = f(\tau)$ , which is sharply marked on the logarithmic graph (Figure 20), characterizes the transition from damped strain to permanent strain, i.e. it determines the long-term strength.

For the samples examined, the values of  $\tau_{1t}$ , determined by this method, were as follows: experiment 22,  $\tau_{1t} = 0.75 \text{ kg/cm}^2$ , and in experiment 28,  $\tau_{1t} = 0.5 \text{ kg/cm}^2$ . According to indirect determinations (Table 16), these quantities are also equal to  $0.75 \text{ kg/cm}^2$  and  $0.5 \text{ kg/cm}^2$ .

In Table 17, the experimental values of  $\gamma$  and those computed from equation (24) are given; the dotted line indicates the beginning of the divergence between these values, which corresponds to the inflection of the curve.

### 5. Visco-plastic flow

The mechanism of deformation in the stage of visco-plastic flow is characterized by a relationship between stress and rate of flow. Pull-out experiments of model piles have shown that in a definite range of stresses that does not exceed the limiting value of  $\tau_{1t}$  by

Table 17. Experimental and theoretical values of the displacement

Experiment 22					Experiment 28				
$\tau, \text{kg/cm}^2$	$\gamma \cdot 10^4$		$-\ln \gamma$		$\tau, \text{kg/cm}^2$	$\gamma \cdot 10^4$		$-\ln \gamma$	
	Expmt.	Theor.	Expmt.	Theor.		Expmt.	Theor.	Expmt.	Theor.
0.2	8.57	8.7	7.06	7.04	0.2	17.1	17.1	6.37	6.37
0.4	22.8	23.0	6.08	6.07	0.3	30.0	29.0	5.81	5.84
0.6	40.0	41.0	5.52	5.50	0.4	40.0	42.0	5.52	5.46
0.8	74.3	61.5	4.89	5.09	0.5	57.1	58.0	5.17	5.15
1.0	148.5	84.0	4.21	4.78	0.6	88.5	75.0	4.73	4.91
1.2	337.1	108.0	3.39	4.53	0.7	137.0	92.0	4.30	4.71
1.4	Pile pulled out				0.8	246.0	109.0	3.71	4.52
					0.9	Pile pulled out			

much, i.e. for moderate rates of deformation, the relationship between the steady rate of displacement of the pile ( $dy_{f1}/dt = \xi_{f1} = \text{const}$ ) and the excess stress ( $\tau - \tau_{1t}$ ) can be described by

$$\xi_{f1} = \frac{1}{\eta} (\tau - \tau_{1t})^\beta, \quad (25)$$

where  $\beta > 1$  and  $\eta'$  are parameters depending upon the type of soil, its temperature, moisture content, and the method of emplacing the rods. However, for some (plastic) soils the value of  $\beta$  is close to unity for a narrow range of stress variation. Therefore in such cases, we can use the linear relationship (Figure 21) between  $\xi_{f1}$  and  $(\tau - \tau_{1t})$  in the Bingham-Shwedoff form,

$$\xi_{f1} = \frac{1}{\eta_{pv}} (\tau - \tau_{1t}), \quad (26)$$

where  $\eta_{pv}$  is the plastic viscosity, appearing as functions of  $\theta$  and  $\underline{W}$ .

The value of  $\tau_{1t}$ , corresponding to the transient conditions from damped to permanent deformation, can be determined from the graph  $\xi = f(\tau)$  (Figure 21) through the value of the segment of the ordinate axis intercepted by the continuation of the straight line (or the smooth curve); this follows from the condition  $\tau = \tau_{1t}$ , for  $\xi = 0$ . The values of  $\tau_{1t}$  obtained by this method, as well as the values determined indirectly from experiment, are given in Table 18. From that table, one can see that the agreement obtained is quite satisfactory. In that table, the values of  $\eta_{pv}$  are also given, computed as the slope of the curve  $\xi_{f1} = f(\tau)$ , for  $\theta = -0.4C$ .

In shear, the coefficient of viscosity for ice (according to the literature) ranges between  $10^{14}$  and  $10^{15}$  poises; hence, it is larger than the value for rods surrounded by frozen soil. For frozen-in rods, the coefficient  $\eta$  is larger than for driven rods by a factor of 2 to 8; this is explained by the effect of the ice film. In shear, most of

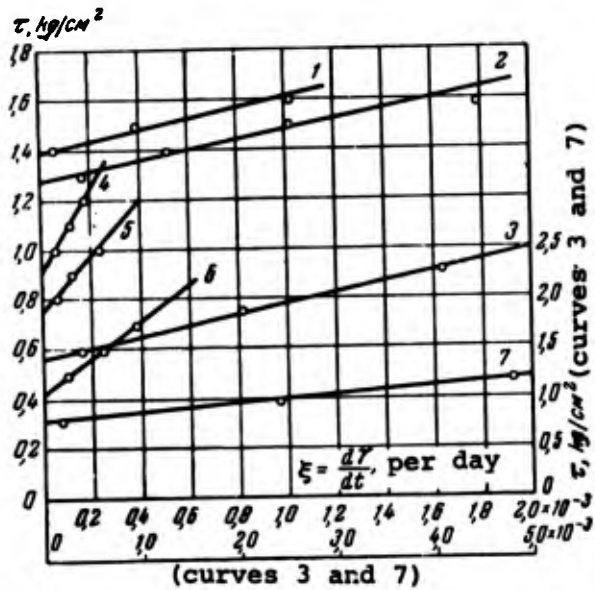


Figure 21. Relationship between the rate of displacement of model piles and the applied stress.

(1), (2), (3), are for driven model piles; (4), (5), (6) for frozen-in piles; (7) is for frozen-in piles with indentations. Soils (1) and (7) are varved clay (experiment 16 and 35); (2), (3), (4) are heavy, sandy loam (experiment 24, 24a, and 25); (5) is silty, muddy soil (experiment 23); (6) is light loam (experiment 28).

Table 18. Values of  $\tau_{1t}$  and  $\eta_{pv}$  ( $\theta = -0.4C$ )

Number of the experiment	Soil	Driven piles			Frozen-in piles		
		$\eta \cdot 10^{-13}$ Poise	$\tau_{1t}$ , kg/cm <sup>2</sup>		$\eta \cdot 10^{-12}$ Poise	$\tau_{1t}$ , kg/cm <sup>2</sup>	
			Analyt.	Expmt.		Analyt.	Expmt.
22,23	Silty, muddy	4.0	0.75	0.8	9.75	0.75	0.7
24,25	Heavy, silty, sandy loam	1.75	1.3	1.25	14.4	0.9	0.9
24	The same, according to the data of tests with constant stresses	1.85	1.1	1.30	-	-	-
21	Damp, heavy, silty, sandy loam	0.75	0.8	0.8	-	-	-
28	Light, silty loam	-	-	-	6.2	0.40	0.45
26,27	Light loam	0.9	1.2	1.1	4.5	0.65	0.6
16,35	Varved clay	1.95	1.4	1.3	2.7	0.8	0.7
35	The same, pile with an indentation	-	-	-	0.7	0.8	0.75

the properties are deduced from the results of pull-out tests of frozen-in rods having annular notches (experiment 35) in which shearing of soil against soil is occurring. In addition, since the influence of the ice film was almost insignificant, the values of the coefficient of viscosity obtained were not significantly lower than for smooth rods.

The displacement of rods has been previously examined. However, in addition to sliding of the rod itself, a shearing deformation occurs in the surrounding soil, caused by the moving of its particles as the rod moves. First, the soil is displaced together with the rod; secondly, when the strain reaches a limiting value, the cohesion between the soil and the rod is broken and the rod slides through the ground. Proceeding from the Bingham-Shwedoff law for viscoplastic flow (4), for an arbitrary point at a radial distance  $\rho$  and a displacement  $u$  of the rod, we can write (Figure 22),

$$\frac{P}{\omega_\rho} - \tau_{lt} = \eta \frac{dv}{d\rho},$$

where  $\omega_\rho = 2\pi\rho l$  is the area of the shearing surface;  $r$  is the radius of the rod, and  $\frac{dv}{d\rho}$  is the gradient, along the normal  $\rho$  to the direction of motion, of the rate of displacement ( $u$ ) of the soil particles,  $v = \frac{du}{dt}$ .

Hence the deformation of the soil surrounding a pile is governed by the following differential equation:

$$-2\pi\rho l \eta \frac{dv}{d\rho} + 2\pi\rho l \tau_{lt} = P.$$

Integrating this equation and using the boundary conditions:  $v = v_0$  at  $\rho = r$  and  $v = 0$  at  $\rho = R$ , where  $R$  is the radius of the region of deformation of the soil, we get  $\eta v_0 = \frac{P}{2\pi l} \ln \frac{R}{r} - \tau_{lt} (R - r)$ .

$v_0$  denotes the rate of displacement of the soil particles at the soil-rod interface.

Considering that

$$\frac{P}{P_{lt}} = \frac{2\pi R l \tau_{lt}}{2\pi r l \tau_{lt}} = \frac{R}{r},$$

we obtain

$$\eta v_0 = \frac{P}{2\pi l} \ln \frac{P}{P_{lt}} - \tau_{lt} r \left( \frac{P}{P_{lt}} - 1 \right);$$

or setting

$$P = 2\pi r l \tau \quad \text{and} \quad \frac{P}{P_{lt}} = \frac{\tau}{\tau_{lt}},$$

we shall have

$$\eta v_0 = r \left[ \tau \ln \frac{\tau}{\tau_{lt}} - (\tau - \tau_{lt}) \right].$$

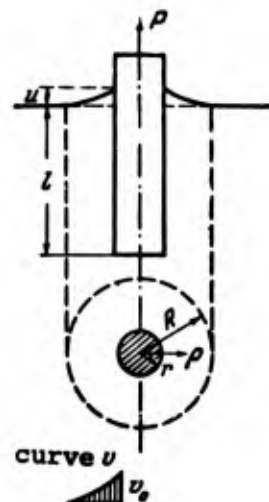


Figure 22.

Region of viscoplastic deformation of the soil.

This equation can also be expressed as an average rate of relative shear:

$$\epsilon_{av} = \frac{v}{r \ln \frac{R}{r}} = \frac{1}{\eta} \left( \tau - \frac{\tau - \tau_{lt}}{\ln \frac{\tau}{\tau_{lt}}} \right)$$

To simplify these relations, we shall expand  $\ln \left( \frac{\tau}{\tau_{lt}} \right)$  in a power series; keeping the first non-zero term, we get

$$\eta \frac{v_0}{r} = \frac{(\tau - \tau_{lt})^2}{\tau - \tau_{lt}}, \quad (27)$$

and

$$\epsilon_{av} = \frac{1}{2\eta} (\tau - \tau_{lt}).$$

Hence for shear, the viscosity of frozen soil particles (for  $\theta = \text{const}$ ) is determined by the expression,

$$\eta = \frac{r}{v_0} \frac{(\tau - \tau_{lt})^2}{\tau - \tau_{lt}}, \quad (27a)$$

it will be different from the value of the apparent coefficient of viscosity for the sliding of the rod through the soil, as determined by equation (26). The displacement of the rod does not obey equation (27), obtained for an axially symmetric loading; it is governed by Bingham's equation (26). This is explained by the different character of the processes of sliding of the rod through the soil, and of shearing of the particles around this rod. On the other hand, it can indicate a non-linear relationship between stress and the rate of flow of frozen soil for pure shear, as described by equation (25).

#### 6. Conditions for similarity of piles of various dimensions

The investigations have shown that the specific pull-out stress, i.e. the stress per  $\text{cm}^2$  of lateral surface of the pile, depends upon the dimensions of the piles both for the instantaneous and long-term cases. The influence of the dimensions of the piles on the instantaneous adfreezing strength was noted even earlier by N. A. Tsytoich, I. C. Vologdina, and N. I. Saltykov. The latter showed that the strength diminishes as the diam of the piles increases, in accordance with a dampening law; he suggested that for  $d > 16 - 20$  cm, the change of the diameter ceases to influence the value of  $\tau_{inst}$ .

In order to investigate this question more thoroughly, pull-out tests on frozen-in and driven pile models with various  $l/d$  ratios were performed. The stress was applied both instantaneously and in stages which were maintained for equal time intervals (Figure 23). For driven piles, the diameter of the holes was  $0.9d$  of the pile, whereas for frozen-in piles it was  $1.45d$ . The experiments were conducted with varved clay and sandy loam at  $\theta = -0.4^\circ\text{C}$ . The experiments showed that the value of the displacements of the piles increases as their

diameters increase, since this is related not only to the absolute value of the displacement  $\lambda$ , but also to relative value  $\gamma = \frac{\lambda}{d}$  (Figure 23). Consequently, the pull-out of piles of larger diameter occurred for a smaller value of the specific stress  $\tau = \frac{P}{\pi d l}$ . An analogous phenomenon occurs for frozen-in piles. In order to eliminate the influence of deformation of the soil surface, and to obtain the shear directly at the soil-pile interface, an experiment was conducted with a load on the surface. In this case, the pull-out resistance of the pile decreased, confirming the role of the soil mass in the work of the pile. However, even under that condition, the value of the pull-out stress was found to depend upon the diameter of the pile.

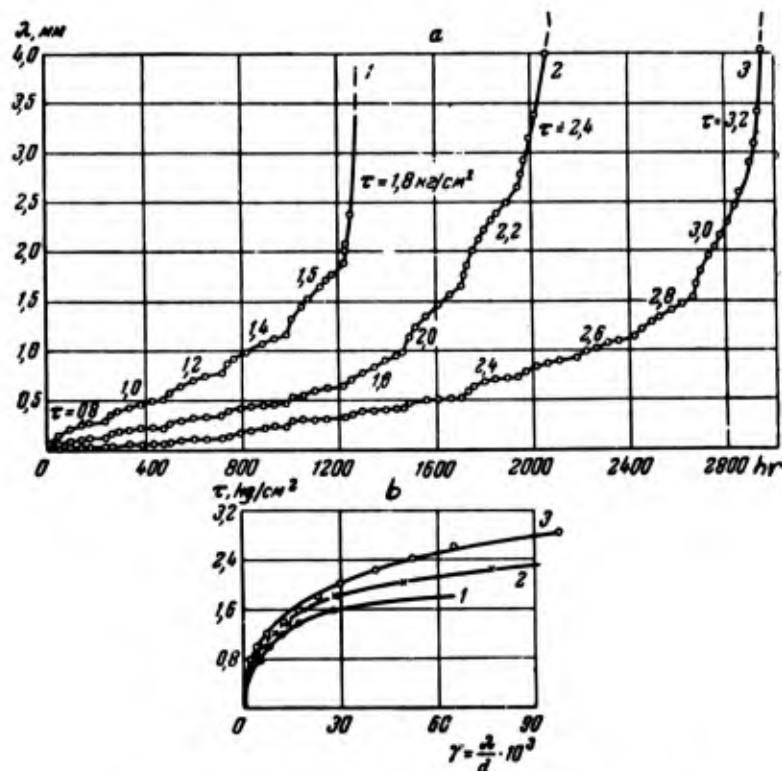


Figure 23. Pull-out tests of model piles of various diameters.

a. Displacement of the pile for loading in steps. b. Relation between the stress and the relative displacement. (1), (2), and (3) are respectively  $d = 70$  mm;  $35$  mm; and  $17.5$  mm.

From Figure 24a, one can see that as  $d$  increased by a factor of 4 (for  $l = \text{const}$ ), the specific strength under long-term pull-out decreased by a factor of approximately 1.8. It was also noted that  $\tau$  decreases as  $d$  increases, even when the length and diameter of the



pile increases in such a way as to maintain  $l/d$  constant (Figure 24b). On the other hand, when only the length of the pile is increased, keeping  $d = \text{const}$ , the adfreezing strength decreases somewhat. Thus, the tests of model piles of small dimensions give excessive values of the adfreezing strength as compared to the values for real piles. The actual values are asymptotic limits approached by the curves showing the dependence of  $\tau$  upon the dimensions of the piles. Taking into account the damping character of the above-mentioned curves, one must agree with N. I. Saltykov, that for sufficiently large dimensions ( $d > 15 - 18 \text{ cm}$ ), the influence of the diameter of the pile is insignificant. Therefore, results of tests of actual piles must give values of  $\tau_{lt}$  close to the actual values.

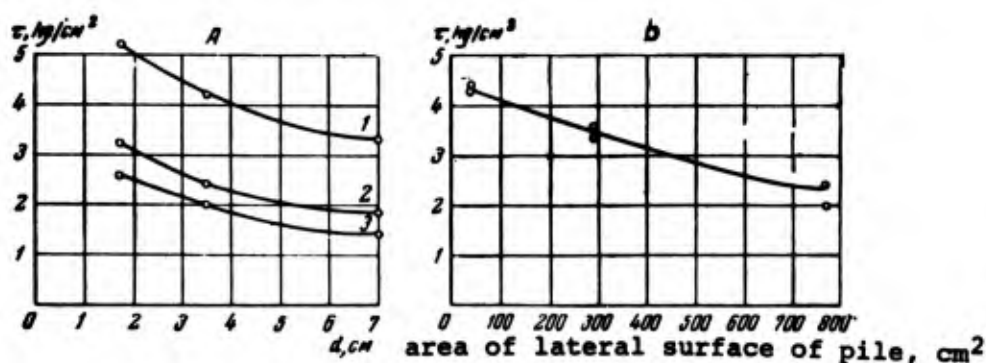


Figure 24. Influence of the dimensions of the pile on the adfreezing strength.

a. Variation of the pull-out stress ( $\tau$ ) vs the diameter ( $d$ ) of the pile for  $l = \text{const}$ , for the following cases: 1) instantaneous loading, 2) loading in steps ( $\Delta t = 240 \text{ hr}$ ), 3) the same as 2, but with loading of the surface. b. Variation of the pull-out stress ( $\tau$ ) vs the area of the lateral surface of the pile for  $l/d = \text{const}$ ; loading in steps ( $\Delta t = 1 \text{ hr}$ ).

In the experiments with models, it is necessary to take into account the conditions of similarity which we shall examine below.

The question of the similarity of the visco-plastic flow has been investigated in general by N. V. Tyabin (1951). At the author's request, he has been so kind as to completely solve the axi-symmetrical problem (unpublished) examined below. The Bingham-Genki-Ilyushin flow equation for the three-dimensional problem is written by N. V. Tyabin as follows:

$$\rho(F - \omega) - \nabla \tau + \eta \nabla v + \nabla \theta = 0, \quad (a)$$

where  $\rho$  is the density;  $F$  is the external force acting on the unit mass;  $\omega$  is the acceleration;  $\tau$  is the mean shearing stress;  $\eta$  is the plastic viscosity;  $\theta$  is the tensor of the yield stresses;  $\nabla$  is the differential operator, and  $v$  is the rate of shear.

For a steady process, the condition of similarity, i.e. the dimensionless form of the solution (a) in the axially symmetric case (Figure 22), is the following

$$E_u = f(R_e, A, \Gamma), \quad (b)$$

where  $E_u = \frac{\tau}{\rho v}$  is the Euler number;  $R_e = \frac{vd\rho}{\eta}$  is the Reynolds number;  $A = \frac{\tau_{lt}}{\rho v^2}$  is the Tyabin number, and  $\Gamma = l/d$  is the ratio of the length of the pile to its diameter.

For both full-sized (N) and model (M) experiments, the density, viscosity and yield stress (adfreeze strength) are equal, namely:

$$\rho_N = \rho_M, \quad \eta_N = \eta_M \quad \text{and} \quad \tau_{lt(N)} = \tau_{lt(M)}.$$

Hence, from the conditions  $R_{e(N)} = R_{e(M)}$ ,  $A_N = A_M$ , and  $\Gamma_N = \Gamma_M$ ,

we deduce

$$v_M d_M = v_N d_N; \quad v_M^2 = v_N^2, \quad \text{and} \quad l_M d_N = l_N d_M. \quad (c)$$

This means that the dimensions of the pile models must be equal to the full-sized piles, or the similarity conditions will not be fulfilled. The experimental data also led to this conclusion. How then is one to proceed to use models under laboratory conditions when the dimensions of the model are significantly smaller than those of full-sized piles? Let us assume that the viscosity and the limiting long-term shearing stress are respectively equal, constant and known for both full-sized and model piles. The rate of flow  $v$  and the dimensions of the pile  $l$  and  $d$  vary. Then the similarity condition takes the form,

$$d_M v_M \rho_M = v_N d_N \rho_N; \quad \rho_M v_M^2 = \rho_N v_N^2 \quad \text{and} \quad \frac{l_M}{d_M} = \frac{l_N}{d_N},$$

hence,

$$\frac{v_N}{v_M} = \frac{l_N}{l_M} = \frac{d_N}{d_M}. \quad (d)$$

This is the similarity condition; therefore, the similarity of the process is ensured when the ratio of the rates of flow equals the length - diameter ratio. Let us assume that  $d_N$  and  $l_N$  are constant and that we wish to model the pull-out of piles under various stresses  $\tau$ , i.e. for various rates of flow, in order to plot the curve of the long-term strength or the graph of the relation between  $\tau$  and  $v$ , and determine  $\tau_{lt}$  through it. Then, to ensure similarity conditions, one must change the values of  $l$  and  $d$  of the model for each different value of  $\tau$ ; this allows the change in the rate to satisfy condition (d). Observing this condition, and changing the rate of flow for each test with a given  $l$  and  $d$ , one can obtain a value of the pull-out force for full-sized piles from the dimensionless relation (b) written in the following form:

$$E_u = K_1 \Gamma^\alpha R_e^\beta + K_2 \Gamma^\gamma A^\delta. \quad (e)$$

The coefficients  $K_1$  and  $K_2$  and the parameters  $\alpha$ ,  $\beta$ ,  $\gamma$ , and  $\delta$  are

determined experimentally from the graphs of the relation  $E_u = f_1(r)$ ,  $E_M = f_2(R_e)$  and  $E_u = f_3(A)$ , other dimensionless numbers remaining constant and  $\rho$ ,  $n$  and  $\tau_{1t}$  being known ( $\tau_{1t}$  can be determined from a test for pure shear). As a result, we get a formula which determines the pull-out stress for any dimensions of the pile,

$$P_{1t} = \pi d l (K_1 r^a R_e^b + K_2 r^c A^d). \quad (f)$$

Nevertheless, one must note the complexity of determining the parameters of this equation, as well as the lack of clarity of the relation between yield stress and adfreeze strength of the soil with piles. These factors render the above procedure inadequate for practical application in laboratory experiments. However, with the accumulation of experimental data, it appears that, using the considerations revealed above, it will be possible to find conversion factors for the transition from laboratory data to full-scale which are acceptable for practical purposes.

One can arrive at the same conclusions concerning the similarity conditions for piles of various dimensions with simple constant criteria, if one examines the condition of its limiting equilibrium, proceeding from the theory of similarity of elasto-plastic media as developed by V. V. Sokolovskiy (1950) and V. A. Florin (1948), instead of the visco-plastic condition of the soil around the pile. For a body obeying:

(1) in the plastic region, the Saint-Venant condition  $\tau = c = \text{const}$ , and

(2) in the elastic region, the non-linear relation  $\bar{\gamma} = \phi(\bar{\tau})$  connecting the shearing strain  $\bar{\gamma}$  and the tangential stresses  $\bar{\tau}$ , any solution of the three-dimensional elasto-plastic problem must satisfy the equations of equilibrium and the equations of compatibility as well as the equation of plasticity. The identity of the equations for full-sized and model piles constitutes the similarity criterion. It is ensured only if the ratios of the scales satisfy the equality,

$$\alpha_\tau = \alpha_u = \alpha_c = \alpha_e \alpha_q,$$

where  $\alpha_\tau$  is the ratio of stresses for full-sized and model piles;  $\alpha_u$  is the ratio of the displacements;  $\alpha_c$  is the ratio of the cohesion forces;  $\alpha_q$  is the ratio of the body forces, and  $\alpha_e$  is the ratio of linear dimensions. It therefore follows that the distribution of stresses and the configuration of the actual and model plastic regions will be similar only if the volumetric weight of the soil in the model is increased in the same proportion as the ratio of the linear dimensions of the full-sized model. Such modelling is only possible in a centrifuge.

#### 7. Limiting long-term adfreeze strength of soil with wooden rods

The combined results of calculations of the instantaneous and long-term yield stresses of soil along the lateral surface of pile models, i.e. the adfreeze strengths, are given in Table 19.

Above, all the fact that the long-term yield strength of driven piles is significantly higher than that of frozen-in piles is worth

Table 19. Resistance of frozen soils to movement along the surface of wooden rods (adfreeze strength) according to laboratory experiments

Soil	Tempera- ture °C.	Moisture Content %		Frozen-in piles		Driven Piles	
		Natural	After adfreezing (for frozen-in piles)	Strength $\tau$ , kg/cm <sup>2</sup>			
				$\tau_{inst}$	$\tau_{lt}$	$\tau_{inst}$	$\tau_{lt}$
Heavy, silty, sandy loam	-3.6	34	42	11.5	2.6	10.3	4.0
The same	-0.4	30	35	4.1	0.75- 1.0	4.8	1.3 - 1.4
The same damp	-0.4	47	44	4.2	0.6	3.8	0.75
Light, sandy, clayey soil	-0.4	36	35	3.5- 4.2	0.5-- 0.7	4.6	1.0
Sandy, silty, muddy soil	-0.4	34	30	-	0.7	4.5	1.0
Varved clay, dense	-0.4	42	45	-	0.5 - 0.6	-	1.0 - 1.5

noting. This can be explained as follows: (1) the strength of the pile emplacement increases due to frictional forces arising from the compression of the soil during driving of the piles; (2) on the other hand, the stability decreases because of the influence of the film. This film, forming around the frozen-in piles, has a weakening influence, since the long-term strength of ice is close to zero. The gradation and plasticity of the soils have a lesser, but appreciable, influence on the adfreeze strength. The greater the clay and silt fractions of the soil, the higher their plasticity and moisture content, and the smaller the adfreeze strength (for driven, as well, as for frozen-in piles). The effects of the unfrozen water, and the small value of the friction in fine-grained soils, are evident in this behavior. Varved clay is an exception, giving quite large values of  $\tau$  for driven piles; this is due to the increased density of these soils. It is interesting to note that when the natural structure of varved clay breaks up during emplacement of piles by the freezing-in method, its adfreeze strength is the lowest in comparison to other soils. This emphasizes the importance of the structure and structural stability of frozen soils.

The adfreeze strength, like other strength properties of frozen soils, depends strongly upon the temperature. Thus a drop of  $\theta$  from -0.4°C to -35°C increases  $\tau_{lt}$  by a factor of approximately 2.5 to 3.5 (Table 19). The influence of temperature on the adfreeze strength is illustrated in Figures 25 and 26. In Figure 26a, the test data for piles placed by steaming into silty, sandy loam and loam soils under field conditions are given. The data concerning the apparent adfreeze strength, obtained by I. N. Votyakov under laboratory conditions, for the punching

of frozen-in rods under short duration loads growing in steps, are given in Figure 26b. The relation between  $\tau$  and  $\theta$  is described by the same type of empirical formula as (23), i.e.

$$\tau = \tau_0 + a\sqrt{|\theta|}, \quad (28)$$

where  $\tau_0$  is the adfreeze strength at a given temperature and  $a$  is a parameter dependent on the type of soil and its moisture content.

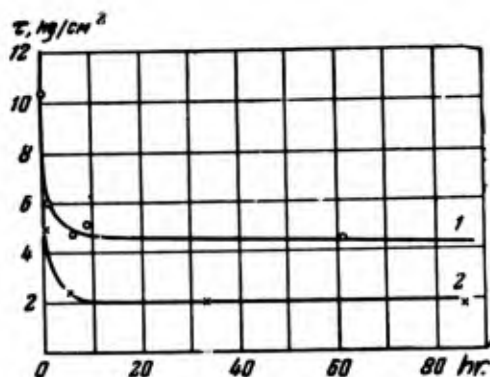


Figure 25. Curves of the long-term adfreeze strength at various soil temperatures. Heavy, silty, sandy loam; (1), and (2) are, respectively, for a temperature of  $-3.6^{\circ}\text{C}$  and  $-0.4^{\circ}\text{C}$ .

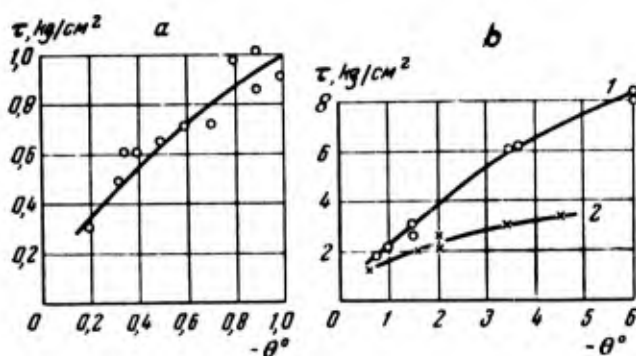


Figure 26. Variation of the adfreeze strength with temperature.

a. Long-term field tests: sandy loam and loam soil; b. Short-term laboratory experiments: (1) sand, (2) loam.

## 8. The adfreeze strength of ice with wooden rods

These tests consisted of pulling out wooden rods frozen into the ice (Figure 27); for this purpose, holes with  $d = 50$  mm and 120 mm were drilled in the floor of the vault. Water was poured into the holes, and model piles were inserted for subsequent freezing-in. For rapidly increasing stresses, the failure had a clearly marked brittle character; it was accompanied by a sharp snap and by the shattering of the ice, separate fragments of which clung to the pulled-out rod. During the long-term action of the stresses, the rod slid through the ice. A characteristic peculiarity of the deformation process is the concavity of the curves representing the growth of the deformation with time (Figure 27b). The last circumstance reflects the tendency of the rate of sliding of the rod to increase continuously. However, for a certain segment of the curves, this rate can be considered approximately constant, especially for small stresses. The concavity of the deformation curves of ice was also noted by other investigators (Kartashkin, 1947), and is obviously caused by the re-orientation of the ice crystals during the flow process.

The duration of the process of viscous flow for small values of the stress turned out to be large enough (up to 3000 hr and more) for this process to end by the pull-out of the piles in all cases, except one, even for  $\tau = 0.5$  to  $0.3$  kg/cm<sup>2</sup>. It is interesting that the displacement of one of the piles (for  $\tau = 0.3$  kg/cm<sup>2</sup>) stabilized itself after reaching 0.2 mm, and did not change for 4150 hr. However, after approximately 12,000 hr, a marked and visible increase of the displacement was detected; 13,000 hr after the beginning of the test the pile was pulled out. In another case, for  $\tau = 0.4$  kg/cm<sup>2</sup>, the displacement of the pile reached 0.65 mm after 6,000 hr, and yet the pile was not pulled out after remaining 9,000 hr under stress. This interesting phenomenon of sudden weakening is explained, according to B. A. Savelyev's theory, by a change in the structure of the ice and by the re-orientation of the crystals bordering its layer, as a result of the long-term action of tangential stresses.

Thus, the limit of the long-term adfreeze strength of ice either does not exist, or is quite small, and at any rate it does not exceed  $0.2$  kg/cm<sup>2</sup> for  $\theta = -0.4^\circ\text{C}$ ; this is significantly lower than  $\tau$  for frozen soils. The low strength of ice under long-term loading may be explained by the instability of the ionic lattice of ice, since there are 100 times less ions of hydrogen than of oxygen and the former possess a great mobility, taking root easily in the inter-nodes of the lattices. The formation of a field of tension increases the intensity of this process significantly. As a conclusion, let us point out that in agreement with the last investigations of Glen (1952, 1955), K. F. Voitskovskiy, S. S. Vialov and others, the flow of ice is described, not by Newton's law (3) for an ideal viscous liquid, but by the power relation  $\frac{dy}{dt} = k\tau^n$  (where  $k$  and  $n$  are constants); this ice flow develops for any  $\tau$  larger than zero.



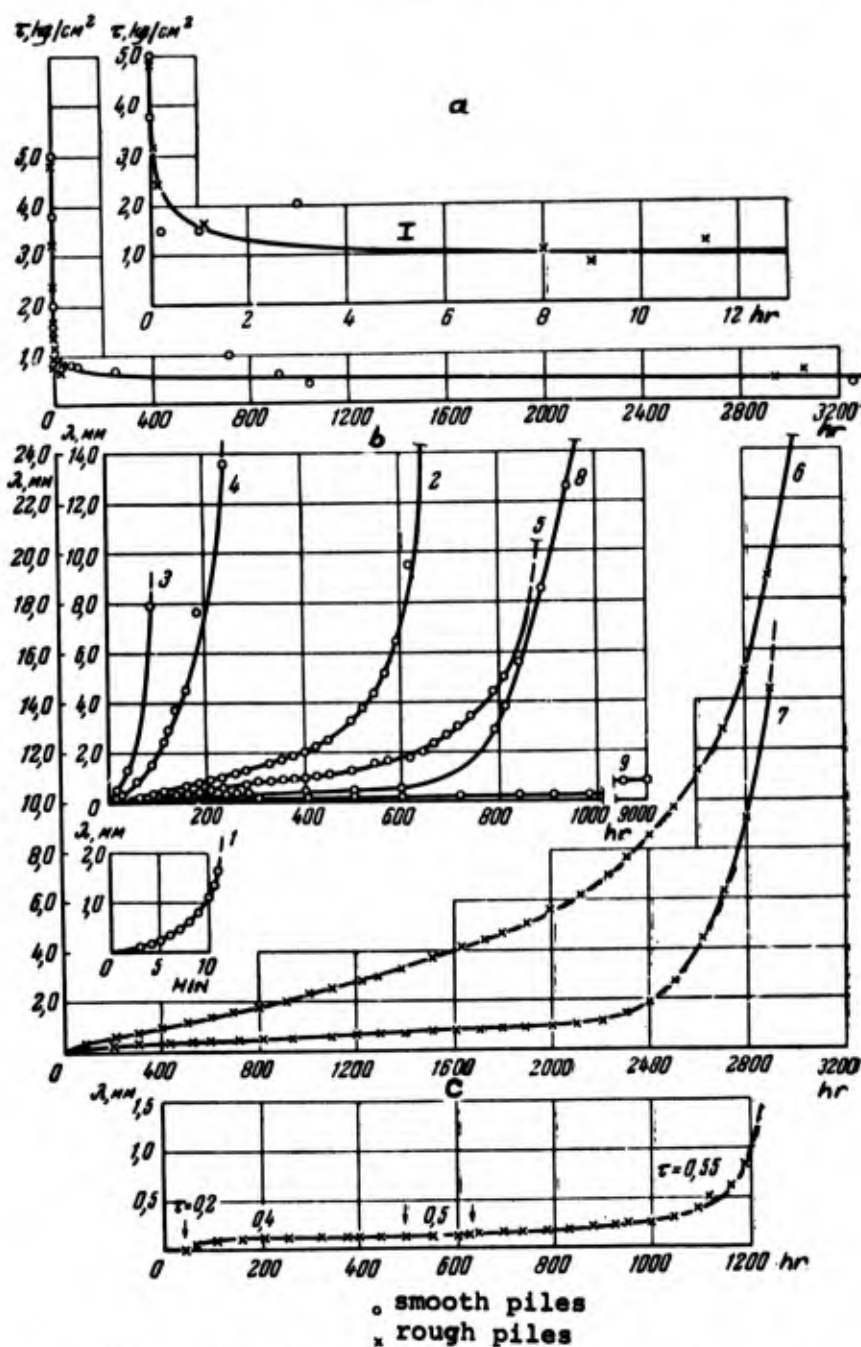


Figure 27. Adfreeze of ice with piles:  $\theta = -0.4C$ .  
 a. Curve of the long-term strength (I is the initial portion of the curve). b. Growth of the deformation in time, for pull-out of piles under various constant stresses  $\tau$  equal to:  
 (1) 1.5 kg/cm<sup>2</sup> (pile 183); (2) 1.0 kg/cm<sup>2</sup> (pile 184);  
 (3) 0.8 kg/cm<sup>2</sup> (pile 209); (4) 0.7 kg/cm<sup>2</sup> (pile 134);  
 (5) 0.6 kg/cm<sup>2</sup> (pile 210); (6) 0.55 kg/cm<sup>2</sup> (pile 64);  
 (7) 0.4 kg/cm<sup>2</sup> (pile 218); (8) 0.4 kg/cm<sup>2</sup> (pile 137);  
 (9) -0.4 kg/cm<sup>2</sup> (pile 212).  
 c. Growth of the deformation for a stress applied in steps (pile 54).



## CHAPTER IV. TENSILE STRENGTH AND COMPRESSIBILITY OF FROZEN SOILS

## 1. Long-term tensile strength of frozen soils.

A study of the strength of frozen soils under tension is necessary, not only for knowledge of the general laws for the simplest types of loadings, but for the development of the condition of limiting stress as determined by the relationship between normal (compressive and tensile) and tangential stresses (see Chapter V). In addition, tensile strength is one of the stability characteristics which must be known, for instance, to evaluate the operating strength of frozen soils, to study the formation process of frost fissures, etc. Investigation of the tensile strength of frozen soils for rapid application of loads was conducted some time ago by Pchelkin, Evdokimov-Rokotovskiy, Faintsimmer, Tsytovich and others. The long-term tensile strength began to be studied for the first time in 1949 (Berezantsev, 1949, 1953). Our experiments were carried out with undisturbed samples, and consisted of the breaking of "figure eight" specimens on the apparatus by Mikhaelis, under various stresses, starting from stresses causing instantaneous rupture and ending with long-term non-rupturing stresses\*.

The curves of the long-term strength (Figure 28) were drawn from the experimental results. It can be seen that these curves are very similar to the curves of the long-term adfreeze strength. They are characterized by a sharp reduction of strength in the initial time interval, and by a long-term (lasting more than 1,000 hr), but small,

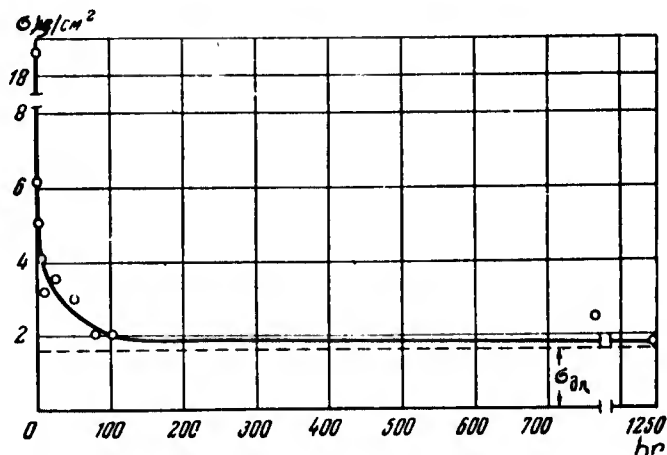


Figure 28. Curve of the Long-term Tensile Strength. Heavy Silty Sandy Loam,  $\theta = -4.2^\circ$  (Exp. No. 23)

\* For more details, see S. S. Vialov, 1954.

weakening afterwards. The results of the tests are compiled in Table 20. Compare the tensile strength of frozen soils with the value of the equivalent cohesion. The determination of this cohesion by the indentation test for the same samples, for which the values of the tensile strength are given in Table 20, gave the following results:

No. of test	212	215	210	211	217
$c_{inst}$ (kg/cm <sup>2</sup> )	11.7	12.8	9.0	8.2	15.1
$c_{lt}$ (kg/cm <sup>2</sup> )	-	2.5	2.0	3.0	3.2

Table 20. Instantaneous ( $\sigma_{tinst}$ ) and limiting long-term tensile strength  $\sigma_{tlt}$  of undisturbed frozen soils

Note: See Table 1 for the properties of these soils.

	Soil	Mois- ture Content %	Temper- ature °C	$\sigma_{tinst}$ kg/cm <sup>2</sup>	$\sigma_{tlt}$ kg/cm <sup>2</sup>
212	Heavy, silty loam	36	-4.2	23.5	1.7-1.8
215	Light, silty loam	30	-4.0	20.4	1.6-1.7
210	Light, silty, damp, sandy loam	31	-4.3	20.0	1.8
211	Heavy, silty, sandy loam	30	-4.6	-	1.7-1.8
217	The same	28	-3.7	23.1	1.4-1.5

We can see by comparing these data with those in Table 20, that the instantaneous tensile breaking strength was larger than the instantaneous cohesion by a factor of 1.5 to 2.2. This more or less obeys the Saint-Venant plasticity condition, according to which  $c = \frac{\sigma_t}{2}$ .

Let us note that analogous data were also obtained in the laboratories of the Permafrost Institute by V. S. Faintsimmer. The long-term tensile strength, on the contrary, turns out to be smaller than  $c_{lt}$ , i.e. 0.5 to 0.7 times smaller (0.9 for damp soil). This can be explained by strengthening of the soil during the long-term penetration of a ball, whereas for tension the broken bonds are not restored; the collapse mechanism in this case is the same as for compression or shear. From this point of view, it is significant that  $c_{inst}/c_{lt} = 3$  to 5 when  $\sigma_{tinst}/\sigma_{tlt} = 12$  to 16. It is known that the tensile strength of frozen soil is less than the resistance to compression, since in the last case, binding of the solid particles causes a strengthening of the bonds and the soil "skeleton" is included in the work. Under tension, stresses are taken only by the forces of molecular attraction between the soil particles, ice and the water film, i.e. by the forces resistant to tension. Proceeding from all these facts, it is impossible to determine the long-term cohesion (in the sense of Saint-Venant) through tension tests (as is sometimes done); there is however a definite connection between the two properties, since cohesion enters

into all types of strength of frozen soil under stress, including the tensile strength.

In conclusion, note that although the weakening of the tensile stresses occurs at a significantly higher rate than the weakening of cohesion forces ( $\sigma_{t\text{inst}}/\sigma_{t\text{lt}} = 12 - 16$ ), it is nevertheless not infinite in practice; this is explained by the high resistance to rupture of frozen soils. From this point of view, the data of experiment 210 are extremely significant:

Stress (kg/cm <sup>2</sup> )	20.0	10.0	6.0	5.0	4.0	2.5	2.0	1.8
Time preceding collapse:	9sec	3sec	27min	4hr	24hr	140hr	766hr	not broken

All the loads, starting with  $\sigma_t = 2 \text{ kg/cm}^2$  are larger, led to failure;  $\sigma_t = 2.0 \text{ kg/cm}^2$  caused failure in 766 hr. For a load of  $\sigma_t = 1.8 \text{ kg/cm}^2$ , failure did not occur although the sample remained under this load for approximately six years (it was protected from the air during this period). For all practical purposes, this conclusively establishes the existence of a fundamental strength characteristic of frozen soils, i.e. a limiting long-term strength.

## 2. Compressibility of frozen soils

Until recently, frozen soils were considered as incompressible rocks. However, by 1951 the author, on the basis of experiments on the penetration of indenters (Vialov, 1954)\* had established that such an assumption is incorrect. Those tests were the first to show that plastic frozen soils, particularly at temperatures close to 0C, are capable of deformation under compression. In order to study this question thoroughly, investigations were conducted on the compressibility of frozen soil. Apparatus adapted for compression tests of thawed soils were used in the experiments. The investigations were conducted with undisturbed soils, the properties of which are listed in Table 1. Associated with the duration of damping of the penetration rate, each test lasted more than 3,000 hr. The test results are given in Table 21; the values of the relative compression  $e = \Delta h/h$  ( $h$  is the initial height of the sample, and  $\Delta h$  is the deformation due to compression) are also given in Table 21, and in Figure 29 where the compression curves are plotted. The data in Table 21 are in agreement with the results of experiments subsequently carried out at the Central Laboratory of the Permafrost Institute. Nevertheless, the figures quoted may be excessive because of errors introduced by the apparatus or by the experimental conditions.

The data reflect the results of loading without subsequent unloading, i.e. they include both residual (consolidational) and recoverable deformations. The latter, under conditions which do not permit lateral expansion of frozen soil, reach a rather large value, equal, for a maximum load of  $20 \text{ kg/cm}^2$ , to 50% or more of the total deformation. Consequently, the coefficient of residual compression for  $p = 20 \text{ kg/cm}^2$  is equal, for the tested soils, to  $e_{p1} = 0.04$  for  $\theta = -0.3C$ ,

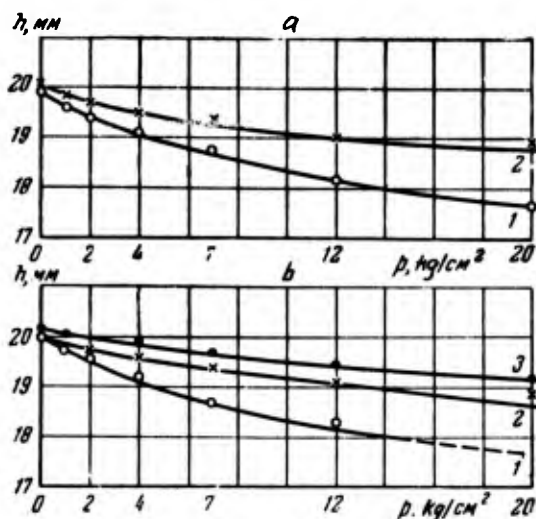
\* See also footnote on p. 40.

Table 21. Relative compression  $e$  of frozen soils

Experiment No.	Soil	Temperature °C	Compression load, kg/cm <sup>2</sup>					
			1.0	2.0	4.0	7.0	12.0	20.0
7.9	Light, silty loam. w = 32%	-0.3	0.0165	0.025	0.039	0.056	0.087	0.112
12		-1.4	0.010	0.016	0.0225	0.032	0.049	0.052
6.8	Light, silty, sandy loam. w = 28.5%	-0.3	0.013	0.0215	0.041	0.066	0.0835	—
10		-1.4	0.008	0.013	0.020	0.029	0.046	0.055
		-3.6	0.005	0.0085	0.014	0.0215	0.035	—

Figure 29. Curves of the compressibility of frozen soils.

- a. Silty loam.  
b. Silty, sandy loam.  
(1), (2), and (3) are, respectively, for high temperatures of -0.3C, -1.4C and -3.6C.



$e_{p1} = 0.025$  for  $\theta = -1.4^\circ\text{C}$ , and  $e_{p1} = 0.01$  for  $\theta = -3.6^\circ\text{C}$ . The air content in the loam examined was equal to approximately 4% of the total volume. Comparing this figure with the data in Table 21, we see that, starting with  $p \geq 4 \text{ kg/cm}^2$  at  $\theta = -0.3^\circ\text{C}$  and  $p > 7 \text{ kg/cm}^2$  for  $\theta = -1.4^\circ\text{C}$ , the compression deformation exceeds the value, which can be explained only by the squeezing out of air contained in the frozen soil. Consequently, for sufficiently large stresses, not only an elastic compression of the constituent components of a soil and a squeezing-out of the air contained in it occur, but also melting and squeezing-out of the ice. This problem will be examined in more detail in Chapter VI. Here, we shall only note that the squeezing-out of the ice during compression tests (with subsequent shear) is verified by the fact that the surface of a sample was covered by an ice film after a test; in addition, the ice also filled the openings of the porous disc, through which the stress was transmitted, although a filter paper was put between the soil and this disc.

This compression of the soil, explained by squeezing-out of the moisture formed as a result of the melting of the ice, occurs only for

values of  $p$  exceeding a certain limit. In accordance with the investigations of V. I. Ivanov ("Data on Laboratory Investigations of Frozen Soils", 1957), the relationship between the rate of filtration of the water film and the hydraulic gradient  $I$  can be expressed by the formula:  $v = k(I - I_0)$ , where  $k$  is the coefficient of permeability.

Therefore, in both frozen and thawed soils, the process of transfer of the moisture film begins only when the hydraulic gradient  $I$  reaches a certain minimum value  $I_0$ , called by S. A. Roz in 1950, the "initial pressure gradient (of percolation)," balancing the surface tension of the water film. In addition, since the coefficient  $k$  is quite small for frozen soils, consolidation of the soils proceed very slowly and stabilization of the settlement occurs after an extremely long time interval.

For frozen soils at low temperature, the value of the total deformation of compression is small, and such soils can be considered as almost incompressible. However, for frozen soils at relatively high temperatures (close to  $0^\circ\text{C}$ ), the total compression reaches an appreciable value, being equal, for instance, to 1.5 to 4 cm per running meter of the compressible stratum at  $\theta = -0.3^\circ\text{C}$  and  $p = 1 - 4 \text{ kg/cm}^2$ ; such a settlement must be taken into consideration. Therefore, in spite of existing opinion, the above-mentioned soils under the given conditions must be considered as compressible. The calculation of the settlement of these soils can be performed by standard methods of Soil Mechanics, taking into account the marked variability of the coefficient of compressibility  $a_0 = e/p$ . To illustrate the variation of this coefficient, its values (for light silty, sandy loam) are given in Table 22 for constant values of  $p$ .

Table 22. Values of the reduced coefficient of compressibility  $a_0$  for silty, sandy loam

Temperature °C	Coefficient of compressibility $a_0$ for a compression load $p$ ( $\text{kg/cm}^2$ ):					
	1.0	2.0	4.0	7.0	12.0	20.0
-0.3	0.0130	0.0110	0.010	0.009	0.007	—
-1.4	0.008	0.006	0.005	0.004	0.004	0.003
-3.6	0.005	0.004	0.0035	0.003	0.003	0.0025

## CHAPTER V. LIMITING STRESS-CONDITION OF FROZEN SOILS

## 1. General principles

It is well known that the loss of soil strength is explained by the growth of irreversible shear deformations along the so-called slip surfaces. These deformations arise when the maximum tangential stress, acting at a given point, exceeds some limiting value corresponding to the shearing strength of the soil. The limiting equilibrium condition for an elementary area of sliding is determined by means of the relation between maximum tangential stress  $\tau_n$  and the normal component of the stress  $\sigma_n$ , at the time preceding shear. In the general case, it is described by the non-linear Mohr relation,

$$|\tau_n| = f(\sigma_n). \quad (29)$$

This condition is represented graphically by a curved envelope. For cohesive, unfrozen soils, the curve is usually approximated by the straight line,

$$|\tau_n| = c + \sigma_n \tan \phi \quad (30)$$

(the parameters  $c$  and  $\phi$ , as usual, designate the cohesion and the angle of internal friction).

For ideally plastic bodies ( $\phi = 0$ ), the limiting stress condition becomes the Saint-Venant condition,

$$|\tau_n| = c = \text{const}, \quad (31)$$

according to which, at any point of the plastic region, the maximum tangential stress has a constant value equal to the internal cohesion. The Mohr envelope becomes, in this case, a horizontal straight line.

The limiting stress condition has an exceptionally important role in Soil Mechanics, since it is the fundamental relation through which the strength of the soil is determined. Until recent times, a normal working hypothesis assumed that the limiting stress condition of frozen soils obeyed condition (31), i.e. the shearing resistance of soils was expected to be independent of the normal component of the stress, and to be determined by the cohesion alone: the so-called friction is equal to zero. However, a series of indirect indications, i.e. the difference between compressive strength and tensile strength, the failure to fulfill the equality  $\tau_{f1} = \frac{\sigma_{f1}}{2} = \text{const}$ , and other data, lead the author to doubt the accuracy of this assumption. To reveal the actual condition of the limiting stress condition of frozen soil, the author carried out in 1952 - 1953 a series of tests on the shear of these soils for various normal pressures (Vialov, 1957). In 1953, analogous tests were also conducted at the Central Laboratory of the Permafrost Institute (Pekarskaya, 1957; Pekarskaya and Tsytovich, 1957).



## 2. Method of testing frozen soils in shear

The investigations of the author were conducted with undisturbed frozen soils (silty, sandy loam and loam; see Table 1) at temperatures of  $-0.3^{\circ}\text{C}$  and  $1.2^{\circ}\text{C}$ . The shear is accomplished by means of a strengthened version of shearing apparatus of the type used by N. N. Maslov. The investigations consisted of tests for "instantaneous" and long-term shear. In the first case, shearing occurred after 5 to 25 sec; this was obtained by a rapid increase in the shearing stresses. In the second case, the shearing stress was increased in steps of  $0.2 \text{ kg/cm}^2$ , and each step was maintained until stabilization of the shearing deformation. The load, which has to be exceeded for a permanent plastic deformation to occur, was considered the limiting shearing strength  $\tau_l$ . After appearance of a permanent deformation, the load was increased in equal steps, which were maintained until the plastic flow stage occurred. The duration of these tests ranged from two to six months.

Each experiment included the testing of three samples under normal pressures  $\sigma = 1.0 \text{ kg/cm}^2$ ,  $3.0 \text{ kg/cm}^2$ , and  $7.0 \text{ kg/cm}^2$ . For long-term shear, the samples were first consolidated under these stresses (in one case, all three samples were consolidated under a stress  $\sigma = 7 \text{ kg/cm}^2$ ). For instantaneous shear, the experiments were conducted with an instantaneous application of stress ( $\sigma$ ) both with an initial consolidation and without it.

## 3. Limiting stress condition of frozen soils taking into account the time factor

It is well known that the shearing strength of a frozen soil depends, above all, upon its temperature and ice-moisture content. In addition, the results of the determination of the instantaneous shearing strength of frozen soils (Table 23) obviously point out that this strength increases as the normal stress becomes larger. It must also be emphasized that the data given in Table 23 are related to the occurrence of shear without preliminary consolidation. Since the stress was rapidly applied, the increase of  $\tau$  was not a result of the strengthening of the soil due to a change in its density; it is explained by the direct influence of the normal stress appearing in the increase of the forces of molecular interaction. The influence of direct consolidation for low-temperature frozen soils is insignificant and does not affect the shearing strength (Pekarskaya, 1953). For relatively high temperatures (close to  $0^{\circ}\text{C}$ ), the preliminary consolidation of frozen soils begins to influence the shearing strength: for example, in experiment 2, the shearing strength after preliminary consolidation was  $\tau = 6.3 \text{ kg/cm}^2$  for  $\sigma = 3.0 \text{ kg/cm}^2$ , and  $\tau = 8.1 \text{ kg/cm}^2$  for  $\sigma = 7.0 \text{ kg/cm}^2$ . During the same time interval, for unconsolidated samples (Table 23), this strength equalled, respectively,  $5.4 \text{ kg/cm}^2$  and  $6.8 \text{ kg/cm}^2$ . In another case (experiment 3), an increase in  $\tau$  also occurred for previously consolidated samples, but to a smaller extent (5 to 10%).

The dependence of the shearing strength of frozen soils on the normal stress is, strictly speaking, non-linear; unlike solid bodies, this dependence changes in accordance with the time of action of the shearing stresses. The limiting long-term shearing strength is smaller than the instantaneous strength by a factor of 4.5 to 7 (Table 24).



Table 23. Instantaneous shearing strength  $\tau_{inst}$  (kg/cm<sup>2</sup>) of frozen soils

Experiment No.	Soil	Values of $\tau_{inst}$ for $\sigma$ (kg/cm <sup>2</sup> ):		
		1.0	3.0	7.0
1	Light, silty loam w = 34% $\theta = -1.2C$ .	6.5	7.1	8.6
		6.5	7.0	8.4
		7.6	8.3	8.7
		7.7	8.1	8.3
		6.9	8.1	8.3
		6.9	7.5	8.2
		7.5	8.3	
		7.5	7.6	
		7.5	7.7	
		7.5	8.3	
	mean	7.2		8.4
2	Light, silty loam w = 32% $\theta = -0.3C$ .	4.7	4.6	6.2
		4.9	4.5	6.2
		4.0	4.5	6.1
		5.4	6.8	6.4
			4.5	
	mean	4.7	5.0	6.2
3	Heavy, silty, sandy loam w = 35% $\theta = -0.3C$ .	3.4	5.4	6.8
		3.4	5.4	6.7
		3.3		7.3
				6.4
	mean	3.4	5.4	6.8
4	Heavy, silty, sandy loam w = 42% $\theta = -0.3C$ .	6.1	6.8	7.5

Table 24. Instantaneous and limiting long-term shearing strength of frozen soils

Experi- ment no.	Soil	Tempera- ture °C.	$\tau_{inst}$ kg/cm <sup>2</sup>			$\tau_{lt}$ , kg/cm <sup>2</sup>		
			for $\sigma$ , kg/cm <sup>2</sup>					
			1.0	3.0	7.0	1.0	3.0	7.0
2	Heavy, silty, sandy loam	-0.3	3.4(?)	5.4	6.8	0.8-0.9	1.0-1.1	1.3-1.4
3	Light, silty loam	-0.3	4.7	5.0	6.2	0.7	0.9-1.0	1.3-1.4

Thus, the shearing strength of a frozen soil is a function of its temperature, the normal stress, duration of the action of the shearing stress (or the rate of the loading), density, and of the moisture content. Consequently, the condition of limiting stress of frozen soils can be written in the following general form,

$$|\tau_n| = F(\theta, \sigma_n, t, w).$$

For  $\theta$  and  $w$  constant, this condition becomes

$$|\tau_n| = f(\sigma_n, t) \quad (32)$$

and is represented graphically by the family of curves  $\tau = f(\sigma)$ , in which the time of action  $t$  of the shearing stresses is the parameter (Figure 30a).

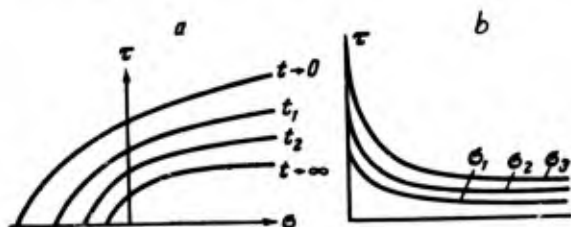


Figure 30. Envelopes (a) and curves of the long-term shearing strength (b) of frozen soils (diagrammatic).

The upper envelope represents the relationship between normal stress and instantaneous strength; the lower represents the limiting long-term shear. When computing the action of constant loads for frozen soils, we must proceed from their long-term shearing strength, i.e. use the long-term envelope.

The Variation of the shearing strength of frozen soils with time is shown by the curve of the long-term strength; each value of  $\sigma$  yields a curve (Figure 30b).

The envelope for frozen soils (Figure 31a) can be described, as was suggested by V. V. Sokolovskiy (1950) and K. V. Ruppineit (1954)

for rock excavation, by a combination of the equation of the cycloid corresponding to the curvilinear part of the envelope,

$$+H = \frac{k}{2} (\psi - \sin 4\psi); \quad \tau_1 = \frac{k}{2} (1 - \cos 4\psi),$$

and the equation of the straight line tangent to the cycloid,

$$\tau_2 = c + \sigma \tan \phi.$$

But, as with rock, it is necessary to take into account the relaxation properties of frozen soils, and of course, the influence of the temperature and moisture content. In these equations,  $2\psi$  is the angle of inclination between slip surfaces; it corresponds to the slope of the normal to the envelope. It is determined by the relation  $2\psi = \frac{\pi}{4} - \phi$ ;  $H$  is the limiting tensile strength, and  $k$  is the diameter of the generating circle of the cycloid which can be computed from the relation,

$$k = \frac{H - c \cdot \cot \phi}{\frac{\pi}{2} - \phi - \cot \phi} \text{ (kg/cm}^2\text{)},$$

where  $c$  and  $\phi$  are the parameters of the straight line.

All these parameters are time-dependent, changing from instantaneous values to limiting long-term values. The curve represented in Figure 31a is plotted according to the data from instantaneous tests. The curved envelope reflects more accurately the physical

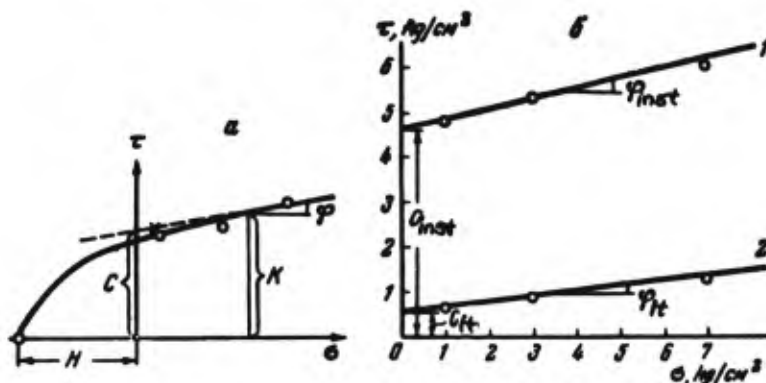


Figure 31. Test of frozen loam for shear.  $\theta = -0.3C$ . a. The true envelope. b. The diagram of the instantaneous (1) and limiting long-term (2) shearing strength.

nature of the stability of frozen soils, taking into account their different strengths under compression and tension. However, the use of such a curve requires determination of additional computed characteristics: this involves several complications. At the present state of our knowledge, we can proceed from a consideration of the linear

part of the envelope alone. The limiting stress condition for frozen soils then takes the form,

$$\tau_t = c_t + \sigma \tan \phi_t. \quad (33)$$

This condition differs from the Coulomb equation (30) in that the parameters  $c_t$  and  $\phi_t$  are time-dependent and change from instantaneous  $c_{inst}$  and  $\phi_{inst}$  to the limiting long-term value  $c_{lt}$  and  $\phi_{lt}$ . In addition, they are functions of  $\theta$  and  $W$ .

When plastic flow arises, the viscous resistance to shear is again increased:

$$\tau = c_{lt} + \sigma \tan \phi_{lt} + \eta_{pv} \frac{dy}{dt},$$

where  $\frac{dy}{dt}$  is the rate of the steady flow, and  $\eta_{pv}$  is the plastic viscosity. The parameters  $c$  and  $\phi$ , following standard nomenclature, can be called cohesion and the angle of internal friction. However, such a division of the shearing strength is complicated, and strictly speaking,  $c$  and  $\phi$  must only be considered as parameters of the linear relationship (33) between shearing, and normal, stresses. In addition, the parameter  $c$  characterizes the "initial" shearing strength of the soil, which depends upon the internal bonds, existing in the absence of a normal component of the stress. The parameter  $\phi$  characterizes the increase of the shearing resistance under the action of normal stress as a result of the reversible compression of the particles; consequently, it reflects the increase in the molecular forces of interaction. The values of these parameters are critically dependent upon the temperature of the soil.

For instantaneous shear, the value of the angle of friction turns out to be appreciably large. This indicates the essential influence of the normal stress on the shearing strength for rapidly applied stresses. We must also take into account that the resistance to rapid shear was determined, not at the moment corresponding to the beginning of the collapse, but after it, when the sliding of the soil particles against each other occurred. During this process, the role of friction with respect to the condition of limiting equilibrium, obviously, becomes more important. For long-term shear, the values of both  $c$  and  $\phi$  sharply decrease: in particular,  $c$  is smaller. This is in complete agreement with the experimental data of the penetration of a spherical indenter. According to the data from experiment 3, the instantaneous values of the above-mentioned parameters were:  $c_{inst} = 4.8 \text{ kg/cm}^2$  and  $\phi_{inst} = 10^\circ$ ; the limiting long-term values decreased to  $c_{lt} = 0.7 \text{ kg/cm}^2$  and  $\phi_{lt} = 6^\circ$  (Figure 3lb). The value of the parameter  $c_{lt}$ , determined from the  $\sigma - \tau$  diagram as the magnitude of the intercept on the vertical axis, is in satisfactory agreement with the value of  $c_{lt}$  obtained from the ball-penetration test. From all the samples tested, those with a large moisture content (see Table 23) and a few of the samples having ice inclusions had the maximum strength for instantaneous shear.

Let us return to Figure 3lb. It can be seen that for long-term shear, the parameter  $\phi_{lt}$  is significantly less than  $\phi_{inst}$ . For frozen clay soils, at a temperature close to  $0^\circ\text{C}$ , the envelope of the shear curve is close to a horizontal straight line; this is analogous to the

situation for plastic (clay) unfrozen soils. Therefore, for these frozen soils, it is sometimes possible to disregard the value of  $\phi_{1t}$  in making allowance for strength, and to take the condition of limiting equilibrium in the simplest form (Tsytoich, 1952; Berezantsev, 1953)  $\tau_{1t} = c_{1t} = \text{constant}$ , where  $c_{1t} = f(\theta, w)^*$ .

For sandy frozen soils, the value of  $\phi_{1t}$  will obviously be significant, and it must always be taken into account. Both this question and the question of the value of  $\phi_{1t}$  for frozen clay soils at low temperatures demand further study. The appropriate investigations are extremely effective and can be conducted by means of tests on frozen soils in triaxial compression, taking creep into account. Apparatus for such tests has already been constructed.

---

\* The dependence of  $c$  upon  $\theta$  is shown by formula (23).

## CHAPTER VI. THE LAWS OF DEFORMATION AND RESISTANCE OF FROZEN SOILS UNDER LOAD

## 1. The nature of frozen soil deformation

The cohesive strength of frozen soil, i.e. strength of internal bonding, depends on several factors, which in turn depend upon the interactions between the soil components. Experiments show that the cohesion of frozen soil decreases with rising temperature, and falls sharply after thawing. However, in the unfrozen state, soils have a definite strength which increases with compression. It was also established that undisturbed frozen soils have a higher cohesion than remolded soils, even if the density and moisture content are the same.

According to recent ideas on the nature of the strength of cohesive unfrozen soils, introduced by N. Ya. Denisov (1951), the bonding of unfrozen soils may conditionally be classified as a natural, molecular (primary) bond and a structural (secondary) bond. In recent works, the author has separated, for specific frozen soils, an independent third form of bonding, i.e. ice cementing; this bond has a fundamental value for any given soil and is its distinguishing characteristic. Thus, the cohesion of frozen soil may be analyzed as though it consisted of three parts.

(1). The natural molecular bond that depends upon the strength of the molecular attraction between solid particles of soil separated by a film of connecting water. This part of the bond depends on the surface area of the particles, and the distance between them, i.e. on the density of the soil. When the particles move closer together the molecular attraction increases; this also explains the strengthening of the soil when it is compressed. After thawing, the molecular attraction does not disappear, but increases with the density of the thawed soil.

(2). The structural bond that reflects the actions of a variety of physical, physico-chemical, mechanical and other processes occurring in a soil layer in the course of its geological formation; and giving rise to an increase in the cohesion in comparison with the original state. In frozen deposits, this bond reflects the same changes in its structure as occurred upon freezing. The structural bond is removed upon distortion of the natural structure of the soil, which also explains the differences, up to 2 to 3 times (section 5, Chapter II), in the strength between undisturbed and remolded samples. In experiments performed in 1955 in the MGLL by L. D. Pikulyevich under the guidance of the author, the difference  $\Delta c$  in the value of the cohesion of samples with undistorted and distorted structures, characterized by structural bonding, showed a comparatively small dependence on the temperature of the soil (compare Table 25). The relative role of the structural bond  $\Delta c$  with a decreasing temperature significantly decreases, since it is superimposed on the influence of the cementing ice bond.

Table 25. The cohesion of frozen clayey soil, undisturbed and remolded

Temperature °C	$c_{inst}$ , kg/cm <sup>2</sup>			$c_{lt}$ , kg/cm <sup>2</sup>		
	Undisturbed	Remolded	$\Delta c$	Undisturbed	Remolded	$\Delta c$
-2	4.2	2.1	2.1	2.4	1.5	0.9
-5	13.6	12.1	1.5	4.6	3.5	1.1
-10	16.3	14.9	1.4	-	-	-

(3). The bond of the cementing ice that depends on the cementing action between the ice crystals and the mineral particles. The bond being discussed is accomplished, not by direct contact of the ice and the mineral particles, but through a liquid layer, which envelops the solid particles and the ice crystal. This bond depends on the volume of the ice, the interface area of ice and the mineral particle, and the temperature of the frozen soil; upon thawing, the bond disappears completely. The cementing ice bond is the least stable and under natural conditions changes continuously with changes of temperature of the frozen mass.

Of course, this classification of bonding (in itself an assumption) is arbitrary, insofar as all the forms of bonding considered are determined by the strength of molecular attractions. The fact that this bonding may assume various aspects is emphasized by such classification; it simultaneously permits graphic presentation of the role of the various factors which affect the strength of frozen soil and formation of hypotheses about the physical nature of the deformation processes of the designated soil. These hypotheses, which were introduced by the author (Vialov, 1954, 1955), are considered below.

It is well known (Tsytovitch, 1937, 1952) that a load applied to a frozen soil leads to a stress concentration at the contact between the mineral particles and the ice crystals; even with a comparatively small applied pressure, the stress at a contact can reach 100 kg/cm<sup>2</sup>. An increase in the stress leads to a plastic deformation of the ice which is forced from a high stress region to a region of lower stress; it also gives rise to a plastic flow of the ice (with no phase transition) which depends on the difference in pressure at the contacts and around them. At the same time, the increase in the stress at the contact leads to a disturbance of the equilibrium state between the film of water and the ice in contact with it. This finally leads to a melting of the ice. If the phenomena described take place in a closed volume or at hydrostatic pressure, then water would be formed only at the squeezed-out contact region and would refreeze; thus, the entire process would amount to a redistribution of the ice and an insignificant increase in the amount of unfrozen water. However, in the presence of a local stressed region, a difference in stress between this region and the outer zone is formed. Under the influence of the pressure gradient, moisture, which is being added because of the phase transition of the ice into a water film, is moved from a region of high pressure into a region of lower stress. The water squeezed into this region refreezes and reaches an equilibrium state



at a given temperature and pressure (but partially squeezed out onto a free surface). All this agrees well with the principles of the dynamic equilibrium states of solid and liquid phases of water in frozen soil, as formulated by N. A. Tsytovitch (1945, 1954). The higher the temperature of the soil, the greater the role of this mechanism of deformation. Besides the process already described, a process of squeezing-out of the air contained in the frozen soil also takes place.

The information concerning the melting of the ice, contained in the frozen soil (but not at a very low temperature) under the action of pressure and the squeezing-out which forms water and free ice, was established by the author by experiment and is illustrated in Figures 32 and 33. In Figure 32, a sample of frozen clayey soil is shown after compression and shearing at a temperature of  $-1.2^{\circ}\text{C}$ . The crystals of ice (the moisture, squeezed out from the surface and refrozen at the opening of the punch) can be easily seen in the photograph. Sections of a block of a dense layer of clay after penetration by a punch (at  $\theta = -0.4^{\circ}\text{C}$ ) are shown in Figure 33. On these sections (Figure 33a) the frozen inclusions are distinctly visible. They appear as a consequence of squeezing out the ice water to the limit of the stressed region that marks the fracture surface of the soil.

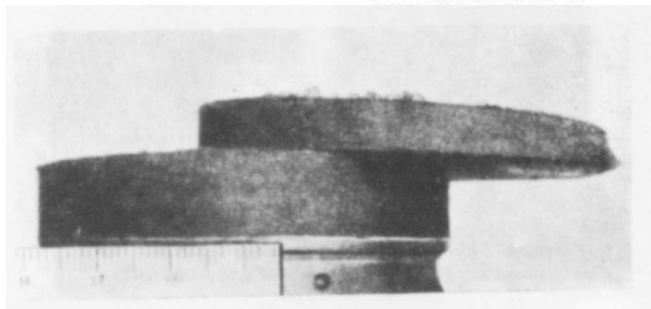


Figure 32. The melting of ice and the displacement of water in frozen soil.

Plastic flow of the ice (with no phase transition) is illustrated in Figure 33b (left), where a section of block of soil is shown with a frozen layer. After testing, this layer showed a compressed ring of soil which was formed under the punch. Ice was squeezed out, partially in the soil under the punch, and partially in the space which was formed under the punch. Besides the plastic flow of the ice, melting also took place and the resulting water was squeezed out; some of the meltwater was squeezed out onto the surface where it froze. It is interesting to point out that the appearance of water on the free surface is clearly observed if the load is rapidly applied and if the load is sufficiently great. Thus, with a state of complex stress in the frozen soil a redistribution of the ice takes place which depends directly on the plastic flow of the ice as well as on melting, since the latter obviously appears only when the soil temperature is not very low. Redistribution of the ice in frozen soils under the action of an external load is also verified by determination of the

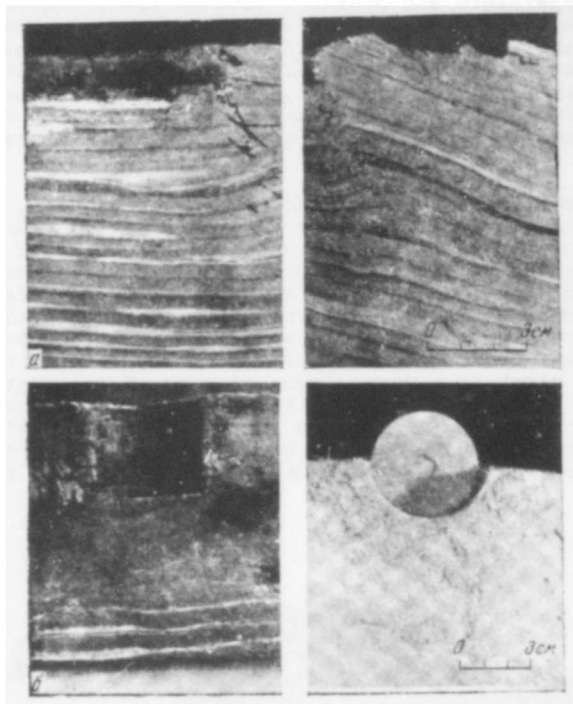


Figure 33. The melting of ice and the displacement of water under pressure ( $\theta = -0.4^{\circ}\text{C}$ ).

- a. Section of a block of varved clay after penetration with a punch, showing ice inclusions which formed on the boundaries of the stressed zone (experiment 5;  $p = 13 \text{ kg/cm}^2$ ;  $t = 2068 \text{ hr}$ ).
- b. Penetration of a punch in clay with ice inclusions. At the left: section showing penetration of the ice layer; at the right, view from above showing the ice projecting from the surface (experiment 33;  $p = 0 - 10 \text{ kg/cm}^2$ ;  $t = 1200 \text{ hr}$ ).

amount of moisture in a block of soil after prolonged compression by a punch (Table 26). A scheme for sampling the water content is shown in Figure 34. In all cases, the least moisture was found in the region of highest pressure, i.e. under the punch. However, the highest water content corresponds to the limit of separation of the stressed zone and the region of soil close to the edge of the punch hole.

Table 26. Redistribution of the moisture in frozen soil after penetration by a punch ( $\theta = -0.4C$ )

Experiment no.	Soil	Moisture content (%) at probe points (Figure 34)					Average moisture content (%) of entire block
		1	2	3	4	5	
15	Varved clay	30	35	47	40	-	37
22	The same	35	43	41	48	-	40
19	The same	34	42	39	51	39	40
7	Sandy loam, heavy	38	-	44	43	45	42
16	Sandy loam, light	22	23	26	31	25	25

The process of ice flow, its melting, and the squeezing-out of the water is accompanied by a structural distortion of the frozen soil, i.e. by a lowering of the structural and cementing bonds. Simultaneously, a mixing and regrouping of the solid particles takes place; as a result, an irreversible structural deformation, proceeding in time, arises, i.e. the phenomenon of creep. We point out that this deformation arises only at that pressure where the tangential stress exceeds the strength of the internal interactions which determine the equilibrium state. Until the previously discussed limits are exceeded, the deformation will depend on the elastic binding of the particles and the squeezing-out of the air contained in the frozen soil.

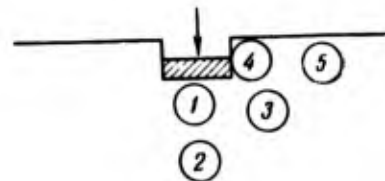


Figure 34. Scheme for probing for the moisture content: probe points: (1) - (5).

Structural deformation leads to a denser packing of the mineral particles, which move into those places that result from displacement of ice, water, and air. As a result, there is a volume change of the soil, i.e. there is a consolidation. Insofar as the binding of the particles by the strength of the molecular interaction is increased, the molecular bond of the soil grows. Thus, in frozen soil under the action of a load, a disturbance of the bond and a weakening of the cohesion takes place, as well as a growth of bonding and strengthening. If the cohesion does not exceed the limits of the long-term strength, then the strengthening compensates for the weakening, and the deformation dies out. This process may be considered as an after-effect, accompanied by a change in volume, i.e. a consolidation. However, if the weakening is not compensated by a strengthening, then a viscoplastic flow develops. When the frozen soil is under tension, the picture will be different, since in such a case the process of deformation depends on two mutually contradictory phenomena, i.e. disturbance of the bond with the formation of a region of plastic collapse of the ice and recovery of this bond, as a result of recrystallization of the ice.

The phenomena of weakening of the structural bond and the cementing ice bond and the plastic deformation of such ice lead to a weakening of resistance of the frozen soil for a load acting over a long period of time. It has been shown that the long-term strength of frozen soil is 5 to 15 times smaller than that of the instantaneous strength.

In conformity with all that has been discussed above, the deformations of frozen soils are analogous to those of unfrozen soils (Denisov, 1951), but considering the special frozen state of the soil, they may be separated into the following forms.

1. Elastic deformation that is associated with the elastic changes in the crystalline lattice of the ice and minerals, and with the elastic compression of the water and the entrapped air contained in the frozen soil. These deformations, which may be analyzed as instantaneous-elastic, designated  $\gamma$  (compare Figure 35), arise immediately upon application of the load and fade away with removal of the load. The fundamental role here is played by the elastic deformation of the ice, which appears at a load significantly smaller than that which can give rise to an elastic compression of the mineral particles. The specific value of the instantaneous elastic deformation of the frozen soil is comparatively small, but may be increased by a repeated loading-unloading cycle.

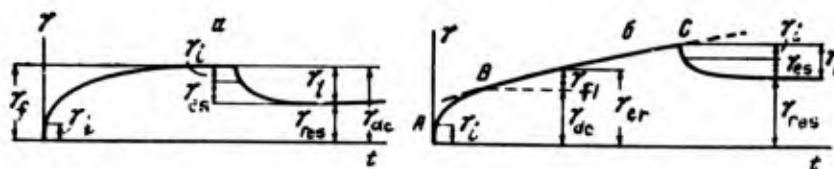


Figure 35. Kinetics of the deformations of frozen soils (schematic) a.  $\tau < \tau_{lt}$  b.  $\tau > \tau_{lt}$ .

2. Structurally reversible (absorptive) deformations that arise as a result of changes in the thickness of the water film at the interfaces of the solid particles under the action of external pressure; they also arise as a consequence of the reversible phase transitions in the ice. This deformation develops with time and is also recovered with time after unloading; consequently, it may be considered as visco-elastic. Its specific role is considerably greater than the elasto-instantaneous.

3. The deformation accompanying consolidation (structural), that is associated with the squeezing-out of air. It is an irreversible phase transition of the ice and the displacement of the water which was formed; as a result, an adjustment of the mineral aggregate occurs, i.e. a change in the structure which is accompanied by a decrease in porosity (volume) of the soil. This deformation proceeds in time with complete irreversibility.

Structural-reversible deformations and deformations of consolidation have an attenuating character and reflect the unsettled phase of the deformation  $\gamma_{dc}$  (Figure 35). However, the first of these may be considered as the elastic part of the deformation reaction (a

delayed elastic deformation)  $\gamma_{es}$ , and the second as a constant part  $\gamma_{res}$  thus  $\gamma_{de} = \gamma_{es} + \gamma_{res}$ . The presence of this constant part, which depends on a volume change as a result of consolidation, also distinguishes the process of attenuation of the deformation of frozen soil from the process of delayed elasticity of an ideal visco-elastic body.

4. Plastic deformation that depends on the irreversible displacement of solid particles and flow of ice. This deformation develops with time and may be analyzed as visco-plastic flow  $\gamma_{fl}$  (see Figure 35). The growth of a plastic deformation leads to an irreversibly distorted structure which corresponds to a transition to a stage of progressive flow, resulting in complete failure of the soil (subsidence).

Each of these deformations does not proceed, of course, separately; they all accompany one another and appear to some degree in each stage of the process of deformation. Depending on the value of the loading, one or another form of deformation is dominant. However, the specific value of any kind of deformation depends on the state of the soil, and most of all on its temperature: the higher the temperature, the more the plastic properties of the soil are developed.

We emphasize once more that a classification of the deformation on attenuation or non-attenuation is arbitrary, since the relation of it to one or another type depends to a great extent on the duration, degree, and precision of observation. Theoretically, from the character of the deformation of solid bodies (section 2, Chapter I), it can be assumed that even with small loads on frozen soil, very long (secular) deformations may develop. However, these deformations are so insignificant and so slow that they virtually do not need to be considered.

## 2. Distinguishing the rheological processes of frozen soils from the deformation processes of an idealized solid

Frozen soil may be considered as an elasto-plasto-viscous solid; its elastic properties appear as reversible, linear deformations, the plastic as irreversible displacements, and viscous in development of the deformation with time. However, frozen soil, differing essentially from an idealized elasto-plasto-viscous solid, depends on the complex and unusual bonding of the frozen soil, which is a non-homogeneous and anisotropic system, the properties of which continuously change in accordance with changes of the water temperature regime. In addition to what has been said, the special character of frozen soil is its ability to change its physical properties under the action of an external load; such action is accompanied by changes which correspond to the liquid and solid phases of water, a rise in the viscosity of the latter, readjustments of solid particles, changes in density, etc.

Similarly, the rheological characteristics of the soil are changed, as well as the parameters of deformation, viscosity and the period of relaxation. We point out that the above is correct for bonding in unfrozen soil as well, the difference being that in unfrozen soil the phase transformation of water is absent, and the influence of temperature is very small.



For an analytical description of the rheological processes in frozen soils, in particular the processes of relaxation and decreasing stability (Goldshtein, 1941, 1948; Saltykov, 1944; Berezantsev, 1949, 1953; Tsytovich, 1952), the Maxwell-Shwedoff equation (8) has been used. However, some investigators have already pointed out deviations between the theoretical and analytical data (Berezantsev, 1953); the introduction into the results of a proportional coefficient was proposed (Tsytovich, 1954). Our investigation (Vialov, 1954, 1957) showed that, for frozen soil, the [Maxwell] equation is generally unsuitable. Equally unsuitable also is the initial equation (7) for a linear deformation of an ideal elasto-plastic solid; this equation does not properly reflect the true rheological processes which proceed in such a complex body as frozen deposits. The non-correspondence between the analytical and experimental data is graphically demonstrated in Figure 36a, which shows the relaxation curve for the cohesive strength. This curve was experimentally obtained by ball-penetrations and by calculation from the Maxwell-Shwedoff formula (8),\* according to the values of  $\underline{n}$  and  $c_{inst}$  which are known from experiment.

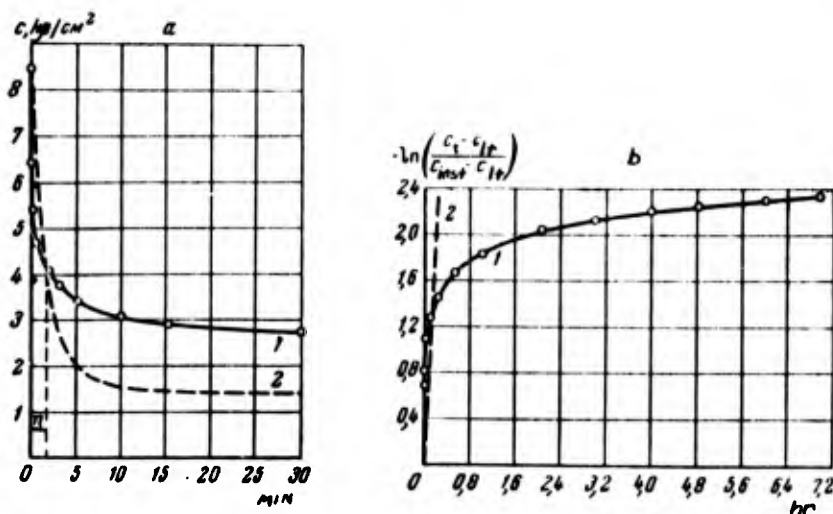


Figure 36. Experimental (1) and calculated according to the Maxwell-Shwedoff formula (2) curves of relaxation of the cohesion in normal (a) and semilogarithmic (b) coordinates; sandy loam,  $\theta = -1.2C$  (experiment 36).

As is seen, the curves diverge sharply. If in correspondence with expression (13), a determination of the value of  $c_{lt}$  from the known experimental values of  $c_1$  and  $c_2$  (determined for two arbitrary moments of time connected by the condition  $t_2 = 2t_1$ ) is attempted, then, depending on the fact that such values of  $c_1$  and  $c_2$  would be substituted in formula (13), we obtain some different value of  $c_{lt}$ . This was shown by the author earlier (Vialov, 1954).

\* Substituting  $\underline{c}$  in place of  $\tau$  in formula (8).

Thus, formulas (8) and (13) are to be considered entirely unsuitable for determining the long-term strength of frozen soils (even considering the introduced arbitrary proportional coefficient).

In principle, the non-correspondence of the basic laws of linear deformation (7) to real processes which proceed in frozen soils may be demonstrated as follows: equation (7) and the laws of relaxation (3) following from it were obtained on the assumption that the basic parameter, i.e. the relaxation time, is constant. If this assumption is correct for frozen soil, then the experimental points, plotted on a semilogarithmic plot in accordance with the expression  $\ln \frac{c - c_1 t}{c_{inst} - c_1 t} =$

$1/n t$ , which we obtained from equation (8), would lie on a straight line. Actually such points lie on an obvious curve (Figure 36b) that testifies to the variability of the model value of  $n$ . This variability is confirmed by direct calculation of the value of  $\bar{n}$  from experimental data. From Figure 37, where the calculation results are given, it is seen that the parameter  $\bar{n}$  increases almost linearly with increasing time, and decreases by a more complex law with the decrease of stress under the ball indenter which changes with time according to the penetration of the ball:  $\sigma = \frac{P}{\pi d s_t}$ . Thus, for frozen soils, the relaxation

time is a function of stress. It is interesting that the value of  $\bar{n}$  is changed so much in the initial stages of the process with large  $\bar{\sigma}$ . there a sharp bend of the curve  $n = f(\sigma)$ , after which changes in  $\bar{n}$  are very small.

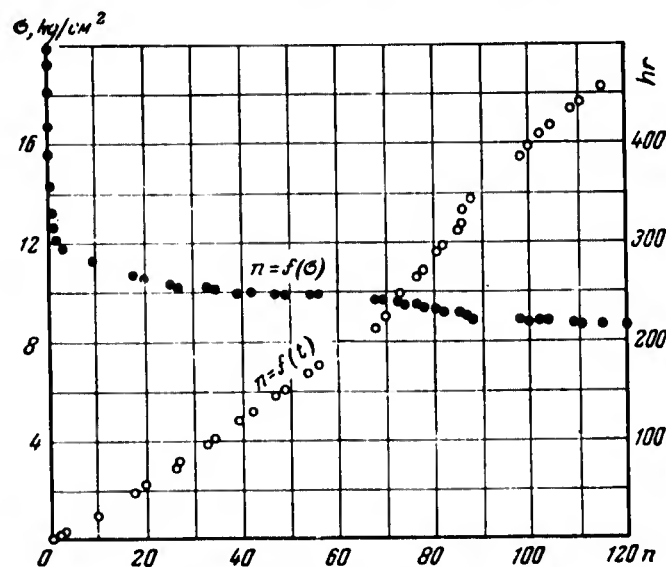


Figure 37. The change of the relaxation time  $\bar{n}$  and its dependence on the time  $\bar{t}$  and the stress  $\bar{\sigma}$ .

An analogous non-correspondence also takes place for the results of experiments on long-term adfreeze strength (Figure 38). Neither formula (12) of Maxwell-Shwedoff, nor formula (15) of Bykovskiy



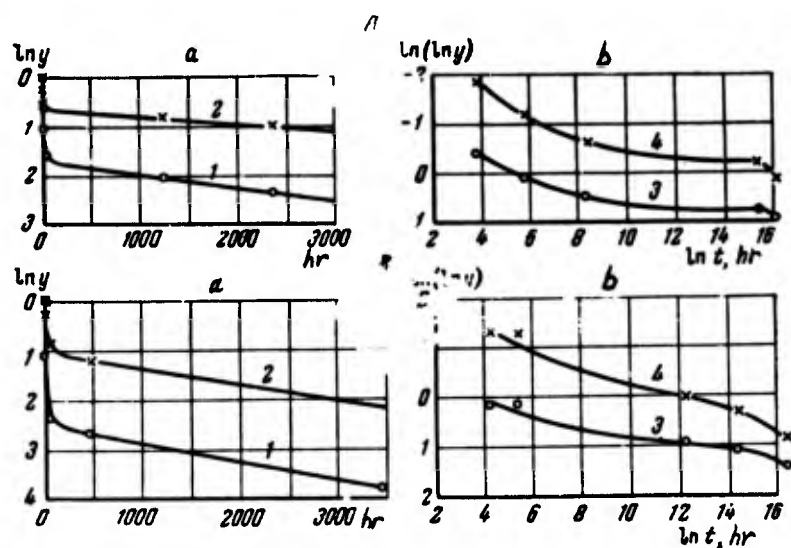


Figure 38. Curve of the long-term adfreeze strength on semilogarithmic (a) and logarithmic (b) coordinates: (1) according to formula (12); (2) according to formula (15); (3) according to formula (14); (4) according to formula (16).

(a) Heavy sandy loam, and silty (experiment 21);  
(b) Silty gravel (experiment 23).

coincides with experimental data. This is illustrated by the absence of any rectilinearity of the experimental curves when they are plotted on a logarithmic scale corresponding to the expression  $\ln y = 1/n \cdot t$ ,

where  $y = \frac{\tau_{inst} - \tau_{lt}}{\tau - \tau_{lt}}$  for formula (12), and  $y = \frac{\tau}{\tau_{inst}} \cdot \frac{\tau_{inst} - \tau_{lt}}{\tau - \tau_{lt}}$

for formula (15). However, straight-line experimental curves were obtained when they were plotted with the coordinates  $\ln(\ln y) - \ln t$  (Figure 38). This verifies the inapplicability, for frozen soil, of laws (14) and (16) for more complicated (according to Bronskiy) powers of  $e$ .

Upon analysis of the curves (Figure 38), the sharp bend of a curve attracts attention; according to I. A. Odinga (1949, 1954), this may be considered as consisting of two parts, which reflect two stages of weakening; and which coincide well with the law for change of the curve  $n = f(\sigma)$ , shown in Figure 37. The first, steeply falling, curved portion corresponds to the stage of intensive weakening, for which the parameter  $n$  seems to be the variable quantity. The second, linear, part of the semi-log curve corresponds to the stage of smooth change of stability; in this stage of the period of lowering stability,  $n$  is an almost constant parameter if it is considered as the reciprocal of the tangent of the angle of slope for the curve  $\ln y - t$ . It is interesting to note that this value of  $n$  was equal to 2700 hr,

while for the other process it was three minutes, thus verifying the extremely slow rate of the weakening process in the second stage. The comparative constancy of the parameter  $n = \frac{\Delta p v}{G_f}$  in the second stage indicates that, in this stage, the process of deformation proceeds in the form of a visco-plastic flow which is established with small changes of viscosity.

What has been said coincides well with the experiments which were analyzed in section 5, Chapter III.

All the data considered strongly imply that the model of an ideal elasto-plasto-viscous solid and the laws of linear deformation flowing from it, give only a quantitative indication; they do not reflect the actual rheological processes which occur in frozen soil. We pointed out that when a process of consolidation develops in a stage of the flow, then the physical properties of the frozen soil change; in particular, the viscosity does not have the described character and these soils can be considered, by applying the theory of a constant continuum to them, as visco-plastic media. Further, it can be shown that in the stages of the frozen soils which have been discussed, the flow equations of Bingham-Shwedoff are applicable in many cases.

### 3. The relationship among load, deformation, and the rate of flow

The relationship between stress and deformation, as is known, is a fundamental law characterizing the stress-deformation conditions of the solid body. We consider this relationship for frozen soils by taking into account the influence of the time factor (Vialov, 1956). From the experimental data, the recoverable portion of the deformation is directly proportional to the stress, but the residual deformation connected with the stress has a nonlinear dependence. So far as the deformation of the frozen soil (the residual, as well as the recoverable) is developed with time, the character of the curves reflecting the relationship between stress and deformations will change corresponding with variation in the time of action of the load or the rate of loading (Figure 39a). Thus, the relationship between stress and the total deformation of the frozen soil can be expressed by the equation,

$$\gamma = \gamma_{el} + \gamma_{res} = \frac{\tau}{G(t)} + \frac{\tau}{A'(t)} \frac{1}{\alpha'} \quad (34)$$

$\alpha' < 1$  is a coefficient of consolidation,  $G$  is the modulus of recoverable deformation, and  $A'$  is the modulus of plastic deformation. The influence of the time factor is reflected in the variability of these parameters, which change from large initial values of  $A'_i$  and  $G_i$  for  $t \rightarrow 0$  to small, final (limiting long-term) values  $A'_{lt}$  and  $G_{lt}$  at  $t \rightarrow \infty$ .

As seen from Figure 39a, the curve of the sum of the deformations deviates slightly from the curve of the residual deformations; the latter, with sufficient precision, may be described by a power law,

$$\gamma = \frac{\tau}{A(t)} \frac{1}{\alpha} \quad \text{or} \quad \tau = A(t) \gamma^\alpha, \quad (35)$$

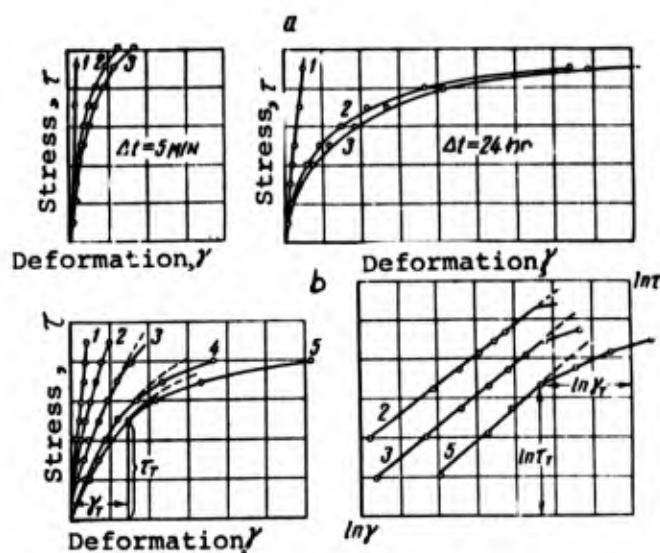


Figure 39. Relationship between the deformation and stress taking into account the time factor.

a. Classification of the sum of the deformations (3) into the recoverable (1) and the residual (2) for various  $\Delta t$ ; the penetration of a punch; sandy loam,  $\theta = -0.4C$  (experiment 21). b. The dependence between the summed deformations, and the loading in normal and logarithmic coordinates for different intervals of time of action of the load. (1) 1 min; (2) 1 hr; (3) 24 hr; (4) 120 hr; (5) 240 hr. Displacement along a rod, clayey soil;  $\theta = -0.4C$  (experiment 28).

where the parameters  $A$  and  $\alpha < 1$  differ somewhat from the purely plastic parameters  $A'$  and  $\alpha'$  in equation (34). Thus, the relationship between stress and summed deformations is graphically reflected in the set of curves  $\gamma = f(\tau)$ , the parameter of which is the  $t$  during which the load acts for the rate of loading  $\dot{\gamma}$  (Figure 39b). For a rapid increase in loading, the curves have a steep slope and are almost straight, i.e.  $\alpha_i \rightarrow 1$  and  $A_i \rightarrow G_i$ . An infinitely long-term, stepped loading or an infinitely slow loading corresponds to the limiting curve,

$$\tau = A_f \gamma^{\alpha_f} \quad (36)$$

Such a curve can be obtained by maintaining each step of loading until complete stabilization of the deformation. The validity of equation (35) is confirmed by placing the experimental points on a logarithmic graph (Figure 39b). By considering these points, it is seen that they lie on a straight line.

In many cases, particularly for frozen soils at low temperatures, the parameter  $\alpha$  is close to unity. Then equation (35) has the form,

$$\tau = G_{\tau}(t)\gamma, \quad (37)$$

which differs from Hooke's law in the variation with time of the parameter  $G_{\tau}$ , where

$$G_{\tau} = \frac{GA}{G + A}.$$

The parameters  $G$ ,  $A$  and  $\alpha$  in equations (34) - (37) are functions of temperature and the moisture-ice content of the frozen soil; they also depend on the type of soil.

As seen in Figure 39b, the curve  $\gamma = f(\tau)$  has a point of inflection, which is especially distinct on a logarithmic graph. This means that relationship (35) is correct only up to that point where the load reaches a certain limiting value, i.e. the yield stress  $\tau_{f1}$ , after which plastic flow occurs.

Up to the latter time, the yield stress of frozen soils is considered constant. Actually, from Figure 39b, it follows that each curve has its own point of bending. This means that the yield point is a varying value, which depends on the speed of loading, or the time of maintaining a step of loading.

It is necessary to show that the point of inflection of the curve  $\gamma = f(\tau)$  lies approximately on a vertical, i.e. all values of  $t$  correspond to one constant value of the deformation  $\gamma = \gamma_{f1}$ .

It follows that the emergence of plastic flow depends on reaching a deformation of some critical value which can be considered as depending only slightly on the rate of loading. This is confirmed also by the following theoretical considerations. We apply the law of deformation of frozen soil at  $\tau < \tau_{f1}$  in the form,

$$\phi \frac{d\gamma}{dt} + f\gamma = \tau + n(\tau) \frac{d\tau}{dt}; \quad (38)$$

this differs from equation (7) in its nonlinear relationship between  $\tau$  and  $\gamma$ , and the variability of the parameter  $n$ .

However, the laws of deformation at  $\tau > \tau_{f1}$  can be written in the form,

$$\phi \frac{d\gamma}{dt} = \tau + n(\tau) \frac{d\tau}{dt} - \tau_{f1}. \quad (39)$$

Because of the smooth transition from one stage to another we have, at  $\tau = \tau_{f1}$ ,

$$\gamma_1 = \gamma_2 \text{ and } \frac{d\gamma_1}{dt} = \frac{d\gamma_2}{dt},$$

from which we obtain the condition for transition into the stage of visco-plastic flow (Rzhanitsyn, 1949),

$$f\gamma = \tau_{f1} \text{ or } \gamma = \frac{\tau_{f1}}{f} = \gamma_{f1}.$$

However, these stages are not continuous, but the growth of the plastic deformation does change to a stage of failure, i.e. progressive flow.

Consequently, for frozen soils there are two limiting conditions which are determined by two criteria of stability.

The first limiting condition is characterized by the potential possibility of failure (consequent) and corresponds to the emergence of plastic flow. It is determined by the deformation reaching a certain critical value  $\gamma = \gamma_{f1}$ .

The second limiting condition is the transition to the stage of failure. It is determined by the development of plastic flow up to the limiting value  $\gamma = \gamma_{lim}$ .

For this condition, the concept of limiting stress is not sensible, since any loading which exceeds  $\tau_{f1}$  leads to failure. The first limiting condition corresponds to reaching a stress value  $\tau_{f1}$  which, however, cannot be considered as a criterion of strength, since it is a variable quantity. For rapid loading, the value of the limiting flow approaches the instantaneous strength  $\lim_{t \rightarrow 0} \tau_{f1} = \tau_{inst}$ , but when the load is maintained for a long time, the value of  $\tau_{f1}$  coincides with the limit of long-term strength. In other words, the limit of the long-term strength is determined by the limiting value of  $\tau_{f1}$  for infinitely slow loading:  $\lim_{t \rightarrow \infty} \tau_{f1} = \tau_{lt}$ .

This limit also can be considered as the basic characteristic of stability. Up to this limit the deformation is virtually stable, and the relation between deformation and stress is well defined, in the general case, at the rate (36), and the particular case as a linear (Hooke) law. When  $\tau_{lt}$  is exceeded, a continuous deformation arises and the well-defined connection between  $\tau$  and  $\gamma$  is broken. The law of deformation in this stage is determined by the relationship between the excess stress and the rate of deformation. For viscoplastic flow established, this relationship for frozen soil is represented in the general case, as shown by experiment, by the expression,

$$\frac{d\gamma}{dt} = \frac{1}{\eta'} (\tau - \tau_{lt})^b, \quad (40)$$

where  $\eta'$  and  $b > 1$  are coefficients which depend on  $\theta$ ,  $w$  and the type of soil. However, in many cases we can assume the law of Bingham-Shwedoff, according to which the rate of steady flow is directly proportional to the excess stress,

$$\frac{d\gamma}{dt} = \frac{1}{\eta} (\tau - \tau_{lt}), \quad (41)$$

where  $\eta = \eta_{pv} = f(\theta, w)$  is the coefficient of plastic viscosity.

The relationship discussed is correct only in a definite interval of the value of  $\tau$ , at not very great rates of flow. A complete rheological curve obviously has points of inflection which correspond to very great and very small stresses, analogous to the concept of N. V. Mikhailov and P. A. Rebinder (Figure 4). At  $\tau < \tau_{lt}$ , the straight

line  $\frac{d\gamma}{dt} - \tau$  could change into a smooth curve, asymptotically approaching the axis  $\tau$ . In other words, in frozen soil a flow type of slow creep with a constant, very large, relaxing viscosity in tangential stress, less than  $\tau_{lt}$ , is possible. In this case  $\tau_{lt}$  may be considered as the limit, which when exceeded changes a slow, secular flow into a visco-plastic flow with perceptible speed. Probably a second limit also exists (in excess of which deformation proceeds at a very high rate) which is accompanied by the failure of the structural bond.

#### 4. The laws of the process of deformation in frozen soils

It has been shown above that the equations of linear deformation (7) are not applicable to frozen soils, since in these soils the parameter  $n$  is a variable quantity, and the connection between  $\gamma$  and  $\tau$  is nonlinear. To use the special equations discussed above, the deformations can be described in the forms (38) and (39). These laws are explained with the help of models (Figure 3) with the difference, however, that the modulus of elasticity of the spring and the viscosity in cylinder (3) are variable (in the manner in which the sinking of a piston into a cylinder compresses a liquid). However, the most useful is the representation of the law of deformation of frozen soil in integral form in accordance with the theory of the so-called "hereditary creep" of Volterra-Boltzmann (Volterra, 1931).<sup>\*</sup> From this comes the law of change with time of the rate of deformation (Figure 40). At  $\tau < \tau_{lt}$  the curve of the speed asymptotically approaches the abscissa:  $\frac{d\gamma}{dt} \rightarrow 0$ , but at  $\tau > \tau_{lt}$  the curve changes to a horizontal direction, which corresponds to the stage of established visco-plastic flow. If the loading far exceeds the limit, then the region of constant rate of deformation is poorly defined: the rate, reaching a minimum value, increases again. This, the usual way in which frozen soil acts, is not present in structural foundations of interest.

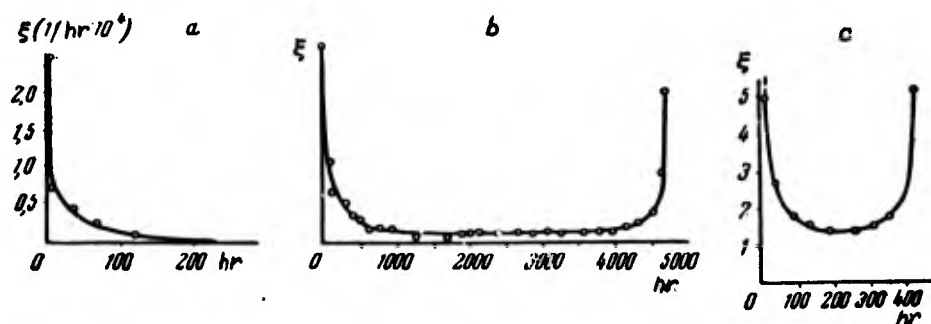


Figure 40. Change of the deformation rate with time.

a -  $\tau < \tau_{lt}$ ; b -  $\tau > \tau_{lt}$ ; c -  $\tau > \tau$ . Displacement along the lateral surface of a rod frozen into the ground;  $\theta = -0.4C$  (experiment 24).

<sup>\*</sup> See also Bronskiy, 1941; Ishlinskiy, 1945; Kachanov, 1948; Rabotnov, 1948; Rzhnitsin, 1949; et al.



We will consider the process of attenuating deformation; initially, we will proceed from the linear relationship between  $\gamma$  and  $\tau$ . The following initial premises are applied. (1) The instantaneous deformation complies with Hooke's law. (2) The elastic (which develops with time) deformation at  $\tau = \text{constant}$  at all moments of time is

directly proportional to the stress  $\gamma_{es} = \frac{\tau}{G_{es}}$  where  $G_{es} = f(t)$ .

(3) The law of superposition for the deformations, i.e. the value of the deformation at some variable loading, can be determined by summing the  $\gamma$ , which arises from the action of an elementary increment of  $\tau$ . It is assumed at the same time that the stress-deformation condition of the body depends not only on the stress, which is assumed at a given moment, but also on the effect of previous loading. Let the time  $v$  be related to the deformation  $\gamma(v)$ , and the duration of the flow interval be  $\Delta v$ . At the subsequent loading at the moment  $t$ , the stress is decreased in comparison with Hooke's by that amount which depends on the first deformation, the influence of which decreases with time according to the law  $R(t)$ .

In summation, proceeding from the law of superposition, we obtain

$$\tau = G_1 \gamma - \int_0^t R(t-v) \gamma(v) dv. \quad (42)$$

Solving this equation for  $\gamma$  and designating the resulting series  $R(z)$  by  $K(z)$ , we have

$$\gamma = \frac{\tau}{G_1} + \int_0^t K(t-v) \tau(v) dv. \quad (43)$$

where the first term represents the elastic-instantaneous deformation; the second represents the visco-elastic deformation, which develops with time. In these formulas  $K(t-v)$  is the aftereffect coefficient which is a function that reflects the influence of loading at the moment of time  $v$  on the deformation at the moment of time  $t$ . The function  $R(t-v)$ , i.e. the relaxation coefficient, reflects the influence of changes of the deformation on the stress. For the case  $\gamma = \gamma_0 = \text{const}$  or  $\tau = \tau_0 = \text{const}$ , equations (42) and (43) take the form,

$$\tau = \gamma_0 G_1 - \gamma_0 \int_0^t R(t) dt; \quad (44)$$

$$\gamma = \frac{\tau_0}{G_1} + \tau_0 \int_0^t K(t) dt. \quad (45)$$

These equations represent the law of relaxation of stress with time at constant deformation and the law of the development with time of the deformation at constant stress. In other words, from (45) the value of the deformation at any time  $t$ , arising under the action of a constant stress  $\tau$ , is determined. However, for the determination of  $\gamma$ , it is necessary to know the form of the function  $K(t)$ , which appears as the kernel of (45), and to integrate the latter. Analogously, for the determination of  $\gamma$ , it is necessary to know the form of the function  $R(t)$ .

The nature of the above functions will now be considered.



Differentiating (44) and (45) we obtain

$$K(t) = \frac{1}{\tau_0} \frac{d\gamma}{dt} \text{ and } R(t) = -\frac{1}{\tau_0} \frac{d\tau}{dt}.$$

Consequently,  $K(t)$  characterizes the rate of change with time of the deformation under the action of a constant unit load  $\tau = 1$ , and  $R(t)$  characterizes the rate of change of stress necessary for maintaining unit deformation  $\gamma = 1$ . From this comes a simple way of determining  $K(t)$ . This function leads to the curve of the changes with time of the rate of deformation  $\frac{d\gamma}{dt} = f(t)$ , if all the ordinates of this curve decrease by  $\tau$  times. Analogously  $R(t)$  is determined from the curve of the rate of relaxation. Between  $K(t)$  and  $R(t)$  there is an analytical connection; therefore, it is sufficient to determine one of these functions. For the processes of attenuating deformation (Figure 40a), the following properties are characteristic of the functions discussed: at  $t = 0$ , the functions  $K(0) = R(0) = \infty$ , and at  $t = \infty$ , the function  $K(\infty) = R(\infty) = 0$ . From the conditions considered above, it follows that the integrals in (44) and (45) with

limits from 0 to  $\infty$  have a finite value, namely:  $\int_0^{\infty} K(t) dt = \frac{1}{G_f} - \frac{1}{G_i}$ .

Equations (42) and (43) are extremely general and include a variety of forms of deformation. Thus, for correspondingly simple values of  $K(t)$  and  $R(t)$  these equations go over into the equations of Newton, Kelvin, Maxwell, Hohenemser-Ishlinskiy (7), Bronskiy, and others.

From the idea of Volterra-Boltzmann comes the theoretical nonlinear, successive creep, worked out by Yu. N. Rabotnov (1948) for solids in which the relationship between stress and deformation is nonlinear:  $\gamma = \phi(\tau)$ . At the same time, it is considered that the curve  $\gamma - \tau$  for various fixed moments of time applies, i.e. the deformation at any moment of time is proportional to some function of the stress. In other words, the curve of  $\gamma - \tau$  can be obtained from the curve of the deformation for  $\tau = 1$  by multiplying its ordinate by some function of the stress  $\phi(\tau)$ . With such an assumption, the equation of deformation takes the form,

$$f(\gamma) = \tau + \int_0^t Q_1(t-v) \tau(v) dv, \quad (46)$$

where  $Q_1(t) = \frac{1}{\tau_0} \frac{d}{dt} f(\gamma)$  is the coefficient of the plastic aftereffect. This equation also can be applied in the general case to frozen soils.

At the same time, for frozen soils, a nonlinear (power) relationship between the deformation and the stress is correct for all moments of time other than the initial; the instantaneous deformation obeys Hooke's law (Figure 39b). Concurrently, with reasonable approximation, it can be assumed that for various moments of time, besides the initial moment, the curves of  $\gamma - \tau$ , which are described by the expression (35), are similar in themselves ( $\alpha = \text{const}$ ); this is verified by the parallelism of the curves when they are plotted on a logarithmic scale (Figure 39b). Then for frozen soils the applicable equation for the deformation (47) (Rozovskiy, 1951) differs somewhat

from (46),\*

$$\gamma = \frac{\tau}{G_1} + \int_0^t Q(t-v) \phi[\tau(v)] dv, \quad (47)$$

where in accordance with (35),  $\phi(\tau) = \tau^{\frac{1}{\alpha}}$ .

At a constant value of the stress  $\tau = \tau_0 = \text{const}$ , equation (47) takes the form,

$$\gamma = \gamma_i + \tau^{\frac{1}{\alpha}} \int_0^t Q(t) dt. \quad (48)$$

In expressions (47) and (48)  $Q(t) = \frac{1}{\phi(\tau_0)} \frac{d\gamma}{dt} = \tau_0^{-\frac{1}{\alpha}} \frac{d\gamma}{dt}$ .

For frozen soil, in those cases where it appears that the linear relationship ( $\alpha = 1$ ) is correct, equations (47) and (48) transform into (43) and (45).

For the correct description of the process of deformation it is necessary to find the correct expression for the function  $Q(t)$  [or  $K(t)$ ]; at the same time, it is necessary to find the relationship between relaxation time and stress  $\tau$  which is introduced finally into the function being discussed. Such a value of  $Q(t)$  can be obtained from experiments, according to data on the rate of deformation, the laws of change of which reflect the physical processes which go on in frozen soils, including the changes of viscosity and time of relaxation. The curve  $\frac{d\gamma}{dt} = f(t)$  for frozen soil is close to a hyperbola.

The simplest expression which represents the curve is, according to Boltzmann, the function  $Q(t) = \frac{a}{t}$ . Upon substitution of this function into equation (48), we see that the development of the attenuated deformation proceeds according to the logarithmic law  $\gamma = \gamma_i +$

$a \ln t$ ; this corresponds to the law of "secular consolidation" of Buisman (1936) according to which the deformation increases without limit, but with ever-decreasing speed (at  $t \rightarrow \infty$ ,  $\gamma \rightarrow \infty$ , but  $\frac{d\gamma}{dt} =$

$\frac{a}{t} \cdot \frac{1}{t} \rightarrow 0$ ). However, the expression does not satisfy the initial con-

ditions, since at  $t = 0$  we obtain  $\gamma = \infty$ . Therefore for the initial moment of time (lower limit of integration) in formula (48), it is necessary to take  $t = 1$ . A stricter adherence to the initial condition is obtained if the function  $Q$  takes the form  $Q(t) = \frac{a}{bt+1}$ .

Upon substitution of this expression into formula (48), the law of attenuation of the deformation is in the form,

$$\gamma = \gamma_i + \frac{a}{b} \tau^{\frac{1}{\alpha}} \ln(bt + 1),$$

\* For greater detail it would follow, in accordance with Figure 39a, that creep deformation should be separated into: (1) initial (elastic), (2) elastic (recoverable), linearly dependent on the stress, and (3) residual, which is connected with the stress nonlinearly:

$$\gamma = \gamma_i + \gamma_{es} + \gamma_{res}.$$

which corresponds (at  $\gamma_i = 0$  and  $\frac{a}{b} \tau^{\frac{1}{a}} = A$ ) to the equation of "secular consolidation" of G. I. Pokrovskiy and A. A. Nekrasov (1934). The reduced equation was assumed by these authors to describe the process of settlement on unfrozen cohesive soil; as shown by A. M. Skibitskiy (Vialov and Skibitskiy, 1957), such a law is correct for deformations of certain unfrozen soils, for example, very dense clays. However, for frozen soils, as follows from our experiments, the function  $Q(t)$  follows the more general form,

$$Q(t) = \frac{ae^{-bt}}{t^{1-c}} \quad (49)$$

This function, which was assumed at one time by A. D. Rzhnitsin (1949) for crystalline solids, is a combination of a hyperbolic function, giving the law of "secular consolidation" deformation, and an exponential function, giving the asymptotic attenuation according to Maxwell.

The function (49) satisfies the limiting conditions considered earlier; at  $t = 0$ , the function  $Q(0) = (\infty)$ , and at  $t = (\infty)$  the function  $Q(\infty) = 0$ . This reflects the asymptotic approach of the rate-time curve to both coordinate axes (Figure 40a). At  $b = c = 0$ , (49) changes into the Boltzman function. The parameters  $a$ ,  $b$ ,  $c$  ( $0 < c < 1$ ) of expression (49) can be determined from the change of the rate of deformation with time by means of its rectification.

The values of these parameters which have been calculated by such means (experiment 37 on the penetration of a ball indenter) are applicable to the case of a linear relationship between  $\gamma$  and  $\tau$ ; that is  $\alpha = 1$  and  $Q(t) = K(t)$  were shown to equal  $a_0 = 0.009 \text{ cm}^*$ ;  $b = 0.2 \text{ hr}$  and  $c = 0.3$ . Consequently, for a given case, we have:  $v = \sigma K(t) = 0.09 e^{-0.2t} t^{-0.7} \text{ mm/hr}$ , where  $v = \frac{ds}{dt}$  is the rate of the absolute deformation penetration and  $\sigma$  is the stress under the indenter.

Table 27 is a comparison of the value of the rate of deformation  $v$ , calculated according to formula (49), and the value obtained directly from experiment.

Table 27. Rate of deformation  $v$ , mm/hr

Value of $v$	Time, hr									
	0.25	0.5	1.0	1.5	2.0	3.0	4.0	5.0	6.0	7.0
Theoretical	0.223	0.132	0.073	0.049	0.037	0.023	0.015	0.010	0.008	0.006
Experimental	0.250	0.140	0.075	0.050	0.035	0.022	0.015	0.013	0.011	0.008

\* The quantity  $a_0$  (or  $a\tau$ ), generally speaking, is unmeasured if the rate of the related deformation is considered. However, in a given instance, we operate with an absolute deformation by penetration of the indenter.

Thus, substituting the value of  $Q(t)$  from expression (49) into formula (48), we obtain for the case of constant loading,

$$\gamma = \gamma_i + \frac{1}{b^c} \frac{\alpha \tau_0}{c} \Gamma(bt, c), \quad (50)$$

where  $\Gamma(bt, c) = \int_0^{bt} e^{-z} z^c - 1 \, dz$  is the incomplete gamma function.

According to this formula, we can determine the deformation of frozen soil at any moment. For a final stabilized deformation, let  $t = \infty$ ; then  $\Gamma(bt, c)$  goes into the complete gamma function

$$\Gamma(c) = \int_0^{\infty} e^{-z} z^c - 1 \, dz,$$

the value of which is tabulated and is given in the reference. As already pointed out, for many cases the relationship between stress and the deformation of frozen soils may be taken as linear. Then  $\alpha = 1$ ,  $\phi(\tau) = \tau$ ,  $Q(t) = K(t)$  and equations (47), (48), (50) are correspondingly simplified.

The theory of successive creep permits, in principle, the calculation of the effect of varying the temperature of the frozen soil in the process of deformation, thus representing a case of substantial practical interest. The theory worked out by N. K. Arutyunyan (1952) for the creep of materials, the properties of which change with time, can be applied here. For example, for the simplest case of a linear deformation in equation (45), the modulus of instantaneous deformation  $G_i$  and the coefficient  $K(t)$  should be considered as functions of temperature; these appear, in turn, as functions of time,

$$G_i = \phi(\theta) = \phi[f(t)] = G_i(t), \quad (51)$$

and

$$K(t - v) = \frac{d}{dv} \left[ \frac{1}{G(v)} + C(t, v) \right]. \quad (52)$$

where  $C(t, v)$  is the measure creep deformation at the moment of time  $t$  from the action of a unit stress, which was applied at the moment of time  $v$ .

The laws which were analyzed above were related to the stage of attenuated deformation. For the stage of unattenuated creep, equations of the same type as (46) - (48) are applied, but with a form of the function  $Q(t)$ , which must reflect the curve of rate of unattenuated deformation (figure 40b). The integral of this function, for the

limits 0 and  $\infty$ , is infinitely large:  $\int_0^{\infty} Q(t) \, dt = \infty$ ; but the same function at sufficiently large values of time must have a constant value,

$$Q(t) = \frac{1}{(\tau - \tau_{1t})^\beta} \frac{d\gamma}{dt} = \frac{1}{\eta} = \text{const},$$

which corresponds to the rate of the established visco-plastic flow described by formula (40). When this flow conforms to Bingham's law,

then  $Q(t) = \frac{1}{\eta_{pv}} = \text{const}$  -- the reciprocal of the plastic viscosity.

However, with some approximation we can represent the deformation of undamped creep as the sum of the deformations of the aftereffects  $\gamma_{dc}$  and the flow  $\gamma_{fl}$ ; expressing  $\gamma_{dc}$  by equation (47), and  $\gamma_{fl}$  with the help of the limiting value considered above:  $Q(t) = \frac{1}{\eta_{pv}}$ .

Then,

$$\gamma_{cr} = \gamma_{dc} + \gamma_{fl} = \frac{\tau}{G_i} + \int_0^{t_1} Q(t - \nu) \phi[\tau(\nu)] d\nu + \frac{1}{n} \int_{t_1}^t [\tau(\nu) - \tau_{fl}] d\nu, \quad (53)$$

where  $t_1$  is the time to reach the deformation value  $\gamma_{fl}$ , i.e. the time which corresponds to the start of flow. Such time amounts to 100 to 500 hr.

For constant loading  $\tau = \tau_0 = \text{const}$ , and taking (40) and (50) into account we obtain

$$\gamma_{cr} = \gamma_i + \tau_0^\alpha \int_0^{t_1} Q(t) dt + \frac{1}{n} (\tau - \tau_{fl})^\beta (t - t_1),$$

or

$$\gamma_{cr} = \gamma_i + \frac{\alpha \tau_0^\alpha}{bc} \tau (bt, c) + \frac{(\tau - \tau_{fl})^\beta (t - t_1)}{n}. \quad (54)$$

For long durations  $t_1$  can be neglected. For engineering calculations, in many cases we can take  $\alpha \approx 1$  and  $\beta \approx 1$ ; then formula (54) is simplified.

##### 5. The laws of the reduction in strength of frozen soils

The relationship between the distorting force and the duration of its action is one of the basic laws which must be known in order to calculate the strength of frozen soils. In section 2, Chapter VI, it was shown that for frozen soil this law does not correspond to the Maxwell-Shwedoff equation of relaxation. However, at the same time, it was shown that the experimental points lie well on a straight line, if the reciprocal of the distorting force  $\left(\frac{1}{\tau}\right)$  is plotted vertically and the logarithm of the time, during which the distortion takes place ( $\ln t$ ), is plotted horizontally. Such a graph constructed from experimental data on frozen soil for the displacement along the lateral surface of a wooden bar is presented in Figure 41. From this it follows that the law of loss of strength (in particular, adfreeze strength) of frozen soil is described by the expression,

$$\frac{\beta}{\tau} = \ln \left( \frac{t}{B} \right), \quad (55)$$

where  $\beta$  (in kg/cm<sup>2</sup>) and  $B$  (in hr) are parameters which depend on the type of soil, its temperature, and the moisture-ice content. The reduced formula has great practical value, since with its help and with data from short-term experiments, it is possible to calculate the value of  $\tau$  at which the strength of frozen soils decreases in a given period of time, e.g. in the life of a building. The physical nature of formula (55) was shown by Tyler, who applied it to the development of a theory for strength of amorphous solids, based on Eyring's idea

(Nadai, 1954); it has been analyzed in section 2, Chapter I. Taking the logarithmic law as a measure of the rate of the molecular processes which depend on an activation energy, and also considering the determined rate of chemical reaction, Tyler assumed that the chemical bonds in the substance are destroyed upon stretching to some definite characteristic value  $\gamma_{lim}$ . This condition agrees well with the second condition of strength, which we obtained for frozen soils (section 3, this chapter).

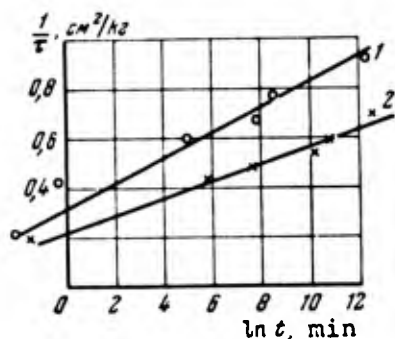


Figure 41. Rectification of the curves of the long-term adfreeze strength ( $\theta = -0.4^\circ\text{C}$ ); (1) silty, muddy soil (experiment 22); (2) heavy, silty, sandy loam (experiment 24).

To calculate the activation energy necessary for rebuilding the atomic structure, the relationship between the time necessary for failure of the elastic body and the action of the stress are expressed according to Tyler by the formula,

$$t = B \exp \left( \frac{G \alpha}{k T \tau} \right),$$

where  $\alpha$  and  $k$  are constants,  $G$  is the modulus of deformation, and  $T$  is the absolute temperature.

Taking the logarithm of this expression and setting  $\frac{\alpha G}{k T} = \beta$ , we obtain formula (55). The value of the parameters  $B$  and  $\beta$  can be determined either directly from the graph of  $\frac{1}{\tau} - \ln t$ , or by treating the experimental data by the method of least squares. Designating  $b = \frac{1}{\beta}$  and  $a = \frac{\ln B}{\beta}$ , we represent formula (55) in the form,  $\frac{1}{\tau} = a + b \ln t$ .

Then the values of  $a$  and  $b$  are determined from the common solution of the equations,

$$\left. \begin{aligned} n a + b \sum_{i=1}^n \ln t_i &= \sum_{i=1}^n \frac{1}{\tau_i} \\ a \sum_{i=1}^n \ln t_i + b \sum_{i=1}^n (\ln t_i)^2 &= \sum_{i=1}^n \frac{1}{\tau_i} \ln t_i, \end{aligned} \right\} \quad (56)$$

where  $n$  is the number of experimental points.

Processing the data of experiment 24 by such a method gives results shown in Table 28.

Table 28. Results from experiment 24

n	t	$\tau$ kg/cm <sup>2</sup>	ln t min	$\frac{1}{\tau}$	(ln t) <sup>2</sup>	$\frac{1}{\tau} \ln t$
1	14 sec	4.8	- 1.47	0.208	2.16	-0.243
2	5.3 hr	2.3	5.76	0.435	33.2	2.500
3	33 "	2.1	7.59	0.475	57.6	3.605
4	77 "	1.9	10.15	0.526	103.0	5.35
5	788 "	1.7	10.76	0.588	116.8	6.32
6	4735 "	1.5	12.55	0.666	157.5	8.36
		$\sum_{i=1}^n$	45.34	2.90	470.3	25.89

Substituting the obtained values in (56), we have  $6a + 45.34b = 2.9$  and  $45.34a + 470.3b = 25.89$ , from which  $\beta = \frac{1}{b} = 31.9$  kg/cm<sup>2</sup> and  $B = e^{-\frac{a}{b}} = 6.5 \cdot 10^{-6}$  hr. Having substituted these values in formula (55), we determine the theoretical value of  $\tau$  for a given moment of time  $t$ . Designating the ratio of the experimental value of  $\tau$  to the theoretical  $\frac{\tau_{\text{ex}}}{\tau_{\text{theor}}} = \tau^*$ , and assuming that for the case of ideal correspondence of all theoretical and experimental points  $\tau^*_{\text{av}} = \frac{\sum \tau^*}{n} = 1$ , we can calculate the value of the standard deviation for one determination, which for experiment 24 is

$$\sigma_1 = \sqrt{\frac{\sum_{i=1}^n \delta_i^2}{n-1}} = 4.6\%,$$

where  $\delta_i = \tau^*_{\text{av}} - \tau^*$  is the deviation of the ratio  $\frac{\tau_{\text{ex}}}{\tau_{\text{theor}}}$  for a given point from the ideal coincidence. Hence, the coefficient of variation, characterizing the general degree of deviation of the experimental points from the theoretical curve (55), is described by the equation,

$$\rho = \frac{\tau_i}{\tau^*_{\text{av}} \sqrt{n}} = 1.9\%.$$

As we can see, the level of accuracy is adequate.

Application of formula (55) for describing the process of loss of strength of frozen soil, and the direct comparison of the experimental and theoretical (calculated by the means discussed above) values of  $\tau$  are shown in Table 29. In this table, values of  $\tau$  were calculated in a manner somewhat different from the empirical method of formula (55) used by some authors for crystalline solids ("Proceedings of Sessions OTN and OFM, Academy of Sciences USSR", 1954).

$$\frac{\tau}{a} = \ln \frac{A}{t}, \quad (57)$$

where  $a$  (in kg/cm<sup>2</sup>) and  $A$  (in hr) are the parameters.



Table 29. Experimental and theoretical values of  $\tau$  (kg/cm<sup>2</sup>), calculated according to (55) and (57)

Experiment 22				Experiment 24			
t	$\tau$ Experi- mental	$\tau$ Theoretical		t	$\tau$ Experi- mental	$\tau$ Theoretical	
		Accord. to formula (55)	Accord. to formula (57)			Accord. to formula (55)	Accord. to formula (57)
7 sec	4.5	4.55	2.4	14 sec	4.8	5.0	3.2
45 "	2.3	3.3	2.2	5.3 hr	2.3	2.35	2.3
2.5 hr	1.7	1.75	1.75	33 "	2.1	2.05	2.1
42 "	1.5	1.45	1.5	4.29 "	1.9	1.75	1.75
77 "	1.3	1.35	1.4	788 "	1.7	1.7	1.7
4247 "	1.1	1.05	1.05	4735 "	1.5	1.55	1.5

As follows from Table 29 and as verified by the good co-linearity of experimental points when plotted in the coordinates  $\tau - \ln t$ , formula (57), as well as (55), gives satisfactory agreement with a given experiment. However, considering the good coincidence of the initial points\*, the greatest expressed slope at large  $t$ , and finally, the physical basis of formula (55), for frozen soil this formula is preferred. Formulas (55) and (57) characterize the process of unlimited reduction of strength with increasing  $t$ , i.e. they verify the concept of a limited long-term strength of which we have already spoken. However after a sufficiently large interval of time  $t_{lim}$ , the reduction of strength will take place more slowly, and for practical purposes it can be neglected. This value of  $t_{lim}$  will also correspond to the condition of limited long-term strength,

$$\tau_{lt} = \frac{\beta}{\ln\left(\frac{t}{\frac{t_{lim}}{B}}\right)}$$

The limit characterizes the stress at which, if exceeded, the rate of growth of the deformation becomes practically significant. This limit is a practical characteristic of frozen soil, necessary for engineering calculations. The reality and practical significance of the limit of long-term strength are verified by experiment. For illustration, this was recognized once again in the experimental data on failure

\* With formula (57) the initial condition was not satisfied: as  $t \rightarrow 0$ ,  $\tau \rightarrow \infty$ , which cannot be valid. Formula (55) also does not satisfy the initial condition, but owing to the smallness of the parameter  $B$ , coincidence with the initial points is obtained, entirely satisfactorily, even at  $t = 10$  sec.

presented in section 1, Chapter IV on frozen soil, since all loads exceeding  $1.8 \text{ kg/cm}^2$  led to failure. However at a loading of  $1.8 \text{ kg/cm}^2$ , failure did not arise, even though the sample was held in a loaded condition more than six years.

The value of the limiting time of reduction of strength  $t_{\text{lim}}$  is estimated. For experiment 24 (see Table 29), a direct experimental determination of the long-term strength was given, in accordance with Table 15,  $\tau_{1t} = 1.35 \text{ kg/cm}^2$ . Proceeding from formula (58) this value

corresponds to  $t_{\text{lim}} = B \exp\left(\frac{B}{\tau_{1t}}\right) = 6.5 \cdot 10^{-6} \exp [31.9/1.35] = 115,000 \text{ hr.}$

Further increases in time must, consequently, have an extremely small effect on the quantity  $\tau_{1t}$ . Actually, if  $t_{\text{lim}} = 50$  years is taken, then  $\tau_{50} = 1.28 \text{ kg/cm}^2$ ; if  $t_{\text{lim}} = 100$  years, then  $\tau_{100} = 1.26 \text{ kg/cm}^2$ , i.e. only 5 to 7% smaller than found from experimental data. Just as for experiment 22, the value obtained was  $\tau_{1t} = 0.9 \text{ kg/cm}^2$ , this value for  $t_{\text{lim}} = 50$  years decreased only to  $0.85 \text{ kg/cm}^2$ , and with  $t_{\text{lim}} = 100$  years only up to  $0.83 \text{ kg/cm}^2$ . Thus, considering the usual life of a structure, the calculated value of the limit of the long-term strength can, with sufficient accuracy, be determined according to formula (58) by substituting into this formula the value of  $t_{\text{lim}} = 50 \text{ yr.}$

#### 6. Methods of determining the limits of long-term strength

On the basis of the results already discussed, the following method of experimental determination of the limit of long-term strength of frozen soil follows.

First, the most widespread method consists of a direct loading according to experimental data of a series of identical samples; each sample is under a different constant load, beginning from that causing instantaneous failure and finishing with those that are indestructible over the long term. On the graph (Figure 19), the value of the failure load is plotted on the vertical axis, and the time to failure horizontally. The ordinate of the asymptote of the curve also determines  $\tau_{1t}$  (or  $\sigma_{1t}$ ). This method is the most reliable; but it, together with the necessary experiments in sufficiently large number (not less than 6-8) on identical samples, is naturally complex and requires a great expenditure of time, since the duration of the experiments at small  $\tau$  is extremely great.

The second method of determining the limit of long-term strength consists of finding points of inflection on the curve of stress and deformation. Experiments are performed under a load with an increasing rate, first holding it until the deformation stabilizes, and then until the beginning of flow. A graph is constructed of  $\gamma$  and  $\tau$  on a logarithmic scale (Figure 20) from the test data; the obtained lines will have points of inflection, the ordinates of which also determine the values of  $\tau_{1t}$ . The advantage of this method is the possibility of conducting an experiment with a single sample with the required repetition; the deficiency lies in the duration of the experiment.

The third method consists of determining the limits of the long-term strength from a graph of load and the rate of plastic flow which is caused by the load (Figure 21)\*. The value  $\tau_{lt}$  can be obtained as an intercept on the ordinate axis of a straight line, or of a smooth curve

$$\frac{d\gamma}{dt} = \tau,$$

as follows from formula (40) or (41): at

$$\tau = \tau_{lt} \frac{d\gamma}{dt} = 0.$$

The experiment can be carried out with one sample under an increasing rate of loading, as well as with a series of identical samples under different constant loads. The value of the load and the time it is held must be such that the rate of flow becomes constant and at the same time does not become extremely large. For construction of the graph we can confine ourselves to three or four points (with the necessary repetitions). This limitation simplifies the experiments and shortens the time. To conduct the experiment on loading, it is necessary to maintain the flow for a sufficiently long time. Otherwise, error may occur, e.g. taking a slowly attenuating deformation as plastic flow, or, on the other hand, considering a slow flow as a stabilization of the deformation. This error leads to a subsequent error in the determination of  $\tau_{lt}$ . Finally, in all cases it is necessary to ensure constancy of the temperature, since its variation leads to quite appreciable errors in the results. It is also necessary to protect the samples being tested from air drying; this is especially important for long-term tests.

The fourth method consists of an analytic determination of  $\tau_{lt}$  on the basis of formula (58). This method allows us to determine  $\tau_{lt}$  by means of a short experiment; this is its fundamental advantage over other methods. The testing is done with not less than three different loadings  $\tau$ , the values of which ensure rapid failure. As a result, the test time  $t$  is determined at which failure occurs. The experimental data are plotted on a graph of the type in Figure 41; along the vertical axis the values of  $\frac{1}{\delta}$  are plotted, and along the horizontal axis  $\ln t$ . The slope of the line, which is obtained on the graph, determines the value of  $\frac{1}{\delta}$  in formula (58). The intercept of this line and the vertical axis gives the value  $y = \frac{1}{\delta \ln B}$ , from which is found the parameter  $B = e^{-y\delta}$ . Knowing parameters  $B$  and  $\delta$  and setting  $t_{lim} = 50$  years (or any time depending on the period of service of the structure), the value of the limiting long-term strength is determined according to formula (58). The values of the parameters  $B$  and  $\delta$  can also be calculated, using equation (56), as was shown above.

\* In another interpretation, such a method was used by N. A. Tsytovitch (1940) for determining the limit of viscosity of frozen soil.

In conclusion, we may say that the formulas introduced in the present chapter are, in principle, correct (with more exact definitions) for plastic unfrozen soil as well, as was shown by the investigations of N. N. Maslov (1955), N.Ya. Denisov (1956), Geuse (1954), M.N. Goldshtein (1957); creep and a reduction of strength also develop with long-term loads. However, an essential distinguishing feature of frozen soils is that their parameters, in all the formulas introduced above, greatly depend on temperature, while for unfrozen soil the influence of the latter is insignificant; of course, the quantitative value of the parameters for frozen and unfrozen soils will be substantially different. Finally, the presence of ice in the frozen soils and the influence of phase transitions of water on them sharply affect the rate of flow of the rheological processes in these soils in comparison with unfrozen soils. In particular, in frozen soils the strength is significantly lowered (in relation to the instantaneous value) as compared to unfrozen soils, even though in the end the long-term strength of frozen soils in all cases turns out to be larger than in unfrozen soils.

## PART II. THE RESISTANCE OF FROZEN SOILS IN STRUCTURAL FOUNDATIONS

## CHAPTER VII. EXPERIMENTAL INVESTIGATIONS ON THE RESISTANCE OF FROZEN SOIL TO INDENTATION BY A PUNCH

At the present time, calculations for ordinary foundations of structures are based on two limiting conditions: the stability (structural) and the limiting deformation. For frozen soil at low temperatures, taking into consideration its low compressibility, the calculations are based on the first limiting condition, which arises when the loading exceeds a limiting value.

At the same time, under a limited load, as will be shown later, one should take, not the loading which gives rise to a bulging of the soils and failure settlement, but a loading small enough so that the settlement tends to stabilize at an amount (for frozen soil at low temperature) so small that for practical purposes it need not be considered. When the limiting load is exceeded, there arises an unattenuated settlement (creep), which can lead to an impermissible deformation of the structure. Thus, calculations using the limiting long-term resistance of the frozen soil also satisfy the conditions of a limited deformation, since this resistance, if it is not exceeded, is the criterion ensuring that deformations unsafe for the structure will not arise. The exception is plastic frozen soil at temperatures close to  $0^{\circ}\text{C}$ , which with  $p < p_{\text{lim}}$  may give a large consolidation settlement and for which deformation tests are necessary.

In the remaining cases, calculations of the deformations of frozen soils are necessary only when taking into account the action of a load larger than the limiting load; i.e. which unattenuated settlement occurs. Such calculations are performed from the development of the settlement with time, in a manner analogous to calculations of creep.

Study of the onset of the limiting state and determination of the limiting load can be performed with the help of an indenter penetrating into a soil model rigid footing for structures.

## 1. Experimental methods

Tests of the penetration of an indenter are performed in laboratories (in caves) as well as under field conditions. Laboratory experiments were carried out with blocks (30 cm x 30 cm x 30 cm and 15 cm x 30 cm x 30 cm) of undisturbed frozen soil, which were sealed into the "floor" of a cave (see section 1, Chapter I) and directly with soils in the cave under naturally occurring conditions. The characteristics of these soils are presented in Table 1. For transmission of the load to the indenter, a lever device with a vertical rod was used. The latter had bilateral screws, which allowed one to regulate, during the process of the experiment, the horizontal position of the arm. Some tests were performed on a lever press (0.5T); in these cases, the block of soil was held in a container. A dial indicator measured the deformation (readable to 0.01 mm) with three

indicators on each indenter. In isolated cases other self-recorders were used. In most of the experiments, the indenter was applied to the surface of the soil, but in some cases the tests were made with deep penetration. For protection from the air, the surface of the soil block was covered with moist sawdust.

Table 30. The Physico-mechanical Characteristics of The Soils

Gradation, % Fractions, mm			Plasticity, %			Density <sub>3</sub> tons/m <sup>3</sup> or Sp. Gr.
Sand >0.05	Silt 0.05- 0.005	Clay <0.005	Liquid limit	Plastic limit	Plasti- city index	
1.0	38	61	64.5	27.5	37	2.72

Temperature observations were made with thermometers and thermocouples.

For the laboratory tests, circular flat-faced punches with diam of 5.0 cm, 7.13 cm, and 10.14 cm were used. The apparatus was placed on the smoothed and leveled soil surface. Tests were made under constant loads and under loadings which increased by steps. In the basic experiments, each step of loading was maintained until the settlement stabilized, and went on until continuous deformations occurred, over the course of sufficiently large (from 500 to 1600 hr) intervals of time. In some experiments the loading, beginning with the first step, was maintained for equal intervals of time.

In the same cave, experiments were carried out under semi-industrial conditions with a circular indenter of larger dimensions:  $d = 50.5$  cm. In these tests, the ball was pressed directly into the soil of the cave. The loading was applied by a 100-ton hydraulic jack acting against the roof of the cave, which provided reaction through a special construction. Measurements of the penetration were made with three indicators, which were set up on deep-anchored pipes. These pipes were also used for measurements (by thermometers) of the soil temperature. Furthermore, thermocouples were put in the base of the indenter.

The tests discussed above also served at the same time for measurement of the reactive pressure of the soil under the base of the indenter for which an electrical device for measuring the deformations (see Chapter IX) was used. The soil with which the above-described semi-industrial tests were made was a dense, varved clay of the same type as discussed in Chapter I. The physico-mechanical characteristics of this soil are shown in Table 30.



## 132 RHEOLOGICAL PROPERTIES AND BEARING CAPACITY OF FROZEN SOILS

The moisture content of the soil according to depth (taken from the base of the indenter) was:

Depth, m	0.0-5	0.5-1.0	1.0-1.5	1.5-2.0	2-2.5	2.5-3.0
w, %	55	43	45	43	50	61

In the stratum of soil there was a large number of ice lenses, the thickness of which reached 3 to 5 cm. A graphic representation of the structure of the soil is given in Figure 44. The moisture content of the mineral layers of the soil (not including the ice inclusions) was equal to 38%.

The chamber in which the experiments were carried out was placed at a depth of 10 m from the surface. The natural temperature of the soil at this depth, which was maintained throughout the experiment, was  $-0.5^{\circ}\text{C}$  to  $-0.6^{\circ}\text{C}$ .

Experiments on the penetration of a punch were also carried out under field conditions. A circular punch of 70.5 cm diam was set up on a section of the permafrost station. The soils of this section below the bases of the punches had the following variations: punch no. 1 in a heavy, silty, sandy loam, with a thickness of 2.0 m, underlaid by a dense varved clay; punch No. 2 in a heavy, silty, sandy loam, underlaid at a depth of 3.0 m by a layer of gravel, and followed by a dense varved clay; punch no. 3 in a 25 cm layer of light, clayey soil, and below, a heavy, silty, sandy loam, underlaid at a depth of 1.8 m by an 80 cm layer of gravel, below which was a layer of varved clay. The moisture content of the sandy-clayey soil varied from 20 to 30% and reached 35%; in isolated and comparatively few places, where the soil contained ice inclusions, it reached 50 to 60%. The depth of the summer thawing at punch nos. 2 and 3 was about 1.5 m; punch No. 1 was set up on a portion of the so-called "non-fusing permafrost," the upper surface of which occurred at a depth of 2.25 m. The punch was sunk to a depth of 2.95 m. The temperature of the soil at this depth and below was from  $-0.1^{\circ}\text{C}$  to  $-0.3^{\circ}\text{C}$  at punch nos. 2 and 3, and  $-0.1^{\circ}\text{C}$  at punch no. 1.

The loading on the punch was done with the help of a lever (Figure 42); the short end was fastened to two anchors made of two metallic pipes ( $d = 89$  mm) to which brackets were welded in a staggered arrangement. The pipes were placed in a 15 m hole and later frozen in. For regulation of the horizontal position of the lever, the connection with the anchors was with the help of the turnbuckle. The loading of the lever on the punch was applied (with a fulcrum) through a wooden post, rigidly connected to the punch. To keep the soil from being melted by the post, the latter was inclosed in a wooden case filled with grease. The deformation of the soil was measured with a dial indicator (three indicators on each punch) fastened to an immovable supporting pipe which was set into the ground to a depth of 6 m. To control reading of the indicator, a systematic leveling of all the setups was carried out. Observations of the temperature of the soil were made with a sluggish thermometer at depths of 0 m, 0.5 m, 1.0 m, 1.5 m, and 2.7 m from the base of the punch, and by three thermocouples, which were fixed in the punch. The setting up of the apparatus was done in May, when the temperature of the air was positive; as a result, the soil





was somewhat warmed. The punch was loaded at the end of the summer. At this time, the temperature of the soil under the base of the punch was about 0 C, and at punch no. 1 it was even + 0.05 C. Later, the temperature reached its natural value. To reduce the cooling of the soil during the winter its surface was covered with a layer of sawdust. The horizontal variations of temperature at the greater depths were insignificant: at a depth of 2.75 m temperatures varied, equaling -0.1C at punch no. 1, -0.2 C at punch no. 2, and -0.3 C at punch no. 3.

2. The character of the failure of frozen soil under penetration by a punch

The idea of a limiting equilibrium of unfrozen soil under local loading comes from the assumption, experimentally verified for dense sand, that the disturbance of the equilibrium is accompanied by a heaving of the soil from under the base. However, for frozen soil, the deformed state is shown to be different from this. Actually, all the experiments performed with rapid increases of the loading up to 60 kg/cm<sup>2</sup>, as well as with long-term experiments, showed that heaving is absent in frozen soil. This is well illustrated in Figures 43, 44, and 45 where photographs are presented of sections of blocks of various soils, from sandy loam to varved clays (at  $\theta = 0.4$  C), after deep penetration into them of punches under various loads and for different time periods\*. Of course, the general rise of the surface of the soil

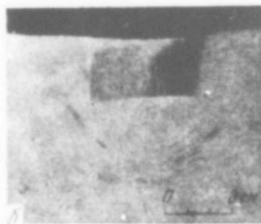
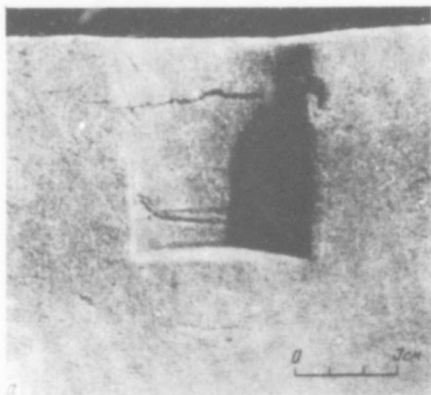


Figure 43. Section of a block of soil after the penetration of a punch.

a. Silty, muddy soil (experiment 16,  $p = 0$  to 25 kg/cm<sup>2</sup>). b. Light, sandy, soil; view of the compacted region of the soil under the punch (experiment 21c,  $p = 0 - 18$  kg/cm<sup>2</sup>,  $t = 432$  hr).

\* The designation  $p = 0 - 18$  kg/cm<sup>2</sup> and so on in the indicated photographs means the application of loads in equal steps, beginning at 0 and finishing at 18 kg/cm<sup>2</sup>; the time  $t$  is the total duration of the tests.

and some curving of this surface around the punch takes place as a result of the penetration of the punch. This deformation is far less than the heave that could be expected from calculations and which is observed in loose soil.

A more important characteristic of the disturbance of the structure is the appearance of cracks on the surface of the soil, directed radially from the axis of the punch; these were observed in many experiments under laboratory conditions, with small punches, as well as under working conditions with punches of  $d=50\text{cm}$  (Figure 44). The photographs of soil sections (Figures 33, 43, 44, 45) well illustrate the character of the deformed condition of frozen soil. Of especial significance are the photographs of banded soils, in which the distortion of the natural calcareous layers in the soil is distinctly seen. The photographs show the densification region of the so-called "elastic" (point densification) "kernel," which is formed in frozen soil under the base of the punch\*, similar to that which takes place in thawed soils. This kernel is especially easy to see in Figure 45a, where a section of the block separated like a walnut from its shell. The fact that the density of the kernel which has been discussed is greater than the density of the surrounding soil is indicated by the external form, as well as by direct comparison of the moisture content inside as well as outside the kernel (Table 26).

Of special interest is the fact, that the displacement of the frozen soil with a disturbance of the equilibrium proceeded not along the curvilinear slip surface, which is directed from the punch toward the free surface of the soil (as it is for unfrozen, loose soil), but at the side and below the punch in several lines, beginning at the punch edge at an angle to the vertical axis (Figures 33a and 45b).

Between the kernel and the line of displacement there is found a region of deformed soil, but above this line and in the kernel itself, the layers of soil maintain a horizontal position. It is characteristic that the ice inclusions, seen in Figure 33a, were formed as a result of the squeezing-out of ice and water just along the line of displacement (in the locality of fracture surfaces). This verifies the fact that the previously referred-to lines delimit the region of plastic deformation, and possibly, are also lines of discontinuity of stress.

From the above discussion it follows that structural disturbance of frozen soil under the action of a local loading is accompanied not by a heaving, but by a separation of the surrounding soil from the dense kernel which is formed under the punch. We point out, that in our opinion, an analogous phenomenon also takes place under certain conditions in plastic unfrozen soils. As shown by the recent, extremely interesting investigations of V. G. Berezantsev and V. A. Yaroshenko

---

\* The presence of such a kernel in the frozen soils was first pointed out in the experiments of V. G. Berezantsev (1949), who performed investigations of the resistance of frozen soils under local loading.

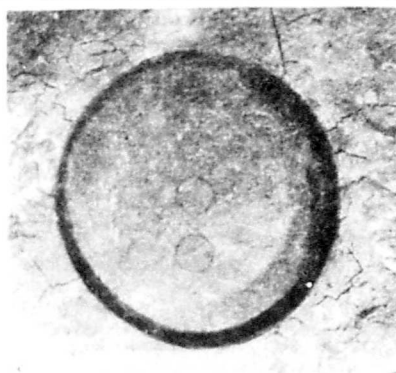
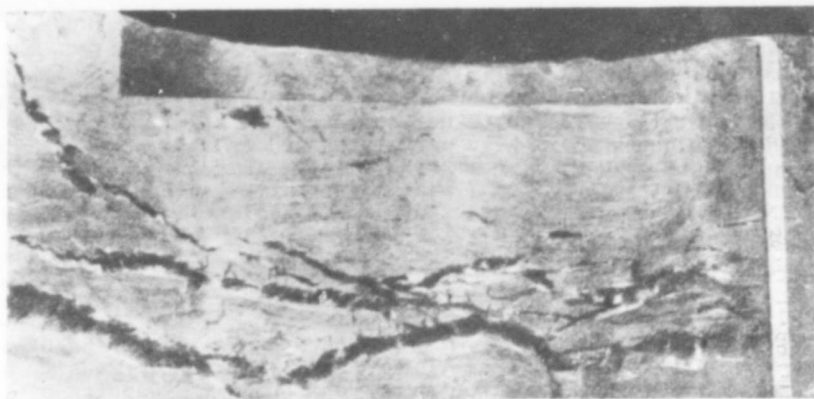


Figure 44. The character of the deformation of soil when a punch penetrates it.

Test under field conditions; the punch has  $d = 500$  mm. The soil: varved clay,  $\theta = -0.6C$ . a. Section of a soil block, showing the densified region under the punch and the bending of the clay layers. b. Top view showing the cracks on the surface of the soil.

(reported by them in 1956 in the All-Union Scientific Investigations of the Institute of Transport-Construction), an analogous picture of the structural disturbance is observed under certain conditions even in sand. Those authors established the fact, that depending on the density of the sand and the depth of the foundation, the fundamental character of the distortion of sandy soils will be different. With a shallow depth of foundation, a heaving of the soil occurs, but with a large depth in dense sand, and with any depth in loose sand, an expansion and densification of the surrounding soil (by the densification of the kernel) takes place. For argillaceous, unfrozen soils, the absence of heaving was pointed out in the works of B. I. Dalmatov (1951) and Sylvestrowicz (1953).

We established that the deformation of frozen soils takes place in this way: with small loadings on the punch there are only elastic and structurally reversible deformations, which characterize the first,

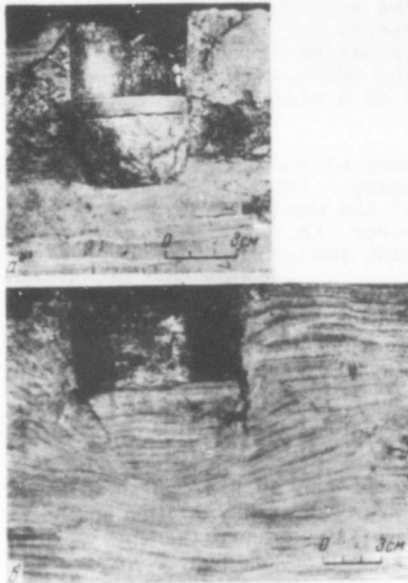


Figure 45. A sectioned block of frozen soil (varved clay) after the penetration of a punch.

- a. A clear view of the densified kernel, which was formed under the punch (soil with inter-stratified ice, experiment 22,  $p = 0 - 10 \text{ kg/cm}^2$ ,  $t = 1200 \text{ hr}$ ).
- b. View of the densified kernel under the punch and the deformation of the surrounding soil (experiment 19,  $p = 0 - 25 \text{ kg/cm}^2$ ,  $t = 6043 \text{ hr}$ ).

linear portion of the settlement-load curve. When the loading exceeds a certain critical value, there arises in the soil a non-reversible structural deformation of densification. These deformations, as was shown in Chapter IV, are a consequence of the flow of ice, its melting at the contacts between the mineral particles, the squeezing-out of the water and ice, which is formed from the region of high pressure under the punch, and the movement of mineral particles. As a result, a dense region of soil begins to form under the punch. Since in the process of densification, the physico-mechanical properties (density, the ratio between the solid and liquid phases of water and so on) are changed, then simultaneously with the rise in load the modulus of the total deformation also changes. Similarly, the relationship between the loading and the total deformation is nonlinear.

With any increase in the load, the region of densification is always increased. This leads to the formation of the dense kernel which has been described above. Finally, when the load reaches a limiting value and the greatest tangential stress in the neighborhood of the dense kernel exceeds the limit of the long-term resistance of frozen soil to displacement, there arises visco-plastic flow; the growth speed of this flow depends on the amount by which the load exceeds the limit. At this stage the densified kernel begins to separate from the surrounding less-dense soil, and together with the fundamental flow of ice which arises in it, there is also introduced a melting in the surrounding soil, a squeezing-out of water in the less stressed region, and so on. Further development of the visco-plastic deformation leads to structural failure of the soil.

Thus, the total settlement of a penetrating punch depends, in the first place, on the densification of the soil due to the squeezing out of air, ice and water; secondly, it depends on the total upheaval of the surface of the soil (with local distortion about the edge of the punch) due to the sinking into it of the punch with an abutting kernel, similar to the upheaval of the surface of a viscous medium when a cone is pressed into it.

Of course, the schematic development of the settlement which has been presented is to some degree arbitrary. Actually, all the enumerated factors affecting the character of the development of the settlement probably act simultaneously. However, in various stages, one or another of the phenomena has the dominant influence; this is reflected in the theory presented.

### 3. The development of the penetration of frozen soil with time

Figures 46 and 47 show the results of experiments on the penetration of a punch into varved clay under a constant load, which was  $13 \text{ kg/cm}^2$ , in consideration of the high density of the given soil. Figure 46 shows the exceptionally large influence which the temperature of the frozen soil has on the process of deformation. From this graph it can be seen that the settlement at  $-0.4^\circ\text{C}$  is 20 times larger than that at  $-7.6^\circ\text{C}$ .

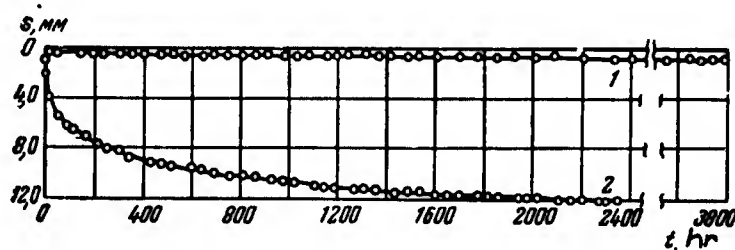


Figure 46. The settlement of frozen soil (varved clay) upon the penetration of a punch with  $p = 13 \text{ kg/cm}^2 = \text{const}$ , at various temperatures. (1)  $\theta = -7.6^\circ\text{C}$  (experiment 12), (2)  $\theta = -0.4^\circ\text{C}$  (experiment 5).

However, even at a temperature of  $-7.6^\circ\text{C}$  the settlement is not attenuated at once, but proceeds to flow for a very long time, although its value and intensity of growth are extremely small. At high temperatures the settlement reaches significant dimensions, building up in 2.5 months to  $0.12d$  (where  $d$  is the diameter of the punch). In all cases the rate of settlement decreases with time corresponding with the law (48).

The influence of the size of the punch is illustrated in Figure 47. As in unfrozen soils, with the increase of size, the duration of the growth of the settlement and its absolute value grow, since the size of the compressed region is also increased. As a first approximation, one can assume in analogy to unfrozen soils, that the settlement will be directly proportional to the diameter of the punch; however, this condition needs to be specifically checked.

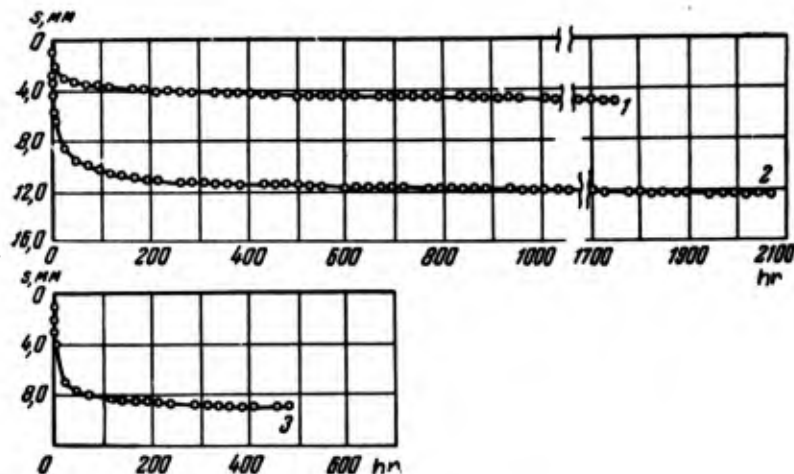


Figure 47. The settlement in frozen soil of a punch under a constant load of  $p = 13 \text{ kg/cm}^2$ , varved clay,  $\theta = -0.5^\circ\text{C}$ . (1) punch has  $F = 20 \text{ cm}^2$  applied to the surface of the soil (experiment 13); (2) punch has  $F = 40 \text{ cm}^2$  applied to the surface of the soil (experiment 11); (3) punch has  $F = 80 \text{ cm}^2$  sunk to a depth of  $3d$  (experiment 8). [ $F$  = area]

At the present time, in Soil Mechanics the depth of a foundation is considered only as a minor consideration [in settlement]. Actually, the role of depth is apparently quite significant. From a comparison of curves 2 and 3 in Figure 47, it is seen that a depth of  $3d$  ( $d = 10\text{cm}$ ) of the punch gives a settlement significantly smaller than a punch which is applied to the surface, even if in the first case the area is twice as large. The theoretical solution of the problem applies only to the case of a central force applied inside the elastic region. One can assume that the soil which lies above the bottom of the foundation not only counteracts the loading of its own weight, but, owing to the large force of the adhesion, takes part in the reaction of the entire deformed body.

The role of the foundation depth will be still more significant if we consider the relieving effect of the freezing of the soil to the lateral surface of the foundation in permafrost\*. As was shown (Table 19), the adfreeze strength is appreciably large, and at a proper foundation depth the force of adfreeze can take a significant portion of the load, thus relieving the soil below.

The results of field tests on the penetration of a punch will now be considered (Figure 48). As has already been shown, this punch is at  $3\text{m}$  from the daily [sic] surface, but it was insulated from the covered soil with the result that all the pressure was transmitted to the base. First, notice the extremely long period of settlement which

\* With the condition, of course, that the permafrost table is not lowered by the presence of the foundation.



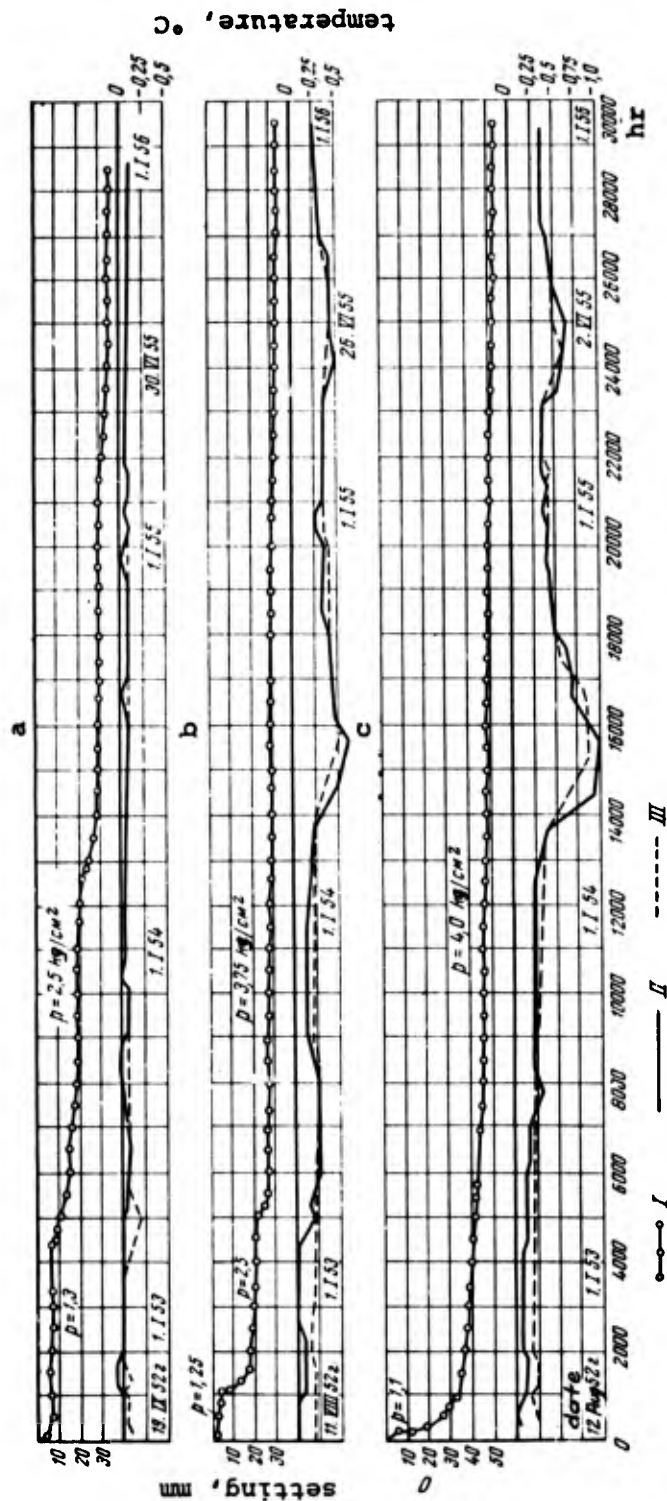


Figure 48. Tests of the penetration of a punch ( $d = 71 \text{ cm}$ ) into plastic frozen soil under field conditions.

I. Settlement of the punch. II. Temperature of the soil under the base of the punch. III. Temperature of the soil at a depth of 0.5 m below the base of the punch. a, b and c: data from the tests on punches number (1), (2), and (3). Note: the experiments are being continued at the present time, i.e. over a period of more than 7 years.

continued to increase for four years and is continuing at the present time, i.e. over a period of more than 7 years, though the rate of growth is extremely small. Punch no.1 with a load of  $1.3 \text{ kg/cm}^2$ , acting over a period of 4400 hr, settled (which was stabilized) about 7 mm, though the temperature of the soil under the punch was about  $0^\circ\text{C}$ . An increase of the load up to  $2.5 \text{ kg/cm}^2$  increased the settlement after 24,000 hr (by 1/1/1956) to 35 mm; during the growth of the settlement (at an extremely small rate), sharp changes were observed, the causes of which are not clear. Several increases of the rate of settlement (even though not large in absolute value) were also noticed in the first half of 1955. At that time, the increment of settlement was 4 mm, but after the second half of 1955 the settlement increased altogether by 0.7 mm (at  $\theta = -0.1^\circ\text{C}$ ).

Punch no.2, under loads of  $1.25 \text{ kg/cm}^2$  and  $2.5 \text{ kg/cm}^2$ , gave stabilized settlements of 5.5 mm and 21 mm. An increase of the load to  $3.75 \text{ kg/cm}^2$  increased the settlement after 24,300 hr to 31.5 mm. At that time a noticeable increase of the settlement was noted only in the initial period. Subsequently the growth of settlement proceeded at an extremely small rate: about 1.6 mm/year. At this intensity, the settlement continued to grow also in the second half of 1955 ( $\theta = -0.3^\circ\text{C}$  to  $0.4^\circ\text{C}$ ).

Punch no.3 was placed under a constant load of  $4 \text{ kg/cm}^2$ . The most intense rate of growth of the settlement was in the initial period when the temperature was close to  $0^\circ\text{C}$ ; during the first year the settlement was 44 mm. In the following two and a half years it was only 1 mm. By January 1, 1956 (at  $\theta = -0.2^\circ\text{C}$  to  $-0.3^\circ\text{C}$ , with isolated dips to  $-1^\circ\text{C}$ ) the settlement increased altogether by 5 mm, including in the last half year only 0.7 mm (at  $\theta = -0.4^\circ\text{C}$  to  $-0.5^\circ\text{C}$ ).

Thus, plastic frozen soil at a temperature close to  $0^\circ\text{C}$  has the ability to develop long-term settlement. For sandy, clayey soils at a temperature of  $-0.1^\circ\text{C}$ , this settlement under a load of  $2.5 \text{ kg/cm}^2$  continues to grow even at the present time (1959) at a rate of 3.3 mm/year (for the last three years), and for soils, at temperatures of  $-0.3^\circ\text{C}$  to  $-0.4^\circ\text{C}$  under loads of  $3.75 - 4.0 \text{ kg/cm}^2$  settlement continues to grow at the rate of 1.5 mm/year.

#### 4. The relationship between the penetration and the load

At the present time, calculations are made on the basis of the widely used principle of a linearly deformed region, according to which: 1) the recoverable, as well as the residual portion of the settlement depends linearly on the loading; 2) both parts of the settlement are related to the so-called total deformation, which is apparent from the form of deformation of the soil under the punch and in the surrounding soil. Only the recoverable portion of the settlement should in fact be related to the total deformation; this follows from the elastic-instantaneous and the elastic-delayed deformations, which are recovered with time (Figure 49). The remaining portion of the settlement (consolidation and plastic deformation) has a local character which develops directly under the punch. At the edge of the punch, a tension deformation occurs, the amount of which determines the local settlement. The diagram of such a region, which was assumed by I. I. Cherkasov (1955), is represented in Figure 50a.

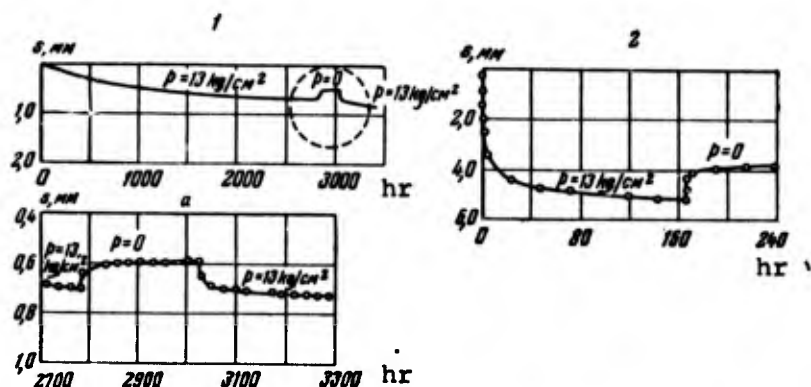


Figure 49. The recoverable deformation with long-term penetration of a punch into clay at: (1)  $\theta = -7.6^\circ\text{C}$  (experiment 12); (2)  $\theta = -0.4^\circ\text{C}$  (experiment 10); (a) portion of curve (1) to a larger scale.

A graph of the relationship between the load and the final settlement of frozen soil, with separation of the settlement into recoverable and residual portions, is presented in Figure 50b. This graph was obtained from the data of tests under semi-industrial conditions (the punch  $d = 505$  mm, varved clay,  $\theta = -0.6^\circ\text{C}$ ), with removal of the punch after each step of loading.

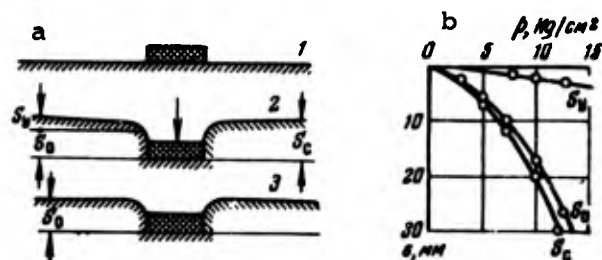


Figure 50. The deformation of frozen soil upon the penetration of a punch.

a. Diagram of the deformation of the soil. b. Graph of the dependence of the settlement on the load. (1) Initial position, (2) punch loaded, (3) punch unloaded;  $s_c$ -total settlement,  $s_0$ -residual settlement,  $s_y$ -recoverable settlement.

From the previous discussions, the complete settlement of the punch (circular and flat) for frozen soil is determined from the following expression

$$\frac{s}{d} = \frac{s_{lim} + s_{res}}{d} = \frac{1}{4} C(t) p + \sqrt{\frac{P}{A'(t)}} \quad (59)$$

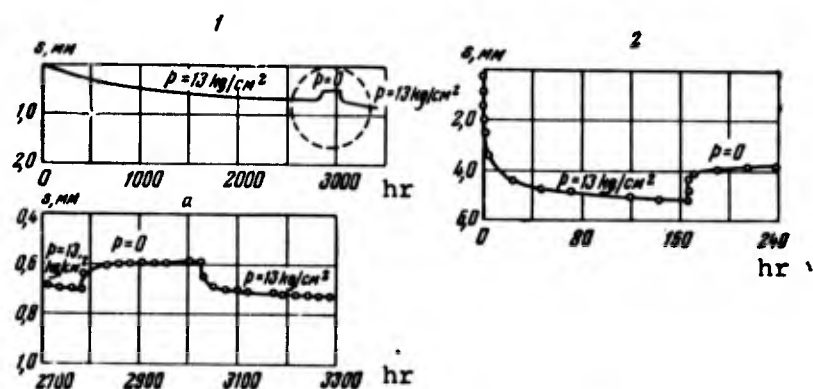


Figure 49. The recoverable deformation with long-term penetration of a punch into clay at: (1)  $\theta = -7.6^\circ\text{C}$  (experiment 12); (2)  $\theta = -0.4^\circ\text{C}$  (experiment 10); (a) portion of curve (1) to a larger scale.

A graph of the relationship between the load and the final settlement of frozen soil, with separation of the settlement into recoverable and residual portions, is presented in Figure 50b. This graph was obtained from the data of tests under semi-industrial conditions (the punch  $d = 505 \text{ mm}$ , varved clay,  $\theta = -0.6^\circ\text{C}$ ), with removal of the punch after each step of loading.

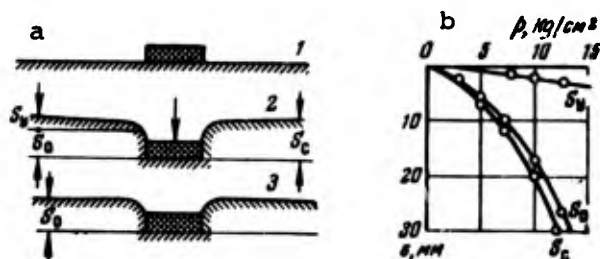


Figure 50. The deformation of frozen soil upon the penetration of a punch.

a. Diagram of the deformation of the soil. b. Graph of the dependence of the settlement on the load. (1) Initial position, (2) punch loaded, (3) punch unloaded;  $S_C$ -total settlement,  $S_0$ -residual settlement,  $S_Y$ -recoverable settlement.

From the previous discussions, the complete settlement of the punch (circular and flat) for frozen soil is determined from the following expression

$$\frac{s}{d} = \frac{s_{\text{lim}} + s_{\text{res}}}{d} = \frac{\pi}{4} C(t) p + \sqrt{\frac{P}{A'(t)}}, \quad (59)$$

which is analogous to the formula of I. I. Cherkasov (1952, 1955) for cohesive unfrozen soils, but it accounts for the variability with time of the parameters  $C$  and  $A'$ .

In this formula,  $C(t)$  is the coefficient of the linear half-space, which equals  $C(t) = \frac{1 - \nu^2}{E(t)}$ , where  $E$  is the time-dependent Young's modulus, and  $\nu$  is Poisson's ratio.

The parameter  $A'(t)$  is the coefficient of residual deformation, numerically equal to the specific loading at which the punch is embedded to a depth equal to its diameter. The unmeasured parameter  $\alpha' < 1$  is the coefficient which characterizes the slope of the curve  $s = f(p)$ ; this coefficient may be taken as independent of time.

The exponent  $\alpha$  expresses the rate of consolidation of the soil, that is, the influence of the structural cohesion. The nonlinearity of the process of penetration of the punch is demonstrated by the changes of the physical properties of the soil with deformation, as well as by the fact that the residual deformation in the soil under the punch is developed gradually, as the stress in the soil block increases and passes to the limit. We point out that the parameters  $\alpha$ ,  $A$ , and  $C$  are functions of the temperature and the moisture content of the soil.

The deformation of the soil surface around the punch can be described by the well-known expression from the theory of elasticity:

$$\frac{s_{\text{sur}}}{d} = pC(t) \arcsin \frac{d}{2\rho},$$

where  $d$  is the distance from the considered point on the surface to the center of the punch.

Taking into consideration the small effect of the recoverable portion of the settlement on the form of the curve between the total settlement of the frozen soil and a sufficiently large range of loading (Figure 50b), the curve, in accordance with Formula (35), can be approximated by a monomial degree equation that is correct in the limits  $0 < p < p_{\text{lim}}$ .

$$p = A(t) \left[ \frac{s}{d} \right]^\alpha, \quad (59a)$$

where  $s$  is the total settlement, and  $A$  and  $\alpha$  are parameters, analogous to  $A'$  and  $\alpha'$  in Formula (59); numerically they are different, since parameter  $A$  changes with time within the limits  $A_i > A(t) > A_f$ . For basic calculations with a constant load there should follow from the final, limited long-term value of  $A_f$ , a corresponding stable settlement  $s_f$ .

The correctness of the degree of dependence of the total settlement on the load (for frozen soils), especially the plastic settlement, is verified by the data of experiments (Figure 51); experimental points, plotted on a logarithmic scale, lie well on a straight line. Deviation from a power law is noticed only after the limiting value of the loading is exceeded. However, from these graphs the values of the parameters  $\alpha$  and  $A$  are found: the first from the slope of the logarithmic

curve and the second from the intercept on the ordinate axis which determines  $\ln A$ .

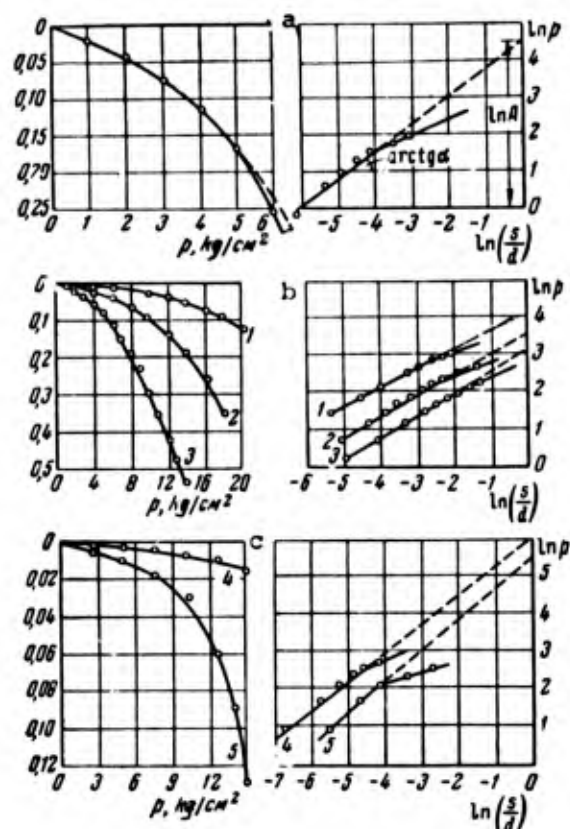


Figure 51. The relationship between the settlement and the load in the penetration of a punch into frozen soil (in normal and logarithmic coordinates).

a. Light, sandy loam;  $\theta = -0.4C$  (experiment 17). b. Silty, light, sandy loam,  $\theta = -0.4C$ ; time of action of the load  $\Delta t$ : (1) 5 min, (2) 24 hr, (3) 504 hr (experiments 21a, 21b, 14). c. Dense banded clay,  $\theta = -0.6C$ ; time of action of the load  $\Delta t$ : (4) 30 min, (5) 72 hr (field experiments 7 and 1).

The nonlinearity, in particular of the power law between the load and the settlement of natural and thawed soil, has been spoken of previously by several investigators (G. I. Pokrovskiy and M. N. Troitskaya, N. Ya. Denisov, and others); at the present time it has been convincingly shown by the experimental and theoretical investigations of I. I. Cherkasov (1952, 1955), N. V. Laletin (1954), A. S. Smirnov, A. K. Biruli, V. D. Zinchenko,\* and others.

Into Table 31 are brought values of parameters  $A$  and  $\alpha$ , introduced in Formula (59a), which were determined by means of processing the experimental data according to the method of least squares:

$$\alpha = \frac{n \sum (\ln p \cdot \ln \frac{s}{d}) - \sum \ln p \sum \ln \frac{s}{d}}{n \sum (\ln \frac{s}{d})^2 - (\sum \ln p)^2}$$

$$\ln A = \frac{\sum \ln p - n \sum \ln \frac{s}{d}}{n}$$

\* The determination of the modulus of deformation of soil. Report, Auto Transport Publication, 1955.



Table 31. The values of the parameters A and  $\alpha$  for plastic frozen soil

Experiment No.	Soil	Temperature °C	Time $\Delta t$	A kg/cm <sup>2</sup>	$\alpha$
21, a	Silty, light sandy loam	-0.4	5 min	61	0.51
21, b	The same	-0.4	24 hr	27	0.57
14	The same	-0.4	504 hr	23	0.60
7	Silty, heavy sandy loam	-0.4	1600 hr	20	0.67
4 (field)	Dense, varved clay	-0.6	1 hr	900	0.88
1 (field)	The same	-0.6	72 hr	220	0.81
9	The same	-0.4	1200 hr	48	0.81

where  $n$  is the number of experimental points.

It follows from Figure 51 and Table 31 that the coefficient A depends significantly on the time of exposure to the loading step  $\Delta t$ . Particularly in the experiment which is under consideration, the value of this coefficient changed from 61 kg/cm<sup>2</sup> to 23 kg/cm<sup>2</sup> for sandy loam, and from 900 kg/cm<sup>2</sup> to 50 kg/cm<sup>2</sup> for dense varved clay. It is necessary to take into consideration this time factor in order to evaluate the deformation properties of the soil, since the determination of A (or E) for a given short duration test, as sometimes is done in practice, leads to a significant misinterpretation. In regard to the coefficient  $\alpha$ , the laws of its changes, with its dependence on  $\Delta t$ , have as yet not been established. For sandy soil at  $\theta = -0.4^\circ\text{C}$ , the value of  $\alpha$  was shown to be 0.5 to 0.6, and for dense varved clay for  $\theta = -0.4^\circ\text{C}$  to  $-0.6^\circ\text{C}$ ,  $\alpha = 0.8$  to 0.9. Note that for unfrozen soils the value of  $\alpha$  ranges between 0.3 and 0.9.

Table 32 gives a comparison of the analytic values computed from formula (59a) and the experimental values of the settlement. As can be seen, the coincidence which was obtained is satisfactory; the coefficient of variation  $\rho$  varies between the limits 1 to 5% and only in one case reaches 9% because of the fall of the first point. These data illustrate well the correctness of formula (59a). Note that only the rate law describes the process of penetration of the punch, which has a close contact with the surface of the soil (with a preliminary grinding or pressing, etc). Where the contact is not a close one, a local compression of the soil occurs and the curve  $s = f(p)$  is concave in the initial portion.

It is known that a calculated characteristic of the deformation properties of soil serves as the modulus, of the total deformation,  $E_0$ , which for the linear deformation of a homogeneous medium is a constant value. For a nonlinearly deformed soil, the modulus  $E_0$  itself has a variable value which decreases with the growth of the pressure (Cherkasov, 1955). For separate calculations of the recoverable and the residual settlements, the value of this modulus can be determined in accordance with (59)



Table 32. Experimental and analytical values of the settlement in the penetration of a punch

Experiment 21a			Experiment 21b			Experiment 14			Experiment 17		
P, kg/cm <sup>2</sup>	s/d · 10 <sup>3</sup>		P, kg/cm <sup>2</sup>	s/d · 10 <sup>3</sup>		P, kg/cm <sup>2</sup>	s/d · 10 <sup>3</sup>		P, kg/cm <sup>2</sup>	s/d · 10 <sup>3</sup>	
	Exp.	Anal.		Exp.	Anal.		Exp.	Anal.		Exp.	Anal.
Silty, sandy loam											
4.0	4.8	4.5	2.0	5.2	5.6	1.0	6.0	5.7	1.0	2.0	1.5
6.0	10.6	10.1	4.0	20.0	19.5	2.0	17.6	17.6	2.0	4.2	4.2
8.0	17.4	17.8	6.0	38.6	39.2	3.0	33.5	34.7	3.0	7.3	7.9
10.0	26.2	27.6	8.0	63.3	65.9	4.0	64.6	55.6	4.0	11.2	12.0
12.0	38.0	39.6	10.0	95.0	97.3	5.0	79.0	81.3	5.0	16.4	17.3
14.0	53.2	53.9	12.0	138.6	135.3	6.0	109.5	109.7	6.0	25.2	22.8
16.0	71.2	70.7									
$\sigma_i=4.45\%$ $\rho=1.7\%$			$\sigma_i=4.05\%$ $\rho=1.65\%$			$\sigma_i=3.3\%$ $\rho=1.35\%$			$\sigma_i=20.8\%$ $\rho=9.3\%$		
Experiment 7 (field)			Experiment 1 (field)			Experiment 9 (lab)			Experiment 15 (lab)		
P, kg/cm <sup>2</sup>	s/d · 10 <sup>3</sup>		P, kg/cm <sup>2</sup>	s/d · 10 <sup>3</sup>		P, kg/cm <sup>2</sup>	s/d · 10 <sup>3</sup>		P, kg/cm <sup>2</sup>	s/d · 10 <sup>3</sup>	
	Exp.	Anal.		Exp.	Anal.		Exp.	Anal.		Exp.	Anal.
Dense, varved clay											
2.5	1.2	1.25	2.5	4.1	3.9	2.0	20.0	20.0	3.0	5.9	6.1
5.0	2.8	2.85	5.0	8.9	9.35	4.0	47.4	46.9	5.0	16.5	17.9
7.5	4.8	4.70	7.5	15.9	15.4	6.0	74.2	77.3	7.0	34.0	35.4
10.0	6.7	6.65				8.0	110.0	110.8	9.0	70.8	61.4
						10.0	147.0	146.6			
						12.0	176.0	180.9			
$\sigma_i=2.2\%$ $\rho=1.1\%$			—			$\sigma_i=2.1\%$ $\rho=0.75\%$			$\sigma_i=10.6\%$ $\rho=5.1\%$		

NOTE:  $\sigma_i$  = standard deviation %       $\rho$  = coefficient of variation %

$$\frac{E_0}{1 - \nu_0^2} = \frac{1}{C(t) + \frac{4}{\pi} \sqrt{\frac{a'}{P} \frac{1 - a'}{A'(t)}}}$$

For calculation of the total settlement, proceeding from Formula (59a), the value of  $E_0$  is determined by the expression

$$\frac{E_0}{1 - \mu_0^2} = \frac{\pi}{4} \sqrt[A(t) p^\alpha - 1]{} = \frac{\pi}{4} A(t) \left[ \frac{s}{d} \right]^{\alpha - 1}, \quad (60)$$

where  $E_0 = f(t)$ , while  $E_0(i) > E_0(t) > E_0(f)$ .

The value of the exponent  $\alpha$  depends on the properties of the frozen soil: the denser the soil and the lower its temperature, the closer to unity is the exponent. For example, for dense varved clay even at  $\theta = -0.6^\circ\text{C}$ ,  $\alpha = 0.8 - 0.9$ . In many cases (soils at low temperature), the value of  $\alpha$  can be taken equal to unity. Then  $A = \frac{\pi}{4} \frac{E_0}{1 - \mu_0^2}$ ,

and formula (59a) transforms into the well known equation of a deformed linear medium:

$$p = \frac{\pi}{4} \frac{E_0(t) s}{1 - \mu_0^2}, \quad (61)$$

with the difference, however, that  $E_0$  is a function of time.

The nonlinear character of the relationship between  $s$  and  $p$  correctly reflects the physical nature of the process of the deformation of frozen soil. At the same time it allows one to take into consideration the behavior of the soils in a broader region of load changes up to its limiting value, whereas the application of the rule of linear deformation is restricted to the limit of proportionality. However, in view of the undeveloped state of the theory of nonlinear elasticity, the direct utilization of the power law for calculation from fundamentals has practical difficulties. Therefore, these calculations can be carried out by the method of the theory of linear elasticity by replacing the actual curves  $s = f(p)$  by broken straight lines. In specific cases, one can prove that straight lines are a satisfactory approximation for the entire curve, so that the assumed value of  $E_0$  for the actual value of the deformation can be taken.

CHAPTER VIII. DETERMINATION OF THE BEARING CAPACITY OF FROZEN SOILS  
TAKING THEIR RHEOLOGICAL PROPERTIES INTO ACCOUNT

## 1. Theoretical value of the limiting stress

The analytical computation of the limiting stress is achieved by means of the theory of limiting equilibrium (Sokolovskiy, 1950, 1954). According to Novotortsev and Sokolovskiy, for cohesive soils possessing both cohesion ( $c$ ) and friction ( $\phi$ ), the limiting stress (for a two dimensional problem in which gravity is neglected) is equal to:

$$P_{lim} = c \cot \phi \left[ \frac{1 + \sin \phi}{1 - \sin \phi} e^{\pi \tan \phi} - 1 \right] + q \frac{1 + \sin \phi}{1 - \sin \phi} e^{\pi \tan \phi}, \quad (62)$$

where  $q = \gamma_s h_f$  is the load ( $\gamma_s$  is the unit weight of the soil, and  $h_f$  is the depth of the foundation).

For soils which do not possess internal friction, i.e. which obey condition (31), the above formula can be written, according to Prandtl, as

$$P_{lim} = (\pi + 2) c + q. \quad (63)$$

N. A. Tsytovich (1937, 1952) suggested the use of formula (63) for frozen soils. Using a limiting long-term value of the cohesion,  $c_{lt}$ , to account for the rheological properties of frozen soils, the direct application of formula (63) to frozen soils is possible when the values of  $\phi_{lt}$  are small and can be neglected in the calculations. If the soils possess both cohesion and friction, then one must use formula (62) introducing in it limiting long-term values of the strength parameters  $c_{lt}$  and  $\phi_{lt}$ .

At the same time, as S. S. Vialov and N. A. Tsytovich (1956) have shown, it becomes possible to use the results of a ball-test to determine the limiting stress on such soils by means of the complex characteristic  $c_e$  called "equivalent cohesion" (section 2, Chapter II). From a comparison of the computations, it follows that if one substitutes the value of the equivalent cohesion in (63), within certain limits, the value of  $p_{lim}$  obtained will be equal to the value obtained by means of formula (62), which takes cohesion and friction into account separately. For instance, according to experimental data for three different soils, the value of  $c_e$  is equal to 0.75 kg/cm<sup>2</sup>; 2.3 kg/cm<sup>2</sup>, and 4.0 kg/cm<sup>2</sup>. Let us now assume that the value of  $\phi$  for these soils can vary from 0 to 30°. Then by means of formula (19) the following values of  $\underline{c}$  are obtained (Table 33),

Let us further determine the value of  $P_{lim}$  by two formulas, namely, (1) by formula (63), in which  $\underline{c}$  is replaced by  $c_e(lt)$ , and (2) by formula (62), in which  $c$  and  $\phi$  are replaced by the values of  $c_{lt}$  and  $\phi_{lt}$  obtained in Table 33. In addition, the values of the load  $q$  (in kg/cm<sup>2</sup>) are assumed to be varied.

Table 33. Values of  $c$  (kg/cm<sup>2</sup>) for various values of  $\phi$  and  $c_e$

$\phi$	M	values of $c$ for $c_e$ equal to		
		0.75	2.3	4.0
0	1	0.75	2.3	4.0
10	0.615	0.45	1.41	2.46
20	0.285	0.214	0.655	1.14
30	0.122	0.092	0.280	0.49

It can be seen from the range of variations of  $c$  and  $\phi$  (bounded in Table 34 by the dotted line), that the results of calculations by these two formulas are in close agreement. In this way, the limiting stress for frozen (and plastic unfrozen) soils can be determined according to the formulas of the theory of plasticity, using the equivalent limiting long-term cohesion. For strip footings, formula (63) is used as is, whereas for two-dimensional circular footings (Ishlinskiy, 1944; Berezantsev, 1949) we should use

$$P_{lim} = 5.65 c_e + q, \quad (64)$$

Table 34. Values of  $P_{lim}$  (kg/cm<sup>2</sup>) for various  $c_e$ ,  $q$ , and  $\phi$

Method of calculation.	$\phi$	$c_e = 0.75$			$c_e = 2.3$			$c_e = 4.0$		
		$q$			$q$			$q$		
		0.25	0.5	0.75	0.25	0.5	0.75	0.25	0.5	0.75
By formula (68) with the introduction of $c_e$ .	-	4.1	4.4	4.6	12.1	12.3	13.6	20.9	21.1	21.4
By formula (62) taking $c$ and $\phi$ into account separately.	0	4.1	4.4	4.6	12.1	12.3	13.6	20.9	21.1	21.4
	10	4.4	5.0	5.6	12.1	12.8	13.4	20.8	21.5	22.5
	20	4.8	6.4	8.0	11.3	13.0	14.5	18.5	20.1	23.3
	30	7.3	11.8	16.5	12.9	17.4	20.0	19.0	23.7	28.3

For a two-dimensional footing of square cross-section (Shield and Drucker, 1953), we should employ

$$P_{lim} = 5.71 c_e + q. \quad (65)$$

Note that if we take into account the influence of the "elastic kernel" forming under a punch, the limiting stress, for a two-dimensional problem, is equal to (Berezantsev, 1949)

$$P_{lim} = 5.7 c_e + q. \quad (66)$$

In the following computation it will be shown that the possibility of determining the limiting stress through data of ball-tests follows directly from an examination of the nature of these experiments.

2. Determination of the limiting stress from the results of penetration by spherical indenters

A further application of the ball-test method, suggested by N. A. Tsytovich, consists in the direct evaluation of the bearing capacity of frozen and plastic unfrozen soil through the amount of penetration of the spherical indenter. From the solution of the problem of the limiting equilibrium of a plastic medium under penetration by a sphere (Ishlinskiy, 1944), it follows that the normal stresses under the sphere are distributed according to some non-linear law yielding  $\sigma_1 = 4.37 c$  at the edge of the surface of imprint and  $\sigma_1 = 7.0 c$  in the center.

The average normal pressure, per unit area of the imprint surface  $\omega$ , transferable by the spherical indenter penetrating under a concentrated force  $P$ , is equal to

$$p = \frac{P}{\omega_t} = \frac{P}{\pi d s_t}, \quad (67)$$

where  $d$  is the diameter of the sphere, and  $s_t$  is the depth of the imprint.

For the penetration of a sphere in frozen soil, the depth and hence the area of imprint  $\omega_t$  increases with time. Consequently, the average pressure  $p$  decreases. In addition, the curve representing the decrease of  $p$  in time will resemble the relaxation curve for cohesion (Figure 5). The minimum pressure  $p$  corresponds to the final stabilized penetration of the spherical indenter  $s_f$ . This is also the limiting pressure  $p_{lim}$ , i.e. the condition of limiting equilibrium sets in at this value. Any increase of the force  $P = \frac{1}{0.36} \pi d^2 c_e$ , applied to the sphere results in a sinking of the sphere by an amount  $s > \frac{d}{2}$ , and causes a permanent visco-plastic deformation. Comparing expressions (67) and (18) for  $s_t = s_f$ , we get the following formula for the computation of the limiting stress on the soil under a spherical indenter:

$$P_{lim} = \frac{P}{\pi d s_f}, \text{ or } P_{lim} = 5.55 c_e; \quad (68)$$

taking the depth into account,

$$P_{lim} = \frac{P}{\pi d s_f} + q = 5.55 c_e + q. \quad (69)$$

This expression can also be obtained directly, using the plasticity theory. Formula (69) gives values of  $p_{lim}$  which are close to the values of  $p_{lim}$  from formulas (64) - (67). Thus, the limiting stress determined by the depth of the penetration of a spherical indenter can be approximately considered as the limiting stress on a shallow, flat, two-dimensional punch of square or circular (and with some allowance, even rectangular) cross-section.

The method of pressing a spherical indenter of sufficiently large dimensions for field determination of the bearing capacity of frozen (and plastic unfrozen) soil seems promising to us, compared to the standard method of test-loading flat punches. With this method (spherical indenters), the tests are carried out under a unique constant load (as opposed to a series of loads increasing in steps), each of which must be maintained until the stabilization of the deformation. This method shortens significantly the duration of the experiment, and decreases its cost. Furthermore, with the method using test-loads, the value of  $p_{lim}$  is determined by means of the "conventional" point of inflection of the penetration curve (the choice of the point of inflection is to a certain extent subjective). For a test of the penetration of a sphere, the value of  $p_{lim}$  is determined in a very simple, well-defined way, i.e. directly from the value of the stabilized penetration which is, so to speak "automatically" noted by the fact that the pressure reaches a limiting value,  $p_{lim} = \frac{P}{\pi d s_f}$ .

Note that, unlike tests of individual samples, tests with a sphere having a large diameter allow taking into account the influence of the structure of the frozen soils, e.g. the presence of ice inclusions in them. That is they allow to some extent the evaluation of the bearing capacity of the whole soil mass. One need only point out the necessity of a special investigation of the problems of the influence of the sphere's dimensions and the values of the stresses for the final results, i.e. one should investigate the conditions of similarity and invariance of  $p_{lim}$ . In particular, in section 3 of Chapter II it was shown that in the penetration process a certain strengthening of the soil occurs, although it is very small for practical purposes. In conclusion, note in Table 35 the values of  $p_{lim}$  obtained from tests on frozen soils of natural structure for penetration of a ball indenter under laboratory conditions.

Table 35. Values of the limiting pressure of frozen soils

Soil	Moisture content %	$p_{lim}$ (kg/cm <sup>2</sup> ) for a temperature:		
		-0.3C	-1.2C	-4.2C
Dense, varved clay	35	10	14.5	23.0
Silty loam	32-36	3.5-5.0	5.5-8.3	11.0-14.0
Heavy, silty, moist, sandy loam	43	4.2	-	11.0
Silty, sandy loam	34-28	5.0-7.2	8.9-11.0	15.5-18.0
Sand	23	10.0-13.0	15.0	21.0-25.0

### 3. Comparison of the experimental and theoretical values of the limiting stress

In Figure 52, the results of two tests on undisturbed frozen soils by the penetration of flat, circular, punches ( $d = 50$  mm and 71 mm)

are shown. In experiment 17 (light, sandy loam,  $w = 26\%$ ), the penetration for stresses up to  $5 \text{ kg/cm}^2$  (inclusive) was for all practical purposes damped; for stresses equal to or greater than  $6 \text{ kg/cm}^2$ , an undamped penetration arose, leading to collapse\*. When this undamped penetration arises, the well-defined relation between the penetration and the load is no longer valid, and the experimental points begin to deviate from the curve  $p = A \left(\frac{s}{d}\right)^n$ . This is represented by the kink of the curve plotted on a logarithmic scale. Hence, the ordinate of this point determines the limiting stress  $p_{\text{lim}}$ . In the experiment examined,  $p_{\text{lim}} = 5.3 \text{ kg/cm}^2$ .

A power law is not the only law representing the relationship between the stress and the penetration; one can, generally speaking, select another equation for the curve  $s = f(p)$  fitting the experimental data more or less satisfactorily. In all cases, the well-defined relation between  $s$  and  $p$  will be valid only for stresses smaller than  $p_{\text{lim}}$ .

The other example (Figure 52b) refers to a sandy loam of high ice-content ( $w = 42\%$ ) (experiment 7). This soil is highly silty and plastic; its plasticity index (16%) is close to that of clay soils. The peculiarities of this soil explained the long duration of the deformation process: even after 1775 hr for  $p = 2 \text{ kg/cm}^2$ , and after 2376 hr for  $p = 4 \text{ kg/cm}^2$ , the penetration had not become completely stabilized. However, these penetrations increased at an extremely small rate (.005 mm/day and .0075 mm/day) and had a damped character. The value of the limiting stress for this soil, determined by means of the kink of the curves  $\ln \left(\frac{s}{d}\right)$  (vs.  $\ln p$ ), turned out to be equal to  $p_{\text{lim}} = 4.7 \text{ kg/cm}^2$ .

Now compare the above experimental values to the values of  $p_{\text{lim}}$  computed by formula (68) according to the data of laboratory tests of penetration with a ball indenter. For experiment 17, these tests yielded  $c_e = 1.0 \text{ kg/cm}^2$ , hence  $p_{\text{lim}} = 5.55 \text{ kg/cm}^2$ . For experiment 7,  $c_e = 0.88 \text{ kg/cm}^2$  and  $p_{\text{lim}} = 4.9 \text{ kg/cm}^2$ . The results of similar comparisons for other experiments are given in Table 36.

It can be seen that the analytical and experimental values of  $p_{\text{lim}}$  obtained are sufficiently close to each other. This proves the applicability of formula (68) for the evaluation of the bearing capacity of frozen soils.

#### 4. Influence of ice inclusions on the bearing capacity of frozen soils

Let us now examine the results of pressing punches into frozen soils having ice layers; for this purpose, consider first the case in which these layers occur close to the base of the punch. Under the action of pressure, plastic deformations arise in the ice, which for relatively small stresses develop into a permanent bending of the ice layers (Figure 53a). With the growth of stress, the strengthened

\* On the graphs of Figure 52, the results of the tests are not completely shown; actually in experiment 17, the load reached  $20 \text{ kg/cm}^2$  and in experiment 7,  $12 \text{ kg/cm}^2$ .



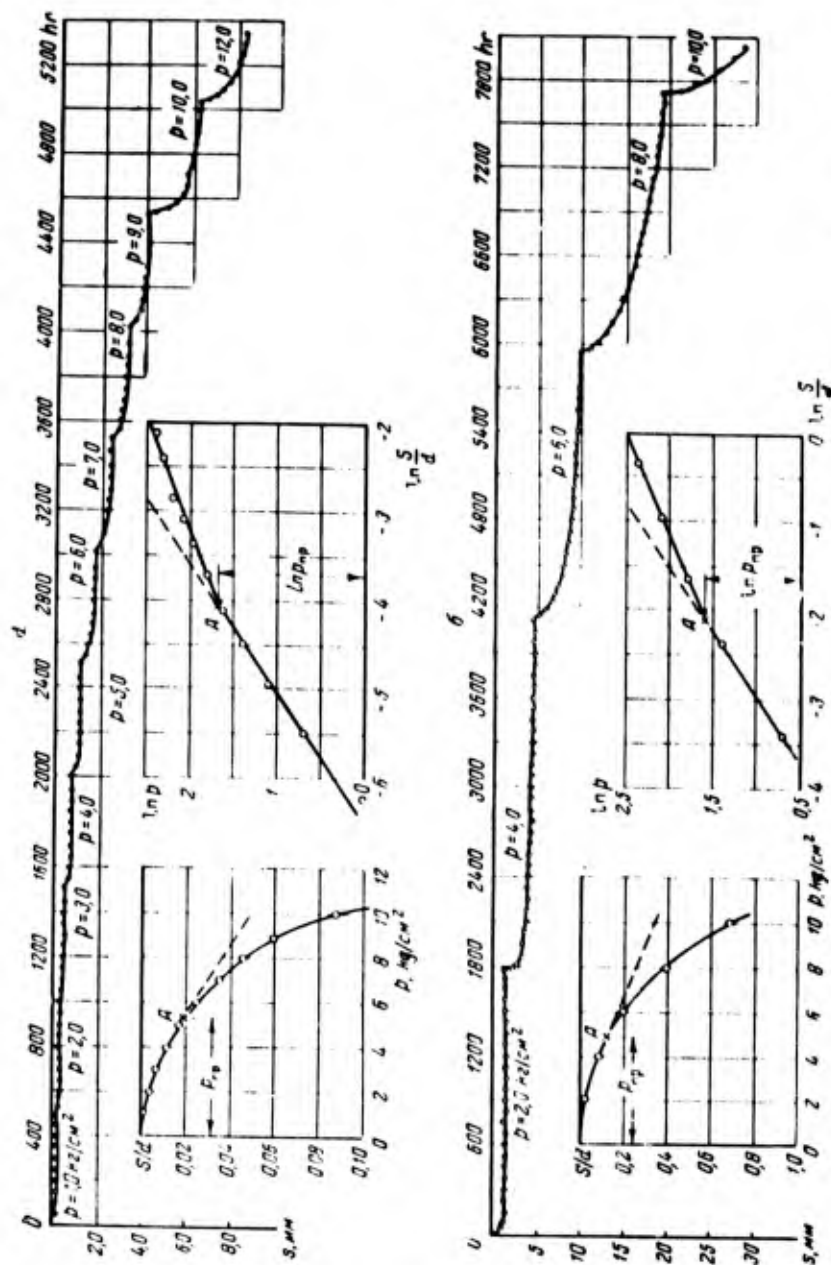


Figure 52. Investigation of frozen soils by punching. Growth of penetration in time, and relationship between the load ( $p$ ) and the relative penetration ( $S/d$ ) in ordinary and in logarithmic co-ordinates.

- a. Light, sandy loam,  $w = 26\%$ ;  $\theta = -0.4C$  (experiment 17)  
 b. Heavy, silty, ice-saturated sandy loam,  $w = 42\%$ ;  $\theta = 0.4C$  (experiment 7).

154 RHEOLOGICAL PROPERTIES AND BEARING CAPACITY OF FROZEN SOILS

Table 36. Experimental and analytical values of the limiting stress  $P_{lim}$  (kg/cm<sup>2</sup>)

No. of the experiment	Soil	Experimental values	Analytical values	
		$P_{lim}$	$C_e$	$P_{lim}$
19	Dense, varved clay	10.0	1.8	10.0
15	The same (mineral layer)	9.0	1.8	10.0
17	Light, silty, sandy loam	5.3	1.0	5.6
16	The same	6.0	1.2	6.7
14	The same	6.3	1.2	6.7
7	Ice-saturated, heavy, silty, sandy loam	4.7	0.88	4.9

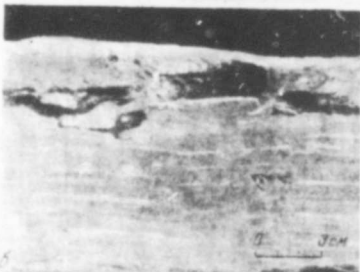
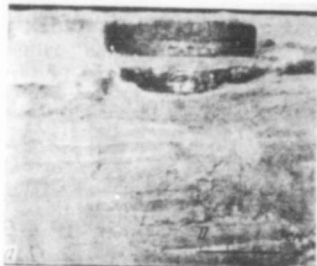


Figure 53. Cross-section of blocks of frozen soil with ice inclusions after punching.

a. Beginning of the penetration: the ice layer is only bent. b. The ice layer is partially pierced through. c. The ice layer is completely pierced through.

soil nucleus begins to be embedded in the ice layer (Figure 53b), piercing a hole through it (Figure 53c). Thus, the presence of ice layers in the immediate vicinity of the base of the punch increases the rate and the amount of the penetration, and decreases the bearing capacity of the soil. These facts are illustrated in Figure 54, where results of tests with a punch ( $d = 50$  mm) in varved clay, with and without ice inclusions, are compared\*. It can be seen that for small stresses, the penetration is almost identical in both situations. However, as the stress increased, the penetration of soil with ice layers sharply increased: the punch, together with the strengthened kernel sank in the ice as in a viscous medium. When the ice layer was completely pierced through and the nucleus under the stamp "encountered" the soil under the layer, the rate of penetration sharply decreased. This deceleration is well-reflected by the changes of slope of the curves  $s = f(p)$  and  $s = f(t)$  (Figure 54). It is significant that the total penetration in experiment 20 was half that in experiment 22, since the thickness of the ice inclusion was approximately 8 mm in the first case, and 20 mm in the second.

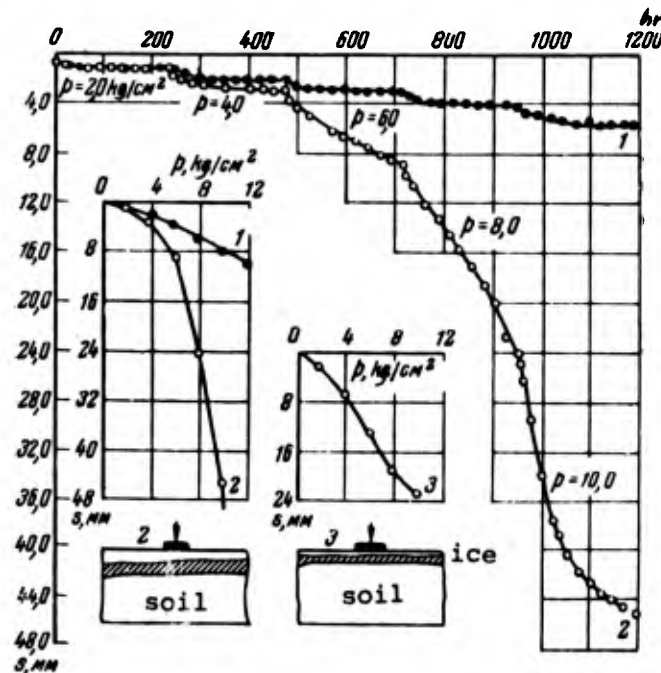


Figure 54. Influence of the structure of frozen soil on the strength under punching. Growth of the settlement with time, and the relationship between stress ( $p$ ) and ( $s$ ) settlement.

1. Dense, varved clay without ice layers;  $\theta = 0.4C$  (experiment 9);
2. The same, with an ice layer 20 mm thick (experiment 22);
3. The same, with an ice layer 8 mm thick (experiment 20).

\* The photographs in Figure 53 are related to these experiments.

Now consider the case in which the ice layers are located at a certain distance from the base of the punch. Ice layers pressed between mineral layers of soil, turn out to have a significantly smaller weakening effect on the strength of the whole block. The ice is in a sort of sheath and cannot be pierced through the layer of frozen soil; hence, the ice layers are bent only in a plastic manner, and even this occurs only in a small region (Figure 4a). Interesting data about the influence of ice layers on the bearing capacity of frozen soils were obtained independently of our investigations by the Permafrost Station of the Noril'sk Mining Combine (L. P. Gavelis, G. N. Maksimoviy, and others)\*. As in our case, these experiments showed that the punching depends not only upon the total thickness of the ice inclusions, but also upon their dimensions and distribution. For instance, soils with thick but rare ice layers gave large settlements, whereas the presence, even in large amounts, of thin isolated ice inclusions decreased the settlement in comparison.

Summarizing these facts, one can suggest the following: the presence of ice layers lowers the total strength of frozen soils under long-term stresses†. However, if the ice layers are not distributed in the immediate vicinity of the base of the footing, but are separated from it by a layer of mineral soil, then the loss of strength is not very large. Thus, in our experiments, we found that the limiting stress for varved clay without ice layers was  $10 \text{ kg/cm}^2$ , and with ice layers (having a width of 3 to 5 cm)  $7.5 \text{ kg/cm}^2$ .

The effect of the ice inclusions will differ according to their thickness, their total width, and their distribution. Separate, isolated ice inclusions, surrounded on all sides by mineral soil, will be much less distorted than uniform horizontal layers. It is significant that frozen soils with isolated ice inclusions yield less settlement, even when they thaw, than soils with uniform layers (Bakulin and Zhukov, 1955). When continuous horizontal ice layers are present, their deformation, which occurs as plastic bending, will obviously increase as the thickness of the layer decreases.

Finally as a conclusion, let us note that, regardless of the weakening effect of the ice inclusions, the apprehension regarding these inclusions prevalent among many engineers is, in our opinion, unjustified, if the preservation of the frozen state of the foundation is ensured, and if the ice inclusions are not located directly under the base of the footing. From the above qualifications, it is recommended that a fill of moistened sand which will subsequently freeze, be constructed under the footing. If this recommendation is followed, soils with ice layers can have a satisfactory bearing capacity. This is verified by our experiments and by those of the Noril'sk Combine. For instance, according to their data, the penetration in silty, sandy loam and loam soils with ice inclusions ( $\theta = -2^\circ\text{C}$ ) of the punch in the

---

\* Partial data for the experiments are published in the journal "Osnovaniya, Fundamenty i Mekhanika Gruntov", 1959, No. 3.

† On the contrary, for rapidly applied stresses, e.g. when excavating frozen soils, the presence of ice layers increases the strength of the soil.

field tests ( $p = 10 \text{ kg/cm}^2$ ) did not exceed 3 cm. Therefore, one can already increase (in comparison with N and TU 118-54) the values of the permissible pressure on soils with ice layers. At the same time, one must note that the question of the effect of the structure of frozen soils on their stability still requires thorough study.

#### 5. Computed strength of frozen soils in structural foundations

The computed strengths (permissible pressures)  $R = p_{\text{per}}$  of soils under foundations are determined by the value of the limiting stress, and by introducing a safety factor,  $R = \frac{p_{\text{lim}}}{k}$ ; for frozen soils, the value of  $p_{\text{lim}}$  can be calculated by means of formula (69).

From the experimental data, it follows that a slight increase of the stress, beyond the value of  $p_{\text{lim}}$ , does not lead to an instantaneous loss of strength and a subsidence, but only to the emergence of a visco-plastic flow which can develop during an extremely long time interval without causing catastrophic deformations of construction. Hence, the safety factor need not be excessively large. With a sufficient margin, dictated by the newness of the suggested computed values, one can choose  $k = 1.5$  (and up to 1.75). For such a value of  $k$ , the value of  $p_{\text{lim}}$  is close to the so-called critical (marginal) stress  $p_{\text{crit}} = c_e + q$ , for which any essential visco-plastic deformations of the frozen soil are not acceptable; the settlement (although it can develop in an extremely long time interval) is explained on the basis of the structural deformation due to consolidation.

Taking the slight compressibility of frozen soils at a low temperature into account, the observance of the condition  $N \leq R$  (where  $N$  is the average pressure transmitted to the soil on the base of the foundation) will also satisfy the conditions for the calculation of the deformation of a frozen foundation soil. The only exception is for plastic soils having a relatively high temperature (close to  $0^\circ\text{C}$ ). Since such soils can settle appreciably (section 2, Chapter IV), it is necessary to test them, like unfrozen soils, for the condition of limiting deformation,  $s \leq \bar{s}$ , where  $\bar{s}$  is the limiting value of the deformation of the foundation, determined according to the character of the surface construction; this value is fixed by the standards (N and TU 127-55). The value of  $s$  is found either by formula (59a), or by the usual Soil Mechanics methods, through the experimentally known values of  $E_0$  (section 4, Chapter VII) or of  $a_0$  (section 2, Chapter IV), taking into account the variation of these parameters with stress.

In Table 37, some values of our recommended design strength (permissible pressures) of frozen soil under footings are given\*. These values were obtained by analysis of the results of field and laboratory experiments, and also on the basis of the results (Table 35) of penetration tests by a ball indenter, together with formula (69).

---

\* The values of the computed strength, given in Table 37, are somewhat more precise than the ones suggested earlier by the author (Vialov, 1954, 1959), with respect to their differentiation and factor of safety.

Table 37. Computed strength (permissible pressures) of frozen soils under footings

No. of the experiment	Soil	R(kg/cm <sup>2</sup> ) for a temperature of °C			
		-0.5	-1.5	-2.5	-4.0
1	Rubble and gravel soils, coarse and medium sands.	6.0	10.0	12.0	15.0
2	Fine and silty sand (w up to 25%).	5.0	8.0	10.0	12.0
3	Sandy loams, including silty ones (w up to 35%).	3.5	6.0	8.0	10.0
4	Loams and clay soils including silty ones (w up to 45%).	3.0	5.0	6.5	8.0
5	All kinds of soils with large ice inclusions and ice layers.	2.5	4.0	5.0	6.5

- Notes: (1) The physico-mechanical properties of the tested soils are given in Tables 1, 2 and the value of the cohesion in Table 10.
- (2) Numbers 1 - 4 are accurate for soils having only separate, isolated ice inclusions of small dimensions (with thickness from 3 - 5 mm).
- (3) Number 5 refers to ice-saturated soils, the liquidity index of which exceeds  $B > 1.3$ , and to soils with a large content of uniform ice inclusions and ice layers (with a thickness greater than 3 - 5 mm) covered by layers of mineral soil, provided that these layers are at a distance from the base of the foundation of not less than 0.2 - 0.4 m. Otherwise, one must place under the foundation a fill of moistened sand (of 0.25 - 0.5 m thick) which will subsequently freeze.
- (4) The computed strength of dense varved clay of the types described earlier (of glacial-lake sediments; see Table 11) can be used for mineral layers, in agreement with point 1 of this table. However, when ice inclusions are present, values 20 - 50% smaller should be used.

The factor of safety for the calculation of  $p_{per}$  was chosen equal to  $k = 1.5$ ;  $k = 1.75$  was selected for soils at a temperature of  $-0.4^{\circ}\text{C}$ , and the value of the load  $q = 0.4 \text{ kg/cm}^2$  ( $h_0 = 2.5 \text{ m}$ ). The dependence of the quoted values of  $R$  upon the temperature is described by a formula of the same type as (23).



The computed value of the temperature of frozen soil must be taken from the highest average monthly temperature at the depth of the footing; it can be determined during the process of construction. When computing the stress transmitted to the base of the footing, one can compute the uplift effect of the adfreezing of the soil with the lateral surface of the foundation inside the frozen stratum.

One must say a few words about the permissible pressures on frozen soils with a temperature close to 0C (up to -0.2C to -0.3C). In the literature, there are indications that such soils are comparable to unfrozen soils from the standpoint of bearing capacity. However, such an approach is equivalent to recognizing that plastic frozen soils, in general, are not stable for foundations. For instance according to Table 1, silty, sandy loam from pit No. 31-k has even in the absence of ice layers a void ratio of  $e = 1.15$  and a liquidity index  $B = w - \frac{w_p}{I_p} = 1.05$ . This means that after thawing the soil will be in a flowing condition, and the values of  $R$  recommended by N and TU 127-55 for thawed soil are generally inapplicable. Actually, the above-mentioned soil, for  $\theta = -0.1C$  to  $-0.2C$  is in a plastic state, and possesses a definite bearing capacity. Thus, according to the data of field experiments (Figure 48), silty, sandy loam soils, at a temperature from 0C to  $-0.15C$  support without trouble a load of  $1.3 \text{ kg/cm}^2$ , and even for  $p = 2.5 \text{ kg/cm}^2$ , they have an extremely slow rate of settlement, equalling only 3.5 cm after three years. Hence, frozen soils with a temperature close to 0C to  $-0.2C$  must be compared not to frozen soils, but to plastic unfrozen soils, evaluating their consistency not by the total moisture content, but only by the content of unfrozen water.

Now compare the values of  $R$  in Table 37 to those recommended by the standards. In the accepted standards (up to 1955) and in the technical standards of OST 90032-39, as well as the Technical Specifications MPS of 1941, the values of  $R = p_{per}$  were chosen on the basis of laboratory tests (performed up to 1936 and 1937) of cubes of frozen soil in compression. The underestimation of these values is now generally known. Therefore, when new and more progressive standards were compiled in 1955 (N and TU 118-54), the computed strength of frozen soils was increased. However, even these new values contain a large reserve and can be increased as the data from the latest investigations have shown; this is reflected by the values we recommended in Table 37. In Table 38, a comparison of the values of  $R$  used in N and TU 118-54, for frozen soils at  $\theta = -1.5C$ , and of the values we recommend is given.

Again note the following differences in the design strengths we recommend (Table 37). In the standards, silty soils (i.e. soils having a content larger than 50% of particles ranging from 0.05 to 0.005 mm in size) are put into a separate group. Since siltiness is one of the inherent properties of permafrozen sandy-loam and loam soils, then for practical purposes one must use (in agreement with No. 4 of the standards) lower values of  $R$  for the majority of these soils. At the same time, experiments show that the bearing capacity of silty, sandy loams differs from that of silty loams. Hence in Table 37, we have not combined such soils into one group, but have kept them separate; Nos. 3 and 4 are related to silty, sandy loams and to silty loams. Taking into account the circumstances recommended by



Table 38. Comparison of the values of R, kg/cm<sup>2</sup>

Experiment No.	Soil	Values of N and TU-118-54*	Values recommended by the Author†
1	Sand	4.5-5.0	10.0
2	Sandy loam	4.0	6.0
3	Loam	3.5	5.0
4	Silty soils	3.0	-
5	Soils with ice layers	2.5	4.0

the author, the values of the design strengths turned out to be 1.5 to 2 times larger than in N and TU 118-54.

The validity of the increased values of the strength of frozen soils is verified also by the experiments of other investigators, in particular by those of the Yakutsk Permafrost Scientific Research Station (YaNIMS), conducted according to the method of N. A. Tsytoovich and S. S. Vialov (Votyakov, 1955). The values of the design strengths chosen, at the suggestion of YaNIMS, as the standards for construction in Yakutya\*\*, are in good agreement with the data in Table 37.

The introduction of new and increased values of the design strengths given in Table 37 simplifies significantly the construction of foundations on frozen soils, and has an extremely appreciable result economically. Note that the values of the design strength quoted in Table 37, especially in relation to soils with ice layers, are approximate and do not completely exhaust the strength resources of frozen soil. Through a practical check, and by means of the accumulation of experimental data, these values can be made more precise.

Thus, calculations for foundations on frozen soils must be carried out as follows:

- (1) by means of the limiting long-term strength in the case of frozen soils with a low temperature (the so-called "hard frozen" soils)
- (2) By means of the limiting long-term strength and of the limiting deformation in the case of "plastic-frozen" soils.

In addition, one must treat frozen soils with a relatively high temperature (up to -0.5C to -0.7C), salt soils, etc, as plastic-frozen

\* When taking into account simultaneously the action of the dead and live loads, the values of  $R$  are increased by a factor of 1.2.

† The sandy loams and loams are silty.

\*\* Report by P. I. Melnikov on Interdepartmental Conferences No. VII (March 1956) on permafrost investigations.

when their long-term cohesion is less than 1.0 to 0.9 kg/cm<sup>2</sup>, or when their 2 hr cohesion is less than 1.5 kg/cm<sup>2</sup>.

Calculations by means of the limiting long-term strength are valid, if the pressure from the code load does not exceed the design strength  $R$  (permissible pressure) under the base of the footing; in addition, one may calculate the uplift effect of the adfreeze forces of the soil on the lateral surface of the footing by,  $N \leq Rf + kS_M F$ , where  $N$  is the code load in kg, and  $R$  is the design strength of the soil under the base of the footing in kg/cm<sup>2</sup>. It is determined from Table 37, and for plastic-frozen soil with a temperature higher than -0.5°C, as well as for salt and damp soils, it is determined by experiment. For approximate calculations it is determined by the code value of  $R$  for unfrozen soils, depending upon the actual physical condition of the plastic-frozen soils.  $S_M$  is the limiting long-term adfreeze strength of the soil (in kg/cm<sup>2</sup>) with the lateral surface of the foundation; its values will be given later (Table 47).  $f$  is the area of the base of the footing in cm<sup>2</sup>;  $F$  is the minimum area in cm<sup>2</sup> of the lateral adfreezing surface of the soil and foundation on which shearing of the soil can arise: this area is determined by taking into account the maximum depth of the upper boundary of frozen soil, computed before the time of construction.  $k$  is the uniformity coefficient (adding to safety) which can be chosen equal to 0.7.

When one designs a foundation on such soils by the limiting deformation method, the settlement of plastic-frozen soil can be determined by the standard methods of Soil Mechanics on the basis of experimental determination of the modulus of compressibility  $E_0$ , or on the basis of the coefficient of compressibility  $a_0$  (section 2, Chapter IV). The settlement can be determined by the method of equivalent layers (Tsytoich 1951, 1958), using the formula:  $s = h_s a_{om} p_0$ , where  $s$  is the computed settlement (in cm) under the center of the footing;  $p_0$  is the average pressure (in kg/cm<sup>2</sup>) on the soil under the footing, after subtracting the existing natural pressure;  $a_{om}$  is the average corrected coefficient of compressibility in cm<sup>2</sup>/kg;  $h_s = bA_w$  is the thickness of the equivalent layer (in cm), depending upon the width of the footing  $b$  and upon the coefficient  $A_w$ . The values of the latter, depending upon the Poisson ratio and the ratio between the width and the length  $l$  of the foundation, are given in Soil Mechanics treatises (Tsytoich, 1957, 1958). In particular, for frozen soils one can take  $\frac{b}{l} = 1 - 2 - 3 - 5 - 10$ :

(1) for flexible foundations,  $A_w = 1.5 - 2.16 - 2.51 - 2.96 - 3.6$ , respectively;

(2) for rigid foundations,  $A_w = 1.24 - 1.72 - 2.01 - 3.0$ , respectively.

The value of  $a_{om}$  is computed by means of the following formula,

$$a_{om} = \frac{1}{2h_s} \sum_{i=1}^n a_{oi} h_i z_i$$

where  $n$  is the number of compressible layers under the foundation. The compressibility of the soils is computed only up to the depth at which the pressure of the foundation equals 20% of the weight of the

overlying soil (existing pressure).  $h_i$  is the thickness of the layer (cm) under consideration;  $z_i$  is the distance from the center of the layer examined, to a depth of  $2h_i$  (in cm).  $a_{oi}$  is the reduced coefficient of compressibility of each layer  $i$  of frozen soil, depending on the temperature, and upon the actual pressure;  $a_{oi} = \frac{e}{p_i}$ , where  $e$  is the relative compression, and  $p_i$  is the additional (excess over the actual) pressure acting in the middle of the layer examined. The value of  $p_i$  is determined by well-known Soil Mechanics methods; the value of  $e$  is determined from compression tests at various temperatures and pressures (section 2, Chapter IV). Some values of  $e$  are given in Table 21. Since  $e$  depends upon the temperature of the soil, for the calculations of  $a_{oi}$ , one must determine the temperature distribution throughout the depth of the compressed stratum.

Note also that in special cases, the values of  $R$  can be chosen equal to, or even somewhat larger than  $p_{lim}$ , but one must then take creep-settlement into account. Design of the foundation must then be executed not from the stability condition, but from the condition of permissible rate of deformation, or from the condition of the permissible value of the settlement during a fixed time interval, e.g. the working-life of the structure, as for structural design based on creep.

## CHAPTER IX. PRESSURE DISTRIBUTION IN FROZEN SOILS UNDER A FOOTING

## 1. Survey

It is well known that the curve of distribution of contact pressure at the base of a rigid footing in an ideally elastic medium has, according to the theoretical solution of Boussinesq-Sadovskiy, a so-called saddle shape (Figure 55a), which is described, for a two-dimensional circular footing, by the following equation:

$$\sigma_{z=0} = \frac{P}{2\pi r \sqrt{r^2 - p^2}} \quad (70)$$

where  $P$  is the total load (kg),  $r$  is the radius of the footing, and  $p$  is the radial polar coordinate of the point examined.

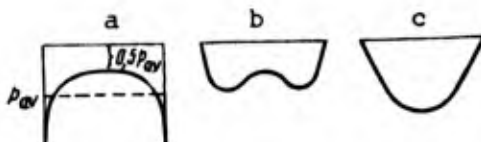


Figure 55. Diagram of the reaction pressure of unfrozen soils on a rigid footing at the soil surface. a. Theoretical. b, c. Actual (according to the experiments with sand of A. G. Rodshtein).

However in real soils, infinitely large stresses cannot occur at the edge of the footing, as in the theoretical solution; hence in these regions, plastic deformations inevitably arise. The reaction-pressure diagrams change their aspect, according to the rate of growth of these deformations (Florin, 1948). Considerable attention has been devoted, in recent years, to the study of the actual stress distribution in soils (Rodshtein, 1950, 1951; Lipovetska, 1953; and others); however at present, no complete understanding has been reached.

Experiments with frozen soils were conducted for the first time by V. G. Berezantsev (1953), who measured the stresses at several depths below the base of the footing by means of "heat electro-tensometers" under laboratory conditions (models with a width of 4.5 cm). To our knowledge, the determination of the reaction pressures for frozen soils under the base of a footing has not been obtained up to now. Results of such experiments with frozen soils, carried out under natural freezing conditions, are examined below.

## 2. Experimental determination of the frozen soil reaction at the base of the rigid footing,

In order to measure the stresses, we used the electro-tensometer

gauge\* system of A. G. Rodshtein (Institute of VODGEO), with a recording device in the form of a balancing bridge with a galvanometer having a sensitivity of  $10^{-9}$ . It is well-known that gauges of this type are built on the principle of the measurement of extremely small mechanical strains in electric units. The gauge is used as a steel shell with a thin bottom (a membrane) on which an operating electro-tensometer made of a constantan wire having (in our case) a resistance of 200 ohms is cemented. Another electro-tensometer, fastened to a special membrane, serves to compensate for the temperature fluctuations in the circuit. Measurements of the stresses are performed by means of the recording (null method) of changes of the ohmic resistance caused by the longitudinal deformation of the active wire electro-tensometer when the membrane deflects. The above-mentioned equipment and the operational method appropriate for it are described in detail in the literature of A. G. Rodshtein (1950, 1951). Therefore, we shall not deal any further with these questions. Only note that we used these gauges with a membrane diameter of 28 mm and a thickness of 0.8 mm. The measurements were conducted with a precision of  $0.05 \text{ kg/cm}^2$ . The cast-iron punch had a diameter of 50.5 cm; seven gauges were mounted on it, five main ones, and two for control purposes. On the whole, the apparatus manufactured by VODGEO functioned satisfactorily; however, there were a few shortcomings. In order for the apparatus to record small pressures with the necessary precision, the membrane must be sufficiently thin. But, in that case, for increased stresses, the deflection of the membrane became excessively large. In the soil under the gauge, "unloading" crests were formed, etc. Therefore, for large stresses, a so-called "remainder" of the stresses occurred, i.e. the sum of the measured stresses turned out to be less than the value of the load applied to the stamp. For small loads, the agreement of the measured and total pressures was relatively satisfactory. As is well known, these shortcomings have also been observed by other investigators when testing unfrozen soils.

The experiments for determination of the stresses were carried out in underground vaults, with varved clay having ice layers (Figure 53) at a temperature of  $-0.6^\circ\text{C}$ . A punch, on which a load was applied increasing in steps from  $1.25 \text{ kg/cm}^2$  or  $2.5 \text{ kg/cm}^2$  to  $15 \text{ kg/cm}^2$ , was operated by means of a jack. In the various experiments, each load was maintained for a time ranging from 30 min to 72 hr. The stresses were measured immediately after each increase of the load, and during the following time interval: altogether 12 tests were carried out. A description of the soil and of the experimental conditions was given in great detail in section 1 of Chapter VII.

In unfrozen, sandy (compact) soils, when the punch is applied, the profiles of the reacting pressures change as the stresses grow from a two-humped saddle-shaped to a convex parabolic, and even to a peak shaped, curve, corresponding to the condition of limiting equilibrium of loose soil (Figure 55b,c.). This is in agreement with the experiments of A. G. Rodshtein (1950), as well as with the theoretical investigations of V. A. Florin (1948). The parabolic character of the curves was observed even for small stresses, if the sand was in a dense condition. In T. F. Lipovetska's experiments (1953), the parabolic curve was observed even for stresses in the sand measured far from the base of the punch (in all cases). A. G. Rodshtein observed a profile having a saddle shape close to the theoretical one only when the punch penetrated.

\* Electrical resistance strain gauge.

The results of our experiments with frozen soils turned out to be different. When a punch was forced through the surface of the soil, previously compressed by means of a  $15 \text{ kg/cm}^2$  load and levelled by means of a thin layer of dry sand, the reaction pressures were distributed in the following manner (Figure 56). For small and medium loads (in this experiment, the loads reached  $5.0$  to  $7.5 \text{ kg/cm}^2$ ), the profiles had a two-humped saddle-shaped contour, differing substantially from the theoretical solution for an ideally elastic medium (the theoretical profile is shown in Figure 56 as a dotted line). As the load increased, the "humps" of the profile decreased, and its contour became saddle-shaped, resembling more and more the theoretical contour. Note that for all the loads, the ordinate of the actual curve under the center of the stamp was larger than the theoretical one, being  $0.6$  to  $0.7$  times the average pressure; according to formula (70) they should have equalled  $\sigma_{z=0, \rho=0} = 0.5 P_{av}$ .

This is explained by the decrease of stresses at the edge of the punch, in comparison with the theoretical solution. The small number

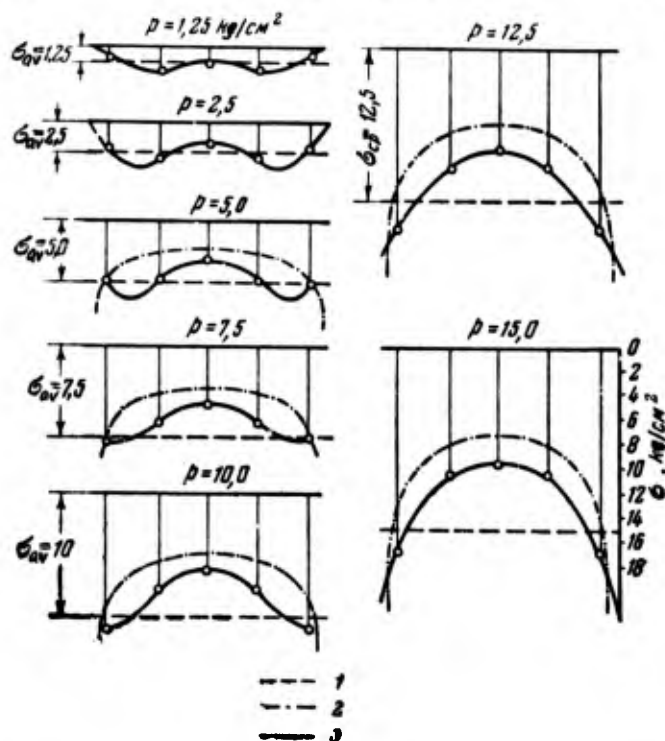


Figure 56. Profiles of the reaction pressures of frozen soil under rigid punches for various loads. Varved clay,  $\theta=0.6C$ ; punch  $d=50 \text{ cm}$ , without load (experiment 6). (1) Average value of the stress, (2) theoretical contour of the curve (for an elastic medium), (3) actual contour.

of gauges mounted on the punch does not allow the plotting of the pressure curves with sufficient accuracy. Hence, the profiles shown are provisional to a certain extent. However, the variation of the profiles, partially characterized by the systematic change of the relation between the ordinate at the edges and at the center of the punch, is apparent

and definite enough from the data. The load on the punches was increased until permanent deformations, and even progressive flow arose. However, in these cases, different profiles of the reacting pressure are not convex (as in the experiments with thawed sand), but saddle-shaped and fairly similar to the theoretical ones.

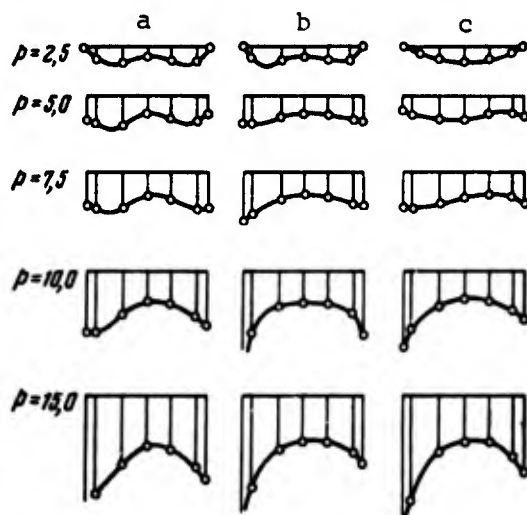


Figure 57. Diagrams of the reaction pressures of frozen soils under various loads ( $p$ ,  $\text{kg/cm}^2$ ) on the punch. a. Previously compressed soil. b. Strongly compressed soil (repeated test). c. Uncompressed soil.

Several unexpected results of the experiments, differing from the existing data on the character of the redistribution of reactions with respect to the increase of the load, necessitated repeated tests. In all these tests, the punch was applied to the surface of the soil, but conditions of preparation of the foundation varied from preliminarily compressed to uncompressed soils, as well as from soils with a thin filling of sand to soils without it. It turned out that in the initial stage of the punching process, i.e. for small  $p$ , the above conditions influence, to a definite extent, the character of the distribution of the reacting pressures. The profiles shown in Figure 57a are the most typical. They are analogous to the ones in Figure 56\* and correspond to the case of complete contact of the punch with the surface of the soil, with a preliminary  $15 \text{ kg/cm}^2$  compression of the last load. For extensive compaction of the soil (which occurs for instance when reloading), the profile had a two-humped contour only during the loading. It began to assume a concave saddle shape, not only for large pressures (as in the first case), but even for moderate values of the load (Figure 57b). For tests without preliminary compression of the soil, the profiles had in some cases a character analogous to that of Figure 57a; in other cases, they had a parabolic character for small loads, and a saddle-shape for large pressures (Figure 57c). Thus the type of

\* In Figure 56, the so-called smoothed profiles are shown; their ordinate corresponds to half the sum of the stresses measured at two symmetrical points. In Figure 57, the actual contour of the diagram is shown.



Table 39. Value of the reaction pressures  $\sigma_{z=0}$  (kg/cm<sup>2</sup>)(for a moderate load on the punch,  $p_{av}=15$  kg/cm<sup>2</sup>)

No. of the experiment	Conditions of preparation of the base soil	Distance from the center of the punch, cm		
		0	10	12
1	Without sand filling and without preliminary compression of soil	10.6	10.5	14.9
9	Without sand filling, but with compression of twice the load 15 kg/cm <sup>2</sup>	7.7	12.2	18.1
7	With sand filling, but insignificant compression (7.5 kg/cm <sup>2</sup> )	9.1	10.1	15.0
5	With sand filling and with compression by a load of 15 kg/cm <sup>2</sup>	9.3	10.4	18.5
6	The same	9.8	11.8	17.0
8	With sand filling, repeated test (i.e. very strongly compacted soil)	9.0	9.8	16.8

preparation of the foundation may influence the profile only in the initial stage of the loading; the distribution of reaction pressures, in the subsequent stages of the loading, is in all cases saddle-shaped and close to the theoretical distribution (Table 39).

In our opinion, the results obtained from the tests are in good agreement with the above considerations. for the behavior of the strength of soils under punching, and can be explained precisely from these estimations.

If a punch is placed on the surface of the soil, a local movement of the soil under the edges occurs even under the action of a small load. Consequently, the stresses at the edge take a value close to, or equal to, zero, and the stress diagram becomes two-humped instead of being saddle-shaped. The less the soil is compacted, the larger the influence of this movement, until a parabolic profile is obtained when loose contact of the punch with the surface of the foundation occurs. As the load increases, a strengthening of the soil occurs, i.e. a dense kernel starts to form under the stamps. The local push of the soil under the edges stops, and the stresses at the rim begin to grow; the diagram assumes a contour intermediate between a two-humped and a saddle-shaped curve. If the condition of limiting equilibrium is violated, for a further increase of the load, a bulging of the soil under the stamp occurs, and the profile of the reaction pressures takes a parabolic shape, as in the case of loose soils. It was shown earlier that in frozen soils, an expansion of the surrounding soil, due to the strengthened kernel, occurs rather than a bulging. We measured the stress precisely at the point of contact of the punch with the strengthened kernel, which is in an almost elastic condition. In accordance with this condition, the distribution of the reaction pressures is close to the theoretical distribution. If one establishes even for

loose soils, conditions under which bulging is impossible, e.g. by burying the punch, then as A. G. Rodshtein's experiments have shown, the profiles of the reaction pressures will also have in this case, a saddle shape rather than a parabolic shape.

As is well known, the influence of a rigid punch ceases to be felt at a certain depth from the base. V. G. Berezantsev's experiments (1953) show that for small stresses (significantly smaller than the limiting stress), the profiles of the normal stresses in horizontal cross-sections, at depths equal to 0.5 d and 1.5 d of the punch, have a contour close to that given by the theory of elasticity, but differing somewhat from it numerically.

In conclusion, let us consider the influence of the time factor on the distribution of reaction pressures. The measurement of the stresses for  $p = \text{const}$ , at various times during a 72 hr period, have shown that no major change in the character of the distribution of pressures occurs (Figure 58). However, local redistributions of the stresses were noted, even though the general aspect of the profile was preserved. These redistributions are explained by the heterogeneity of the soil: at the points where the soil is denser, the reactions grow only until warping occurs; after that, the reactions are redistributed. In this respect, the influence of ice layers is particularly important, since they offer, at first, a large resistance to punching, and then secondly they become distorted.

In several experiments, a tendency of the stresses to grow with time was noted, particularly in comparison with the initial values (after the application of significant loads).

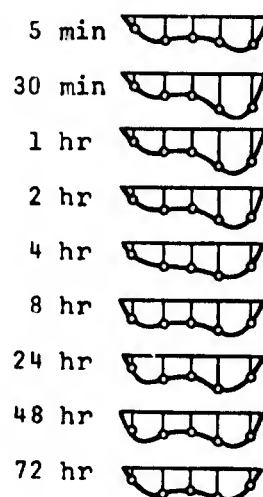


Figure 58. Variation of the reaction pressures with time.  $p = 5.0 \text{ kg/cm}^2 = \text{const}$ .

## PART III. RESISTANCE OF PILE FOUNDATIONS IN FROZEN SOIL

## CHAPTER X. BEHAVIOR OF PILES IN FROZEN SOILS

## 1. General principles

Pile foundations receive more and more use in the construction of buildings on permafrost (permanently-frozen) soil. The use of piles significantly simplifies foundations engineering, since with them expensive excavation work is eliminated, a year-round cycle of production is guaranteed, and the opportunity for broad use of mechanized equipment is made available. In addition, with a pile foundation greater reliability is guaranteed (in comparison with ordinary foundations) in case of an unexpected drop of the upper boundary of the permafrost.

It is possible to view piles driven into frozen soil as frozen columnar foundations, whose load is transferred to some volume of the surrounding soil, which is joined with the surface of the piles by the forces of adhesion (adfreezing). Calculation of such piles should make use of the limiting conditions, with regard to the relaxation properties of frozen soil. Before the emergence of the limiting condition, the stress on the pile is absorbed by the adfreeze forces of the soil with the lateral surface of the pile, and deformations are caused, basically, by the compression of low-lying layers; these deformations for soil with a temperature lower than  $-0.5^{\circ}\text{C}$  to  $-0.7^{\circ}\text{C}$  are exceedingly small. It is possible to avoid taking them into account in actual design. The only exceptions are with plastic frozen soils having a temperature higher than  $-0.5^{\circ}\text{C}$  to  $-0.7^{\circ}\text{C}$ , for which, as we have already said, verification according to the maximum deformations should be made.

The state of limiting equilibrium corresponds to the attainment of adequate long-term resistance of the soil to displacement along the lateral surface of the pile and the long-term resistance of the soil under its point. Disturbing the limiting equilibrium causes a separation of the pile from the surrounding soil and its displacement, with the transmission of excess load onto the soil under the point. As a result, visco-plastic flow of soil occurs causing a continuous settlement of the pile, i.e. its unbroken sinking into the soil as into a viscous medium.

These problems will be examined in greater detail later on; here we will observe that the limiting load on a pile embedded in frozen soil  $P_{\text{lim}}$ , i.e. the load in excess of which the phenomena pointed out above are caused, can be expressed by:

$$P_{\text{lim}} = T_{\text{lim}} + R_{\text{lim}}, \quad (71)$$

where  $T$  is the limiting resistance of the soil to displacement along the lateral surface of the pile, and  $R$  is the limiting resistance of the soil under the point of the pile.

In order to locate the components  $T$  and  $R$ , it is necessary to know the distribution of stresses in the soil around the pile. The resistance

along the lateral surface of a single pile in unfrozen soil is caused by the forces of friction,

$$T = \pi d \int_0^l \tau_{fr} \cdot dz, \quad (72)$$

which arise as a result of the pressure of the pile against the soil, and which depends on the coefficient of friction ( $\mu$ ) and the magnitude of the horizontal pressure,  $\tau_{fr} = \mu p$ . A great deal of work has been devoted to the problem of the character of the distribution of  $\tau$  along the length of the pile (in unfrozen soil); however, this problem has as yet not been solved.

In frozen soil the resistance along the lateral surface of the piles (driven with steaming) is caused chiefly by the forces of adhesion of the soil which is being frozen to the piles (Chapter III). The problems of the character of distribution and of the magnitude of the stresses which have been pointed out is still more complicated, since it is combined with the necessity of calculating the rheological processes which occur in frozen soil.\*

In view of the absence of data and the generally unexplored character of the problem today, it is possible to employ a simplified plan, evaluating the bearing capacity of the piles just as is done for non-frozen soil, according to the total resistance of the piles to the loads. In this case, it is possible to get the values  $T$  and  $R$  from the parallel tests of the piles for pressing-down and pulling-out; as a result, the total limiting stress on the pile  $P_{lim}$  and the resistance along the lateral surface  $T$  are correspondingly determined. The resistance of the soil under the point is determined by the difference  $R = P_{lim} - T$ . It is conditionally possible to refer the magnitude  $T$  to a unit of area of the lateral surface of the pile, which corresponds to the mean (for the length of the pile) value of the strength of adfreezing; the magnitude  $R$  may be conditionally referred to a unit of area of the cross-section, which corresponds to the mean reaction pressure of the soil under the point. The correlation between  $T$  and  $R$  depends on the size of the pile, the magnitude of the load, and the time of its action. Since it is necessary to make a calculation of the piles at the limiting state, the long-term values  $T_{lim}$  and  $R_{lim}$ , i.e. the values corresponding to the emergence of the visco-plastic flow, are of interest. The problem of the bearing capacity of pile foundations in frozen soil is examined below, proceeding from the principles of the theory of rheology which were presented in the first part of the present work.

## 2. Conditions for conducting field tests

Experimental investigations were carried on from 1951 to 1953 and consisted of experimental driving of piles by different methods and

\* Interesting investigations with the help of electro-tensometry on the problem that we have pointed out have been begun by my scientific colleague, K. E. Egerev (1958), at the Permafrost Institute; preliminary data give evidence that less than limiting tangential stresses are distributed over the length of the pile according to some non-linear law, while the character of their distribution changes in time.

testing these piles by static loads for prolonged resistance to pressing-down and pulling-out. In the organization and conducting of the experimental work, which was carried out together with the Igarskiy Permafrost Research Station and the Northern Exploration Project Expedition GUSMP under the general leadership of the author, scientific colleague S. G. Tsvetkova of the INIMS, research worker N. E. Fedotov, and colleagues of the SPIE, engineers P. N. Pavlov and S. I. Ostrozhenko, observer V. E. Petrukhin and others, took part.\* Driving the piles was accomplished in four sections, three of which (sections 1a, 1b, 1c) were distributed in the territory of the research station, and the fourth (section 2) beyond its limits. In this situation each of the sections had different frozen-ground conditions.

Section 1a, on which the greatest number of piles (no. 1 to 12 and no. 14 to 25) is driven, is characterized by considerable variations of depths to the upper surface of permafrost (from 1.2 to 3.5 m), as well as of values of the temperature of this permafrost (from -0.1°C to -2°C). This is caused by differences in snow accumulation in this area. The variation in the temperature of the soil within the limits of one area permitted us to demonstrate the effect of this factor on the bearing capacity of the piles. The soil of the section within the limits of the depth of driving of the piles has silty, blanketing clayey soil (light) and sandy loam (heavy). This soil, as we have already observed, possesses an increased siltiness (65 to 75%) and plasticity (in light argillaceous loam  $W_n = 12$  to 14, in heavy sandy loam  $W_n = 10$  to 13). Thus, if we wish to classify the soil by the plasticity index, then most of the heavy sandy loam should be called argillaceous. The soils possessed no observed ice inclusions. The total moisture content of this soil varies from 25 to 35%.

Section 1b, in which piles no. 26 to 34 are driven, is characterized by the presence of "non-fusing frozen ground", whose upper surface lies at a depth of 2.5 to 2.6 m; the temperature of the soil of the frozen stratum is from 0°C to -0.2°C. The soil is silty, light, and argillaceous; under this layer, from a depth of 5 m, is a heavy and light sandy loam. The plasticity index of the argillaceous loam is 7 to 14, of the sandy loam 5 to 9. Ice inclusions in the form of segregations are observed only at lower levels. The total moisture content varies from 25 to 40%.

Section 1c, in which piles no. 13 and nos. 35 to 41 are driven, is distinguished by the presence of ice-saturated soil which is represented by silty, heavy argillaceous loam (clay fraction 29%); this graduates into varved clay. The plasticity index of this argillaceous soil is 18 to 23. Ice inclusions are contained in the form of solid intercalations with a thickness of from 5 to 8 cm alternating with the layers of mineral soil. The total moisture content of the whole stratum within the limits of the depth of driving of the piles is 65 to 100%. But the moisture content of the mineral

\* Simultaneously, as an independent part of the operation, S. G. Tsvetkova conducted an investigation of the temperature regime of the soil around the piles which were being driven with the help of steaming; the results of these investigations were presented in the work of S. G. Tsvetkova (1953, 1954).

layers equals 42%.\* The temperature of the soil varies between  $-0.5^{\circ}\text{C}$  and  $-0.7^{\circ}\text{C}$ .

Section 2, which has piles nos. 1 to 34, is composed of heavy and light sandy loam with inclusions (at a depth of 3.5 to 5 m) of gravel and pebbles, which compose up to 20% of the contents. The siltiness of the soil of this area is somewhat less than that of the soil of the sections examined above; it is on the average 40% for sandy loam and 50% for argillaceous soil. Correspondingly the plasticity index equals 5 to 9, and only in rare cases does it go up to 14. In the soil, ice layers are encountered, but their thickness is small (from 1 to 7 m, and rarely from 10 to 15 mm). The total moisture content of the soil is from 30 to 45%. The temperature of the soil (at a depth of 3 to 4 m) varies between  $-0.7^{\circ}\text{C}$  and  $-1.4^{\circ}\text{C}$ , but in individual places it rises to  $-0.3^{\circ}\text{C}$ . The depth of the summer thawing is 1.5 m. The average data concerning the mechanical composition of the soil of the sections being investigated are presented in Table 40.

In order to explain the effect of the method of emplacement of piles on their bearing capacity, the piles in our experiments were driven by different methods:

(1) with preliminary steaming of the soil, with the diameter of the thawed zone ("hole") greater than the diameter of the pile; the pile itself was placed (embedded) by hand;

(2) with temporary steaming of the soil, while the diameter of the thawed zone ("hole") was less than the diameter of the pile; the pile was driven with the help of a pile driver;

(3) with preliminary drilling of the hole and with driving the piles with a pile driver.

The essence of the first method, which is described in sufficient detail in the literature (Bykov, 1940; Liverovskiy, 1941; Lukin, 1952; Tsvetkova, 1953, 1954, etc.), lies, as is well known, in the fact that the frozen soil is thawed and liquefied with the help of steam fed under pressure through a so-called steam point. As a result, the free embedding of the pile is ensured; after some time, the liquefied soil mass freezes and the pile is frozen into the soil.

The diameter of the zone of steaming in our experiments exceeded the diameter of the piles by 5 to 10 cm, and in individual cases even up to 20 cm. The period of steaming, depending on the type of soil and its temperature, ranged from 30 min to 2.5 hr.

As the investigations of S. G. Tsvetkova showed (1953, 1954), the period of freeze-back of the steamed soil (the transition of the chief

\* Let us recall that, under the total moisture content  $w_c$  we are considering (Pchelintsev, 1954) the overall content in percent for the dry weight of ice inclusions, ice cement and unfrozen water; under the moisture content of the mineral layers  $w_{mn}$  we are considering the content of the ice-cement and the visible ice inclusions  $c$ ; the difference  $w_c - w_{mn} = w_{incl}$  determines the content of the ice inclusions in the soil.



Table 40. Mechanical gradation of the soils in locations of driven piles

No. of the section	Soil	Sand more than 0.05 mm			Silt .05-0.005			Clay less than 0.005 mm		
		av	max	min	av	max	min	av	max	min
1a.	Sandy loam heavy, silty	20	30	11	72	84	62	8	9	5
	Argillaceous loam light, silty	14	21	9	75	82	67	12	14	10
	Argillaceous loam heavy, silty	2	--	--	70	--	--	28	--	--
1b.	Sandy loam light, silty	30	--	--	65	--	--	5	--	--
	Sandy loam heavy, silty	38	--	--	52	--	--	10	--	--
	Argillaceous loam, light silty	35	--	--	54	--	--	11	--	--
1c.	Argillaceous loam light, silty	2	--	--	85	--	--	13	--	--
	Argillaceous loam heavy, silty	1	1.5	0	76	84	70	23	29	17
	Clay, silty	5	--	--	63	--	--	32	--	--
2	Sandy loam light	55	66	36	39	46	30	4	6	3
	Sandy loam heavy, silty including gravel (1 to 21%)	35	47	20	53	70	37	7.5	10	6

part of the water into ice) was from 20 to 30 days with the temperature surrounding the frozen stratum from  $-0.8^{\circ}\text{C}$  to  $-1^{\circ}\text{C}$ , and from 2 to 3 months with  $\theta = -0.2^{\circ}\text{C}$  to  $-0.5^{\circ}\text{C}$ . But the period of full restoration of the temperature character of the soil ranges from 1 to 4 months. In the conditions of Yakutsk ( $\theta = -7.5^{\circ}\text{C}$ ), the period of adfreezing, according to the data of G. O. Lukin (1952), is considerably decreased. The case is somewhat different in the presence of so-called non-fusing freezing, when a layer of winter freezing does not interlock with the upper surface of the frozen stratum. Since the temperature of such a stratum is from  $-0^{\circ}\text{C}$  to  $-0.2^{\circ}\text{C}$ , the freeze-back of the soil after steaming occurs after an exceedingly long period (8 months and more), and may even not occur at all.

In the cases that have been pointed out, an exceedingly effective method is the use of hollow (metal or reinforced concrete) piles with artificial cooling by means of flooding with brine or circulation of outside cold air. Experimental driving of such a pile (of 160 mm metal pipe) showed that for a temperature of the frozen soil from  $-0.2^{\circ}\text{C}$  to  $-0.4^{\circ}\text{C}$  flooded with brine ( $\theta = -12^{\circ}\text{C}$ ), freezing of the steamed soil was assured even within a week.

As is well known, loading the piles, which are driven with the help of steaming, can be accomplished only after the thawed soil is frozen with the pile. But in this case, we should take into account the possible heaving of the piles in the process of freezing of the steamed soil, if driving was carried out in autumn or winter. To avoid such



heaving of the pile, we should make the steamed zone deeper and also accomplish partial loading of the piles after driving, taking at the same time general measures for decreasing the forces of heaving.

In driving the piles with a pile driver with preliminary temporary steaming, the diam of the steamed holes, depending on the temperature and type of soil, was taken as equal to 0.6 to 0.9 times the diameter of the pile. The process of steaming took in this case 20 to 40 min. For driving, an ordinary pile driver with an electric hoist and a suspended hammer (660 kg) were used. The piles did not have shoes (except in those cases of driving into gravel soil). The driving was accomplished rather easily. Piles were especially easily driven into soil having a temperature near 0C and not having ice lenses.

Driving the piles into the drilled holes was accomplished with the same pile driver. The drilling of the hole was accomplished by the usual drill assembly. Piles were easily driven into plastic soil where the ratio of the diameter of the hole to the diameter of the pile was 0.7 to 0.9. It is extremely curious that we succeeded in driving piles immediately into the frozen stratum without any steaming or drilling of holes when we worked with plastic sandy clayey loam with a temperature about -0.1C (without ice layers). Driving piles (with shoes) into the designated soil can be compared in complexity to driving into unfrozen soil of tight plastic or hard consistency. Thus, for example, the set of the pile (from the last blows) was 0.75 cm with a hammer drop of 1 m.

It is significant that the determination of the maximum stress on piles driven into the frozen ground, with respect to the size of the failure load (a dynamic test), does not give reliable results. For example, with calculations according to the well-known Gersevanov formula, we find that the maximum load on piles driven immediately into a permafrost stratum should equal 15 to 18 T. In fact, however, this stress, as the result of long static tests showed, turned out to be equal to 5 to 8 T. Such a discrepancy is explained by the relaxation properties of frozen soil, the long-term resistance of which is significantly less than the resistance to rapid loading.

In view of the necessity for using rather large loads for static tests of piles and the absence of special loading devices, it was necessary to limit the size of the piles to 15 to 22 cm in diam. The depth of driving of the piles was from 4 to 6 m, depending on the depth of the frozen stratum. With the object of eliminating the effect of the layer of seasonal freezing and thawing, the soil of this layer was dug up after driving, but subsequently the pits were filled with sawdust with the installation of clay waterproofing. In addition to this, the surface of the piles at the limits of the pit were greased with technical vaseline, and bindings were placed on the upper part of the piles. In order to preserve a constant temperature of the frozen soil, the surface of the soil around the piles was insulated by a layer of sawdust (75 cm), and winter snow was not removed from the surfaces. In these conditions, as experiments showed, the temperature of the frozen soil in the limits of the working length of the piles changed almost not at all in the process of the tests. But on one of the sections (no. 2), tests were conducted with the intention of studying the behavior of the piles under a varying temperature. Therefore, on the designated area the insulation at the surface of the soil was not installed.

The load on the piles was transferred by levers. In tests for pressing-down, these levers are made fast to anchors (metal pipes with welded "jags") sunk 10 to 15 m. But in the pull-out tests, the support was a standpipe sunk into the soil 0.5 to 1.0 m. For recording the deformations, we used dial indicators (0.01 mm) fastened to pipe supports sunk 2 to 3 m into the frozen soil. In addition, a control levelling was conducted (twice a month). Temperature observations were made with the help of thermocouples mounted on the body of the pile. In addition, for the purpose of temperature control there were established thermometer openings in which measurements were made with mercury thermometers.

Analogously to the laboratory experiments described in Chapter III, tests were conducted under constant loads as well as under gradually increasing loads. In the first case, different pulling-out loads were applied to several piles which were driven into identical soils, beginning with the load causing instantaneous pulling-out (in practice the loading continued 10 to 20 min), and ending with the long-term load. In the second case, the load on the given pile was increased gradually up to the start of continuous flow. The majority of tests were prolonged from several months to a year and more.

3. On the nature of the resistance of frozen soil to displacement along the lateral surface of the pile

In placing the piles by hand into steamed holes, whose diameter is greater than the diameter of the piles (Figure 59a), the strength of embedment is basically ensured by the adhesion between the frozen soil and the surface of the pile. In addition, with the method of driving being examined there develops in the soil a frictional resistance caused by the lateral pressure of the frozen soil under the effect of its own weight and the pressure arising as a result of the volumetric change of water as it freezes.

The total magnitude of adhesion and friction which causes the resistance to displacement along the lateral surface of the piles (the adfreeze strength) depends first of all on the temperature and the type of soil (see Chapter III); but the measured effects on the magnitude of this resistance and especially of its principal component adhesion shows the moisture pattern in the soil around the pile. The initial moisture content of the soil thawed by means of an open steam point becomes, as a result of the additional humidifying by the steam condensate, extremely high (from 50 to 120% and more), as is well known. However, during the freezing of steamed soil, this moisture content, as was shown by S. G. Tsvetkova (1953, 1954) on the basis of a large number of actual observations, sharply decreases, since as a result of the migration of water to the cold front, the surplus of moisture content is diverted to the periphery, and the layer of soil adjoining the pile is dehydrated. In fact, the moisture content ( $w$ ) of this layer becomes significantly less than the initial moisture content ( $w_i$ ), approaching a definite limit, i.e. the natural moisture content of the mineral layers ( $w_{mn}$ ) of the surrounding unbroken permafrost stratum.

The redistribution of moisture around the piles is graphically illustrated by Figure 60, from which it is evident that the greater the initial moisture content of the steamed soil-mass, the greater was the quantity of water that traveled to the boundary of the hole. The final

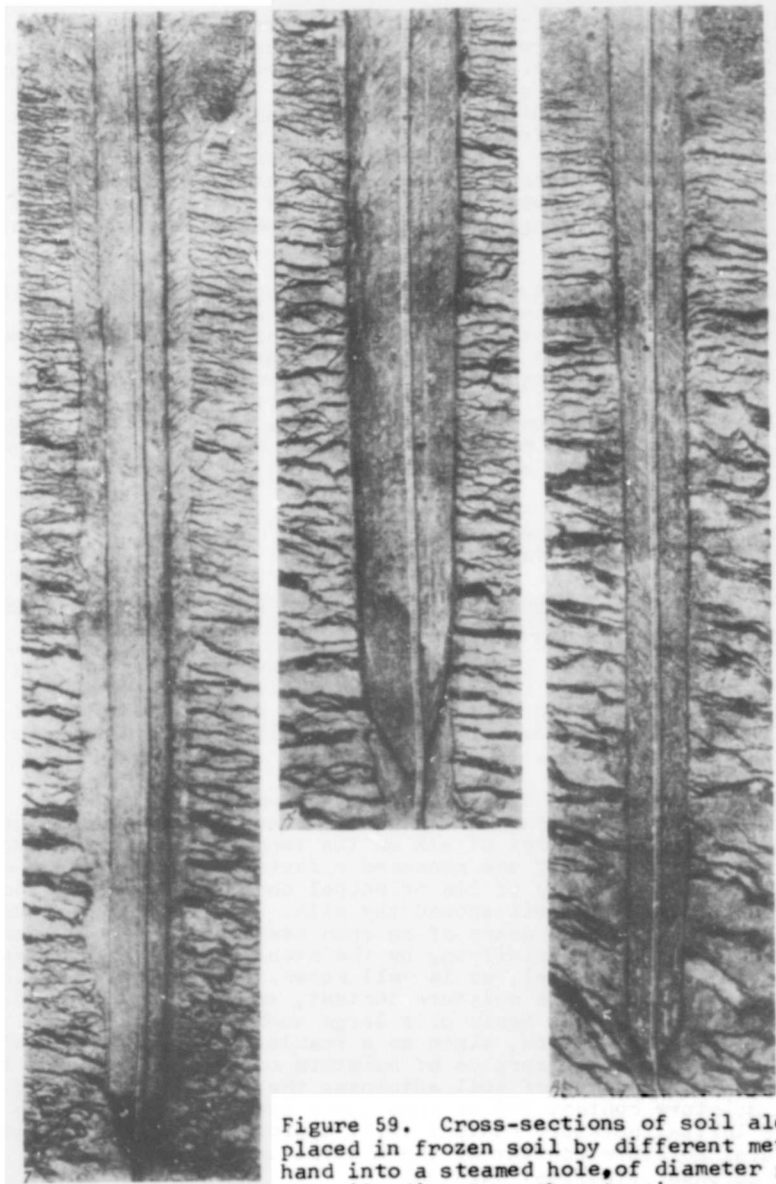


Figure 59. Cross-sections of soil along piles placed in frozen soil by different methods. a) By hand into a steamed hole, of diameter greater than the pile diameter; the steaming zone is clearly visible. b) With the pile driven into the steamed hole, of diameter smaller than the pile diameter; the steaming zone is visible beneath the point of the pile; around the surface of the pile is visible a layer of soil which has been pressed out. c) With a pile driven into a drilled hole; around the surface of the pile are visible deformations of the soil and ice layers.

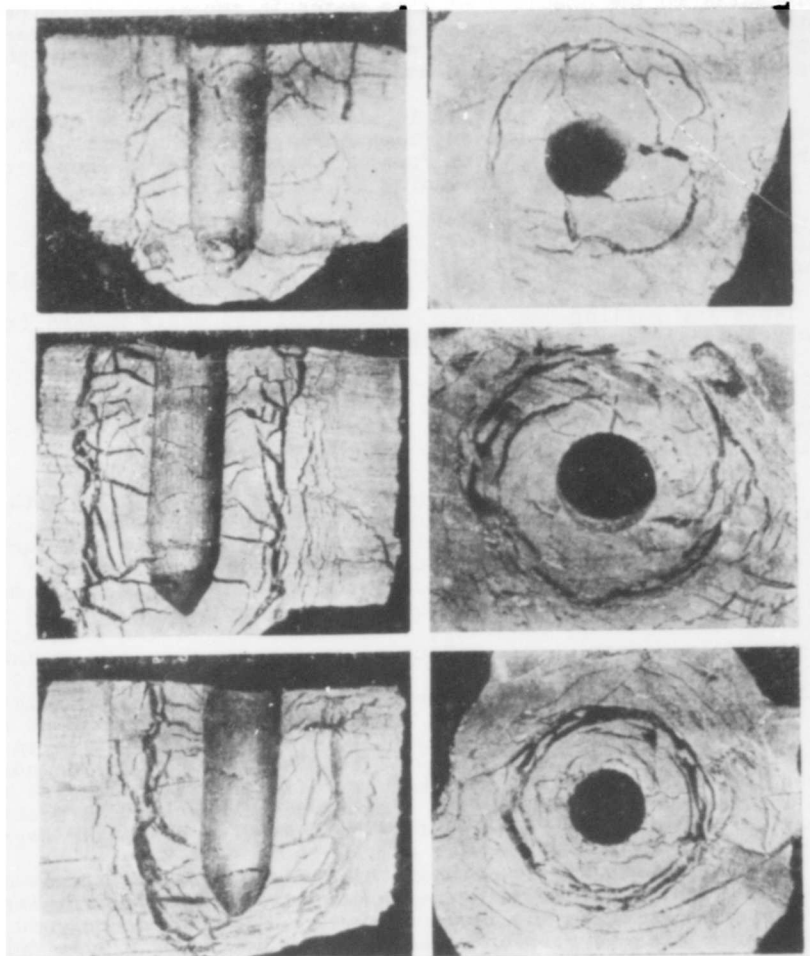


Figure 60. The redistribution of moisture during the freezing of argillaceous soil around the model piles. The initial moisture content of the steamed soil equalled: a) 80%; b) 110%; c) 145% (the piles are 35 mm in diam).

moisture content of the frozen soil turned out to be approximately the same and close to  $w_{mn} = 40$  to 45%.

Initial moisture content, % . . .	80	110	145	155	160	260
Final moisture content, % . . .	40	46	50	46	51	46

It is significant that the amount (36%) of non-frozen water in the steamed, and on the other hand, frozen soil around the piles is approxi-

mately equal to the quantity of this water in the surrounding permafrost stratum (35%); this agrees well with existing ideas concerning the practical lack of dependence of the content of the liquid phase of water in soil on its moisture content and texture.

Another interesting problem is whether the magnitude of the initial moisture content affects the adfreeze strength of the soil with piles. The results of laboratory tests for pulling out piles frozen into sandy loam soil under gradually increasing loads are the following:

Initial moisture content, (%) . . . . .	40	65	90
Final moisture content, (%) . . . . .	34	34	38
Failure stress, (kg/cm <sup>2</sup> ) . . . . .	0.9	0.8	1.0

Tests for pulling-out under constant stress  $\tau=0.8$  kg/cm<sup>2</sup> (the soil is varved clay) showed the following:

Initial moisture content, (%) . . . . .	70	95	110	130
Final moisture content, (%) . . . . .	51	57	60	60
Period within which the pile was pulled out (hr) . . . . .	40	70	131	178

From the data which we have presented, it follows that with the increase of the initial moisture content of the soil-mass the adfreeze strength grows somewhat. This evidently is explained by the fact that with an increase of the absolute content of water the forces of compressing the soil, which develop with the volumetric expansion of water as a result of its freezing, are increased. But if the initial moisture content is lowered very severely, then adfreezing of the soil with the pile cannot in general occur. Such a case occurred in one of the laboratory experiments with silty sandy loam ( $w_c = 30\%$ ,  $\theta = -0.40$ ), when the initial moisture content was equal to 34% and the final moisture content was decreased up to 20%. On the other hand, an extreme increase of moisture content leads to a lowering of the adfreeze strength. It should be observed that under natural conditions, when the boundary between the steamed and the unbroken soil (Figure 59a,b) is not as clear as in laboratory experiments, the influence of the initial moisture content of the steamed ground will be evidently of a smaller degree.

The ice coating exerts substantial influence on the adfreeze strength of soil with piles driven with the help of steaming. It is interesting that in our experiments the ice coating was detected not only in piles surrounded by steamed soil but also in piles driven by a pile driver into narrow, steamed holes (Figure 59, b). But in the first case the coating was unbroken and had a thickness from tenths of a millimeter to 1 to 2 mm; in the second case the coating was broken and thinner.

In order to evaluate the effect of the ice coating on the adfreeze strength we conducted contrasting tests for pulling out models of wooden piles, in one of which annular grooves were made, by which the shearing of soil on soil was ensured. Two other piles had smooth surfaces, but one of them was dried and the other was saturated with water. The tests were conducted under gradually increasing loads with equal time intervals (10 days) for each load. The soil was clay,  $w_f=155\%$ ,  $w_f=42$  to 49%,  $\theta=-0.40$ . The results of the tests showed that the piles having annular grooves had the greatest resistance.



Table 41. The effect on the adfreeze strength of grooves in the pile

Type of pile.	Period within which pulling-out occurred, hr.	Stress under which pulling-out occurred, kg/cm <sup>2</sup>
Smooth, water saturated	820	1.0
Smooth, air-dry	1008	1.2
With annular grooves	1230	1.4

This agrees well with the data of M. N. Goldshtein (1948), and confirms the expediency of his recommendations concerning the installation on the piles of notches and grooves, the installation of shaped piles, etc. From Table 41, it also follows that the smallest stability of adfreezing occurred with the wetted pile. This is explained by the formation around such a pile of a thicker ice coating in comparison with the ice coating around the air-dry pile. The contradictory results received by I. S. Vologdina, N. A. Tsytoich, and others (Proceedings of the KOVM, 1936), i.e. the rise of the adfreeze strength for wetted piles, are explained by the fact that the designated results refer to tests with quick loading, since in that case the resistance of ice is high. However, the long-term strength of ice, on the contrary, is very small, hence the resistance of piles saturated by water to prolonged stresses is decreased.

It is significant that the adfreeze bond between the frozen ground and the surface of the pile, once broken, is not fully reestablished. Thus, one of the piles driven with steaming was in the first test pulled out under a stress  $\tau = 1.2$  kg/cm<sup>2</sup> in 63 hr. In a repeat test, however, conducted 13 days after the first one, this pile under the same stress was pulled out in just 2 hr 45 min, and in the third test (a day later) in 55 min.

In driving piles with a pile driver into steamed holes of diameter smaller than the pile diameter (Figure 59,b), the role of the resistance of friction increases considerably. In the driving process, part of the liquefied soil-mass is pressed into the surrounding frozen soil radially compressing it.

The question arises: will not the pressed-in layer of the steamed ground turn out to be so compressed and dehydrated that adfreezing with the pile will not in general occur? Our experiments showed that with the temperature lower than  $-0.2^{\circ}\text{C}$  these fears are unfounded: the final moisture content of the soil around the piles driven by such a method is less than in the case of the free embedment of piles in steamed holes of a larger diameter, but nevertheless, it is sufficiently high. The adfreezing of the soil with the pile occurred fully in all cases, considerably more quickly than with the first method of driving.

The resistance to displacement along the lateral surface of piles being driven (by a pile driver) into holes drilled in frozen soil (Figure 50c) is ensured basically by the forces of compression (friction). Placing a pile with a pile driver causes the displacement of the sides of

the drilled hole and forces the displaced soil into the surrounding frozen stratum. In this case, some layers of displaced soil thaw at the expense of converting part of the kinetic energy into heat. But part of the energy of the blow is spent on breaking the structure of the soil, i.e. on irreversible deformations. Finally, the portion of the energy causing elastic deformations becomes heat in the soil (Denisov, 1951), and if the pile were withdrawn from the soil immediately after driving, then the accumulated energy would be spent on the reduction of the deformations, i.e. contraction of the hole. Since the pile in the soil hinders such reduction, then the initial stresses, acting on the soil itself and causing in it a weakening of structural and ice-cementing bonds, will relax, attaining after a fixed period some very small value. This radial compression mobilizes friction forces that ensure the stability of the pile.\*

Observe that even with the present method of driving piles, in addition to the forces of friction, adhesion arises, although it plays a secondary role. The adhesion is caused by the adfreezing of the soil (thawed with the driving of the pile) to the layer bordering it.

4. The relationship between the resistance of piles to loads and the method of placement

The demonstration of dependence of the bearing capacity of the piles on the method of placing them is of great practical interest. A comparative evaluation of the resistance of soil to displacement along the lateral surface of the piles driven by a pile driver into drilled holes and by hand into the steamed holes of larger diameter was made in Chapter III (Table 19). These two methods are the limiting cases: in the first, friction plays the chief role in the resistance, and in the second, it is adhesion. But other, intermediate, methods of placing piles into frozen soil can occur. For comparison, the author made pull-out tests (in the laboratory) on model piles placed in the following ways:

1. Piles were driven into drilled holes, but the walls of these holes were thawed by an electric "needle" just before driving.
2. The piles were driven into drilled holes of diameter 0.9 of the pile diameter.
3. The piles were driven into drilled holes (with  $d_{\text{hole}}/d_{\text{pile}}=0.9$ ) filled with a soil mass, which was modelled after piles driven with a pile driver into steamed holes whose diameter was less than the diameter of the piles.
4. The piles were driven into holes thawed by an electric needle; the diameter of these holes was somewhat less than the diameter of the piles.
5. The piles were frozen into a soil-mass placed in holes whose diameter was greater than the diameter of the piles ( $d_{\text{hole}}=50$  mm and

\* An analogous, although rather complicated phenomenon, will occur even with the method of driving piles with a pile driver into steamed holes of small diameter.



120 mm, and  $d_{pile}=35$  mm), which modelled the placement of piles by hand with steaming.

The tests were conducted with silty argillaceous loam (experiment 45) and with varved clay (experiment 41). The natural moisture content of these soils was, respectively, 43% and 40% (the clay did not have ice layers); the physical and mechanical characteristics of the soils are presented in Table 1. The tests consisted of pulling out the models of the piles under loads applied "instantaneously", and under loads applied gradually, with the holding of each step during equal intervals of time, i.e.  $\Delta t=240$  hr. In the last case, the stress under which rupture  $\tau_{rupt}$  occurred was the provisional criterion of stability. The results of the tests are presented in Table 42.

Table 42. Adfreeze strength of soil with piles driven by different methods

Methods of driving the piles	Instantaneous loading $\tau_{inst}$ , kg/cm <sup>2</sup>		Loading by steps, $\tau_{rupt}$ , kg/cm <sup>2</sup>	
	Varved clay	Silty argillaceous loam	Varved clay	Silty argillaceous loam
Driven into drilled holes:	5.0	3.3	2.0-2.4	1.8
The same with the thawing of the wall of the hole:	4.1	4.0	2.0	1.4
Driven into the soil, thawed with an electric needle:	2.4	3.25	1.8	1.8
Driven into holes filled with soil-mass; diameter of the holes less than the diam of the piles:*	2.75	3.0	1.2	1.4
The same, the diameter of holes greater than the diameter of piles:*	2.1	2.8	0.6-1.0	1.2

From the data presented in Table 42 and data previously examined (Table 19), it follows that piles driven by a pile driver into drilled holes exert the greatest resistance; piles driven by hand into steamed holes, whose diameter is greater than the diameter of the piles, exert

\* The initial moisture content of the soil-mass equalled: for clay 120%, and for sandy loam 80%.

the least. For sandy loam and argillaceous soils, the long-term strength in the first case is 1.25 to 1.6 times greater than in the second. This shows that the forces of friction (compression), between the frozen soil and the pile with the appropriate diameter of the hole, turn out to be greater than the forces of adhesion of the steamed, and subsequently frozen soil, particularly taking into account the weakening effect of the ice coating. It is natural that the resistance of the piles driven into the drilled holes will be greater since the diameter of the hole is smaller, and the frozen soil is more compact. Thus, for compact, varved clays the resistance of the driven piles turns out to be 2 to 4 times greater than the resistance of the frozen-in piles. The thawing of the walls of the holes, which is done to facilitate the driving of the piles, somewhat decreases the resistance of the piles to loads. This is explained by the lowering of the compressive forces, since the thawed layer of soil is solidified more easily than the frozen.

The decrease of adfreeze strength is observed also in the driving of piles with preliminary thawing of the soil by electric needles, and also "closed" steam (without the escape of steam into the soil) points. This decrease is explained not only by the lowering of the compressive forces, but also by strength characteristics of piles which were driven (by a pile driver) into steamed holes of diameter smaller than pile-diameter. With this method, just as in driving with the thawing of the electric needle, adhesion as well as friction arises in the soil. The resistance of these piles is less than that of piles driven into drilled holes, but greater than that of piles "frozen" into steamed holes of greater diameter. Depending on the diameter of the hole and the compactness of the soil this increase is from 15% (argillaceous) to 100% (compact varved clay). There are, however, cases when the adfreeze strength of the piles driven by a pile driver into holes of small size (steamed or drilled) is not greater than the strength of piles "frozen" into steamed soil. This can, for example, occur in soil containing many ice layers, since in such a case the ice contacts the surface of the pile and its long-term adfreeze strength is smaller than the adfreeze strength of the soil. In such soil, the installation of steamed holes whose diameter is greater than the diameter of the piles can be more expedient.

The effect of the methods of emplacement strongly influences, particularly, the bearing capacity of piles driven into frozen ground with a high temperature (near 0°C). Thus, we tested in field conditions four piles ( $d=22$  cm) driven into sandy loam with a temperature from -0°C to -0.2°C (section 1,b) by the following methods: (1) by hand, into a steamed hole with a diameter greater than 24 cm; (2) with a pile driver, into a steamed hole with a diameter of about 18 cm; (3) with a pile driver into a steamed hole with a diameter of 19 cm; (4) with a pile driver, immediately driving the pile into the frozen stratum.

The tests, which were carried out within 4.5 months after placement, consisted of pulling out the piles under gradually increasing forces ( $\tau=0.1$  kg/cm<sup>2</sup>; 0.2 kg/cm<sup>2</sup>; 0.3 kg/cm<sup>2</sup>; and so on) with the holding of each phase for 20 days. As a result of the test, the rupture stress  $\tau_{rupt}$ , the time  $t$  after which the rupture occurred, and the approximate limit of the long-term adfreeze strength  $\tau_{lt}$  were determined (Table 43).

As is obvious, the long-term strength for the pile driven by hand with steaming was three times smaller than for the pile driven by the

Table 43. Adfreeze strength of the soil with the temperature 0 to  $-0.2^{\circ}\text{C}$  with piles driven by different methods

Method of driving the piles	t, hr	$\tau_{\text{rupt}}$ kg/cm <sup>2</sup>	$\tau_{\text{lt}}$ kg/cm <sup>2</sup>
Driving by hand into steamed hole of larger diameter:	688	0.3	0.1
Driving with a pile driver into a steamed hole of smaller diameter:	1400	0.5	0.15-0.2
Driving with a pile driver into drilled hole:	1460	0.7	0.3
Driving immediately into frozen soil:	1610	0.7	0.35-0.4

pile driver into the drilled hole. Such a great difference is explained by the fact that with the temperature of the frozen stratum near  $0^{\circ}\text{C}$ , the steamed soil assumed the temperature  $0^{\circ}\text{C}$  to  $-0.2^{\circ}\text{C}$ , but even after 4.5 winter months it remained in a non-frozen state. It is interesting to compare the data presented in Table 43 with the standard values of the frictional resistance of non-frozen soil  $\tau_{\text{fr}}$ . According to "Technical Conditions" of the Ministry of Heavy Buildings I - 100 - 40, this resistance equals:

Sandy loam, depending on compactness	0.1 - 0.2	kg/cm <sup>2</sup>
Argillaceous and hard clay	0.3 - 0.4	"
The same, plastic	0.15 - 0.2	"
The same, in fluid condition	0.05 - 0.1	"
Soft silt, depending on consistency	0.0 - 0.05	"

In comparison we should divide our data by a safety factor, for example  $k=1.5$ , since permissible, and not maximum values of  $\tau_{\text{fr}}$  have been presented in the standards. Then the values  $\tau_{\text{lt}}$  for the piles driven immediately into frozen soil and driven into drilled holes will be approximately equal to the frictional resistance of non-frozen soil which is, respectively, in hard, and plastic, states. But the resistance to adfreeze force for the pile driven by the pile driver into the steamed hole of small diameter corresponds to the frictional resistance of the non-frozen soil, which is in a state halfway between fluid and plastic; for the pile driven by hand into the steamed hole of large diam, it corresponds to the frictional resistance of non-frozen soil of fluid consistency.

In conclusion, let us compare the advantages and disadvantages of the methods of driving piles. Driving piles by hand into steamed holes whose diameter is greater than the diameter of the piles is the simplest method from the operating point of view. The effectiveness of the designated method of driving increases in soil with a low temperature, when the use of other methods is inconvenient. The same applies to the case of driving square (reinforced concrete) piles. However, this method has a number of disadvantages, among which are the decreased bearing capacity of the piles, the length of the process of adfreezing

of the steamed soil, the possibility of heave of the piles in this period, and so on. The presence of gravel inclusions seriously complicates hand driving. But in soil with a temperature that is high and close to 0C, the use of this method is generally not permissible.

Driving of piles with a pile driver into steamed holes is more expedient. In this case the time of adfreezing of the steamed soil is considerably shortened, and the reliability of sealing the piles in the soil and their bearing capacity are increased. The complexity of the process of driving the piles and the necessity of additional machinery (a pile driver) is compensated for by the shortening of the time of steaming and the general increase of work output. Driving piles into drilled holes is the most reliable method, ensuring an increased bearing capacity. However, this method involves additional complexities as related to the necessity of drilling holes. In addition, in the presence of soil with a low temperature the driving itself is inconvenient. If the soil has a comparatively high temperature, than this method is perhaps the only acceptable one. In soil with a low temperature the driving of piles can be performed in drilled holes sealed by a soil back-fill, and in this case, the diameter of the hole becomes greater than the diameter of the pile.

## CHAPTER XI. LIMITING LOAD CAPACITY OF PILES

1. Pull-out tests on piles

The laboratory tests for pressing-down the model piles described in Chapter III permitted us to propose general laws for the processes of deformation and resistance to displacement of frozen soil along the lateral surface of the piles. However, as it follows from the condition of similarity (section 6, Chapter III), the absolute values of the forces of resistance derived from these tests cannot be mechanically transposed to piles of real dimensions. Determining the real value of these forces demands correction by actual tests. The results of such tests, which consisted of determining the resistance of piles to pressing-down, are examined below. The field tests confirmed the general laws proposed according to the data of laboratory experiments. In quick loading, failure occurs as a result of the brittle breaking-away of the pile from the soil. The instantaneous resistance attains a comparatively high value (for example,  $\tau_{inst.} = 3.8 \text{ kg/cm}^2$  at  $\theta = -0.8^\circ\text{C}$ ), which, however, is less than in the laboratory experiments. This is explained on one hand by the slower loading (10 to 20 min) in comparison with the laboratory tests (5 to 30 sec), and on the other hand by the effect of the dimensions of the piles. In the prolonged action, the process of deformation has a visco-plastic character; the curves of creep with different constant stresses  $\tau = \frac{T}{\pi dl}$  ( $\text{kg/cm}^2$ ) and at a differ-

ent temperature of the soil are presented in Figure 61. With large values of the stresses (pile nos. 9, 11, 4), the curves of deformation, in distinction from similar curves for ideal visco-plastic bodies, are S-shaped, not concave. In this we see the effect of the ice coating\*, since the similar character of curves reflecting continuous acceleration of the process of deformation is typical for ice; this we have discussed previously.

But with small values of the stresses (pile nos. 13, 20, 8), the curves take the form of ordinary creep curves, having a clearly expressed linear portion corresponding to the phase of the visco-plastic flow which has been established. The duration of this phase reaches 2000 to 3000 hr and more. Nevertheless, some effect of the ice coating which appeared in the presence of the large concave portion of the curve is seen in the present case. Observe that the bend of the creep curves begins with the deformations, composing in all 1.5 to 3% of the effective length of the pile, and consequently, the decrease of the area of adfreezing cannot be cited as the principal reason for the rise of the gradual flow rate.

The available results of the pull-out tests of piles under constant stresses are presented in Table 44.

\* These curves are derived from tests of piles driven with steaming. For piles which are driven into drilled holes, the curves of deformation approach the ideal form; a comparison of the curves was presented in Figure 17.

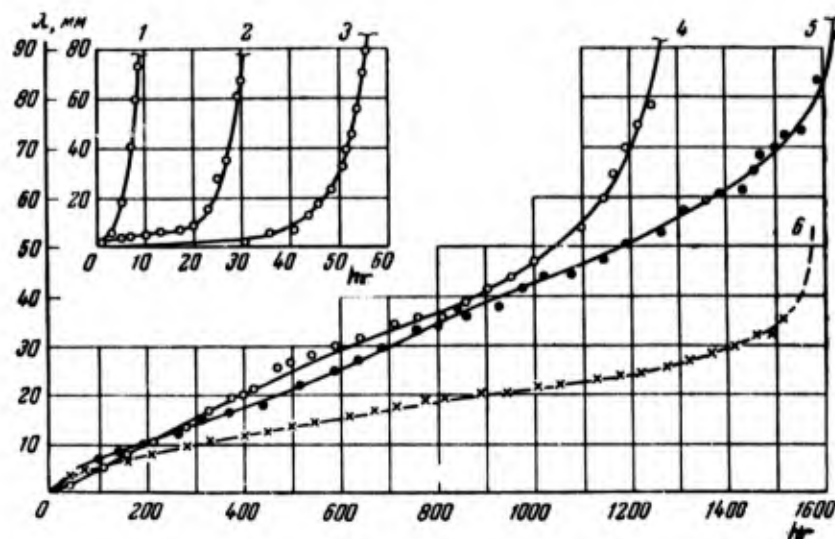


Figure 61. Test for pulling-out piles driven by hand with steaming. Development of deformations in the period under constant stresses:

- (1)  $\tau = 1.65 \text{ kg/cm}^2$ ,  $\theta = -0.8^\circ\text{C}$  (pile no. 9);
- (2)  $\tau = 1.5 \text{ kg/cm}^2$ ,  $\theta = 1.8^\circ\text{C}$  (pile no. 11);
- (3)  $\tau = 1.2 \text{ kg/cm}^2$ ,  $\theta = -0.5^\circ\text{C}$  to  $0.7^\circ\text{C}$  (pile no. 4);
- (4)  $\tau = 0.55 \text{ kg/cm}^2$ ,  $\theta = 0.2^\circ\text{C}$  (pile no. 13);
- (5)  $\tau = 0.4 \text{ kg/cm}^2$ ,  $\theta = -0.2^\circ\text{C}$  (pile no. 20);
- (6)  $\tau = 0.75 \text{ kg/cm}^2$ ,  $\theta = -0.35^\circ\text{C}$  (pile no. 8).

Table 44. Results of pull-out tests on piles under constant stresses driven by hand with steaming into sandy loam and argillaceous, silty loam.

Pile no. Area no.	Temperature $^\circ\text{C}$	Stress $\tau$ $\text{kg/cm}^2$	Time during which the pile was pulled, hr	Comment
10/1	-0.8	3.8	Instantaneous	Approximate value of the long-term adfreeze strength $\tau_{lt} \approx 1.0 \text{ kg/cm}^2$
1/2	-0.8	2.55	0.25	
9/1	-0.8	1.65	10	
11/1	-1.8	1.5	47	
2/2	-0.8	1.25	993	$\tau_{lt} \approx 0.6 \text{ kg/cm}^2$
4/1	-0.5-0.7	1.2	63	
7/2	-0.5-0.6	1.0	11	
8/1	-0.4	0.75	1520	
5/1	-0.1	1.05	Instantaneous	$\tau_{lt} \approx 0.3 \text{ kg/cm}^2$
6/2	-0.2	0.75	113	
13/1	-0.1-0.3	0.55	1306	
20/1	-0.2	0.4	1720	



In addition to the tests under constant stresses, tests under gradually increasing stresses were also performed (Figure 62), holding each phase during a sufficiently long period, i.e. up to several months and even up to a year, in order to establish the fact of transition from the attenuated deformation to the continuous one. Thus, pile no. 12 (argillaceous loam,  $\theta = -0.1C$  to  $-0.2C$ ), when it was under a stress of  $0.15 \text{ kg/cm}^2$  which acted during 380 hr, was not completely displaced. But with the increase of the stress to  $0.25 \text{ kg/cm}^2$ , a continuously growing deformation arose. Although this deformation was developed with an exceedingly small rate, reaching 3.5 mm in all for 2600 hr, the consistency of its rate serves as proof that with a longer time of action of the present stress the pile would have been pulled out. With subsequent increase of the stress up to  $0.35 \text{ kg/cm}^2$ , the displacement of the pile occurred with continually increasing speed, and after 500 hr the pile was pulled out. In other cases, the transition to the phase of gradual flow is expressed more sharply. Thus, pile no. 7 (sandy loam,  $\theta = -0.3C$ ) with a stress of  $0.3 \text{ kg/cm}^2$ , which acted for 2950 hr, had in general no recorded displacement. With a stress of  $0.5 \text{ kg/cm}^2$  which acted for 3380 hr, there were displacements, but they were quickly stabilized. After the increase of the stress to  $0.7 \text{ kg/cm}^2$ , a rapid growth of the deformation began and after 75 hr the pile was pulled out.

Above, we examined the results of field tests of piles with a comparatively constant temperature of the soil (which was achieved with the installation of insulation). The study of the resistance of piles to pulling-out in conditions of variable negative temperature is of substantial interest. With a drop in temperature, the coefficient of

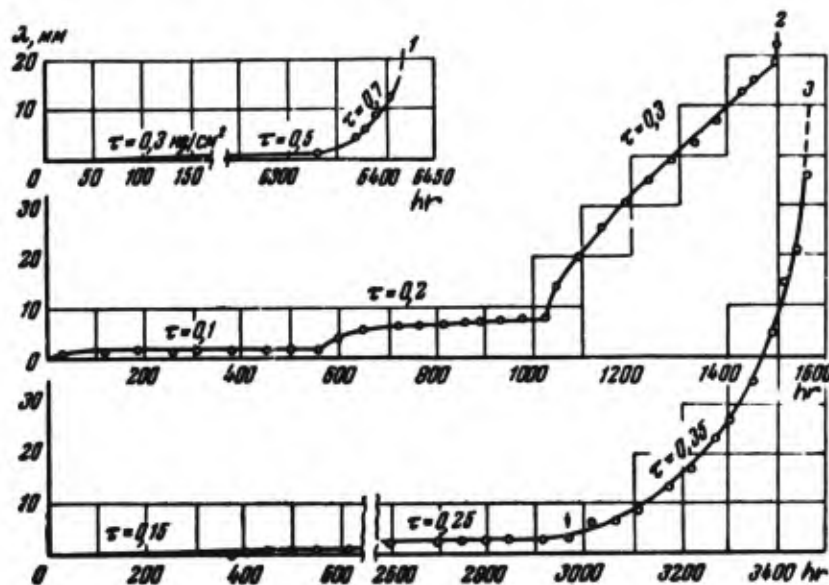


Figure 62. Pull-out test for piles driven by hand with steaming. Development of deformation in time under a stress which rises gradually.

- (1) Data of pile test no. 1 for  $\theta = -0.3C$ ;
- (2) Data of pile test no. 22 for  $\theta = -0.1C$  to  $-0.2C$ ;
- (3) Data of pile test no. 12 for  $\theta = -0.1C$  to  $-0.2C$ .



viscosity of the frozen soil increases, as is well known. Correspondingly, the speed of deformation will decrease. With some value of the temperature of the soil, therefore, the displacement of the pile can in general be discontinued. On the contrary, with a rise of the temperature of the soil the speed of displacement of the pile increases, and the stabilized deformation can turn into a continuous deformation. Similarly, the changes of the character of deformation are graphically illustrated by Figure 63, in which curves of the displacement of the piles and curves of temperature changes of the soil are presented. For example, the tests on pile no. 3 (Graph 5, Figure 63) were begun early in December with the soil temperature  $-0.5^{\circ}\text{C}$ . Under a stress of  $0.75 \text{ kg/cm}^2$  there occurred a slow but continuous displacement of the pile which, however, sharply decreased with the drop of the temperature to  $-0.8^{\circ}\text{C}$ . Further sharp drop of the temperature to  $-1.4^{\circ}\text{C}$  led to a complete halt of the displacement (although  $\tau$  was raised to  $1.1 \text{ kg/cm}^2$ ). The spring rise in soil temperature caused only an insignificant movement of the pile in the beginning. But after some time, with a continuing even rise of the temperature, a sharp intermittent increase of the displacement with subsequent intensive development resulted. After some more time, the process graduated into the phase of gradual flow and the pile was pulled out.

The intermittent change of the speed of displacement of the piles with a rise of the temperature of the soil and the sharp change into the phase of failure are evidently not accidental phenomena, since they were observed in a number of pile tests. It is possible to assume that the rise of the soil temperature causes a gradual decrease of the adfreeze strength and a corresponding gradual change of the speed of displacement of the piles only, until the resistance of adfreezing becomes less than the applied tension. At this moment, there occurs a "disruption" of the pile and subsequent intensive displacement of it.

In conclusion, we present the values of the maximum adfreeze strength of the soil with piles, derived from data of the field experiments examined above under constant as well as under gradually increasing stresses (Table 45). From a comparison of Tables 45 and 19 it follows that the values  $\tau_{lt}$  derived from field tests are somewhat smaller than the values determined under laboratory conditions. Thus, in the first case for sandy, argillaceous loam (at  $\theta = -0.3^{\circ}\text{C}$  to  $-0.4^{\circ}\text{C}$ )  $\tau_{lt} = 0.5$  to  $0.6 \text{ kg/cm}^2$ , and in the second case  $\tau_{lt} = 0.6$  to  $0.9 \text{ kg/cm}^2$ . The designated deviations are explained by the effect of the size of the piles, which we discussed previously in our examination of the conditions of similarity.

## 2. Pile testing for resistance to penetration [Down loads]

Let us examine first the results of laboratory experiments conducted with the forms of the piles frozen into light silty argillaceous loam.\* The experiments consisted of parallel tests for pressing-down and pulling-out these piles under constant, as well as increasing stresses.

\* The natural moisture content, undisturbed soil  $w = 29\%$ ; the initial moisture content of the soil-backfill sealed into the hole  $w_i = 86\%$ ; the final moisture content after adfreezing  $w_f = 29\%$ , the temperature of the soil is  $-0.4^{\circ}\text{C}$ . See other characteristics of the soil in Table 1.

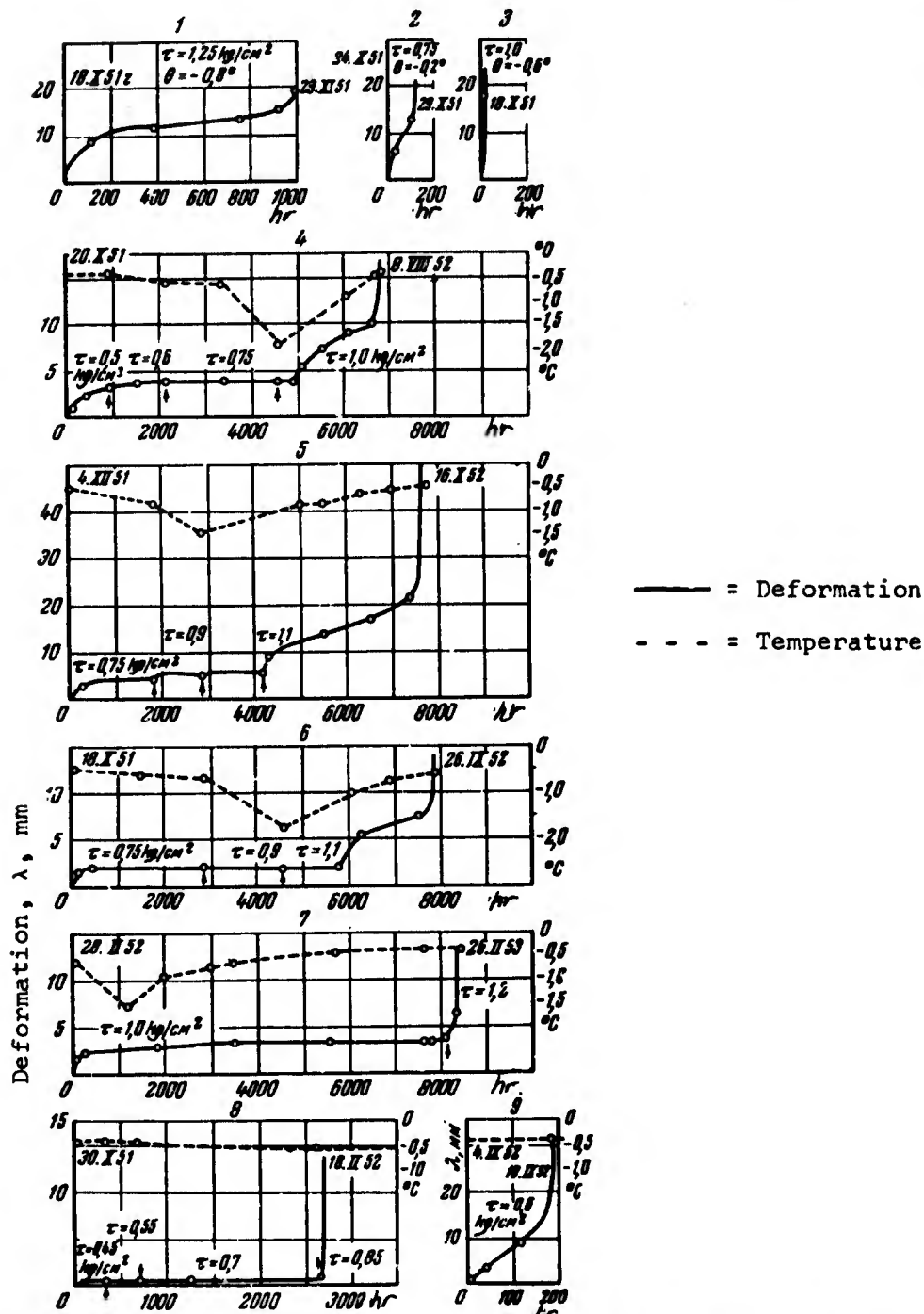


Figure 63. Test for pulling-out of piles driven by hand with steaming. Development of deformations in time with variable soil temperature. (1), (2), (3), (4), (5), (6), (7), (8), (9), are respectively the data for pile nos. 2, 6, 7, 8, 3, 11, 12, 9.

Table 45. Values of long-term adfreeze strength of soil with piles driven by hand with steaming

Pile no. Area no.	Soil	Tempera- ture °C	Moisture content, %		$\tau_{lt}$ kg/cm <sup>2</sup>
			Nat- ural	After adfreez- ing	
	<u>Constant stress</u>				
3/2	Silty clayey sand, and heavy silty sandy loam	-1.0	33	--	0.9
4/2	Heavy silty sandy loam	-0.9	45	28	0.8-0.9
2/2	Light silty sandy loam	-0.9	33	25	1.0
3/1	Light argillaceous, and heavy silty sandy, loam	-0.8	29	27	0.9-1.0
3/2	Silty clayey sand, and heavy sandy loam	-0.7	33	30	0.7
	<u>Gradually increasing stress</u>				
4/2	Silty, light, and heavy, sandy loam	-0.6	45	25	0.7
8/2	The same	-0.5	28	--	0.6-0.7
12/2	Light silty sandy loam	-0.4	40	--	0.6
8/1	Light argillaceous, and heavy silty, sandy loam	-0.3 to -0.4	33	28	0.6
7/1	Heavy silty sandy loam	-0.3	29	26	0.5
20/1	Light argillaceous, and heavy silty sandy loam	-0.2	41	--	0.3
12/1	Light silty argillaceous loam	-0.1 to -0.2	26	25	0.2
22/1	Heavy sandy loam, and light silty argillaceous loam	-0.1 to -0.2	29	--	0.15

The results of the tests of the piles for pressing-down under constant stresses are presented in Figure 64 in the form of curves of development of the displacement settlement of the piles with time. Let us analyze the law of the process of the resistance of frozen soil to penetration by piles, proceeding from an examination of these curves. In loading a pile, the external stress is absorbed first only by the resistance of the soil along the lateral surface of the pile (the resistance of adfreezing), but the point of the pile does not take part in the operation. But in proportion to the relaxation of these lateral stresses, there occurs a gradual pressing-down of the point of the pile, and the soil under it begins to absorb part of the load. If the stress exceeds the maximum long-term adfreeze strength, then at a fixed moment, the weakened forces of resistance to displacement will be less than the acting tangential stresses and a "disruption"

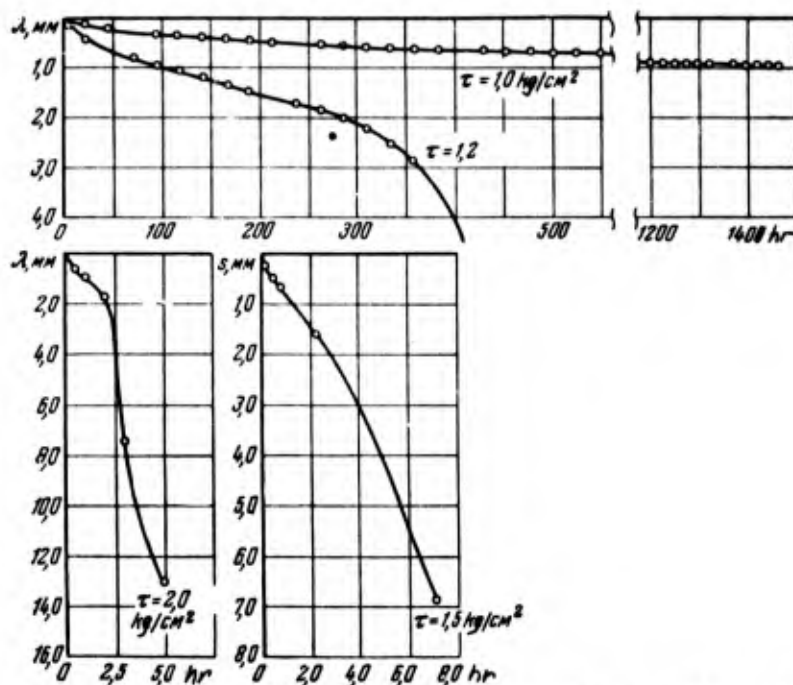


Figure 64. Curves of the development of deformation in pressing-down piles under constant stresses ( $\text{kg/cm}^2$ ) in light, silty argillaceous loam.  $\theta = -0.4^\circ\text{C}$  (experiment 29).

of the pile in contact with the soil will occur. The designated moment is reflected by the inflexion of the curves of Figure 64, particularly, very clearly in the curve for  $\tau = 2.0 \text{ kg/cm}^2$ . The further process of pressing-down is accompanied by the opening of the surrounding soil by the point and by the penetration of the pile in the soil, as in a visco-plastic medium. This process is reflected by the sharp fall in the curves  $s=f(t)$ , i.e. it corresponds to the development of collapse. But if the stress is not very great, then the process of pressing-down is characterized by a continuous growth of the settlement with constant speed; this process corresponds to the phase of the established visco-plastic flow, which can last for an exceedingly long time.

It is extremely significant that the curves of the development of settlement in time according to their character (but not according to absolute value) are analogous to the curves of creep in pulling-out piles, a fact which can be ascertained by comparing the curves of Figure 64 with those of Figure 16. Particularly interesting is the case in which even in pressing-down, when the area of adfreezing is not decreased, the phase of steady flow still merges into the phase of progressive flow.

Laws analogous to those set forth above can be demonstrated also in tests under gradually increasing stresses (Figure 65). In the case of small loads, when the active tangential stresses are significantly less than the long-term adfreeze resistance, the displacement of the pile is exceedingly small and has a broken character. Corresponding to

this, the point of the pile does not take part in the operation and the whole stress is absorbed by the soil along the lateral surface of the pile. In proportion to the rise of the stress and the increase of settlement, a continually increasing part of the stress is diverted to the point. The maximum correlation between the forces of resistance along the lateral surface of the pile and under its point will occur in a state of limiting equilibrium.

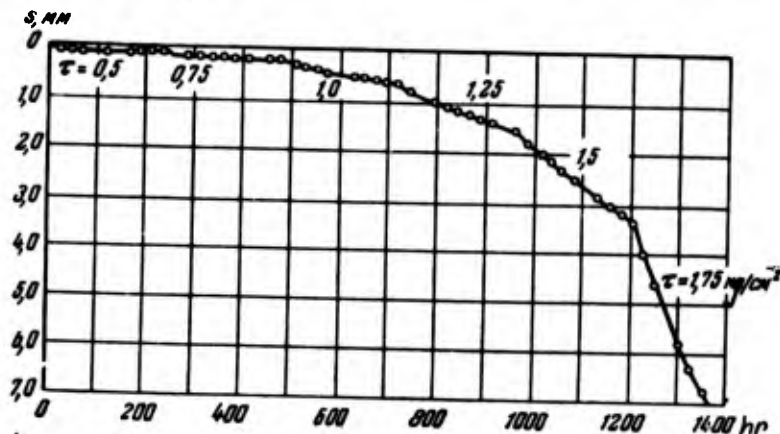


Figure 65. The growth of settlement in pressing down a pile under load increasing by steps. The argillaceous loam is light and silty, the pile is frozen, and  $\theta = -0.4^\circ\text{C}$  (experiment 29).

Before reaching this state, i.e. with  $P < P_{\text{lim}}$ , the relation between settlement and stress is described by the power law analogous to (24) for the case of pulling-out the piles,

$$P = A \left( \frac{s}{d} \right)^n. \quad (73)$$

The corresponding graphs for the data of the parallel tests for pressing-down and pulling-out are presented in ordinary and logarithmic coordinates in Figure 66; let  $s$  designate the settlement of the pile in pressing-down, and  $\lambda$  the displacement of the pile in pulling-out. With the increase of the stress value  $P_{\text{lim}}$ , the settlement assumes a continuous character while formula (40), which establishes the relation between the speed of this settlement and the excess stress, will assume for the case of pressing-down the following form:

$$\frac{ds}{dt} = \frac{1}{n} (P - P_{\text{lim}})^{\frac{n-1}{n}}. \quad (74)$$

For plastic soil  $n \approx 1$ , and equation (74) takes a form analogous to (41). Figure 67 presents graphs of the relation between the stress  $\tau = P/F$  and the speed of the relative displacement of the piles  $\xi = \frac{dy}{dt}$  for

the cases of pressing-down ( $Y = s/d$ ) and pulling-out ( $Y = \lambda/d$ ). Thus, laws of the processes of deformation in pressing-down piles and in pulling them out are analogous; this gives evidence of the community of laws of the resistance of frozen soil to stresses. But, of course, the absolute values of the determinations and of their speeds in pressing-down and pulling-out piles are different, since in the first case, the resistance of the soil is increased because of the participation of the point of the pile in the operation. For example, in

pressing-down model piles the visco-plastic flow approached with a stress  $\tau = 1.0 \text{ kg/cm}^2$ , but in pulling-out this phase corresponded to  $\tau = 0.7 \text{ kg/cm}^2$ . Exactly in the same way the time after which the break occurred was greater (in identical stresses) in the case of pressing-down piles than in the case of pulling them out (Table 46).

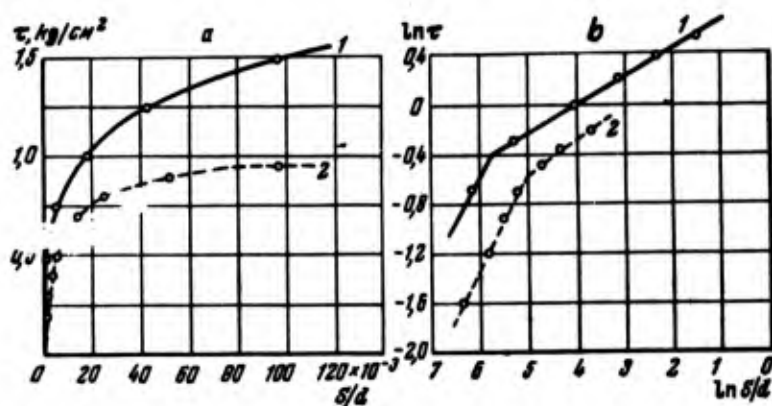


Figure 66. Relation between the deformation (relative) and the stress in (a) ordinary and (b) logarithmic coordinates.

(1) Pressing-down piles (experiment 29);  
(2) pulling-out piles, (experiment 28).

The effect of the resistance of the soil under the point of the pile reveals, of course, the magnitude of the parameters entering equations (73) and (74). The coefficient  $A$  in pressing-down is greater than the same coefficient from formula (24) in pulling-out. But the coefficient of viscosity  $\eta$ , on the contrary, is in pressing-down less than in pulling-out; for the examples which have been examined (Figure 67), it is equal respectively to  $1.4 \times 10^{13}$  poise and  $6.2 \times 10^{13}$  poise (the speed of the deformation in the first case is less than in the second). From this point of view it is interesting to recall that in the installation of notches on the piles, when the effect of the ice coating is eliminated, the value  $\eta$  in pulling-out piles is also decreased (Figure 21); it reaches the values in pressing-down "frozen-in" piles.

Let us pass on to an examination of the results of field tests of piles for pressing-down (Figure 68). Such tests were conducted with stepped loads with piles driven with steaming into sandy, argillaceous, and silty loam.\* The tests of one pile (no. 1) were conducted under stresses of 0.7 to 0.85 to 0.1  $\text{kg/cm}^2$  and continued 5.5 months. With  $\tau = 0.7 \text{ kg/cm}^2$  there occurred an exceedingly slow but, all the same, a continuous, growth of the settlement (0.04 mm per day), while it was characteristic that the steady phase of the process advanced after 1.5 months. With a rise of the stress of 0.85  $\text{kg/cm}^2$ , the rate of deformation sharply increased (1 mm/day) and the magnitude of the settlement

\* The natural moisture content of the soil is 29 to 34%; the initial moisture content of the steamed soil is 76%, the final (after adfreezing) is 28 to 31%. The temperature of the soil  $\theta = -0.30$  to  $-0.40$ .



for 2 months reached 110 mm. The further rise of the stress to 1.0 kg/cm<sup>2</sup> led to the appearance of collapse; in 40 hr the pile penetrated 54 mm.

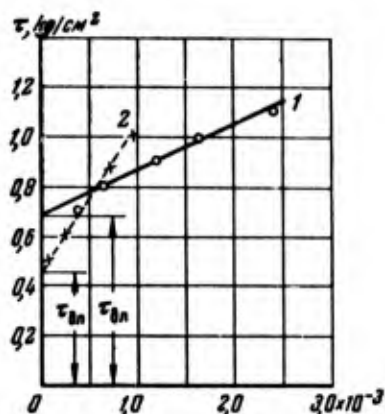


Figure 67. Relation between the stress and the speed of the relative displacement of the piles.

- (1) In pressing-down;  
(2) in pulling-out.

speed of displacement,  $dY/dt$

Analogous results were obtained in the test of pile no. 25. With stresses 0.3 kg/cm<sup>2</sup> and 0.5 kg/cm<sup>2</sup>, the settlements of the pile were small and discontinuous. With  $\tau=0.75$  kg/cm<sup>2</sup>, there was a continuous settlement which grew with catastrophic speed, up to 40 mm per day. The pile began to penetrate the frozen soil as in a plastic medium, and the general settlement reached 380 mm.

Table 46. Comparison of the results of tests for pressing-down and pulling-out piles under constant stresses

Experiment no.	Form of the experiment	Time (in hr) after which there occurred the break in the reaction for stresses $\tau$ kg/cm <sup>2</sup> equal to						
		8.25	4.2	2.0	1.5	1.2	1.0	0.7
28	Pressing-down	Instantaneous	---	3	56	450	more than 2000	not penetrating
29	Pulling-out	---	Instantaneous	0.3	5.3	8	130	more than 2500

### 3. Point-bearing resistance of frozen soil

In conjunction with formula (71), the maximum resistance of the soil under the leading edge of the pile is determined by the difference  $R_{lim} = P_{lim} - T_{lim}$ . Expressing  $P$  and  $T$  by the specific forces of resistance to pressing-down  $\tau_{pr} = P/F$  and to pulling-out  $\tau_{pul} = T/F$  (where  $F$  is the area of the lateral surface of the pile), we find that the maximum pressure transmitted to the soil under the point of the



pile, referred to the unit or area of the cross-section of the pile  $f$ , will equal

$$\sigma_{\text{lim}} = \frac{R_{\text{lim}}}{f} = (\tau_{\text{pr}} - \tau_{\text{pul}}) \frac{F}{f} \quad (75)$$

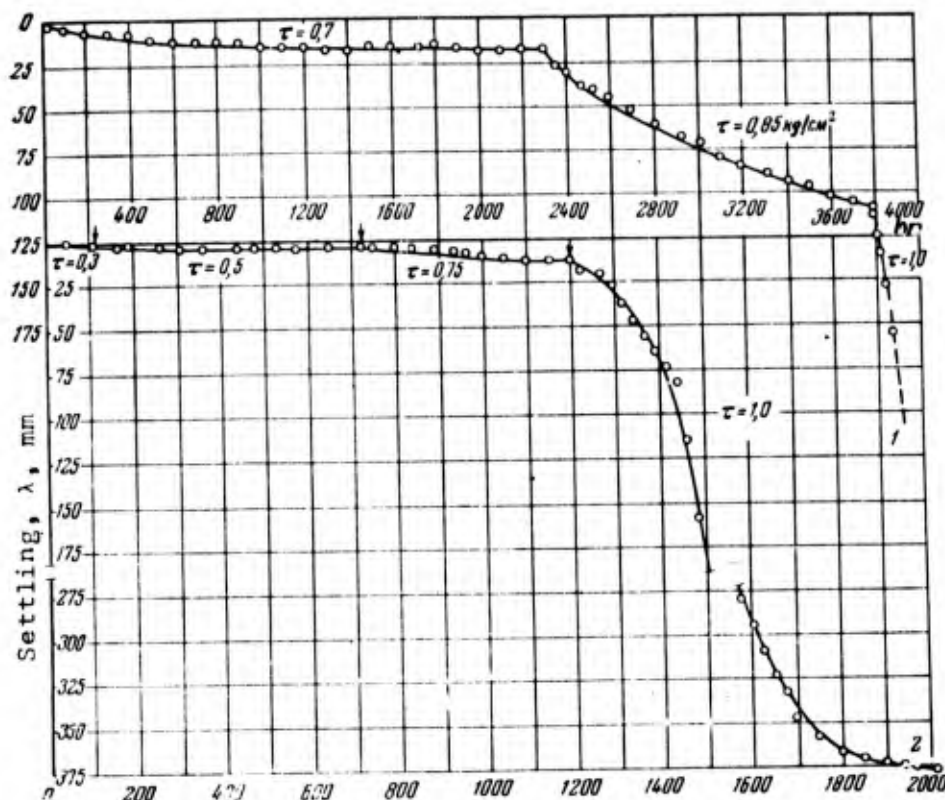


Figure 68. Test for pressing-down piles driven by hand with steaming. Development of deformations in time under gradually increasing stresses.

- (1) Data of the tests of pile no. 1 with  $\theta = -0.3C$ ;
- (2) Data of the tests of pile no. 25 with  $\theta = -0.3C$  to  $-0.4C$ .

According to the data of the above-examined laboratory tests for pressing-down (experiment 29), conducted with four piles, the value of the limit stress was equal to  $\tau_{\text{pr}} = 0.7$  to  $0.8 \text{ kg/cm}^2$ . But the maximum resistance to pulling-out for this soil is (Table 15, experiment 28)  $\tau_{\text{pul}} = 0.5 \text{ kg/cm}^2$ . Hence, with  $F = 126 \text{ cm}^2$  and with  $f = 9.6 \text{ cm}^2$ , the limiting pressure under the point equals  $\sigma_{\text{lim}} = (0.2 \text{ to } 0.3) \times 13.1 = 2.6 \text{ kg/cm}^2$  to  $3.9 \text{ kg/cm}^2$ .

Let us compare this magnitude with the value of adhesion. For the given soil, the value of the equivalent long-term cohesion from experiments,  $c_e = 0.55 \text{ kg/cm}^2$ . Hence,

$$\frac{\sigma_{\text{lim}}}{c_e} = 4.7 \text{ to } 7.1$$

In actual tests of the piles it turned out (Figure 68) that the resistance to pressing-down was  $\tau_{pr} \approx 0.65 \text{ kg/cm}^2$ , but the resistance to pulling-out  $\tau_{pul}$  (Table 45) in one case was equal to  $0.5 \text{ kg/cm}^2$ , and in two cases to  $0.6 \text{ kg/cm}^2$ . With  $F = 11250 \text{ cm}^2$  and  $f = 250 \text{ cm}^2$  we get, on the average,  $\sigma_{lim} = 0.80 \times 45 = 3.6 \text{ kg/cm}^2$ . The value of the equivalent adhesion, determined for the sample of soil taken immediately from beneath the point of the pile after its being dug up, was equal to  $c_e = 0.5 \text{ kg/cm}^2$ . Hence, taking into account the depth of the pile  $l = 4 \text{ m}$  (with  $\gamma_s = 1.7 \text{ T/m}^3$ ), we get  $\sigma_{lim}/c_e = 5.8$ .

As can be seen, the value  $\sigma_{lim}$  is close to the value ( $5.55 c_e$ ) determining the limiting resistance to the pressing-down of the round punch according to formula (69), which corresponds to the assumed approximate calculation scheme of pile behavior. Proceeding from what we have said, it is possible in the series of the first approximation to assume that the resistance of the soil under the point of the pile is determined by the formula,

$$\sigma_{lim} = 5.55 c_e + \gamma_s l \quad (76)$$

where  $l$  is the depth of embedment of the pile.

In conclusion, let us point out that for the piles which were examined, the point resistance of the soil was about 10 to 15% of the resistance along the lateral surface. Observe once again that the soil under the point of the pile is fully engaged in operation only when the state of limiting equilibrium, i.e. when  $P \geq P_{lim}$ , occurs. But since we conduct the calculation of the pile precisely according to such a state, then the resistance of the soil under the point should be taken into account, if, of course, the possibility of the heaving of the piles in the period of construction is excluded.

#### 4. Bearing capacity of piles and design values of the adfreeze strength

For an approximate evaluation of the bearing capacity of a single pile driven into frozen soil we can assume the following simplified formula,

$$P_{lim} = \sum_{i=1}^n \tau_{lt(i)} F_i + f \sigma_{lim} \quad (77)$$

Substituting the value of  $\sigma_{lim}$  from (76) we get the formula which the author proposed for determining the maximum stress for piles hammered into frozen soil,

$$P_{lim} = u \sum_{i=1}^n \tau_{lt(i)} h_i + f(5.55 c_e + \gamma_s l), \quad (77a)$$

where  $P_{lim}$  is the limiting stress on a single pile;  
 $\tau_{lt}$  is the limiting long-term adfreeze strength of the soil with the lateral surface of the pile (taking into account the change of the temperature of the soil according to depth);  
 $h_i$  is the thickness of the layer of frozen soil under examination;  
 $\gamma_s$  is the unit weight of the soil;

- $F_i = u h_i$  is the area of adfreeze of the soil with the lateral surface of the pile (the area of the possible displacement of the soil) within the limits of  $i$ -th portion of the length of the pile under examination;  
 $c_e$  is the equivalent long-term cohesion of the frozen soil at the pile point (taking into account the temperature of the soil at this depth);  
 $u$  is the perimeter of the pile for which upheaval of the soil can occur  
 $f$  is the area of the cross-section of the pile;  
 $l$  is the overall depth of embedment of the pile.

If the value  $c_e$  is not known, then it is possible immediately to use formula (77), approximately taking  $\sigma_{lim} = 1.5 R$ , where  $R$  is determined from Table 37. The symbol  $\Sigma$  in formula (77) indicates the addition of values  $\tau_{lt}$ , which change according to the length of the pile in conjunction with the change of the temperature for the depth of the frozen stratum. With this it is also possible to allow for the heterogeneous strata of the soil. As the design temperature of the soil we should take not the highest absolute values, as is sometimes done, but the highest monthly-average value. Tentative values of the long-term adfreeze strength of sandy loam and argillaceous loam with wooden piles, taken from the data of the above-described tests of piles in field conditions, are quoted in Table 47. These values are included for design in the All-Union "Standards and Technical Specifications for Planning Ordinary Building Foundations in Permafrost Conditions" (N and TU 118-54).

It is necessary to make the following explanation of Table 47.

(1) The design values of the adfreeze strength are given by generalizations for silty sandy loam and argillaceous loam, since the great siltiness of the frozen test-soil, the presence of the ice coating, and other factors even out the differences in magnitude of  $\tau_{lt}$  for this soil. In cases when the soil is sharply distinguished from the soil tested, the values of  $\tau_{lt}$  can be somewhat different than those presented in the table. In particular, for coarser soils (sand, and light non-silty sandy loam) these values, evidently, will be 1.25 to 1.5 times greater than those in the table; but for clay and strongly organic soil, on the contrary, some decrease of  $\tau_{lt}$  is possible.

(2) The values of  $\tau_{lt}$  presented in Table 47 refer to the case of driving piles by hand in steamed holes whose diameter is greater than the diameter of the piles. In driving piles with a pile driver into steamed holes whose diameter is 0.6 to 0.9 of the diameter of the piles, the values of  $\tau_{lt}$  will be approximately 25% greater than those in the table. However, in view of the difficulty of controlling the radius of steaming the values of  $\tau_{lt}$  which have been presented can be extended also for the designated method of driving.

In the case of driving piles into drilled holes whose diameter is 0.6 to 0.9 of the diameter of the piles, the values of  $\tau_{lt}$  should be taken to be 1.3 to 1.5 times greater than those presented in the table.

(3) The values of  $\tau_{lt}$  at  $\theta = -0.2^\circ\text{C}$  to  $-0.3^\circ\text{C}$  are presented on the assumption of complete freezeback of the soil after steaming, e.g. by the cooling of the soil from the surface in winter time.

Table 47. Design values of long-term adfreeze strength of sandy loam and argillaceous silty loam with wooden piles driven with steaming\*

Temperature, °C	-0.2-0.3°	-0.5°	-0.7°	-1.0°	-2.0°	-3.0°
$\tau_{lt}$ , kg/cm <sup>2</sup>	0.3	0.6	0.8	1.0	1.6	2.0

The values of  $\tau_{lt}$  for  $\theta=0^\circ$  to  $-0.2^\circ$  with different methods of driving piles are presented in Table 43 or can be taken analogously for unfrozen soil of corresponding consistency; the last designation is correct even for low moisture-content and quick-frozen soils.

(4) With stresses not exceeding the tentative values of  $\tau_{lt}$ , the possibility of the occurrence of deformations of the visco-plastic flow is eliminated. In a number of cases, it is possible to tolerate these deformations, taking into account their extremely slow growth. Then the calculated stress can be taken as greater than the values of  $\tau_{lt}$  presented in the table; its magnitude should be determined proceeding from the permissible speed of deformation, or from the permissible settlement for an assigned period of time (for example, the useful life of the building) in conjunction with formula (74).

Let us now compare the values presented in Table 47 with data in the literature.

In "Technical Specifications Applying to Surveys, Planning, and Building of Railroads in Permafrost Areas" of 1941, the value of 1 kg/cm<sup>2</sup> was given for all cases, without differentiation, according to the temperature index.

Such an approach, which was caused by the absence of sufficient experimental data, is of course completely incorrect and is full of dangerous consequences. This is graphically proved by the results of the tests examined above (Figure 68). With  $\theta=-0.3^\circ$  to  $-0.4^\circ$  the piles under the specific stress  $\tau=1$  kg/cm<sup>2</sup> gave disastrous settlements which reached 50 cm in one month. On the other hand, for soil with a low temperature the value  $\tau=1$  kg/cm<sup>2</sup> is low; it corresponds to reality only in the particular case  $\theta=-1^\circ$ .

Precisely with this mean soil temperature and the designated magnitude of  $\tau_{lt}$ , the field tests of N. I. Bykov and P. N. Kapterev (1940) gave the values  $\tau=0.75$  kg/cm<sup>2</sup> at  $\theta=-0.6^\circ$  and  $\tau=1.1$  kg/cm<sup>2</sup> at  $\theta=-1^\circ$ . As is clear, our data (Table 47) agree well with these particular values. There is precisely the same agreement with the data of other authors (Tsytoich, 1952), whose determination of the resistance of adfreezing, taking into account the phenomenon of viscosity, equals 0.6 kg/cm<sup>2</sup> at  $\theta=-0.5^\circ$  and 1.5 kg/cm<sup>2</sup> at  $\theta=-1.5^\circ$ . Thereby the reality of our tentative design values of  $\tau_{lt}$  is confirmed. But we should keep in

\* The dependence of  $\tau_{lt}$  on  $\theta$ , which is presented in Table 47, is described by the equation  $\tau_{lt} = \sqrt{1.65\theta} - 0.3$ .

mind that these values were found for particular soils and should be verified for other regions with a warning as to the necessity for corresponding refinements of accuracy.

The values of the adfreeze strength presented in Table 47 refer to silty sandy loam and argillaceous loam, in which the moisture content of the mineral layers is 25 to 30%. The presence of ice inclusions in the soil in driving the piles with steaming does not have any particular effect on the adfreeze strength, since the final moisture content of the steamed, and then refrozen, soil around the pile does not, in effect, depend on the total moisture content of the frozen stratum.

The case is somewhat different in driving the piles into drilled holes (and into steamed holes of smaller diameter), if ice layers are included in the frozen stratum; they will immediately freeze on to the surface of the pile, thereby lowering its bearing capacity, since the adfreeze strength of ice sharply differs from that of soil. In this case on the basis of the data concerning the differentiated moisture-ice-content which are easily determined in field conditions (A. N. Pchelintsev, 1954), we should calculate the general thickness of the mineral layers of the soil and the ice inclusions, and assuming for them the listed values of  $\tau_{1t}$ , we should substitute the latter into formula (77). Thus, if the total moisture content of the whole frozen stratum  $w_c$  and the moisture content of the mineral layers  $w_{mn}$  are known, then the general content of the ice inclusions of this stratum (by percentage of the dry weight) will be

$$w_{incl} = w_c - w_{mn} = \frac{\sum_1^n w_{c(i)} h_i - \sum_1^n w_{mn(i)} h_i}{\sum_1^n h_i},$$

where  $h_i$  is the thickness of the layers of the soil for which the differentiated moisture content was determined, and  $w_i$  is the values of the differentiated moisture content (by percentage of the dry weight) in these layers:

$$\sum_1^n h_i = H_M$$

corresponds to the depth of driving of the pile into permafrost. Expressing  $w_{incl}$  in percentage of the volume of the frozen soil, it is possible to determine easily the total thickness of the ice inclusions\* (in cm),

$$h_{incl} = 0.01 \frac{100 \Delta w_{incl}}{90 + \Delta w} H_M,$$

where  $\Delta$  is the unit weight of the frozen soil.

In its turn, the general thickness of the mineral layers of the soil is

$$h_{mn} = H_M - h_{incl}.$$

\* We disregard the effect of the non-frozen water on the unit weight of the soil, since the error from this approximation does not exceed 2%.

# 200 RHEOLOGICAL PROPERTIES AND BEARING CAPACITY OF FROZEN SOILS

Hence, the limiting stress on the pile driven (by a pile driver) into frozen soil having ice inclusions is determined by the formula,

$$P_{lim} = u \sum_{i=1}^n (h_{mn} \tau_{mn} + h_{incl} \tau_{ice}) + f \sigma_{lim} \quad (78)$$

where  $\tau_{mn}$  and  $\tau_{ice}$  are the long-term adfreeze strengths of the mineral layers of the soil and ice with the pile at the given temperature.

The rest of the symbols are the same as in formula (77).

The size of  $c_e$ , which can be determined from testing by the spherical indenter, enters into formulas (77a) and (78). This size depends essentially on the fact that such soil, i.e. of undisturbed texture or disturbed by steaming, is located under the point of the pile. In the first case, corresponding to driving the piles with a pile driver,  $c_e$  will be considerably higher than in the second case, which corresponds to driving the piles by hand with steaming. What we have said is confirmed by the data presented in Table 25 and also by the results of determining  $c_e$  for undisturbed frozen soil, and for steamed and refrozen soil (Table 48).

Table 48. Limiting long-term adhesion of undisturbed frozen soil and soil disturbed by steaming

Soil	Experiment no.	Temperature °C	Moisture content of the soil, %		$c_e$ ; kg/cm <sup>2</sup>	
			undis- turbed	steamed	undis- turbed	steamed
Light, silty argillaceous loam	29 (lab.)	-0.3	29	29	1.0	0.55
Heavy, silty, slightly peaty sandy loam	Pile no. 1 (field)	-0.3	29	28	0.9	0.5

It is interesting that the cohesion  $c_e$  of the frozen soil corresponds approximately (but still is somewhat greater) to the adfreeze strength,  $\tau_{lt}$ . In this case,  $c_e$  for disturbed soil is close to the values of  $\tau_{lt}$  for the case of driven piles with steaming. The values of the equivalent long-term adfreeze strength for undisturbed frozen soil are presented in Table 6. The adhesion of disturbed frozen soil will be 1.5 to 2 times smaller. Compact soil of the type of Igarska varved clay, in which the value of  $c_e$  by remolding can be decreased 2.5 to 3 times, is an exception.



Formulas (77) and (78) determine the size of the limiting stress on the pile. But for determining the design stress  $N$ , it is necessary to introduce the appropriate safety factor,

$$N = P_{lim} k.$$

Taking into account the fact that the break at the limiting state of the frozen soil with  $N$  somewhat exceeding  $P_{lim}$  leads to the appearance of only slowly developing visco-plastic deformations, it is possible to take  $k$  as not less than 0.7 to 0.8.

As usual, the calculated stress on the pile should also be verified for the strength of the pile material:  $N \leq f R_{cp}$ , where  $R_{cp}$  is the estimated strength of the pile point, and  $f$  is the area of its cross section.

As far as the design of the pile foundation for limiting deformations is concerned, with stress on a single pile not exceeding  $P_{lim}$ , the necessity of such a calculation for the frozen soil recedes. Only the driving of piles into plastic frozen soil with a temperature around 0°C (section 5, Chapter VIII) constitutes an exception, e.g. as in the design of ordinary foundations. Finally, calculation for the deformations is necessary in a case in which the calculated stress will exceed  $P_{lim}$ . As we have already said above, in this case there will arise a visco-plastic flow whose permissible speed of growth will determine the design value  $N$ .

#### 5. Heave forces

As is well known, foundations built on permafrost should be designed for their resistance to heave forces arising in the seasonal freezing of the active layer. For this the condition,

$$\frac{N + Q + T}{k} \geq S, \quad (79)$$

should be satisfied, where  $S$  is the heave force,  $N$  is the constant (calculated) load on the foundation,  $Q$  is its own weight,  $T$  is the forces of adfreezing of the soil with the foundation (within the limits of embedment in the permafrost stratum) opposing the heave, and  $k$  is the safety factor (for the working conditions) taken as equal to 1.1 to 1.2.

The value  $T$  is determined from the expression,

$$T = u \sum_i^h \tau_{lt(i)} h(i), \quad (80)$$

where  $u$  is the perimeter of the base of the foundation,  $h$  is the depth of foundation below the boundary of the seasonal layer, and  $\tau_{lt}$  is the long-term adfreeze strength (Table 47) taking into account the temperature of the soil according to depth.

A special article (S. S. Vialov and N. I. Yegorov, 1958) is devoted to the problem of determining the forces of heaving  $S$  in field conditions; in the article, the arrangement for observations of the heaving is



described and some results of studies carried out by S. S. Vialov, S. G. Tsvetkova, and N. I. Yegorov in 1950-1953 in Igarka are quoted.\*

In principle, the arrangement consists of the following: two secure anchor supports made from pipes with welded cleats are placed in the stratum of permafrost (in the conditions of Igarka for a depth of 12 to 15 m). A horizontal metal beam is fastened to the upper ends of the supports with a span of about 3 m; the foundation to be tested (the support), which has been sunk through the active layer of the soil to the level of the upper surface of the permafrost, touches the beam.

The horizontal beam prevents the heaving of the foundation and absorbs the heaving forces which are developing along the lateral surface. The total value of these forces can be determined from the deflection of the horizontal beam (the idea for such an arrangement belongs to V. F. Zhukov), or immediately by a spring dynamometer placed on one of the anchor supports.

The designated arrangements, which are distinguished by simplicity of construction and facility of observation, permit us to study the dynamics of the forces of heaving and to determine their value at any moment of the process of heaving. For completeness of the study of this process, it is expedient to conduct simultaneous observations of the size of heave according to the depth of the soil, the temperature (of air and soil), the depth of freezing, etc.

The equipment was placed in section no. 1a (described in Chapter X), whose active layer of soil was a silty sandy loam and argillaceous loam with a mean moisture content of 40%; the depth of the summer thaw was 1.5 m. Some of the results of the observations conducted at one of the installations are presented in Table 49.

As a result of the analysis of the experimental data the following conclusions were made:

(1) The process of the growth of the heave forces follows basically the process of freezing of the soil; however, there occur certain deviations. The onset of heave comes somewhat after the beginning of freezing: it occurs when the soil has frozen to 8 to 10 cm. Then, in proportion to the increase of the depth of freezing and the drop of the temperature the heave forces grow intermittently.

Heaving stops before the whole active layer freezes (if the boundary of freezing fuses with the upper boundary of the permafrost soil). This is explained by the fact that as a result of the travel of moisture to the freezing front, the lower levels of the active layer are dehydrated, and the transfer of water from these layers stops even before the process of freezing is concluded.

If the boundary of the freezing layer does not fuse with the upper boundary of the permafrost soil ("non-fusion freezing"), then the process of heave ends with the conclusion of the freezing, since in this case inflow of water from low-lying thawed layers is assured.

---

\* In subsequent years these studies were continued by V. O. Orlov.

Formulas (77) and (78) determine the size of the limiting stress on the pile. But for determining the design stress  $N$ , it is necessary to introduce the appropriate safety factor,

$$N = P_{lim} k.$$

Taking into account the fact that the break at the limiting state of the frozen soil with  $N$  somewhat exceeding  $P_{lim}$  leads to the appearance of only slowly developing visco-plastic deformations, it is possible to take  $k$  as not less than 0.7 to 0.8.

As usual, the calculated stress on the pile should also be verified for the strength of the pile material:  $N \leq f R_{cr}$ , where  $R_{cr}$  is the estimated strength of the pile point, and  $f$  is the area of its cross section.

As far as the design of the pile foundation for limiting deformations is concerned, with stress on a single pile not exceeding  $P_{lim}$ , the necessity of such a calculation for the frozen soil recedes. Only the driving of piles into plastic frozen soil with a temperature around 0°C (section 5, Chapter VIII) constitutes an exception, e.g. as in the design of ordinary foundations. Finally, calculation for the deformations is necessary in a case in which the calculated stress will exceed  $P_{lim}$ . As we have already said above, in this case there will arise a visco-plastic flow whose permissible speed of growth will determine the design value  $N$ .

#### 5. Heave forces

As is well known, foundations built on permafrost should be designed for their resistance to heave forces arising in the seasonal freezing of the active layer. For this the condition,

$$\frac{N + Q + T}{k} \geq S, \quad (79)$$

should be satisfied, where  $S$  is the heave force,  $N$  is the constant (calculated) load on the foundation,  $Q$  is its own weight,  $T$  is the forces of adfreezing of the soil with the foundation (within the limits of embedment in the permafrost stratum) opposing the heave, and  $k$  is the safety factor (for the working conditions) taken as equal to 1.1 to 1.2.

The value  $T$  is determined from the expression,

$$T = u \sum_i^h \tau_{lt(i)} h(i), \quad (80)$$

where  $u$  is the perimeter of the base of the foundation,  $h$  is the depth of foundation below the boundary of the seasonal layer, and  $\tau_{lt}$  is the long-term adfreeze strength (Table 47) taking into account the temperature of the soil according to depth.

A special article (S. S. Vialov and N. I. Yegorov, 1958) is devoted to the problem of determining the forces of heaving  $S$  in field conditions; in the article, the arrangement for observations of the heaving is

described and some results of studies carried out by S. S. Vialov, S. G. Tsvetkova, and N. I. Yegorov in 1950-1953 in Igarka are quoted.\*

In principle, the arrangement consists of the following: two secure anchor supports made from pipes with welded cleats are placed in the stratum of permafrost (in the conditions of Igarka for a depth of 12 to 15 m). A horizontal metal beam is fastened to the upper ends of the supports with a span of about 3 m; the foundation to be tested (the support), which has been sunk through the active layer of the soil to the level of the upper surface of the permafrost, touches the beam.

The horizontal beam prevents the heaving of the foundation and absorbs the heaving forces which are developing along the lateral surface. The total value of these forces can be determined from the deflection of the horizontal beam (the idea for such an arrangement belongs to V. F. Zhukov), or immediately by a spring dynamometer placed on one of the anchor supports.

The designated arrangements, which are distinguished by simplicity of construction and facility of observation, permit us to study the dynamics of the forces of heaving and to determine their value at any moment of the process of heaving. For completeness of the study of this process, it is expedient to conduct simultaneous observations of the size of heave according to the depth of the soil, the temperature (of air and soil), the depth of freezing, etc.

The equipment was placed in section no. 1a (described in Chapter X), whose active layer of soil was a silty sandy loam and argillaceous loam with a mean moisture content of 40%; the depth of the summer thaw was 1.5 m. Some of the results of the observations conducted at one of the installations are presented in Table 49.

As a result of the analysis of the experimental data the following conclusions were made:

(1) The process of the growth of the heave forces follows basically the process of freezing of the soil; however, there occur certain deviations. The onset of heave comes somewhat after the beginning of freezing: it occurs when the soil has frozen to 8 to 10 cm. Then, in proportion to the increase of the depth of freezing and the drop of the temperature the heave forces grow intermittently.

Heaving stops before the whole active layer freezes (if the boundary of freezing fuses with the upper boundary of the permafrost soil). This is explained by the fact that as a result of the travel of moisture to the freezing front, the lower levels of the active layer are dehydrated, and the transfer of water from these layers stops even before the process of freezing is concluded.

If the boundary of the freezing layer does not fuse with the upper boundary of the permafrost soil ("non-fusion freezing"), then the process of heave ends with the conclusion of the freezing, since in this case inflow of water from low-lying thawed layers is assured.

---

\* In subsequent years these studies were continued by V. O. Orlov.

Table 49. Observed data on heave of the soil in Igarka in 1952

Items	Unit of Measurement	Dates of the observations								
		10/1	10/8	10/15	10/22	10/29	11/5	11/12	11/19	11/26
Depth of freezing	m	0.05	0.11	0.22	0.42	0.56	0.75	1.00	1.25	1.50
Speed of freezing	m/day	--	0.01	0.02	0.03	0.02	0.03	0.04	0.04	0.04
Size of heave of the surface	mm	--	20.0	56.0	94.0	112.0	125.0	132.0	131.0	129.0
Speed of heaving of the surface	mm/day	--	3.0	5.0	5.5	2.0	1.0	--	--	--
Forces of heaving $\tau_{heav}$ (per unit of the perimeter of the foundation)	kg/cm <sup>2</sup>	--	8.0	27.0	26.0	27.0	54.5	66.0	55.0	46.5
Rate of growth of the forces of heaving	kg/cm <sup>2</sup> days	--	1.1	2.7	0	0	4.0	1.6	--	--
Unit forces of heaving $\tau_{heav}$ (per unit of area of the lateral surface of the foundation).	kg/cm <sup>2</sup>	--	0.78	1.24	0.62	0.49	0.73	0.66	0.44	0.31

(2) In conjunction with what we have said and as others have observed, in the process of the heaving of the soil whose boundary of freezing fuses with the upper boundary of the permafrost stratum the whole active zone does not take part, but only the "effective" part. According to the data of our experiments, the depth of this zone is  $h_{act} \approx 2/3 h_{fdf}$ , where  $h_{fdf}$  is the full depth of freezing.

(3) In the process of heaving, a folding of the layers of the frozen soil around the foundation occurs, as well as the sliding of this soil along the foundation, observed by V. I. Dalmatov (1954). The folding is observed in the beginning of the process, but later on, in proportion to the growth of the heave forces, there occurs a break of the soil from the foundation and the frozen soil is shifted above, sliding along the lateral surface of the foundation. The heave forces

which develop in this folding correspond, according to B. I. Dalmatov (1954), to the so-called steady adfreeze strength  $\tau_{\text{heave}} = \tau_{\text{steady}}$ , i.e. to the prolonged resistance to displacement of the soil which constantly slides along the shaft (foundation).

(4) As is obvious, the calculated value of the total heave force is determined by the expression  $S = \tau_{\text{heave}} h_{\text{act}} u$ , or  $S = \tau_{\text{heave}} u$ , where  $u$  is the perimeter of the foundation,  $h_{\text{act}}$  is the depth of the active layer,  $\tau_{\text{heave}}$  is the specific heave force in  $\text{kg/cm}^2$ , and  $\tau_{\text{heave}} h_{\text{act}}$  is the heave force per unit of perimeter of the foundation, as recommended by N and TU 118-54. Let us observe that the last method of the expression of the heave forces is not very successful, since the size of  $h_{\text{act}}$  enters here not in a clear but in a concealed form, and the change of the temperature of the soil according to the depth is not taken into account at all. The use of the parameter  $\tau_{\text{heave}}$  can be permitted only as a temporary measure, taking into account the present absence of adequate data.

As follows from Table 49, the specific forces of  $\tau_{\text{heave}}$  attain their maximum value in the beginning of the process. However, the total heave force at this moment is not yet the greatest, and therefore we should introduce into the calculation not maximum  $\tau_{\text{heave}}$ , but a value of  $\tau_{\text{heave}}$  such that the product of  $\tau_{\text{heave}}$  and  $h_{\text{act}}$ , subsequently the total force  $S$  will be a maximum. This value corresponds to the moment at the end of heaving, but not to the conclusion of freezing. At this moment  $\tau_{\text{heave}}$  also attains a maximum.

In the experiment that is being examined (Table 49),  $\max \tau_{\text{heave}} = 1.24 \text{ kg/cm}^2$  (with  $h_{\text{fdf}} = 0.22 \text{ m}$ );  $\max S$  will be with  $\tau_{\text{heave}} = 0.66 \text{ kg/cm}^2$  and  $h_{\text{act}} = h_{\text{fdf}} = 1 \text{ m}$ , to which  $\max \tau_{\text{heave}} = 66 \text{ kg/cm}^2$  corresponds.

(5) The greatest values of the heave forces observed in our experiments in the conditions of Igarka are  $\tau_{\text{heave}} = 105 \text{ kg/cm}^2$  (with "fused freezing"). This corresponds approximately to the values recommended by N and TU 118-54. As far as the heave forces in the condition of deep freezing ("non-fused freezing") are concerned, their value in individual cases (with the possibility of the inflow of water from below) went up to  $300 \text{ kg/cm}^2$  and, as the further observations of V. O. Orlov in Igarka showed, even up to  $400 \text{ kg/cm}^2$ .

## CONCLUSION

The rheological properties of frozen soil caused by the presence of ice and non-frozen water are very important factors, without consideration of which calculations of the stability and steadiness of frozen soil are not possible. In the present work certain principles of rheology and the stability of frozen soil were examined, and proceeding from these principles an evaluation of the bearing capacity of natural [footings] and artificial (pile) foundations was made.

The results of the investigations reduce fundamentally to the following:

(1) On the basis of experimental data we advance an hypothesis concerning the physical essence of rheological processes (creep, lowering of strength) in frozen soil, agreeing well with the principle of the dynamic equilibrium of the solid and liquid states of water contained in this soil. According to this hypothesis, rheological processes in frozen soil are caused by two mutually-opposed phenomena: on one hand by the weakening of inner bonds caused by the flow of ice, and also by the liquefying, squeezing, and shift of the solid portions, and on the other hand by the reduction of broken bonds and their consolidation. The predominance of one of these phenomena over another causes the cessation, or continuous character, of deformation.

(2) We establish the conditions of the stability of frozen soil characterizing the rise of the visco-plastic flow and the transition of this flow into the stage of rupture. It is shown that the limit of viscosity is a variable magnitude, and the long-term strength is a basic characteristic.

In our work the dependence of this limit on different factors was studied and quantitative values of it are given.

(3) Peculiarities of rheological processes in frozen soil are demonstrated, and it is shown that the laws of the classical theory of rheology are inapplicable here.

(4) Laws are proposed which characterize rheological processes in frozen soil and establish a relation between the stress and the deformation (taking time into account), between the stress and the rate of the visco-plastic flow, between the deformation and the time, and between the size of the rupture stress and its time of action. Also presented is the condition of the limiting stress state of frozen soil taking into account its relaxation properties.

(5) It is established that failure at the limiting equilibrium (stability) of frozen soil under foundations occurs as a result of the parting of the frozen stratum under the footing by the compacted wedge [kernel] and of the rise of the visco-plastic flow.

206 RHEOLOGICAL PROPERTIES AND BEARING CAPACITY OF FROZEN SOILS

The presence of ice layers in frozen soil somewhat lowers its bearing capacity, but in certain conditions this soil gives an adequate foundation.

It is shown that plastic frozen soil with a temperature that is high and close to 0C possesses a comparatively high compressibility which should be taken into account in calculations.

(6) The maximum stress on frozen soil can be determined according to formulas of the theory of plasticity, but with consideration of the relaxation properties. According to a joint proposal with N. A. Tsytoich, the concept of the complex character of the adhesion is introduced, and the formula for determining the maximum stress is given. For evaluation the bearing capacity of frozen soil in field conditions we propose a method of testing by the penetration of a ball-indenter which is a development of the Brinell hardness test.

(7) From field and laboratory data we have derived new values-increased in comparison with the standards-of the calculated resistances (permissible pressures) of frozen soils for foundations.

(8) The operation of piles driven into frozen soils by different methods, and their resistance to long-acting loads are investigated. Also presented is the nature of the bonds causing this resistance and the dependence of the bearing capacity of the piles on the methods of emplacement, on the type of soil, its temperature, moisture content, etc.

(9) A design formula for determining the limiting stress on piles in frozen soils is proposed, and, based on field experiments, design values of the long-term adfreeze strength of soils with piles are derived.



## LITERATURE

- Arutyunyan, N. X. Some problems in the theory of creep (Nekotorye voprosy teorii polzuchesti). Moscow, State Technical Printing House, 1952.
- Bakulin, F. G. and Zhukov, V. F. Deformations of frozen dispersed soils on thawing (Deformatsii myorzlykh dispersnykh gruntov pri ottaivanii), "Izvestia AN SSSR, OTN", 1955, No. 7.
- Barnes, L. Permafrost. A challenge to engineers. "The Milit. Engineer", 1946, No. 243.
- Belokrylov, I. D. The forces of adfreezing of concrete and wood with different soils taking into account the plastic deformations of the latter. Candidate's Dissertation (Sily smerzaniy betona i dereva s razlichnymi gruntami s uchyotom plasticheskikh deformatsiy poslednykh). V. I. Lenin State Library, 1944.
- Berezantsev, V. G. On the stability of frozen soil under building foundations (O prochnosti myorzlykh gruntov pod fundamentami sooruzheniy). "Frozen State Research", 1947, Vol. II, extract I.
- Berezantsev, V. G. Some problems of the theory of limiting resistance of soil to stresses (Nekotorye zadachi teorii predel'nogo soprotivleniya gruntov nagruzkam). Doctoral Dissertation. AN SSSR Permafrost Research Institute, 1949.
- Berezantsev, V. G. The resistance of soil to local stress with a constant negative temperature (Soprotivlenie gruntov mestnoy nagruzke pri postoyannoy otritsatel'noy temperature). Materials from laboratory studies of frozen soil. Collection 1. Published in AN SSSR, 1953.
- Berezantsev, V. G. The limiting equilibrium of a cohesive medium under spherical and conical indenters (Predel'noe ravновesie svyaznoy sredy pod sfericheskimi i konicheskimi shtampami). "Izvestia AN SSSR, OTN", 1955, No. 7.
- Bingham, E. C. Fluidity and plasticity, N. Y., 1932.
- Black, R. Permafrost. "Rev. Bull. Geol. Soc. America", 1954, V. 65, No. 9.
- Bronskiy, A. P. The phenomenon of reaction in a solid body (Yavlenie posledeystviya v tvyordom tele). "Occurrences in Mathematics and Mechanics", 1941, Vol. 5, extract 1.
- Buisman, A. S. K. Results of long duration settlement tests. Proc. [1st] Intern. Confer. on soil Mech., 1936, V. I.

- Bykov, N. I. and Kapterev, P. N. Permafrost and building on it (Vechnaya merzlota i stroitel'stvo na ney). Moscow Transzheldorizdat, 1940.
- Bykovskiy, V. N. The change of strength of real materials under the prolonged effect of stress (Izmenenie prochnosti real'nykh materialov pri dlitel'nom vozhdeystvii nagruzki). "Journal of Technical Physics", 1951, Vol. 20, extract 21.
- Carlson, H. Stability of foundations on permanently frozen ground, Amsterdam, 1948.
- Chekotillo, A. M. Permafrost research up to 1955 (Zarubezhnoe merzlotovedenie k 1955 g.). Materials for the study of frozen soil of the earth's crust. extract 3, Moscow, Published in AN SSSR, 1956.
- Cherkasov, I. I. 1. On the connection of the Poisson ratio with the plastic properties of a substance (O svyazi koeffitsienta Puassona s plasticheskimi svoystvami materiala). "Journal of Technical Physics", 1952, Vol. 22, extract 11.
- Cherkasov, I. I. 2. The effect of the method of installing a punch on the results of the test of the soil with a test stress (Vliyanie, metoda ustanovki shtampa na rezul'taty ispytaniya gruntov probnoy itgruzkay). "Report of AN SSSR", 1952, Vol 82, No. 3.
- Cherkasov, I. I. Mechanical properties of soil foundations under the deformation of punching in (Mekhanicheskie svoystva gruntovykh osnovaniy pri deformatsii vdavlivaniya). In the collection "Determination of the Coefficient of Deformation of Soil". Moscow, Avtotranzizdat, 1955.
- Chernyshov, M. Ya. Deformation of wooden bridges from heave of frozen soil (Deformatsiya derevyannykh mostov ot puchin merzlogo grunta). "Railroad Business", 1928, No. 1 - 2.
- Dalmatov, B. I. On determining a safe pressure on the soil (Ob opredelenii dopuskaemogo davleniya na grunt). "Works of the Leningrad Engineering and Construction Institute," 1951.
- Dalmatov, B. I. Study of the tangential forces acting on building foundations in heaving (Issledovanie kasatel'nykh sil, deystvuyushchikh na fundamenty sooruzheniya pri puchinii). Doctoral Dissertation. Leningrad Engineering and Construction Institute, 1955.
- Denisov, N. Ya. On the nature of the deformations of clay soil (O prirode deformatsiy glinistyykh gruntov). Moscow, Rechizdat, 1951.
- Denisov, N. Ya. The construction properties of clay strata and their use in hydraulic construction (Stroitel'nye svoystva glinistyykh porod i ikh ispol'zovanie v gidrotekhnicheskoy stroitel'stve). Moscow, Energoizdat, 1956.

- Dergunov, I. D. Study of heave forces (Izuchenie sil vypuchivaniya). "Technology of Railroads", 1945, No. 1 - 2.
- Dochenko, P. V., Shulman, A. R. First stages of the deformation of ice (Nachal'nye stadii deformatsii l'da). "Works of the State Hydraulic Institute". Leningrad Gidrometeoizdat, 1949, extract 16 (70).
- Dogadkin, B. A. and Reznikovskiy, M. M. Relaxation processes in deformation (Relaksatsionnye protsessy pri deformirovani). "Colloid Journal", Vol. 13, extract, 1951.
- Egerev, K. E. The electrical method of determining the tangential reactions distributed along the lateral surface of piles frozen into the soil (Elektricheskiy metod opredeleniya tangentsial'nykh reaktsiy, raspredelennykh po bokovoy poverkhnosti vmorozhennykh v grunt svay). "Works of the AN SSSR Frozen State Research Institute", 1958, Vol. 14.
- Eyring, H. Viscosity plasticity and diffusion as examples of absolute reaction rates. "J. Chem. Phys.", 1936, Vol. 4, No. 4.
- Fedosov, A. E. Physical and mechanical processes in soil during its freezing and thawing (Fiziko-mekhanicheskie protsessy v gruntakh pri ikh samerznanii i ottaivanii). Moscow, Transzheldorizdat, 1935.
- Florin, U. A. Calculations of the foundations of hydraulic structures (Raschety osnovaniy gidrotekhnicheskikh sooruzheniy). Moscow, stroyizdat, 1948.
- Freezing phenomena in soils (Merzlotnye yavleniya v gruntakh). Collection of articles. Translation from English. Moscow, Foreign Literature Publication, 1955.
- Frenkel, Ya. I. The kinetic theory of fluids (Kineticheskaya teoriya zhidkosti). Moscow, Published in AN SSSR, 1951.
- Genki, G. On the theory of plastic deformations and the residual deformations caused by them in the material. On slow stationary flows in plastic bodies. The theory of plasticity. (K teorii plasticheskikh deformatsiy i vyzyvaemykh imi v materiale ostatochnykh deformatsiy. O medlennykh statsionarnykh techeniyakh v plasticheskikh telakh. Teoriya plastichnosti.) Moscow, Foreign Literature Publication, 1948.
- Gerasevanov, N. M. and Pol'shin, D. E. Theoretical principles of soil mechanics and their practical applications (Teoreticheskie osnovy mekhaniki gruntov i ikh prakticheskie primeneniya). Moscow, Stroyizdat, 1948.
- E. C. W. A. Geuse a. Tan Tjong-Kie. The mechanical behavior of clays. "Proc. second intern. Congress Rheology", London, 1954.
- Glen, J. W. Experiments on the deformation of ice. "J. Glaciology", 1952, Vol. 2, No. 12.

- Glen, J. W. The creep of polycrystalline ice. "Proc. Roy. Soc.", 1955, A. 288, No. 1175.
- Gogoladze, V. G. Some problems in the hereditary theory of elasticity. (Nekotorye zadachi nasledstvennoy teorii uprugosti). "Works of the AN SSSR Seismographic Institute". Moscow, Published in AN SSSR, 1939, No. 87.
- Goldenblat, I. I. Introduction to the theory of creep of building materials (Vvedenie v teoriyu polzuchesti stroitel'nykh materialov). Moscow, State Literature on Construction and Architecture, 1952.
- Goldstein, M. N. On calculating heave forces (O raschete sil vypuchivaniya). "Construction of Railroads and Road Economy", 1941, No. 5 - 6.
- Goldstein, M. N. Deformations of the soil roadbed and building foundations in freezing and thawing (Deformatsii zemlyanogo polotna i osnovaniy sooruzheniy pri promerzanii i ottaivanii). "Works of the All-Union Scientific Research Institute Journal of Transport", 1948, extract 16.
- Goldstein, M. N. and Ter-Stepanyan, N. I. The long-term strength of clay and the sub-surface creeping of slopes (Dlitel'naya prochnost' glin i glubinnaya polzuchest' sklonov). In the book "Materials of the IV International Conference on Soil Engineering and Foundation Engineering". Moscow, Published in AN SSSR, 1957.
- Gorbunov-Posadov, M. I. Plastic deformations in soil under a rigid foundation (Plasticheskie deformatsii v grunte pod zhestkim fundamentom). In the collection of works of the NII of Foundations "Physics and Soil Mechanics", No. 13, Moscow, Mashstroyizdat, 1949.
- Graham, A. The phenomenological method in rheology. "Research", 1953, Vol. 6, No. 23.
- Haefili, R. Kriechprobleme in Boden, Schnee und Eis. "Wasser u. Energiewirtschaft", 1954, Bd. 46, No. 3.
- Hardy, R. and D'Appolonia, E. Permanently frozen ground and foundation design. "Eng. J.", 1946, Vol. 29, No. 1.
- Hemstock, R. Engineering in permafrost in Canada's Mackenzie Valley. "Nat. Res. Council Canada", 1949, No. 13.
- Hohenemser, K. and Prager, W. Fundamental equations and definitions concerning the mechanics of isotropic continua. "J. Rheol.", 1932, No. 3.
- Il'yushin, A. A. The deformation of a visco-plastic substance (Deformatsiya vyazko-plasticheskogo tela). "Study of Moscow State University", 1940, extract 39.
- Il'yushin, A. A. Plasticity (Plastichnost') Moscow-Leningrad, State Technical Printing House, 1948.

- Ishlinskiy, A. Yu. Equations of the deformation of sub-elastic and visco-plastic substances (Uravnenie deformirovaniy ne vpolne uprogikh i vyazko-plastichnykh tel). "Izvestia AN SSSR, OTN, 1945, No. 1 - 2.
- Ishlinskiy, A. Yu. The Axio-symmetrical problem of the theory of plasticity and the Brinell test (Osesimmetrichnaya zadacha teorii plastichnosti i proba Brinellya). "Occurrences in Mathematics and Mechanics", 1944, Vol. VIII, No. 3.
- Ivanov, K. E., Lavrov, V. V. On one peculiarity of the mechanism of the plastic deformation of ice (Ob odnoy oboennosti mekhanizma plasticheskoy deformatsii l'da). "Journal of Technical Physics", 1950, Vol. 20, extract 2.
- Ivanov, Yu. M. The limit of the plastic flow of wood (Predel plasticheskogo techeniya drevesiny). Moscow, Stroyizdat, 1948.
- Jeffreys, H. and Gutenberg, B. Physics of the earth, Vol. 7, Internal Constitution of the Earth. N. Y., 1939.
- Kachanov, L. M. The mechanics of plastic media (Mekhanika plasticheskikh sred). Moscow-Leningrad, State Technical Printing House, 1948.
- Kachanov, L. M. Theory of creep (Teoriya polzuchesti). Moscow-Leningrad, State Technical Printing House, 1949.
- Kartashkin, B. D. Experimental studies of the physical and mechanical properties of ice (Eksperimental'nye issledovaniya fiziko-mekhanicheskikh svoystv l'da). "Works of TsAGI", 1947, No. 607.
- Khanina, S. K. and Shulman, A. Ya. Study of the flow of natural glaciers (Izuchenie techeniya estestvennykh l'dov). "Works of the State Hydraulic Institute", extract 16 (70). Leningrad, Aidrometeoizdat, 1949.
- Laboratory studies of the mechanical properties of frozen soil (Laboratornye issledovaniya mekhanicheskikh svoystv merzlykh gruntov). "Works of KOVM, AN SSSR", collections I and II. Moscow, Published in AN SSSR, 1936.
- Laletin, N. V. Problems in the calculation of non-linear deformations of natural foundations (Voprosy rascheta nelineynoy deformatsii estestvennykh osnovaniy). "Proceedings of the V. V. Kuybyshev Military Engineering Academy", 1954, No. 78.
- Lavrov, V. V. The viscosity of ice as it depends on temperature (Vyazkost' l'da v zavisimosti ot temperatury). "Journal of Technical Physics", 1947, Vol. 17, extract 9.
- Legget, R. Special foundation problems in Canada. Build Resc. Congress. Collected papers (Divis. I) 1951.
- Likhtman, V. I. On the laws of creep of metals (O zakononomernostykh polzuchesti metallov). "Report of the AN SSSR", 1950, Vol. 72, No. 6.

- Lipovetskaya, T. F. Experimental studies of the distribution of stresses on the base of rigid foundations placed on a sand base (Eksperimentl'nye issledovaniya raspredeleniya napryazheniy po podoshve zhestkikh fundamentov, raspolozhennykh na peschanom osnovanii). "Journal of the All-Union Hydraulic Scientific Research Institute", 1953, No. 49.
- Liverovskiy, A. V. and Morozov, K. D. Construction in permafrost conditions (Stroyitel'stvo v usloviyakh vechnoy merzloty). Moscow, Stroyizdat, 1941.
- Lukin, G. O. Tests on the operation of pile foundations with the steaming of frozen soil in Yakutsk (Opyty ustroystva svaynykh fundamentov s preparivaniem merzlogo grunta v g. Yakutske). In the book "Study of Permafrost in the Yakutsk Republic", extract 3. Moscow, Published in AN SSSR, 1952.
- Malinin, N. N. Principles of calculations for creep (Osnovy raschetov na polzuchest'). State Technical Printing House, 1948.
- Maslov, N. N. Conditions of the stability of slopes in hydraulic construction (Usloviya ustoychivosti sklonov i otkosov v gidroenergeticheskom stroitel'stve). Moscow-Leningrad, Gosenergoizdat, 1955.
- McKinley, D. Anchored foundation resists frost heave. "Civ. Eng.", 1952, Vol. 22, No. 2.
- Meister, I. A. and Mel'nikov, P. I. Determination of the forces of adfreezing of soil with wood and concrete and of the resistance of frozen soil to heave in field conditions (Opredelenie sil smerzaniya grunta s derevom i betonom i soprotivleniya sdvigu merzlykh gruntov v polevykh usloviyakh). "Works of the KOVM AN SSSR", Moscow, Published in AN SSSR, 1940, Vol. 10.
- Mewes, E. Untersuchungen von feiesseigenschaften mit einfachen mechanischen modellen. "Kolloid, A.", 1953, Vol. 131, No. 2.
- Mikhailov, N. V. On the viscosity and stability of structured fluids (O tekuchest'i i prochnosti strukturirovannykh zhidkostey). "Colloid Journal", 1955, Vol. XVII, extract 1.
- Mikhailov, N. V. and Likhtgeim, A. M. Study of the full rheological curves and of the formula for calculating the effective viscosity of structured fluids with molecular and kinetic interpretation of the terms entering into it (Issledovanie polnykh reologicheskikh krivyykh i formuly dlya rascheta effektivnoy vyazkosti strukturirovannykh zhidkostey s molekulyarno-kineticheskoy interpretatsiyey vkhodyashchikh v nikh chlenov). "Colloid Journal", 1955, Vol. XVII, extract 5.
- Mikhailov, N. V. and Rebinder, P. A. On the structural and mechanical properties of dispersed and high-molecular systems (O strukturno-mechanicheskikh svoystvakh dispersnykh i vysokomolekulyarnykh sistem). "Colloid Journal", 1955, Vol. XVII, extract 2.
- Muller, S. Permafrost or permanently frozen ground and related



engineering problems. Special Report Strategic Eng. Study No. 62. Milit. Intellig. Div. Office, 1945.

- Nadai, A. Plasticity and fracture of solids (Plastichnost' i razrushenie tverdykh tel). Moscow, Foreign Literature Publication, 1954.
- Nees, L. Pile foundations for large towers on permafrost. "Am. Soc. Civ. Eng", 1951, Vol. 77, No. 103.
- Nye, J. F. The flow of glaciers and ice-sheets as a problem in plasticity. "Proc. Roy. Soc.", Ser. A. 1951, Vol. 207, No. 1091.
- Nye, J. F. The flow law of ice. "Proc. Roy. Soc.", 1953, A-219, No. 1139.
- Oding, I. A. Relaxation and creep of metals (Relaksatsiya i poizuchest' metallov). "Machine Building News", 1946, No. 5 - 10; 1949, No. 2.
- Oding, I. A. Current ideas about the mechanisms of plastic deformation and failure with the creep of metals (Sovremennye predstavleniya o mekhanizmax plasticheskoy deformatsii i razrusheniya pri poizuchesti metallov).
- Odquist and Folke, K. G. Influence of primary creep on stresses in structural parts. "Kyl. tekn. Hogskolans handl", 1953, No. 66.
- Pchelintsev, A. M. Instructions for determining the weight of moisture and the volumetric ice content of frozen soil in field laboratories (Instruktivnye ukazaniya po opredeleniyu ob'emnogo vesa vlashnosti i ob'emnoy l'distesti merzlykh gruntov v polevykh laboratoriyakh). In the book "Proceedings on Laboratory Studies of Frozen Soil". Collection No. 2. Moscow, Published in AN SSSR, 1954.
- Pekarskaya, N. K. Problems of the shear resistance of frozen soil (Voprosy soprotivleniya merzlykh gruntov sdvigu). Official Report for 1953. AN SSSR Permafrost Research Institute.
- Pekarskaya, N. K. On the method of determining the shear resistance of frozen soil (K metodike opredeleniy soprotivleniya merzlykh grunto sdvigu). In the book "Proceedings on Laboratory Studies of Frozen Soil". Collection No. 3. Moscow, Published in AN SSSR, 1957.
- Pekarskaya, N. K. and Tsytoovich, N. A. On the role of friction and adhesion in the general resistance of frozen soil to shear with the rapid increase of stress (O roli treniya i stsepleniya v obshchem soprotivlenii merzlykh gruntov sdvigu pri bystrom vozrastanii nagruzki). In the book "Proceedings on Laboratory Studies of Frozen Soil". Collection No. 3. Moscow, Published in AN SSSR, 1957.
- Perutz, M. F. Direct measurement of the velocity distribution in a vertical profile through a glacier. "J. Glaciology", 1950, Vol. 1, No. 7.



- Prokrovskiy, G. I. and Nekrasov, A. A. Statistical theory of soil (Statiticheskaya teoriya gruntov). "News of the Military Engineering Academy". No. 6. Collection "Bases and Foundations", Moscow, 1934.
- Rabotnov, Yu. N. 1. Equilibrium of a rigid medium with after effect (Ravnovesie uprogoy sredy s posledeystviem). "Occurrences in Mathematics and Mechanics", 1948, Vol. 12, extract 1.
- Rabotnov, Yu. N. 2. Calculation of details of machines for creep (Raschet detaley mashin na polzuchest'). "Izvestia AN SSSR, OTN", 1948, No. 6.
- Rathjens, I. Arctic engineering requires knowledge of permafrost behavior. "Civ. Eng.", 1951, No. 1.
- Rebinder, P. A. Physical and chemical studies of the processes of deformation of solid substances (Fiziko-khimicheskie issledovaniya protsessov deformatsii tverdykh tel). Jubilee collection dedicated to the thirtieth anniversary of the Great October Socialist Revolution. Moscow, Published in AN SSSR, 1947.
- Rebinder, P. A. New methods of the characteristic of elasto-viscoplastic properties of structured dispersed systems (Novye metody kharakteristiki uprugoplastichno-vyazkikh svoystv strukturirovannykh dispersnykh sistem). "Works of the AN SSSR Institute of Physical Chemistry", 1950, extract 1.
- Reiner, M. Ten lectures on theoretical rheology (Deyat'lektsiy po teoreticheskoy reologii). Moscow-Leningrad, State Technical Printing House, 1947.
- Reiner, M. Twelve lectures on theoretical rheology. London, 1949.
- Roberts, P. A. and Cooke, F. Arctic tower foundations frozen into permafrost. "Eng. News. Rec.", 1950, Vol. 144, No. 6.
- Rodshtein, A. G. Distribution of contact under rigid punches on a sand foundation (Raspredelenie kontaktnykh naprazheniy pod zhestkimi shtampami na peschanom osnovanii). Candidate's dissertation. Lenin State Library, 1950.
- Rodshtein, A. G. Experimental determinations of the reaction pressures at the base of rigid foundations (Opytnye opredeleniya reaktivnykh davleniy po podoshve zhestkikh fundamentov). "Hydraulic Construction", 1951, No. 9.
- Roza, S. A. Settlements of hydraulic constructions in clay with low moisture content (Osadki gidrotekhnicheskikh sooruzheniy na glinakh s maloy vlazhnost'yu). "Hydraulic Construction", 1950, No. 9.
- Rozovskiy, M. I. Creep and prolonged failure of metals (Polzuchest' i dlitel'noe razrushenie metallov). "Journal of Technical Physics", 1951, Vol. 21, extract 11.

- Ruppineyt, K. V. Some problems of the mechanics of rock strata (Nekotorye voprosy mekhaniki gornyykh porod). Moscow, Ugletekhizdat, 1954.
- Rzhanitsyn, A. R. Some problems of the mechanics of systems deformed in time (Nekotorye voprosy mekhaniki sistem, deformiruyushchikhsya vo vremeni). Moscow, State Technical Printing House, 1949.
- Saltykov, H. I. On the calculated size of heave forces (O raschetnoy velichine sil pucheniya). "Journal AN SSSR, OTN", 1944, No. 6.
- Savel'ev, B. A. On the problem of the viscosity of frozen soil and ice (K voprosu o vyazkosti merzlykh gruntov i l'dov). Stocks of the AN SSSR Frozen State Research Institute, 1953.
- Savel'ev, B. A. The structure, composition, and properties of the ice coating of sea and fresh water tanks (Stroenie, sostav, i svoystva ledyanogo pokrova morskikh i presnykh vodoemov). Doctoral Dissertation. Stocks of the AN SSSR Frozen State Research Institute, 1955.
- Schulman, A. R. Viscosity of polycrystalline ice (Tekuchest' polikristallicheskogo l'da). "Works of the State Hydraulic Institute", extract 7 (61). Leningrad, Gidrometeoizdat, 1948.
- Segalova, E. E., Rebinder, P. A., Senteryukhina, L. N. The elastoplastic properties of the oleostearate of calcium (Uprugoplasticheskie svoystva oleogeley stearate kal'tsiya). "Colloid Journal", 1951, Vol. XII, extract 6.
- Shield, R. A. and Drucker, D. The application of limit analysis to punch-indentation problems. "J. App. Mech.", 1953, Vol. 20, No. 4; "Mech. Eng.", 1953, Vol. 75, No. 8.
- Shinoda, I. One dimensional consolidation of viscoelastic body. Proc. second Japan. Nat. Congr. Appl. Mech. Sci. Council Japan, Tokio, 1953.
- Shishkin, N. A. and others. The plastic deformation and viscosity of ice (Plasticheskaya deformatsiya i vyazkost' l'da). "Journal of Technical Physics", 1946, Vol. 16, extract 3.
- Shumskiy, P. A. Principles of structural ice research (Osnovy strukturnogo ledovedeniya), Moscow, Published in AN SSSR, 1955.
- Shwedoff, F. N. "J. de physique", 1889, No. 8 (2); 1890, No. 9 (2).
- Sokolovskiy, V. V. The theory of plasticity (Teoriya plastichnosti). Moscow, State Technical Printing House, 1950.
- Sokolovskiy, V. V. The statics of a granular medium (Statika sypuchey sredy). Moscow, State Technical Printing House, 1954.
- Standards and technical specifications for ordinary foundations of permafrost buildings and industrial structures in permafrost areas (Normy i tekhnicheskie usloviya proektirovaniya estesvennykh

osnovaniy zdaniy i promyshlennykh soorusheniy v rayonakh vechnoy merzloty). N and TU 118 - 54. Moscow, Gosstroyizdat, 1955.

Standards and technical specifications for planning ordinary foundations of buildings and industrial structures (Normy i tekhnicheskie usloviya proektirovaniya estestvennykh osnovaniy zdany i promyshlennykh soorusheniy). N and TU 127 - 55. Moscow, Gosstroyizdat, 1955.

Sturgis, J. Arctic engineering known-how gets acid test at Thule. "Civ. Eng", 1953, Vol. 23, No. 9.

Sumgin, M. I. Permafrost within the USSR (Vechnaya merzlota pochvy v predelkh SSSR). Vladivostok, 1927.

Sumgin, M. I. Physical and mechanical processes in moist and frozen soil in connection with the formation of cracks in roads (Fiziko-mekhanicheskie protsessy vo vlazhnykh i merzlykh gruntakh v svyazi s obrazovaniem puchin na dorogakh). Moscow, Tsudortrans, 1929.

Sumgin, M. I. and others. General permafrost research (Obshchee merzlotovedenie). Moscow, Published in AN SSSR, 1940.

Sylwestrowicz, W. Experimental investigation of the behavior of soil under a punch or footing. "J. Mech. and Phys. Solids", 1953, Vol. 1, No. 4.

Terzaghi, K. Permafrost. "J. Boston Soc. of Civ. Eng.", 1952, Vol. 39, No. 1.

Tsvetkova, S. G. The speed of adfreezing of piles driven into permafrost with steaming (Skorost' smerzaniya svay, zabitykh v vechnomerzlye grunty s preparivaniem). Candidate's Dissertation. AN SSSR Permafrost Research Institute, 1953.

Tsvetkova, S. G. The reduction of the frost condition of the soil around piles driven by means of steaming (Vosstanovlenie merzlogo sostoyaniya gruntov okolo svay, zabitykh metodom preparivaniya). In the book "Works of the Igarskiy Scientific Frozen Research Station", extract 1. Moscow, Published in AN SSSR, 1954.

Tsytoich, N. A. The problem of the design of building foundations constructed on permafrost (K voprosu rascheta fundamentov sooruzheniy, vozvodimykh na vechnoy merzlote). Leningrad Gipromeza, 1928.

Tsytoich, N. A. Study of the elastic and plastic deformations of frozen soil (Issledovanie uprugikh i plasticheskikh deformatsiy merzlykh gruntov). "Works of KOVM AN SSSR", Vol. 10, Moscow, Published in AN SSSR, 1940.

Tsytoich, N. A. The theory of the equilibrium conditions of water in frozen soil (K teorii ravnovechnogo sostoyaniya vody v merzlykh gruntakh). "Journal AN SSSR, Series of geography and geophysics", 1945, Vol. 9, No. 5 - 6.

- Tsyтовich, N. A. On non-frozen water in porous strata (O nezamerzayuchey vode v rykh gornykh porodakh). "Journal AN SSSR, Series of geology", 1947, No. 3.
- Tsyтовich, N. A. Soil mechanics (Mekhanika gruntov). Moscow-Leningrad, State Literature on Construction and Architecture, 1951.
- Tsyтовich, N. A. Principles of the mechanics of frozen soils (Printsipy mekhaniki merzlykh gruntov). Published in AN SSSR, 1952.
- Tsyтовich, N. A. Instructions for determining the forces of adhesion of frozen soil (Instruktivnye ukazaniya po opredeleniyu sil stsepleniya merzlykh gruntov). in the book "Proceedings of Laboratory Studies of Frozen Soil". Collection No. 2. Published in AN SSSR, 1954.
- Tsyтовich, N. A. On determining the cohesion of cohesive soil by means of a ball test (Ob opredelenii sil stsepleniya svyaznykh gruntov po metodu sharikovoy proby). "Report of AN SSSR", 1956, Vol. III, No. 5.
- Tsyтовich, N. A. Bases and foundations on frozen soil (Osnovaniya i fundamenty na merzlykh gruntakh). Published in AN SSSR, 1958.
- Tsyтовich, N. A. and Sumgin, M. I. Principles of the mechanics of frozen soil (Osnovaniya mekhaniki merzlykh gruntov). Moscow-Leningrad, Published in AN SSSR, 1937.
- Tyabin, H. V. On the similarity of the currents of a visco-plastic fluid (O podobii potokov vyazko-plasticheskoy zhidkosti). "Colloid Journal", 1952, Vol. XIV, extract 4.
- Tyabin, N. V. Fundamental equations of the rheology of a visco-plastic medium (Osnovnye uravneniya reologii vyazko-plastichnoy sredy). "Colloid Journal", 1951, Vol. XIII, extract 1.
- Volarovich, M. P. Colloids in the food industry (Kolloidy v pishchevoy promyshlennosti). Collection 2. Moscow, Pishchepromizdat, 1949.
- Volarovich, M. P. Study of the rheological properties of dispersed systems (Issledovanie reologicheskikh svoystv dispersnykh sistem). "Colloid Journal", 1954, Vol. XIV, extract 3.
- Volarovich, M. P. and Gutkin, A. M. The flow of a visco-plastic body between two parallel horizontal walls and in the circular gap between two coaxial pipes. "Journal of Technical Physics", 1946, Vol. XVI, No. 3. (Tehenie plastichno-vyaskogo tela mezhdvumya parallel'nymi ploskimi stenkami i v kol'tsevom zazore mezhdvumya koaksial'nymi trubkami).
- Volterra, V. Theory of functions and of integral and integro-differential equations. London-Glasgow, 1931.

- Votyakov, I. N. Some laws on the change of the physical and mechanical properties of permafrost in Central Yakutia depending on its condition and temperature (Nekotorye zakonomernosti v izmenenii fiziko-mekhanicheskikh svoystv mnogoletnemerzlykh gruntov Tsentral'noy Yakutia v zavisimosti ot ikh sostava i temperatury). Candidate's Dissertation. AN SSSR Permafrost Research Institute, 1955.
- Voytkovskiy, K. F. Calculation of foundations of ice and snow (Rachyot sooruzheniy iz l'da i snega). Moscow, Printed in AN SSSR, 1954.
- Voytkovskiy, K. F. Experimental studies of the plastic properties of ice (Eksperimental'nye issledovaniya plasticheskikh svoystv l'da) in the collection: "Seasonal Freezing of Soil and the Use of Ice for Building Purposes". Published in AN SSSR, 1957.
- Vyalov, S. S. Operation of piles in permafrost (Rabota svay v vechnomerzlykh gruntakh). Reports of the Permafrost Research Institute, 1953.
- Vyalov, S. S. Creep and long-term resistance of frozen soil (Polzuchest' i dlitel'noe soprotivlenie merzlykh gruntov). "Report of AN SSSR", 1955, Vol. 104, No. 6.
- Vyalov, S. S. The relation between stress and deformation of frozen soil taking into account the factor of time (Zavisimost' mezhdunarazheniem i deformatsiey merzlykh gruntov s uchyotom faktora vremeni). "Report of AN SSSR", 1956, Vol. 108, No. 6.
- Vyalov, S. S. Rheological processes in frozen soil and the condition of their equilibrium (Reologicheskie protsessy v merzlykh gruntakh i uslovie ikh predel'nogo ravnovesiya). In the book "Materials from Laboratory Studies of Frozen Soil". Collection No. 3. Published in AN SSSR, 1957.
- Vyalov, S. S. The long-term strength of frozen soil and its bearing capacity (Dlitel'naya prochnost' merzlykh gruntov i ikh nesushanaya sposobnost'). VII Interdepartmental Colloquium on Permafrost Research. Materials on the physics and mechanics of frozen soil. Published in AN SSSR, 1959.
- Vyalov, S. S. and Egorov, N. M. Experimental determination of the heave forces of soil (Eksperimental'noe opredelenie sil pucheniya gruntov). In the book "Works of the AN SSSR Permafrost Research Institute", Vol. 14.
- Vyalov, S. S. and Skibitskiy, A. M. Rheological processes in frozen soil and dense clay (Reologicheskie protsessy v merzlykh gruntakh i plotnykh glinakh). In the book "Materials of the IV International Conference on Soil Mechanics and Foundation Engineering". Published in AN SSSR, 1957. See also "Proceedings of the IV International Conference on Soil Mechanics and Foundation Engineering", London, 1957.
- Vyalov, S. S. and Tsytochik, N. A. The cohesion of frozen soil (Tsepleniye merzlykh gruntov). "Report of AN SSSR", 1955, Vol. 104, No. 4.

- Vyalov, S. S. and Tsytovich, N. A. Estimation of the bearing capacity of cohesive soil by the pressure of a spherical indenter (Otsenka nesushchey sposobnosti svyaznykh gruntov po velichine vdalivaniya sfericheskogo shtampa). "Report of AN SSSR", 1956, Vol. III, No. 6.
- Waele, A. a. and Lewis, G. L. The rheological curve. "Nature", 1953, Vol. 172, No. 4372.
- Waterhouse, R. A. and Nelson, S. Thaw-blast prepares permafrost foundation for Alaska power plants. "Civ. Eng.", Febr., 1952, Vol. 22, No. 2.
- Weinberg, B. P. Arctic Magazine, State Technical Printing House, 1940.
- Yoh-Han Pao and Marin, J. A theory for combined creep strain-stress relations for materials with different properties in tension and compression. Proc. U. S. Nat. Congr. Appl. Mech., N. Y., 1952.
- Yoh-Han Pao and Marin J. An analytical theory of the creep deformation of materials. "J. Appl. Mech.", 1953, Vol. 20, No. 2.
- Zaytsev, G. P. The law of mechanical similarity in the deformation of different materials (Zakon mekhanicheskogo podobiya pri deformatsii raznykh materialov). "Factory Laboratory", 1950, No. 5.
- Zener, K. and others. Elasticity and inelasticity of metals (Uprugost' i neuprugost' metallov). Moscow, Foreign Literature Publication, 1954.
- Zhukov, A. M., Rabotnov Yu. N., and Churikov, F. S. Experimental verification of some theories of heaving (Eksperimental'naya proverka nekotorykh teoriy polzuchesti). "Engineering Collection", No. 17, Moscow, 1953.